Co-channel Interference Cancellation in Mobile Cellular Communication Systems

Reza Berangi

B.Sc. (Eng) (Hon), M. E. E.

A thesis submitted in fulfilment of the requirements for the degree of Doctor of Philosophy

School of Communications and Informatics

Faculty of Engineering and Science

Victoria University of Technology

Melbourne, Australia

June 1998

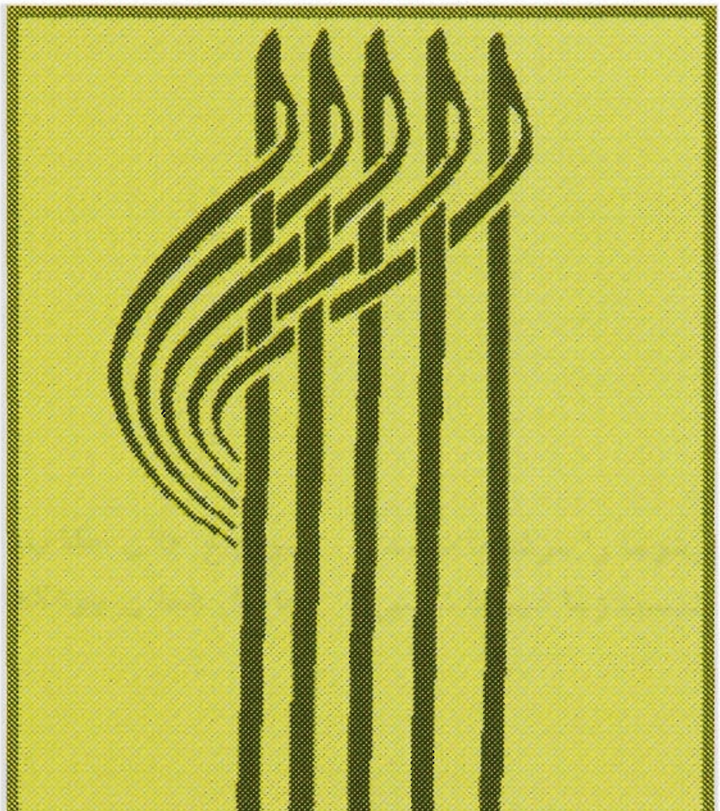
بسم الله الرحمن الرحيم

روز ازل بمهر تو ما را سرشته اند   بر لوح جان حکایت عشقت نوشته اند
زین رو پدید نیست ز ما غیر عاشقی   حاصل همان بود که از او بذر کشته اند

From My Beloved Father

The Great Iranian Poet

Habibollah Berangi Taleghani *(1931-1997)*

ABSTRACT

In recent years, mobile communications has become very popular and the demand for its services has increased dramatically. The capacity of mobile communication systems is mainly limited by co-channel interference caused by frequency reuse. The acceptable co-channel interference at the receiver determines the minimum allowable distance between adjacent co-channel users and hence the system capacity. One approach to increase the capacity is to employ co-channel interference resistant receivers. The research work presented in this thesis deals with the designing of such receivers for cellular mobile communication systems.

A blind co-channel interference cancelling technique, indirect co-channel interference cancelling (ICIC), has been proposed for cancelling of one interferer with constant envelope modulation in mobile communication channels. The main advantage of this interference cancelling technique is that it does not require any knowledge of interference channel and timing, which results in a simple receiver structure. Based on this technique, several detection strategies, including bit-by-bit detection (BB-ICIC), reduced waveform bit-by-bit detection (RW-ICIC), sequential detection using Viterbi algorithm (VA-ICIC), and error detection and correction scheme, are studied by using computer simulations. The VA-ICIC, because of its superior bit error rate (BER) performance has been selected for further investigation.

Effects of various mobile communication system parameters on the performance of VA-ICIC have been examined to assess the sensitivity of the interference canceller to these parameters. The effect of desired signal channel estimation is investigated by applying pilot symbol insertion. The bit error rate of the BB-ICIC in AWGN channel is analysed and an open form expression is obtained. Due to the nonlinearities of relations, some of the required probability density functions (PDF) are obtained by using statistical simulation and approximated by well known distributions. Theoretical BERs, found with certain constraints, closely match with the simulated BERs under high signal to noise ratios, while for low signal to noise ratios, they depart from the simulated BERs. This is due to the inaccuracy of the approximated PDFs and constraints.

Declaration

I declare that, to the best of my knowledge, the research described herein is the result of my own work, except where otherwise stated in the text. It is submitted in fulfilment of the candidature for the degree of Doctor of Philosophy of Victoria University of Technology, Australia. No part of it has already been submitted for this degree or is concurrently submitted for any other degree.

Reza Berangi

June 1998.

ACKNOWLEDGEMENT

Firstly, I would like to thank my supervisor Professor Patrick Leung, Associate Dean, Faculty of Engineering and Science, for his support, and encouragements throughout the work. Special consideration must go to my co-supervisor Associate Professor Mike Faulkner and Dr. Fu-Chun Zheng for their support, constructive comments and help to correct the thesis.

I greatly enjoyed the inspiration and friendly environment provided by the staff of the former Department of Electrical and Electronic Engineering, especially Professor Akhtar Kalam and Associate Professor Wally Evans. I must also appreciate the Ministry of Culture and Higher education of the Islamic Republic of Iran who financially supported me during the research period.

My thanks should also go to my fellow research students in the former Department of Electrical and Electronic Engineering. The memories I shared with Mahmood, Nasser, Mehrdad, Omar, Iqbal, Adrian, Mahabir, Rushan, Zahidul, Vallipuram, Ranjan, Olivia, Tuan, Mark and Scott will always remains with me.

I would like to acknowledge, Melvyn Pereira, Gavin Hill, Professor Akhtar Kalam, Dr. Prem Dassanayake, and Dr. Aladdin Zayegh who kindly gave their time and ideas in helping me to correct the English presentation of this thesis.

Last but not least, I wish to express my gratitude for the support and encouragement I have received from my family. I am specially indebted to my wife Seddigeh (Farideh) Ahmadian who made it all possible with her tremendous support and patience during the long research period. I would like to thank my daughters Tayebeh and Tahereh who helped me in correcting, the final version of this thesis with their excellent command of the English. I should also mention my sweet daughter Sepideh who would lift all the exhaustion of a long hard day with her big smile and hugs whenever I came back from university. Finally, I would like to mention my mother, father, mother in-law and father in-law for all their support.

With Love To my Wife

Farideh

CONTENTS

LIST OF TABLES

List of Figures

ACRONYMS

AM	Amplitude Modulation
ARC-FSK	Asymmetric Raised Cosine FSK
AWGN	Additive White Gaussian Noise
BB-ICIC	Bit-by-Bit ICIC
BER	Bit Error Rate
CCI	Co-channel Interference
CDF	Cumulative Density function
CDMA	Code Division Multiple Access
CIMTS	Co-channel Interference Mitigation in Time Scale Domain
CIR	Carrier to Interference Ratio
CMA	Constant modulus Algorithm
CPM	Continuous Phase Modulation
DD	Discriminator Detection
DDA	Decision Directed Algorithm
DECT	Digital Enhanced Cordless Telecommunications
DF	Decision Feedback
DMI	Direct Matrix Inversion
DPSK	Differential PSK
DS/CDMA	Direct Sequence CDMA
EDC-ICIC	Error Detection Correction ICIC
FALI	Filter and linear interpolation
FBLP	Forward Backward Linear Prediction
$f_D T$, $f_d T$	Normalized fading rate
FM	Frequency Modulation
FQPSK	Filtered QPSK
FRESH	FREquency SHifting

FSK	Frequency Shift Keying
GMSK	Gaussian Minimum Shift Keying
GMSK BT=0.3	GMSK with premodulation Gaussian filter with normalized bandwidth of $BT = 0.3$
GMSK BT=0.5	GMSK with premodulation Gaussian filter with normalized bandwidth of $BT = 0.5$
GSM	Global System for Mobile communication
ICIC	Indirect Co-channel Interference Cancelling
IID	independent identically distributed
I/Q	Inphase and Quadrature
ISI	Intersymbol Interference
ISR	Interference to signal ratio
LDD	Linear Discriminator Detection
LMS	Least mean square
MAP	Maximum A Posteriori
ML	Maximum Likelihood Detection
MMSE	Minimum Mean Square Error
MSK	Minimum Shift Keying
NED	Normalized envelope distance
PAM	Pulse Amplitude Modulation
PDF	Probability Density Function
PIC	Parallel Interference Cancelling
PLL	Phase Locked Loop
PSA	pilot symbol aided
PSK	Phase Shift Keying
QAM	Quadrature Amplitude Modulation
QPSK	Quadrature Phase Shift Keying
rms	root mean square
RWBB-ICIC	Reduced Waveform Bit-By-Bit ICIC
SCORE	Spectral Coherence Restoral

SIC	Serial Interference Cancelling
SIR	Signal to Interference Ratio
SVD	Singular Value Decomposition
TFM	Tamed Frequency Modulation
TDMA	Time Division Multiple Access
VA	Viterbi Algorithm
WLS	Weighted Least Square

NOTATIONS

A	Desired signal amplitude
B	Interference signal amplitude
B_T	Normalized bandwidth
B_N	Noise equivalent bandwidth
B_w	Bandwidth
C	Regenerated desired signal amplitude
$C_{vv}(t_1, t_2)$	Autocovariance of v
$c(t)$	Channel of desired signal
$\hat{c}(t)$	Estimate of desired signal channel
D	Data symbol
D_{ir}	Euclidean distance between $w_i(t)$ and $w_r(t)$
d_{ir}	Normalized Euclidean distance between $w_i(t)$ and $w_r(t)$
$d(t)$	Channel of interference signal
E_b	Energy per bit
$E\{\ \}$	Expectation operator
e_{ij}	Normalized envelope distance between $w_i(t)$ and $w_r(t)$
e_{min}	Minimum envelope distance
$F(x)$	CDF function
f_c	Carrier frequency
f_d	Fading frequency
f_s	Sampling frequency
$g(t)$	CPM modulation index
h	CPM frequency deviation ratio
$h(t)$, $h(n)$	Impulse response
$I(t)$	Interference RF signal
$i(t)$	Complex envelope of interference

L	Normalized length of CPM phase pulse
L_i	ICIC-metric value for the i[th] waveform
L_{ir}	ICIC-metric value for $w_i(t)$ when the received desired signal waveform is $w_r(t)$.
Λ_{ri}	ICIC-metric value normalized with noise power
L_q	Number of quantizer levels
M	Size of alphabet in M-array signalling
M_i	Envelope of residue signal for i[th] regenerated waveform
m	Number of samples per symbol
N	Number of possible waveforms
$N(t)$	Band limited RF noise
N_0	One sided power spectrum of AWGN
$n(t)$	Complex envelope of band limited noise
$n_i(t)$	In-phase band limited noise component
$n_q(t)$	Quadrature band limited noise component
NR	Noise reduction
NRL	Noise reduction limit
P	Pilot symbol
P_e	Probability of error
P_i	I-channel pilot symbol
P_q	Q-channel pilot symbol
Q	Mean squared quantization error
$q(t)$	CPM modulation phase pulse
$R(t)$	Received RF signal
$r'(t)$, $r''(t)$	Received complex envelope signals after fading cancellation
r , $r(k)$, $r(t)$	Complex envelope of received signal
r_i, $r_i(k)$	In-phase received signal
r_q, $r_q(k)$	Quadrature received signal
r_b	Bit rate
V_q	Dynamic range of quantizer

$Ws1$, $Ws2$	Odd and even bits waveform sets of RW-ICIC
$W(t)$	Desired RF signal
W_{ir}	Non-normalized ICIC-metric value.
$w(t)$	Complex envelope of desired signal
$\hat{w}(t)$	Estimate of desired signal's complex envelope
$w_i(k)$	i^{th} possible complex envelope desired signal waveform
$w(n)$	Window
w_{ki}, w_{kq}	In-phase and quadrature waveforms of RWBB-ICIC
$S(f)$	Lowpass fading spectrum
S_i	In-phase data symbol
S_q	Quadrature data symbol
T	Bit timing interval
T_s	Sampling period
$Y(t)$, $Y'(t)$	Interference part of received signal after fading cancellation
α	Sampling frequency to bandwidth ratio
α_i	i^{th} data symbol from alphabet M
a_n	Desired signal symbol at the n^{th} timing interval
$\hat{\alpha}$	Detected data
β_n	Regenerated signal symbol at the n^{th} timing interval
Δ	Step size of quantizer
δ_n	L-tuple phase state
ε	Complex envelope residue signal
ε_I	In-phase component of residue signal
ε_Q	Quadrature component of residue signal
η	Bit energy to noise ratio (E_b/N_0)
$\Theta(t)$	The phase containing the information of interference signal
θ_n	Phase of co-channel interference at the beginning of bit timing interval (phase state).
λ_n	Co-channel interference symbol at the n^{th} timing interval
σ_n	Noise variance

	The phase containing the information of desired signal
ϕ_n	Phase of desired signal at the beginning of bit timing interval
$\Psi_i(k)$	The phase containing the information of regenerated desired signal
ψ_n	Phase of regenerated signal at the beginning of bit timing interval
$\Re$	Channel gain of desired signal
$\hat{\Re}$	Estimated channel gain of desired signal
$\varnothing$	Channel phase of desired signal
$\hat{\varnothing}$	Estimated channel phase of desired signal

Publications

The work on this thesis has produced the following publications:

[1] Reza Berangi and Patrick Leung, "Indirect interference cancelling: Concept and simulation results," is presented in *Multiaccess, Mobility and Teletraffic for Personal Communications conference, Dec, 1997, Melbourne, Australia.* This paper is published in the following book:
D. Everitt and M Rumsewicz, Ed., *Multiaccess, Mobility and Teletraffic Advances in Wireless Networks*, Kluer Academic Publishers: Boston, 1998.

[2] Reza Berangi and Patrick Leung, "Cancelling of a constant envelope cochannel interferer," submitted for publication in the *IEEE Trans. in Veh. Tech.*

[3] Reza Berangi, Patrick Leung and Mike Faulkner, "Signal space representation of indirect cochannel interference canceller," *proceeding of IEEE Vehicular Technology Conference,* Phoenix, Arizona, USA, pp. 145-149, May 1997.

[4] Reza Berangi and Patrick Leung, "Blind Cochannel Interference Cancelling For Mobile Communication Systems," *Proc. of IEEE Singapore International Conference on Communication Systems,* Singapore, pp. 581-584, Nov. 1996.

[5] Reza Berangi and Patrick Leung, "Combined Pilot Symbol Aided Fading and Cochannel Interference Cancellation," *Proc. of IEE Forth UK/Australian International Symposium on DSP for Communication Systems,* Perth, Australia, pp. 25-28, Sept. 1996.

[6] Reza Berangi and Patrick Leung, "A Low Complexity pilot Symbol Insertion Method for GMSK Modulation Scheme," *Proc. of IEE UK/Australian Forth International Symposium on DSP for Communication Systems,* Perth, Australia, pp. 203-209, Sept. 1996.

[7] Reza Berangi, Patrick Leung and Mike Faulkner, "Cochannel Interference Cancellation for Mobile Communication Systems," *Proc. of IEEE International Conference on Universal Personal Communication Systems (ICUPC'96), Cambridge,* MA, pp. 438-442, Sept. 1996.
This paper won the IEEE best student paper award.

[8] Reza Berangi and Patrick Leung, "Detection of Signals In the Presence of Cochannel Interference," *Proc. of IEEE Fourth International Symposium on Signal Processing and its Applications (ISSPA'96)*, Gold Coast, Australia, 26-28 Aug. 1996.

[9] Reza Berangi and Patrick Leung, "A New Receiver Design for CCI Limited Mobile Communication Systems," *Proc. of Iranian Conference on Electrical Engineering (ICEE'96)*, Tehran, Iran, Vol. 2 (communication), PP 279-285, May 1996.

[10] Reza Berangi, Patrick Leung and Mike Faulkner, "Cochannel Interference Cancelling of Constant Envelope Modulation Schemes In cellular Radio Systems," *Proc. of IEEE Vehicular Technology Conference (VTC'96)*, Atlanta, Georgia, PP 1776-1780, April 1996.

[11] Reza Berangi and Patrick Leung, "A New Pilot Symbol Insertion Method for GMSK," *Proc. of First Communication Conference*, Muscat, Oman, March 1996.

[12] M. M. Zonoozi, P. Dassanayake and R. Berangi, "Generation of Non-Uniform Distributed Random Numbers by MATLAB," *Proc. of The 1996 Australian Matlab Conference*, Melbourne, Australia, First paper of Electrical Engineering, Jan. 1996.

[13] Reza Berangi, Patrick Leung and M. M. Zonoozi, "Simulation of A Mobile Communication System," *Proc. of The 1996 Australian Matlab Conference*, Melbourne, Australia, Third paper of Simulation two, Jan. 1996.

[14] Reza Berangi, Patrick Leung and Mike Faulkner, "Cochannel Interference Cancelling Using A New Coherent Demodulation Technique for MSK," *Proc. of Third Iranian Conference on Electrical Engineering (ICEE'95)*, Tehran, Iran, PP 95-103, May 1995.

[15] Reza Berangi, Patrick Leung and Mike Faulkner, "Performance Improvement of Cochannel Interference canceller For MSK Modulation Scheme Using a New Coherent Receiver," *Proc. International Conf. on Mobile and Personal Communication Systems*, Adelaide, Australia, PP. 7-10, April 1995.

[16] Reza Berangi, Patrick Leung and Mike Faulkner,"A Novel Likelihood Function For Mobile Communication Channels with Cochannel Interference," *Proc. of Second International Conference on Mobile and Personal Communication Systems*, Adelaide, Australia, PP. 1-6, April 1995.

[17] Reza Berangi, Patrick Leung and Mike Faulkner, "A Novel Cochannel Interference Canceller for Coherent MSK in Slow Fading Mobile Communication Channel," *Proc. IEEE International Conf. on Universal Wireless Access*, Melbourne, Australia, PP. 99-103, April 1994.

Chapter 1

Introduction

1.1 Background

Frequency reuse and cellular concepts [1] have greatly assisted the establishment of mobile communication networks (systems) that facilitate the mobility of users by using a limited frequency spectrum. The demand for access to these networks, due to their advantages, continually increases. This increasing demand for, and limitation of spectrum resources have motivated mobile communication systems and equipment designers to continually investigate methods of improving system capacity and signal quality. To date, these great have brought several generations of mobile communication systems into existence [2]-[9].

In cellular systems the available spectrum is geographically reused, i.e. the same channels are used simultaneously at different locations [1]. With the cellular concept, the idea is to divide the area into small regions, called cells, each with its own base station and a number of channels corresponding to the expected traffic within the cell. In adjacent cells, different channels are used in order to prevent interference. However, in cells further away, the same channels can be reused. The physical phenomenon in radio communication that makes this possible is that the mean signal strength decreases with the distance between the transmitter and the receiver. Channels that are used in one cell should be reused only the cells located far enough away to ensure a small co-channel interference level. That is, users transmitting on the same channel do not interfere with each other.

Cellular system capacity is often expressed in terms of the number of simultaneous users (number of channels) that can be offered per unit area [10]. The capacity of cellular systems can therefore, be increased by decreasing the channels' geographical reuse distance. However, this increase is constrained by co-channel interference from other users. Co-channel interference reduction or cancelling techniques can effectively relax this constraint and improve efficiency and performance of cellular mobile communication systems. A brief survey of the literature dealing with the problem of co-channel interference in cellular mobile communications is presented as follows.

1.2 Literature Review

During the last two decades, a considerable amount of work has been carried out addressing a wide range of problems in connection with co-channel interference in mobile communication systems. These activities mainly involve evaluation of the performance of different modulation schemes or cellular systems under co-channel interference (CCI), and CCI cancelling techniques. Interference prevention techniques such as sufficiently separating co-channel users, cell sectorization, antenna orientation, changing antenna beamwidth, varying antenna height, controlling transmission power, and dynamic channel assignment [10], have been examined to reduce interference. In the next sections several important topics regarding CCI are reviewed.

1.2.1 Performance of Modulation Schemes in CCI

The problem of detecting signals suffering co-channel interference and Gaussian noise has been studied by a large number of investigators. The literature in this area has been classified into two different branches: linear modulation schemes such as PSK (phase shift keying), QPSK (quadrature PSK) and QAM (quadrature amplitude modulation) as well as nonlinear modulation schemes.

1.2.1.1 Performance of Linear Modulation Schemes in CCI

To the knowledge of the author, the performance of PSK-systems with co-channel interference in addition to Gaussian noise was initially studied by Rosenbaum and Prabhu [11]-[14][1]. In [11], Rosenbaum studied a receiver consisting of an ideal phase discriminator and a perfect slicer. The error performance for a binary system with a co-channel interferer was computed numerically and a bounding technique for the probability of error was given for a M-ary PSK modulation. This research was followed by a discription of analytical probability of error for binary PSK with multiple co-channel interferers and the same type of receiver as in [12]. Prabhu, in [13] and [14], considered M-ary PSK modulation coherent receivers which detect only the phase angle without considering amplitude variations of the signal in the presence of multiple independent additive interferers. In [13], the probability of error is expressed as a power series with the coefficients expressed in terms of Hermite polynomials. The power series converges as the total power of interferers become less than the desired signal power. A simple upper bound on the error probability was

1.Most of the references regarding probability analysis of PSK modulation schemes (including [11]-[20]) are collected in [21].

given in [14] by using the Chernoff bound. The same system model as [13] was later used by Goldman in [15] to express the probability of multiple consecutive errors for both coherent and differential detection. Shimbo and Fang [16] employed a power series expansion technique to evaluate the performance of M-ary PSK with co-channel interference and an ideal receiver, optimized for additive white Gaussian noise (AWGN).

An upper error probability bound for an ideal phase detection of PSK-signals with peak limited interference was derived by Rosenbaum and Glave [17]. This bound is simply used to determine all of the possible interference envelope probability density functions (PDF) with a given rms and peak value, which maximize the probability of error. This bounding technique had already been employed by Rosenbaum and Glave in [18] and [19] for PSK in the presence of adjacent channel interference. A computational procedure for evaluating the error probability bound for PSK in a composite interference channel (including Gaussian noise, intersymbol interference, adjacent-channel interference and co-channel interference) was given by Benedetto et al. in [20].

Bit error rate (BER) performance of differential $\pi/4$-QPSK in the presence of co-channel interference have been investigated using both hardware implementation [22] and software simulation [23], taking into account delay spread, Rayleigh, and log-normal fading channels. BER performance of QPSK in the presence of co-channel interference in both fading and nonfading environments has been analysed in [24]. Three approaches; i.e. a precise method based on the average probability of error, a sum of sinusoids with constant (unfaded) amplitudes model, and a Gaussian interference model, are considered. Comparison between these three methods shows that both Gaussian interference and the sum of sinusoids models, underestimate BER in the fading situation, especially for the case of a single dominant interferer. Furthermore, the obtained BER when the total interference power is equally distributed among six Rayleigh faded interferers, is smaller than that when the interference power is concentrated in a single Rayleigh faded interferer.

Distribution of the phase noise due to AWGN and CCI for differential M-ary PSK (MPSK) in a very slow nonfrequency selective Rayleigh fading with diversity reception was analysed in [25]. Simple closed-form expressions for average probability of error were derived for ideal selection diversity reception. Impacts of the timing offset between the desired signal and the CCI on the overall channel filter impulse response were also investigated. It is shown that continuous phase shift keying (CPSK) is less sensitive to a timing offset than differential PSK (DPSK).

Relating to the references above, receivers were optimized for Gaussian noise. The goal for most of the authors was to find bounds or "easily calculable" expressions of the error probability degradation due to co-channel interference.

1.2.1.2 Performance of CPM Modulation Scheme in the Presence of CCI

Continuous phase modulation (CPM) [26], with constant amplitude, has been shown to provide both good spectral and error properties. Among the different types of CPM modulation schemes, Gaussian minimum shift keying (GMSK) [27], has been adopted as the modulation scheme for the global system for mobile communication (GSM) [28] as well as digital enhanced cordless telecommunications (DECT) [29].

Analytical expressions for the exact error probability of CPM schemes in Gaussian and Rayleigh fading channels with co-channel interference in a linear detector are given in [30] and [31]. The performance of the same detector using a GMSK modulation scheme in the presence of multiple interferers in both Rayleigh and log-normal channels has been studied by Carter et. al. [32] using the Monte Carlo simulation technique. The performances of CPM schemes in co-channel interference and AWGN for Viterbi detectors has been analysed in [33] and [34]. In [33], Wales studied the performance of CPM under interference for large signal-to-noise ratios, based on minimum mismatched Euclidean distances. In [34], Svensson derived a general upper bound on the symbol error probability for a general CPM scheme.

The performance of differential detection (DD) and limiter-discriminator detection (LDD) receivers for different CPM schemes in the presence of CCI has been investigated in [25] and [35]-[38]. Andrisano et. al. [35] analysed the performance of continuous phase frequency shift keying (CPFSK) with LDD and multiple interferers under a Gaussian hypothesis for both co-channel and adjacent channel interferences in a static channel. In [37], Shin et. al. studied the performances of conventional and decision-feedback (DF) differential detection receivers for GMSK signals transmitted in the presence of CCI and AWGN. They showed that two-bit DD with a optimal threshold outperforms one-bit DD in static and Rician fading environments. However, one-bit differential detection offers a better BER performance than the two-bit scheme in a typical Rayleigh fading channel with CCI. They also showed that DF works well in an additive noise and/or interference environment, i.e., a static channel with CCI and AWGN. Nevertheless, in a fading environment, DF offers some reduction in the error floor. In [36], Korn derived a formula for the error probability of partial-response CPM with LDD and DD in a multipath Rayleigh fading channel, taking into account frequency selective fading, co-channel interference, adjacent channel interference, Doppler frequency shift, and AWGN. Performance of the same detectors for GMSK in frequency selective Rayleigh fading and multiple co-channel interferers has also been analysed independently in [38], by giving an exact solution for the average error probability. Since the exact solution that accounts for the effects of Gaussian noise, Rayleigh fading, co-channel interference, and timing delays requires lengthy calculations, a near-exact but less computationally intensive solution was derived. It is shown that, when there are several weak interferers, their combined effect can be represented by an equivalent interferer whose power is the sum of the powers of the individual interferers.

1.2.2 Cochannel Interference Cancelling Techniques

Cochannel interference cancelling simply means the removal of additive interference from the received signal in order to improve the performance of mobile communication systems. The performance and computational complexity of an interference canceller in a practical mobile radio environment mainly depends upon the number of interferers to be cancelled. Single-CCI cancellers are usually simpler than Multiple-CCI cancellers. The objective of a Single-CCI canceller is to cancel the dominant co-channel interferer in order to increase the signal-to-interference ratio. Following the proposal of several CCI cancelling techniques to cancel only one interference, number of authors [39]-[40] attempted to calculate the probability of a dominant co-channel interference. Their investigations reveals that regardless of having, say six possible co-channel interferers in a narrowband cellular radio system with omnidirectional antennas, one co-channel interferer is most dominant. The occurrence of a dominant interference is due to the effect of multipath fading, the asymmetric position of receivers with regard to their interferers, independent shadows in the interferers propagation paths, voice activity factor and the employed cell sectorization scheme.

In this literature review, interference cancelling techniques are classified in five categories. This classification is for exposition and, therefore, some of the mentioned techniques may fit into more than one category.

1.2.2.1 Analog Cellular Communication Systems

Perhaps the earliest research into CCI-cancelling was in analog cellular radio systems using a FM modulation scheme. In [41], a technique to suppress a single FM interchannel interferer was presented. In this technique two phase locked loops (PLL) are used to lock independently on the desired and interference signals. The output of voltage controlled oscillators are cross fedback to cancel interference from the input of PLLs. Another CCI cancelling technique was proposed by Aranguren et. al. [42] to cancel FM interferers using an auxiliary antenna whose output is amplitude and phase weighted and cancelled from the main antenna output. They exploited the envelope variation of FM modulation scheme to control the phase and amplitude weighting. Envelope variation has been also used by Bar-Ness et. al. [43]-[44] to suppress parasitic phase modulation of FM signals resulting from a co-channel interferer. In [45], Welborn and Reed employed forward-backward linear prediction (FBLP) [46] to estimate instantaneous frequencies of two FM interfering signals. They showed that a sixth order predictor can improve the performance by 5-17dB. However a significant disadvantage of this technique is its extensive computational complexity.

1.2.2.2 Narrowband Digital Cellular Communication Systems

One the most straightforward interference cancelling method might be the cancellation of a replica of interference from a received signal. The generation of this replica requires a preliminary knowledge of the co-channel interference channel, timing and transmitted data sequence. Several types of this canceller have been reported in [47]-[50]. The differences between them are mainly due to different approaches used for channel estimation and data detection. To acquire channel information, co-channel signals need to be separated. In code division multiple access (CDMA) systems, signal separation has been optimized by using spreading codes. In narrowband communication systems signal separation is rather difficult but because of independent signal fading, multipath propagation and different received signal powers, signals still may be separated. Assumptions such as synchronization of interference with desired signal can simplify channel estimation as well as timing synchronization. The estimation of interference and transmitted data sequence, especially with intersymbol interference (ISI), results in different situations. Joint estimation of co-channel interference and desired signal is the only way to work out these situations.

In [47] and [48] sequence estimation and symbol detection algorithms for demodulation of co-channel narrowband signals were proposed. The algorithms were based on the maximum likelihood (ML) and maximum a posteriori (MAP) criteria for the joint recovery of co-channel signals. *T/2*-spaced equalizer was used for channel estimation and the symbol timing was assumed to be ideal.

In the joint maximum likelihood sequence estimation (JMLSE), given by Ranta et al. [51], channel estimation is performed based on the joint channel estimation for the desired and interference signals using a training sequence sent in every transmission burst. Timing alignment of desired signal and interferers is also assumed in this approach. They also investigated the performance of their CCI-canceller in a typical cellular [49] environment by examining the network capacity. This investigation shows that their CCI-canceller can have a potential to provide a capacity gain of 15 to 48%, conditional to cancelling the strongest interferer.

Another approach was given by Wales [50] in which joint channel estimation for both co-channel signals, using pilot symbol insertion technique, was considered. For this channel estimation, ideal timing alignment of all co-channel signals was assumed. To reduce the extensive complexity of receiver, for the application of CPM modulation schemes, a sub-optimum receiver based on the superstate trellis [26], was proposed.

Cochannel interference mitigation in time scale domain (CIMTS) is addressed in [52]. In this method of CCI cancelling, a replica of interference is estimated and reconstructed from the null space of desired signal in time domain. Then, this replica is subtracted from the received signal. To enable this receiver to perform properly, a small frequency offset between the desired and the interference signals is necessary. An interference canceller proposed by Yoshino et. al. [53] employs Recursive-Least-Squares Maximum-Likelihood-Sequence-estimation (RLS-MLSE) equalizer with diversity reception to estimate the channel of desired and interfering signals. A similar technique with decision feedback equalizer was used by Uesugi et. al. [54]. The configuration of this interference canceller is such that, for a two element antenna array, one antenna element is dedicated to desired signal and the other one to the interferer. Regenerated replicas of desired signal or interferer from each antenna element is cancelled from the other element.

Joint demodulation of two co-channel QAM signals in static channel is studied by Gooch et. al. [55] using Monte Carlo simulation. In this technique channel estimation for both desired and interfering signals are performed by an adaptive T/2-spaced adaptive equalizer. It is assumed that signal to noise and interference ratios are good enough to support the correct performance of an adaptive equalizer (i. e. BER is at least 0.10 without interference cancelling). Symbol detection in this scheme is a bit by bit error correction scheme which corrects the error of a tentative decision by comparing the received signal and the sum of locally generated co-channel QAM signals with a threshold level.

In [56], Matsue and Murase proposed a CCI canceller to suppress the FM cross-polarization interference from an M-QAM modulated signal. This interference canceller essentially uses a reference signal, correlated with interference, coming from an auxiliary antenna. The same technique has been used by the same authors in [57] to cancel cross-polarization interference when both signals are M-QAM.

1.2.2.3 CDMA Systems

In this section, we focus on direct sequence CDMA (DS-CDMA) because it is the most widely used CDMA scheme for cellular mobile radio systems. In CDMA a desired user signal is subject to both intercell and intracell interferences. In single-user detection [58] (conventional receiver) all user signals from the current cell, except for the desired one, are considered as noise and treated correspondingly in the receiver. The performance of single-user receivers is largely inhibited by interference as well as the near-far problem. Other alternative receivers are those which use joint detection of all the users (multiuser detection) or interference cancelling.

To the knowledge of the author, the first references of multiuser CDMA detection are [59], [60] and [61]. A symbol by symbol receiving scheme, using the output from a bank of matched filters (matched to all users' spreading codes) was derived by Schneider in [60] and [61] to suppresses the effect of the nonorthogonal multiple access interference in a DS/CDMA system. This receiving scheme can individually minimize each error covariance between the information and the estimates produced by the receiver. The fundamental characteristic of the scheme is that performance is independent of the energies from the multiple access interferes. Kohno et. al. [59] and Schneider [60] indicated how the optimum receiver for simultaneous detection of all users in an asynchronous system can be implemented. The optimum maximum likelihood receiver for simultaneous detection of all the users was analysed by Verdu [62]-[63]. He also simulated this receiver as a multiuser generalization of the Viterbi algorithm which was first presented by Schneider in [60].

The significant theoretical steps in analysing the structure and complexity of optimal receivers [59]-[63] triggered new research efforts on sub-optimal algorithms. In [64]-[72], suboptimum receivers were analysed which tried to reduce the detection complexity without significant performance degradation with respect to the optimum performance.

Lupas and Verdu [66], proposed a near-far resistant asynchronous sub-optimum receiver, called a *decorrelating receiver,* which is independent of the signal to interference ratio. The detection process in this receiver is performed in a subspace orthogonal to the space spanned by the interference. A similar decorrelating receiver had been previously proposed by Schneider in [60] for the synchronous case. A family of suboptimum interference resistant detectors, consisting of a linear transformation followed by a set of threshold devices, was suggested by Xie *et al.* in [71]. They used two different performance criteria; weighted least-square (WLS) and minimum mean squared error (MMSE). The receiver, based on the WLS has the same structure as the decorrelating receiver. They followed up their work by investigating parameter estimation in [73] and joint detection and parameter estimation in [72]. In [72], a recursive least-squares (RLS) multiuser parameter estimator along with a sub-optimum tree-search algorithm are used to obtain a performance close to that of the joint ML receiver. A class of synchronous CDMA multiuser receivers, designed to cope with mobile channel variations, were proposed in [74]-[77]. These receivers were mainly extensions of the decorrelator receiver which include knowledge of the signal channel. In [76] and [77], the signals were assumed to be Rayleigh faded, while in [74] and [75], the fading was assumed to be Rician.

Successive (serial) interference cancelling has been studied in [68]-[69] and [78]-[81], while the parallel interference canceller has been addressed in [69]. The successive interference canceller (SIC) has a simple structure which cancels a user's interference at a successive cancellation rate in order of the received powers. It requires high speed hardware to process the total number of active users within a bit interval. On the other hand, for parallel interference cancelling (PIC), all the interfering signals are detected simultaneously. Despite the fact that PIC does not need high speed hardware, it requires a multistage of the same hardware set, which increases the hardware complexity. Furthermore, the performance of PIC degrades when the power of the received signals is widely spread, (as in the case of fading channels) since the detectors for the weak users participate in the cancellation with the corrupted estimates (such as channel parameters and bit decision). An adaptive hybrid serial/parallel interference cancellation is proposed by Kim et. al. [82] which has the same structure as the adaptive SIC scheme except that it performs the addition of the regenerated signal to each detector. It is shown that this scheme outperforms SIC and PIC. The cancelling of an antipodal co-channel interference for a single-user receiver has been studied by Hagerman [83]. Two different scenarios, are with complete knowledge about the co-channel interference channel and the other with only the knowledge about interference energy, were investigated.

1.2.2.4 CCI Cancelling Using Spectral Correlation

Analog and digital carrier modulated signals, such as AM, digital QAM. PSK and frequency shift keying (FSK), exhibit correlation among their spectral components [84]-[86]. That is, spectral components in some bands are highly correlated. This spectral redundancy can be exploited by employing frequency-shifting operations, as well as the usual frequency weighting and phase shifting operations performed by conventional filters, to obtain substantial interference rejection with minimal signal distortion. The results of the study to evaluate the performance capabilities of optimum and adaptive frequency-shift (FRESH) filters for digital communication were presented in [87]-[89]. It was shown by both numerical performance evaluation and limited simulation that severe co-channel interference can be removed from a signal, and that severe frequency-selective fading can be mitigated without substantial noise amplification. These results show that the effective separation of two BPSK or QPSK signals, regardless of the relationship between their carrier frequencies and baud rates, is possible, provided that for QPSK a 100% additional bandwidth is allowed. It is also proved that L individual PSK or digital QAM signals with equal baud rates, but arbitrary carrier frequencies, can be separated if their excess bandwidth is at least (L-1)100%.

1.2.2.5 Interference Cancelling With Adaptive Antennas

Techniques like space diversity have been shown to be beneficial in improving the tolerance of a receiver to co-channel interference by exploiting the uncorrelatedness of the fading upon both desired and interfering signals at different antennas. Diversity combining techniques that explicitly account for the presence of interference have been developed [90]-[91]. More recently, techniques that exploit the angular separation of wanted and interfering signals, using adaptive antennas, have been considered [92]-[96]. The basic operation of adaptive antenna (or smart antenna) is for the antenna pattern to have a maximum gain in a desired look direction and to place nulls in the undesired directions. Different proposed diversity combining algorithms have been proposed. Among them least mean square algorithm (LMS) [97]-[98] has the minimum computational complexity, but its rate of convergence is slow. A variation of LMS is the so called "Decision Directed

Algorithm (DDA)" [98], [99], also suffers from the same limitations. Singular Value Decomposition (SVD) based method [100] (which is also an extension of LMS) seems to have a rapid convergence.

The "Direct Matrix Inversion (DMI)" method [98], on the other hand has the fastest convergence rate, but involves very heavy computational load. Both LMS and DMI need a reference signal to identify the desired signal source. In contrast, blind steering algorithms do not need any reference signal. Constant modulus algorithm (CMA) [101]-[103] is a blind steering algorithm based on maintaining the average modulus of the array outputs. Although CMA has performed well in some cases [101], it may acquire and track the interfering signals rather than the desired one. Another blind steering algorithm, called spectral coherence restoral (SCORE), is based on cyclostationary property of same modulation schemes [104]. However, SCORE suffers from limitations such as slow convergence and high complexity.

1.2.3 Effect of CCI on Timing Recovery

Almost all the mentioned interference cancelling techniques have been studied under the assumption of an ideal timing recovery. The validity of this assumption is addressed by a number of authors who have investigated bit synchronization in the presence of CCI [105]-[107]. In [105], Carruthers et. al. used time domain digital simulation to study bit synchronization of QPSK in the presence of CCI in static channels (i.e. without fading effect). Two synchronization strategies: squarer/bandpass filter and Data-Aided timing recovery circuit were considered. Their study showed that it is possible to achieve bit synchronization circuits in the presence of a strong co-channel interferer. This study showed that the data-aided bit synchronizer outperforms non-data-aided bit synchronizer at the cost of a higher complexity. The impact of the number of interferers and their synchronization with desired signal was also investigated. It was also shown that a single interferer has less deteriorating effect on the BER performance than multiple interferers. The synchronization between interferers and the desired signal can also improve the performance of the synchronizer. Paranchych et. al. in [106]-[107] analysed the performance of a digital symbol synchronizer under co-channel interference using Markov chain modelling. They followed the analysis of bit synchronizer by Payzin [108] in the presence of AWGN. This analysis uses the fact that if a synchronizer advances or retards its timing phase by a fixed amount at T/M, its behaviour may be modelled as random walk with M states. They indicated that the effect of CCI can be accounted for in a Markov chain model without increasing the number of required states. Again, as in [105], static AWGN and CCI channel was assumed. The result of this analysis reveals that even under severe interference, bit timing error can be reduced by increasing the number of states.

1.2.4 Performance Evaluation of Cellular Radio Systems

Performance evaluation of cellular radio systems in CCI has been considered by numerous authors. A parameter sometimes used to evaluate this performance is the average signal to average interference ratio produced at the corner of a coverage area [109]. A more definitive parameter is the expected probability that the signal to interference ratio is below some acceptable level known as protection ratio. This probability (also known as the probability of interference) depends on parameters such as cellular system layout and propagation model within the cell. The protection ratio can be determined by field tests based on the quality of reception [110]. Parameters such as type of modulation scheme, application of interference prevention and cancelling techniques in the cellular systems greatly affect the selection of protection ratio. Outage probability, which may also take traffic and available channels into account, is also of interest in the evaluation of the performance of cellular systems. Propagation model is one of the major factors in calculating the outage probability. For the large or medium size cells, Rayleigh fading or superimposed Rayleigh and log-normal shadowing are reasonable models. On the other hand, for microcellular systems, an interfering signal from a distant co-channel cell may well be modelled by Rayleigh statistics. However, because of a line-of-sight path, Rician fading model is more appropriate for the desired signal [111]-[112]. Among different fading models, Nakagami is the most versatile [113] one. Nakagami distribution not only takes both Rician and Rayleigh distributions as special cases but also approximates log-normal distribution [113]-[114] very well and fits experimental data better than Rayleigh, Rician or log-normal in many cases [113]- [115].

A review of literature on the performance of cellular systems in CCI is now presented as follows. Wojnar in [116] computed the outage probability in the presence of a single Nakagami interferer. French in [117] considered the problem of co-channel interference for Rayleigh fading and log-normal shadowing with one interferer present at any time. Cox in [109], Yeh and Schwartz in [118] and Safak in [119] studied outage probabilities due to multiple log-normal interferers. Muammar and Gupta in [120] used a model that takes the six closest surrounding interferers into consideration and approximates the distribution of the sum of their amplitudes by a normal distribution for the case of Rayleigh fading alone. A log-normal distribution approximation was used for the case of both Rayleigh fading and log-normal shadowing. Sowerby and Williamson in [121] and Williamson and Parsons in [122] considered the problem of outage in the presence of multiple Rayleigh interferers with log-normal shadowing. In [123] and [124], Sowerby and Williamson calculated outage probability when a Rayleigh fading model, a minimum signal requirement, and multiple independent interferers were considered. In [125] and [126], the desired signal is assumed to have Rician statistics and interferers from co-channel cells are assumed to be subject to Rayleigh fading because of the absence of line-of-sight propagation. Abu-Dayya and Beaulieu in [127] and Yao and Sheikh in [128] investigated interference probabilities in the presence of similar and different Nakagami interferers. The case of both Nakagami fading and log-normal shadowing was also studied in [127]. In [129], Tallambura and Bhargava have extracted an expression for the probability of outage with the assumption of multiple Nakagami interferer and desired signal with arbitrary Nakagami fading parameter.

1.3 Scope of the Thesis

The objective of the work in this thesis is to investigate detection of signals in the presence of co-channel interference. A narrowband mobile communication channel is targeted in which the CCI has the same modulation, bit rate and frequency band as the desired signal. The main attention will be paid to the design of receivers which can detect data without much dependence on the knowledge of interference. This eliminates parameter estimation for interference and thus reduces the complexity of the receiver. The main advantage which can be obtained, however, is ability to cancel nonorthogonal interferers. This ability does not exist in the conventional CCI cancelling techniques [47]-[50] which mainly rely on some kinds of orthogonality between interference and desired signals for interference separation and cancellation. For instance, DS/CDMA [68]-[81] assumes orthogonal spreading codes for desired signal and interference. In spatial interference cancelling using adaptive arrays [90]-[104], only those interferences coming from a separate angle from desired signal can be cancelled.

To achieve this goal, a novel interference cancelling concept, known as indirect co-channel interference cancelling (ICIC), will be presented which relies only on the constant modulus property of the applied modulation scheme. Although the concept can be applied to any modulation schemes with constant modulus property, it has been exclusively applied to constant envelope modulation scheme. Based on this concept, several CCI cancelling structures are proposed. GMSK as one of the popular constant envelope modulation schemes is adopted to test the performance of the proposed CCI cancellers. The complexity reduction is targeted in two areas: channel estimation and cancellation. By application of ICIC to constant envelope modulation schemes, there is no need to obtain any information about the channel and timing of CCI. This will reduce channel estimation complexity by 50% compared with a corresponding optimum CCI canceller. The cancellation complexity can be reduced due to the fact that there is no need to generate a replica of co-channel interference. A major limitation of ICIC is that it only cancels one co-channel interference, which makes it more suitable for channels with potentially one co-channel interferer or the channels in which the probability of a dominant co-channel interferer is very high. Examples of such channels are: sectorized cells, dual-polarized communication systems, and adaptive antennas. Furthermore, ICIC can reduce one cancellation stage when it is combined with conventional multiple CCI cancellers. However, this possibility is not studied in this thesis.

The performance of the designed interference canceller will be investigated in Rayleigh fading channels with one dominant co-channel interferer by using Monte Carlo simulation. The other possible interferers and noise will be modelled as AWGN. Some of the possible difficulties in practical implementation will be investigated in terms of sensitivity to practical errors such as those in channel estimation, delay spread, symbol synchronization, and hard limiting. The BER performance of the proposed interference canceller will be investigated with pilot symbol aided channel estimation. The BER performance analysis will be carried out on one of the proposed interference cancellers.

The thesis is organized as follows. First in Chapter 2, the ICIC concept is presented and four different receiver structures are introduced. The BER performance of the proposed receivers are studied in different channels. In Chapter 3, the parameters affecting the BER performances of the ICIC receiver with sequential estimation are investigated. Chapter 4 introduces the pilot symbol aided channel estimation and co-channel interference cancelling for GMSK modulation schemes. In Chapter 5, BER performance of bit-by-bit ICIC in AWGN channel is analysed. Finally, Chapter 6, discusses the results and proposes some potential research topics.

Chapter 2

Indirect Co-channel Interference Cancelling

In this chapter a novel interference cancelling concept, ICIC, is presented. Based on this concept, several receiver structures are proposed which are suitable for detection of CPM schemes such as minimum shift keying (MSK), GMSK [27], tamed frequency modulation (TFM) [130], filtered QPSK (FQPSK) [132], Asynchronous raised cosine FSK (ARC-FSK) [131] and others. The main advantage of these cancellers is that they do not need any information about the channel characteristics or timing of the interferer and therefore can be categorized as blind cancellers. The proposed receiver structures are suitable for cancelling of only one co-channel interferer.

2.1 Concept

The most straightforward approach to cancel co-channel interference is to generate a replica of the co-channel interference and subtract it from the received signal. To do this, additional hardware is required to identify the co-channel signal parameters.

These parameters are symbol, timing information, and channel characteristics. The accuracy of this information is poor because of the jamming effect of the desired signal, which is often considerably larger than the interference signal. An alternative method is blind CCI cancelling which has no requirement to completely identify the co-channel signal. The method proposed in this thesis, *ICIC*, is such a method. The method uses the constant envelope property of the modulation scheme to cancel the co-channel signal and therefore, its application is restricted to CPM schemes.

In ICIC, a replica of the desired signal, $\hat{w}_i(t)$, is regenerated and subtracted from the received signal, $r(t) = w(t) + i(t)$, to leave a residue, $\varepsilon_i(t)$, consisting of the co-channel signal, $i(t)$, and the estimation error $(w(t) - \hat{w}_i(t))$

$$\varepsilon_i(t) = [w(t) - \hat{w}_i(t)] + i(t) \tag{2.1}$$

If the desired signal is correctly estimated, the residue $(\varepsilon_i(t) = i(t))$ will have a constant envelope (Fig. 2.1). On the other hand, if the estimate is not correct, the residue, $(\varepsilon_i(t) \neq i(t))$ will have a varying envelope. By comparing these two different situations, the receiver can identify the correct signal and subsequently detect the data symbols.

In the proposed receiver, shown in Fig. 2.2, all the possible shapes of the desired signal (estimates) are regenerated and cancelled from the received signal. With ideal timing and channel information (and in the absence of noise) one of the residue signals will have constant envelope. A metric can be defined to detect this constant envelope and identify the correct waveform.

By requiring complete knowledge of amplitude, phase and timing characteristics of the desired signal does not involve additional complexity, because these features are required for conventional receivers.

2.2 System Analysis

In the mobile communication system, shown in Fig. 2.3, the desired signal is transmitted over a Rayleigh fading channel. A constant envelope modulated co-channel interferer, assumed to be dominant among all the other co-channel interferers, passes through an independent fading channel and interferes with the desired signal. AWGN and other interference sources are shown by the signal, $N(t)$. Furthermore, the desired signal and its CCI are assumed to have the same bit rate and modulation specifications. Since the CCI canceller operates in the baseband, the received signal is converted to baseband with a quadrature demodulator.

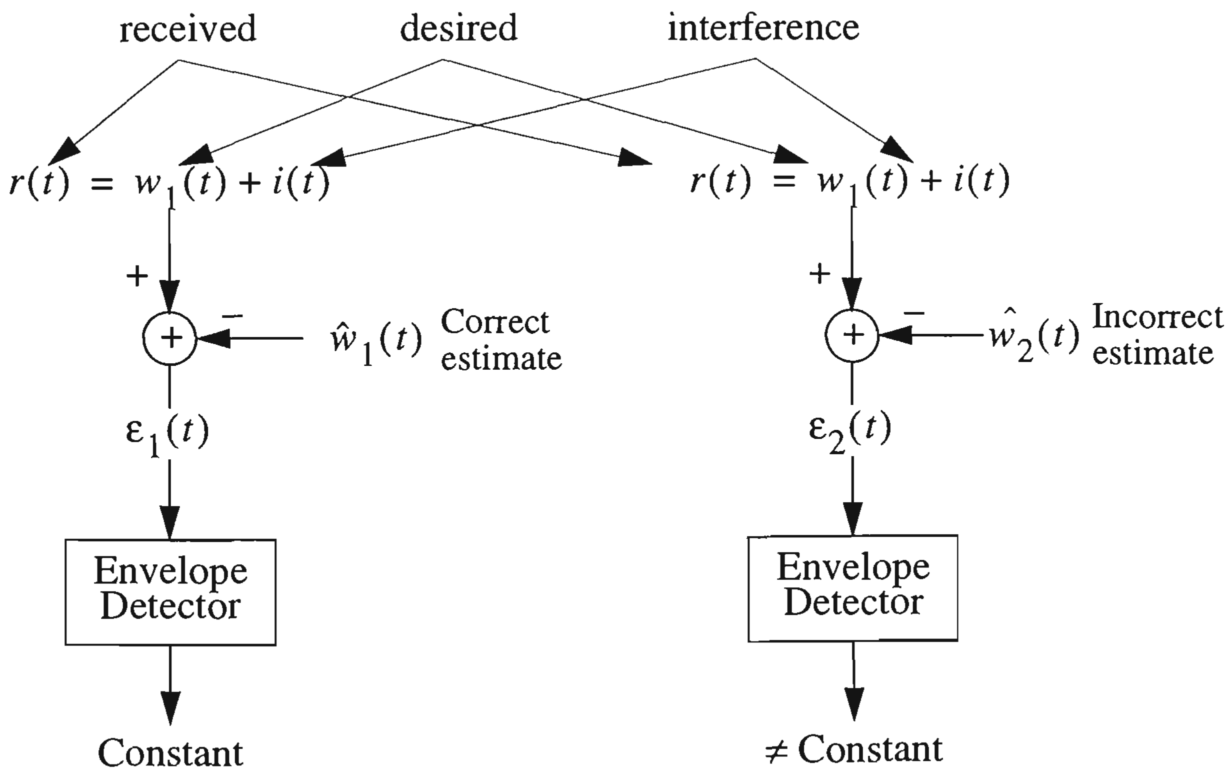

Fig. 2.1. The correct and incorrect estimation in indirect co-channel interference cancelling.

The received RF signal, comprising of the desired signal, AWGN and a dominant interference signal, can be expressed as

$$R(t) = 2A\cos[2\pi f_c t + \Phi(t)] + 2B\cos[2\pi f_c t + \Theta(t)] + N(t) \qquad (2.2)$$

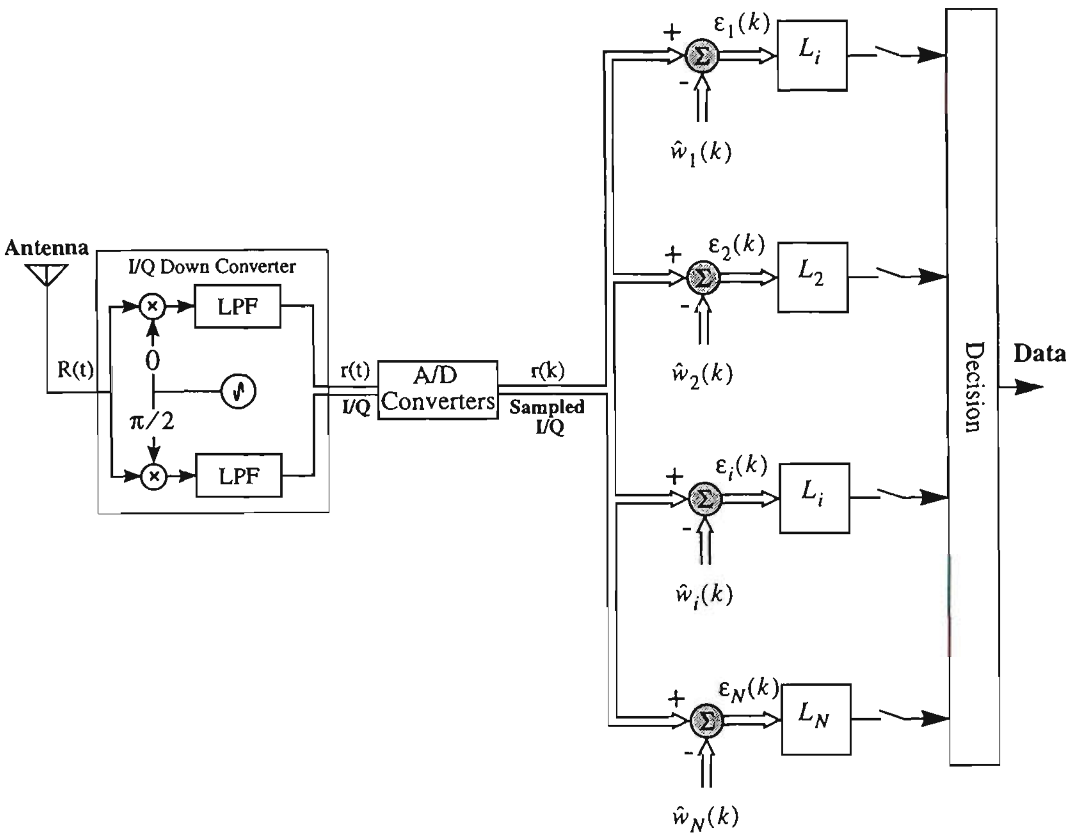

Fig. 2.2. Block diagram of the ICIC receiver.

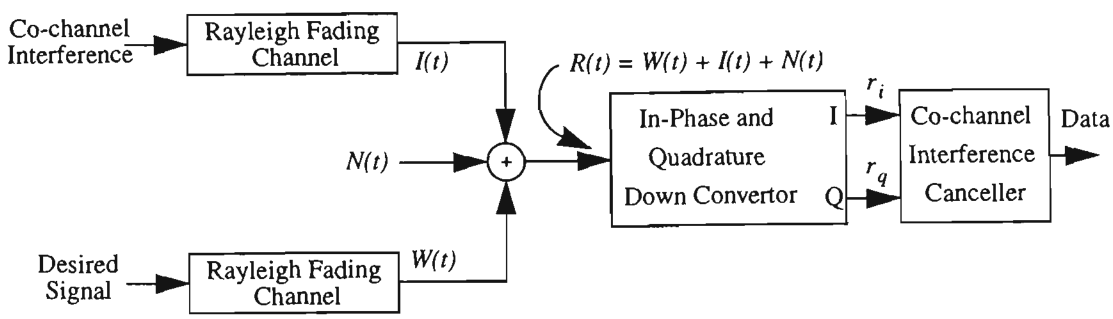

Fig. 2.3. A model of a mobile communication channel with one dominant co-channel interferer.

where $2A\cos[2\pi f_c t + \Phi(t)]$, $2B\cos[2\pi f_c t + \Theta(t)]$ and $N(t)$ denote the desired signal, CCI and the band limited noise respectively. Here, $\Phi(t)$ and $\Theta(t)$ are the data information. Multipath fading affects the carrier phase and amplitudes of both the desired and CCI signals. However, in high bit rates, these can be assumed constant over one bit interval (The validity of this assumption will be discussed in Section 3.4). The in-phase and quadrature components of the received signal after sampling are

$$\begin{cases} r_i(k) = A(k)\cos\Phi(k) + B(k)\cos\Theta(k) + n_i(k), & \text{in-phase} \\ r_q(k) = A(k)\sin\Phi(k) + B(k)\sin\Theta(k) + n_q(k), & \text{quadrature} \end{cases} \tag{2.3}$$

where $r = r_i - jr_q$, $n_i(k)$, $n_q(k)$ are in-phase and quadrature components of the band limited Gaussian noise. The sampling rate is m samples per data symbol. The possible desired signal estimates, $\{\hat{w}_i(k)\}$, $i = 1, 2, \ldots, N$, produced by a waveform generator, are subtracted from $r(k)$ to form the residue, $\varepsilon_i(k)$. This is followed by the processing which selects the most probable signal candidate as the decision output. In constant envelope modulation schemes, the zero variance of the residue envelope can be used to identify the correct estimate. The envelope of the residue is

$$\begin{aligned} M_i(k) &= |\varepsilon_i(k)| \\ &= |r(k) - \hat{w}_i(k)| = \sqrt{[r_i(k) - C\cos\Psi_i(k)]^2 + [r_q(k) - C\sin\Psi_i(k)]^2} \end{aligned} \tag{2.4}$$

where $\hat{w}_i(k) = Ce^{j\Psi_i(k)}$. To avoid the complexity of the square root operation,

$M_i^2(k)$ can be used instead of $M_i(k)$. One method of detecting envelope variation is to use a cost function (metric) equal to the variance of M_i^2 over a single bit interval

$$L_i = Var(M_i^2(k)) = \frac{1}{m}\sum_{k=0}^{m}\left|M_i^2(k) - \overline{M_i^2}\right|^2 \tag{2.5}$$

where $\overline{M_i^2} = \frac{1}{m+1}\sum_{k=0}^{m} M_i^2(k)$. The coefficient $\frac{1}{m}$ can be disregarded because it is identical for all the pulse shapes.

An alternative simplified cost function based on (2.5) is

$$L_i = \sum_{k=0}^{m}\left|M_i^2(k) - \overline{M_i^2}\right| \tag{2.6}$$

This is shown to have similar performance to (2.5) in Appendix A.

Although the cost function (2.6) seems to be similar to the cost function of CMA algorithm[1] [133], there are several differences between them which are:

1- CMA, uses a constant modulus desired signal while in ICIC only the co-channel signal must have a constant modulus.

1.The cost function of CMA algorithm at the i^{th} sampling time for a received signal x and a finite channel impulse response can be explained as: $e = \sum_{k=0}^{m}\left||\hat{h}(k)x(i-k)|^p - 1\right|^q$ where $\hat{h}(k)$ is estimated channel impulse response, p and q are integer values.

2- CMA directly uses the received signal to calculate cost function while the ICIC requires the difference between the received and the desired signal estimates.

3- CMA employs the cost function to update the filter impulse response. While ICIC exploits the cost function to decide the best possible estimate of the desired signal from which the transmitted data bit can be detected.

2.2.1 Criteria for Minimization of Cost Function

The following section analyses the conditions that minimize (2.6).

Lemma: Equation

$$\sum_{k=0}^{m}\left|x(k)-\frac{1}{m+1}\sum_{j=0}^{m}x(j)\right| = 0 \tag{2.7}$$

is a homogenous system with a trivial solution

$$x(0) = x(1) = \ldots = x(m) = 0 \tag{2.8}$$

and a non-trivial solution

$$x(0) = x(1) = \ldots = x(m) \tag{2.9}$$

Proof: Since (2.7) is a summation of absolute values, the only condition that results in zero is that all of the terms be simultaneously equal to zero

$$x(k) - \frac{1}{m+1}\sum_{j=0}^{m} x(j) = 0 \qquad k = 0, \ldots, m \tag{2.10}$$

The system of linear equations (2.10) is a *homogeneous* system with $m+1$ unknowns and $m+1$ equations which always has a solution [134]. One of the solutions is obtained by letting $x(k) = 0$ (trivial solution)

$$x(m) = \ldots = x(1) = x(0) \tag{2.11}$$

The other solution is a non-trivial solution such that $x(k) \neq 0$. To obtain the non-trivial solution (2.10) can be rearranged as

$$\begin{cases} mx(0) - x(1) - \ldots - x(m) = 0 \\ -x(0) + mx(1) - \ldots - x(m) = 0 \\ \qquad \ldots \\ -x(0) - x(1) - \ldots + mx(m) = 0 \end{cases} \tag{2.12}$$

By subtraction of the second row from the first row we have $x(1) = x(0)$ and continuing this by subtraction of other rows from the first row gives $x(m) = \ldots = x(1) = x(0)$. In this system of equations the trivial solution is a special case of the non-trivial solution.

Proposition: If the co-channel interference has constant envelope and the desired signal estimate is equal to the received signal, the value of (2.6) is a minimum.

Proof:

Substituting (2.3) into (2.4) results in

$$\begin{aligned} M_i(k)^2 &= B^2(k) + A^2(k) + C^2(k) + 2A(k)B(k)\cos[\Theta(k) - \Phi(k)] \\ &\quad -2C(k)B(k)\cos[\Theta(k) - \Psi_i(k)] - 2A(k)C(k)\cos[\Phi(k) - \Psi_i(k)] \end{aligned} \tag{2.13}$$

Since the interference is assumed to have constant envelope for all k's, $B(k)$ is constant (i.e. $B(k) = B$). For simplicity of analysis, the noise component of the received signal is not considered. With the assumption that $C(k) = A(k)$ for all k values, (2.13) can be written as:

$$\begin{aligned} M_i^2(k) &= B^2 + 4A(k)B\sin\left[\Theta(k) - \frac{\psi_i(k) + \Phi(k)}{2}\right]\sin\left[\frac{\Phi(k) - \psi_i(k)}{2}\right] \\ &\quad + 4A^2(k)\sin^2\left[\frac{\Phi(k) - \psi_i(k)}{2}\right] \end{aligned} \tag{2.14}$$

Substituting (2.14) into (2.6) yields

$$\begin{aligned} L_i = \Bigg| &\sum_{k=0}^{m} 4A(k)\sin\left[\frac{\Phi(k) - \psi_i(k)}{2}\right]\left\{A(k)\sin\left[\frac{\Phi(k) - \psi_i(k)}{2}\right] + B\sin\left[\Theta(k) - \frac{\psi_i(k) + \Phi(k)}{2}\right]\right\} \\ &- \frac{1}{m+1}\sum_{k=0}^{m} 4A(k)\sin\left[\frac{\Phi(k) - \psi_i(k)}{2}\right]\left\{A(k)\sin\left[\frac{\Phi(k) - \psi_i(k)}{2}\right] + B\sin\left[\Theta(k) - \frac{\psi_i(k) + \Phi(k)}{2}\right]\right\}\Bigg| \end{aligned} \tag{2.15}$$

Since $L_i \geq 0$, the lower bound for the minimum of L_i is zero. From the Lemma, the only condition which makes (2.15) zero is

$$4A(k)\sin\left[\frac{\Phi(k)-\psi_i(k)}{2}\right]\left\{A(k)\sin\left[\frac{\Phi(k)-\psi_i(k)}{2}\right]+B\sin\left[\Theta(k)-\frac{\psi_i(k)+\Phi(k)}{2}\right]\right\}$$
$$-\frac{1}{m+1}\sum_{k=0}^{m}4A(k)\sin\left[\frac{\Phi(k)-\psi_i(k)}{2}\right]\left\{A(k)\sin\left[\frac{\Phi(k)-\psi_i(k)}{2}\right]+B\sin\left[\Theta(k)-\frac{\psi_i(k)+\Phi(k)}{2}\right]\right\}=0 \tag{2.16}$$

The trivial solution for (2.16) has the form

$$4A(k)\sin\left[\frac{\Phi(k)-\psi_i(k)}{2}\right]\left\{A(k)\sin\left[\frac{\Phi(k)-\psi_i(k)}{2}\right]+B\sin\left[\Theta(k)-\frac{\psi_i(k)+\Phi(k)}{2}\right]\right\}=0 \tag{2.17}$$

Equation (2.17) can be satisfied if

$$A(k) = 0 \tag{2.18}$$

or

$$\sin\left[\frac{\Phi(k)-\psi_i(k)}{2}\right]=0 \quad\Rightarrow\quad \psi_i(k) = \Phi(k)\pm 2\pi n \tag{2.19}$$

or

$$A(k)\sin\left[\frac{\Phi(k)-\psi_i(k)}{2}\right]+B\sin\left[\Theta(k)-\frac{\psi_i(k)+\Phi(k)}{2}\right] = 0 \tag{2.20}$$

Equation (2.18) implies no reception of the desired signal and naturally detection is impossible. Equation (2.19), shows that in a special case ($n = 0$) where the phase of the pulse shape is equal to the phase of received desired signal, L_i will be minimum (zero). The $2\pi n$ rotation cannot affect the shape of the pulses, because the in-phase and quadrature components of the pulse shapes are either $\sin[\psi_i(k)]$ or $\cos[\psi_i(k)]$. As a result, the waveforms with the same shape as the desired signal can minimize L_i.

Equation (2.20) shows a rare but possible condition that L_i might be minimized. It can be held if $\psi_i(k)$ satisfies (2.20) for all k values during one bit period. The chance of simultaneous holding of (2.20) for all the k values is poor because A, B, Φ and Θ are independent and their values change during the bit interval. The same condition applies for the non-trivial solution. The non-trivial solution for (2.16) can be found from (2.11) in which

$$x(k) = 4A(k)\sin\left[\frac{\Phi(k)-\psi_i(k)}{2}\right]\left\{A(k)\sin\left[\frac{\Phi(k)-\psi_i(k)}{2}\right]+B\sin\left[\Theta(k)-\frac{\psi_i(k)+\Phi(k)}{2}\right]\right\}. \qquad (2.21)$$

The non-trivial solution can only be held if $x(k)$ remains constant for all values of k. Although the conditions that satisfy (2.20) and (2.21) rarely occur, it makes the decision process suboptimal.

2.3 Waveform Generation

The ICIC can be applied on a wide range of constant envelope modulation schemes. However, this thesis only concentrates on the application of ICIC on CPM schemes, particularly different types of GMSK. This section describes how the waveform estimates are obtained for GMSK modulation scheme.

A large class of constant envelope modulation schemes can be categorised as continuous phase modulation schemes. In CPM modulation schemes, the RF signal envelope is constant and the phase varies in a continuous manner. The signal has a trellis structure and can be generated with a finite state machine. All CPM signals are described by

$$R(t) = (2E_b/T)^{1/2}\cos[2\pi f_c t + \Phi(t, \alpha)], \qquad nT \le t \le (n+1)T \tag{2.22}$$

where E_b is the signal energy per bit, T is the bit timing interval, f_c is the carrier frequency and the information is embedded in the phase

$$\begin{aligned}\Phi(t, \alpha) &= 2\pi h \sum_{i=-\infty}^{n} \alpha_i q(t - iT) = \theta(t, n) + \theta_n \\ &= 2\pi h \sum_{i=n-L+1}^{n} \alpha_i q(t - iT) + \pi h \sum_{i=-\infty}^{n-L} \alpha_i\end{aligned} \tag{2.23}$$

The data $\{\alpha_n\}$ are M-ary data symbol, where M is even and is taken from the alphabet ± 1, ± 2, ..., $\pm(M-1)$; h is a modulation index, which may vary from interval to interval, but here it is considered to be constant over all intervals; $q(t)$ is the phase response function. CPM schemes are denoted by their phase response function, $q(t)$, or by their derivative $g(t)$, the frequency pulse function. The most important CPM schemes are

MSK- minimum shift keying;

LRC - raised cosine, pulse length *L*;

LSRC- spectral raised cosine, length *L*;

ARC-FSK-asymmetric raised cosine;

LREC- rectangular frequency pulse, length *L*;

TFM- tamed FM;

GMSK- Gaussian-shaped MSK;

The frequency pulse functions of the above schemes are listed in Table B.1 of Appendix B. Among CPM modulation schemes, GMSK has been perhaps the most extensively studied. GMSK has been popular modulation scheme for mobile radio telecommunication applications, because of its excellent spectral properties and simple implementation structure. More importantly, GMSK is being currently used in the Pan-European digital cellular system (GSM) [5] with a bit rate of 271 kbits/s, BT=0.3 and a RF carrier spacing of 200kHz. GMSK with BT=0.5 has also been adopted for the DECT with a data rate of 1.152 Mbits/s and radio channel spacing of 1.728MHz. MSK is a simple CPM modulation scheme and has been well investigated. It is equivalent to GMSK with BT = ∞.

Here, we follow the state description of GMSK using the general state description of CPM modulation schemes given by Anderson et.al. [26], with the restriction of binary signalling.

Using (2.22) and (2.23), and the following properties $q(t) \equiv 0, t < 0$ and $q(t) \equiv \frac{1}{2}, t > LT$, $\phi(t, \alpha)$ is uniquely defined by the present data symbol α_n, the $L-1$ past data symbols (known as correlative states: $\alpha_{n-1}, \alpha_{n-2}, \ldots, \alpha_{n-L+1}$), and the phase state θ_n, where

$$\theta_n = \left[\pi h \sum_{i=-\infty}^{n-L} \alpha_i\right] \text{ modulo } 2\pi \tag{2.24}$$

The number of correlative states is finite and equal to $M^{(L-1)}$. Thus, the total states of the transmitted phase is an L-tuple

$$\delta_n = (\theta_n, \alpha_{n-1}, \alpha_{n-2}, \ldots, \alpha_{n-L+1}) \tag{2.25}$$

There are p different phase states with values

$$\theta_n \in \left\{0, \frac{2\pi}{p}, \frac{4\pi}{p}, \ldots, \frac{(p-1)2\pi}{p}\right\} \tag{2.26}$$

where for a rational modulation index h, p can be found from

$$h = \frac{2k}{p} \tag{2.27}$$

where p and k are arbitrary integers with no common factor.

The current data symbol α_n directs the transition from the state δ_n to the next state δ_{n+1}, and this transition defines the actual function of time that is transmitted. Fig. 2.4 shows a phase tree for the GMSK3 (frequency response pulse is truncated to

$L = 3$) with BT=0.3. In this case there are 16 states and each node in the tree has been labelled with the state $(\theta_n, \alpha_{n-1}, \alpha_{n-2})$. The root node at time $t = 0$ has been arbitrarily given the phase state zero. The state trellis diagram can be derived from Fig. 2.4 by viewing the phase modulo 2π. The 16-state trellis of GMSK3 BT=0.3 is shown in Fig. 2.5. The transition from one state to another is equivalent to a pair of in-phase and quadrature waveforms. Fig. 2.6 shows the in-phase and quadrature eye diagram of GMSK BT=0.3 where phase states are numbered as in Fig. 2.5. Close observation of Fig. 2.6 reveals that states are repeated every $2T$. Therefore, the trellis diagram of Fig. 2.5 can be shown in two separate trellises: one for odd and another for even timing intervals (solid and dashed lines in Fig. 2.5). As a result, the number of waveforms in each timing interval is 16. A numbering strategy for the waveforms (pulse shapes) for subsequent use is shown in Table 2.1.

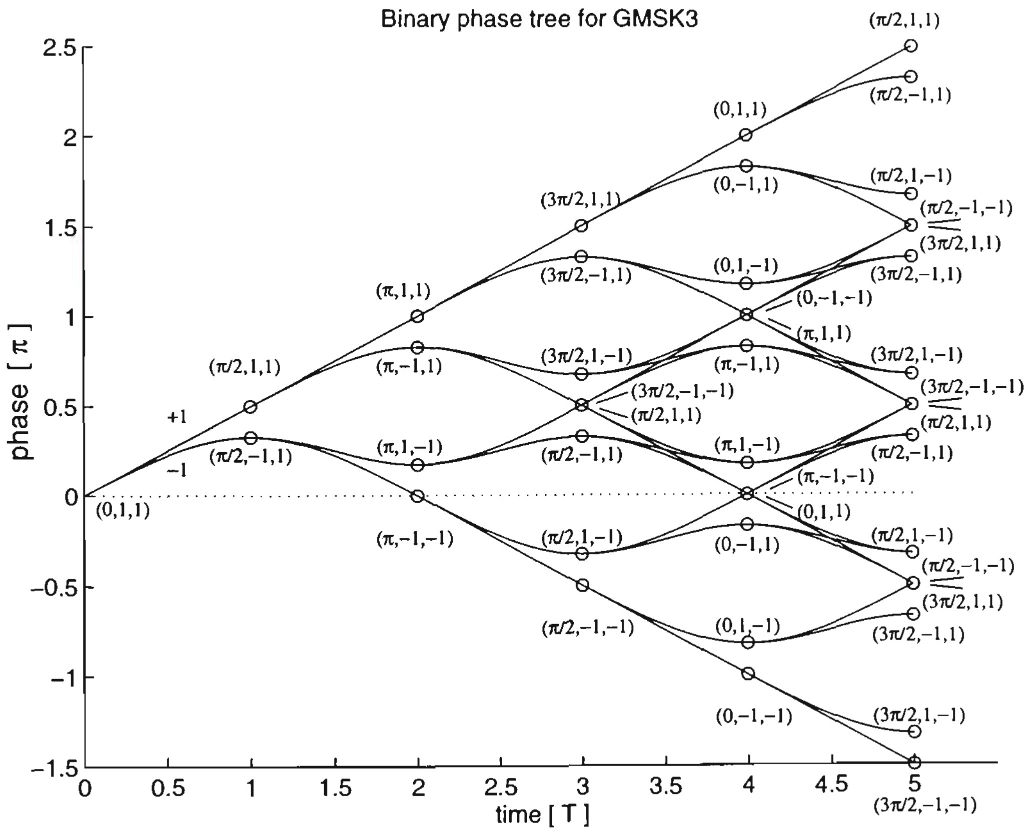

Fig. 2.4. Phase tree for GMSK3 BT=0.3.

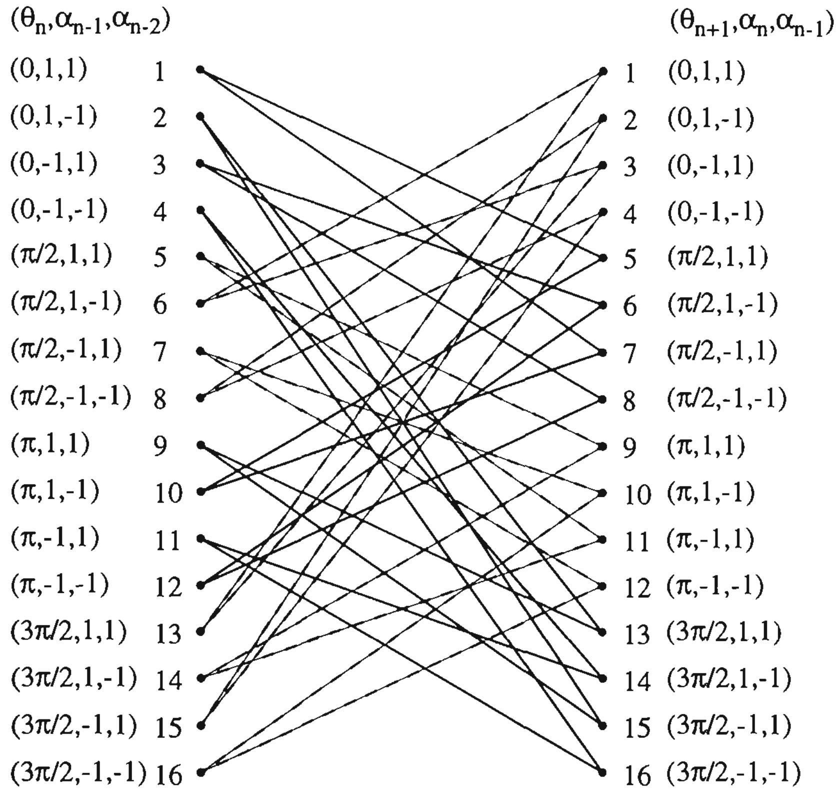

—— odd/even timing intervals
—— even/odd timing intervals

Fig. 2.5. Alternative trellis of GMSK BT=0.3 in odd and even

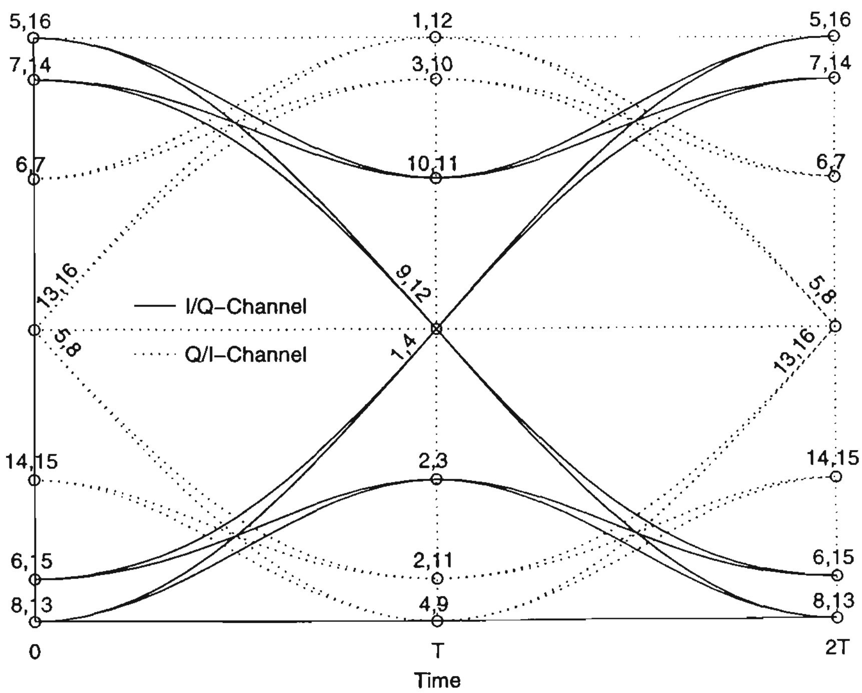

timing intervals.

Fig. 2.6. Eye diagram of GMSK BT=0.3. Phase states are

Table 2.1. States transitions and their corresponding waveforms.

Waveforms (estimates)	State transitions in the first bit interval	State transitions in the second bit interval	Waveform symbol
w1	16⇒12	1⇒5	1
w2	7⇒12	10⇒5	1
w3	14⇒11	3⇒6	-1
w4	5⇒11	12⇒6	-1
w5	16⇒10	1⇒7	1
w6	7⇒10	10⇒7	1
w7	14⇒9	3⇒8	-1
w8	5⇒9	12⇒8	-1
w9	15⇒4	2⇒13	1
w10	8⇒4	9⇒13	1
w11	13⇒3	4⇒14	-1
w12	6⇒3	11⇒14	-1
w13	15⇒2	2⇒15	1
w14	8⇒2	9⇒15	1
w15	13⇒1	4⇒16	-1
w16	6⇒1	11⇒16	-1

In practical applications, the number of waveforms not only depends on the signal phase state, but also depends on the receiver IF-filter bandwidth. Filtering, which is necessary to remove out-of-band noise and also adjacent channel interference, adds additional intersymbol interference to the signal which results in increasing the number of signal states and subsequently the number of waveforms. For instance the number of states in GMSK3 is 16, but when it is filtered in the receiver, the number of states can be increased up to 32. If the filter bandwidth is large enough, the new states are very close to the original nonfiltered states and the change in the states can be ignored to reduce complexity. This ignorance may result in a residual intersymbol interference (RISI) which deteriorates bit error rate performance. The effect of RISI on the BER performance of a conventional coherent receiver is investigated by McLane [135]. He derived the error bound for a truncated state Viterbi detector with the RISI considered as additive interference. The effects of filter type and bandwidth on the RISI, are shown in Fig. 2.7. The frequency responses of these filters is shown in Fig. C.1. The maximally flat filter has less attenuation in the passband and a sharper roll-off in the stopband than the Gaussian filter. Increasing the filter bandwidth or sampling rate reduces RISI. This result shows that on most occasions the maximally flat filter has a better RISI reduction. In this thesis the range of the filter bandwidth is constrained to $0.3<B_bT<0.6$. This limits the additional RISI to less than -33dB and hence, the filtered GMSK BT=0.3 is assumed to have only 16 states.

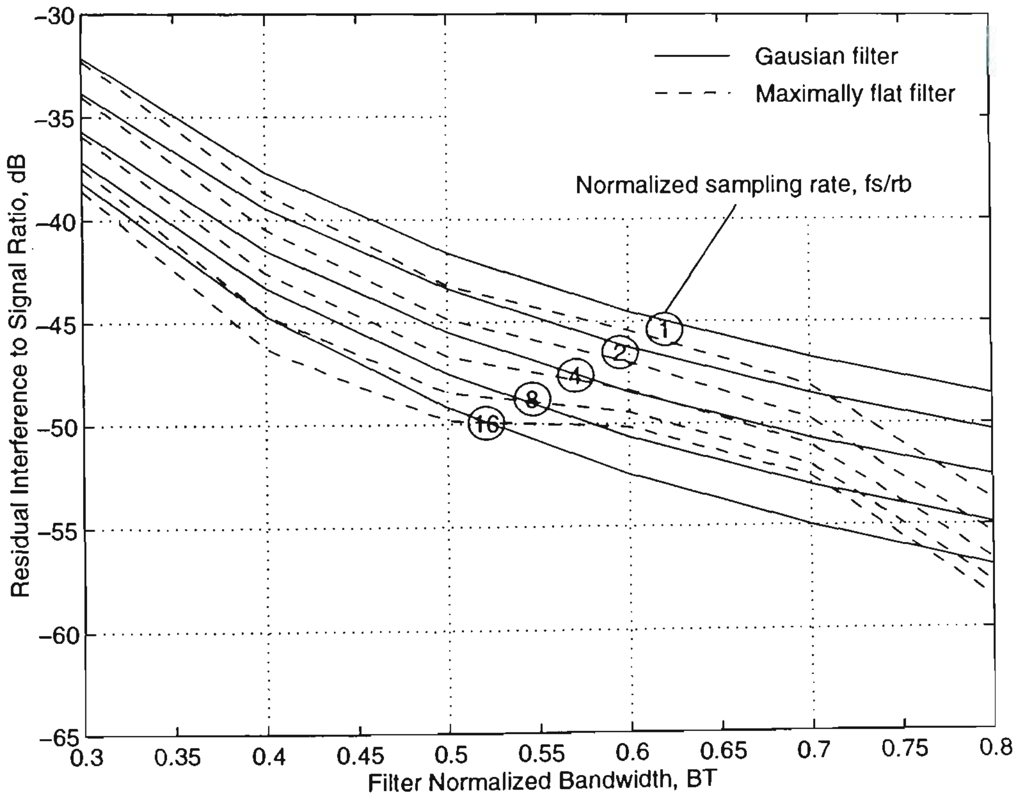

Fig. 2.7. Residual interference to signal ratio with Gaussian and maximally flat filters in different sampling rates.

In maximum likelihood detection, the effect of RISI is very similar to the effect of AWGN because it is an additive interference. The difference between RISI and AWGN is that the AWGN is statistically independent from the desired signal and therefore any change in the signal power does not affect the noise strength. On the other hand, RISI is directly correlated with the signal strength. In conventional coherent detection, RISI can cause irreducible error floor, however, its effect on the ICIC receiver cannot be independently studied, because, it is associated with the envelope distortion introduced by filtering. The envelope distortion will be investigated in the Chapter3.

2.4 Simulation Environment

The complex baseband equivalent model is used to reduce the sampling rate to a multiple of the data rate. The bandpass filters are substituted by equivalent lowpass filters and the bandpass signals are represented by their complex envelopes. The input data is represented by a RBS (random bit sequence). The channel for both desired and CCI signals is Rayleigh with a fading rate of fd=100Hz which is equal to a vehicle speed of 108km/h for a carrier frequency of 1GHz. The multiplicative Rayleigh fading process is generated using the basic quadrature amplitude modulation technique [136] (as shown in Fig. 2.8). A five-pole lowpass filter as introduced by Ball [137] is used to approximate the fade spectrum $S(f) = 1/\sqrt{1-(f/f_d)^2}$. The quadrature noise components, after being filtered, are multiplied by the signal complex envelope to randomly modulate phase and amplitude. AWGN and co-channel interference are then added to the faded signal.

Only one co-channel interferer with independent data sequence, timing and channel characteristics is considered. Moreover it is assumed that the receiver has complete knowledge of the channel and timing of the desired signal. Three modulation

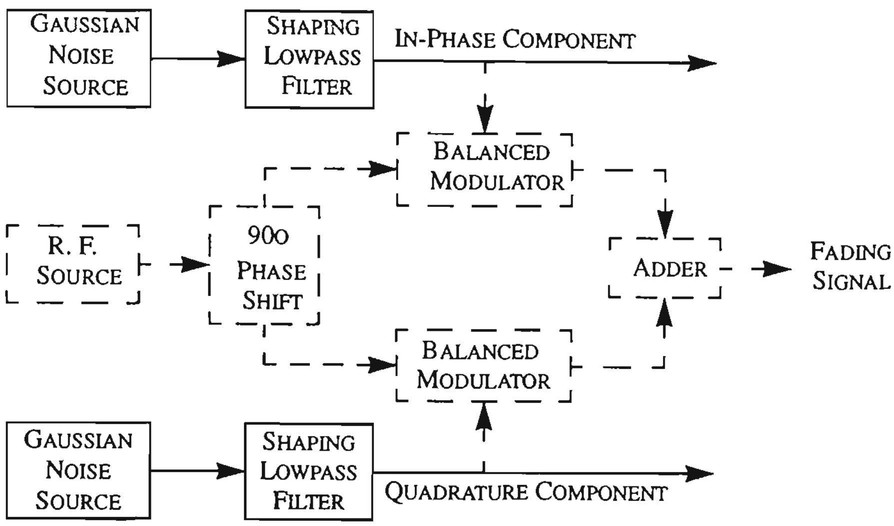

Fig. 2.8. Fading simulator using quadrature amplitude modulation. Only the part shown by solid line has been simulated.

schemes: MSK, GMSK $BT = 0.3$ and GMSK $BT = 0.5$ are used at a data rate of 270 Kbits/s. The phase pulse of GMSK $BT = 0.3$ is truncated to a 3 bit time interval. For analytical purposes, a parallel MSK coherent receiver [26] (or sometimes called conventional coherent receiver) is simulated and its bit error rate performance (BER) is obtained and sketched on the same graph. About 4 million data symbols are simulated for each measurement point to ensure accuracy of the results down to the error probability of 10^{-3}.

An over sampling rate of 16 samples per data symbol has been selected for filtering to avoid aliasing in the spectrum. The sampling rate is reduced to 2 samples per symbol for the interference canceller, due to improved performance (Section 3.1).

2.5 Reference receiver

In this section the two most popular coherent receivers for CPM modulation schemes are compared. One of these receivers is selected as a reference for comparison with the proposed ICIC receivers.

A range of receivers from optimum bit by bit detection [138], optimum Viterbi receivers [26], [139]-[140], serial MSK [141]-[142] and parallel-MSK [26], [143]-[144] have been implemented for detection of CPM schemes. The parallel-MSK receiver (i.e. conventional coherent receiver in some references) is one of the most popular coherent receivers for CPM schemes. This receiver (Fig. 2.9) has only two filters and minimal amount of processing. Although the receiver in general is suboptimum in an AWGN channel, it works well for binary CPM with modulation index $h= 1/2$ [26]. In an AWGN channel (Fig. 2.10), the optimum receiver outperforms parallel MSK by 1dB. In Fig. 2.11, the BER performances of both optimum and parallel MSK receivers are shown in the presence of a single interferer in a Rayleigh fading channel without noise. In addition, their performances in the presence of only noise is shown on the same graph. In the presence of interference, the performance of optimum receiver is 2dB worse than its performance with noise. Since the sum of a large number of interferers has Gaussian statistics [32], the performance of the optimum receiver improves when increasing the number of interferers. On the other hand, the parallel MSK has similar performances in the presence of noise or a single interferer. It outperforms the optimum receiver by 1.5dB in the presence of a single interferer. A similar result can be obtained in combined single CCI and AWGN (Fig. 2.12). As a result of this study, the parallel MSK

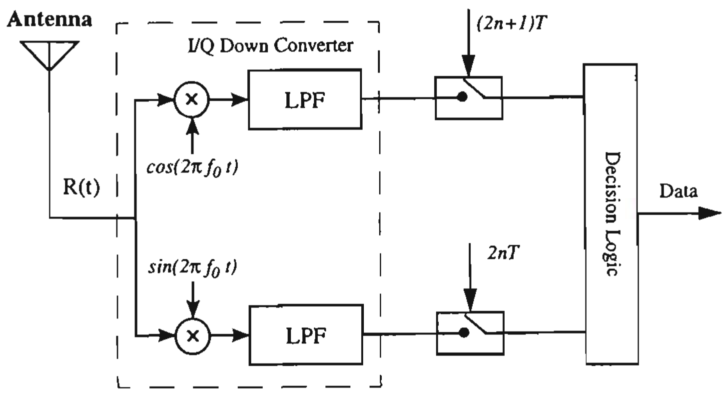

Fig. 2.9. Parallel MSK-type receiver for CPM

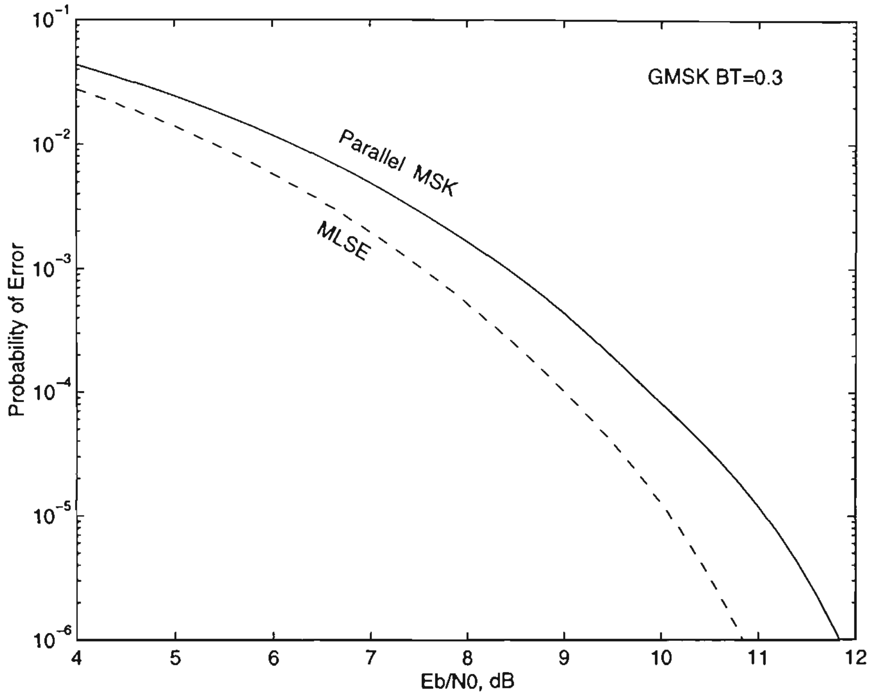

Fig. 2.10. BER performance of maximum likelihood and parallel MSK receivers in AWGN channel for GMSK BT=0.3

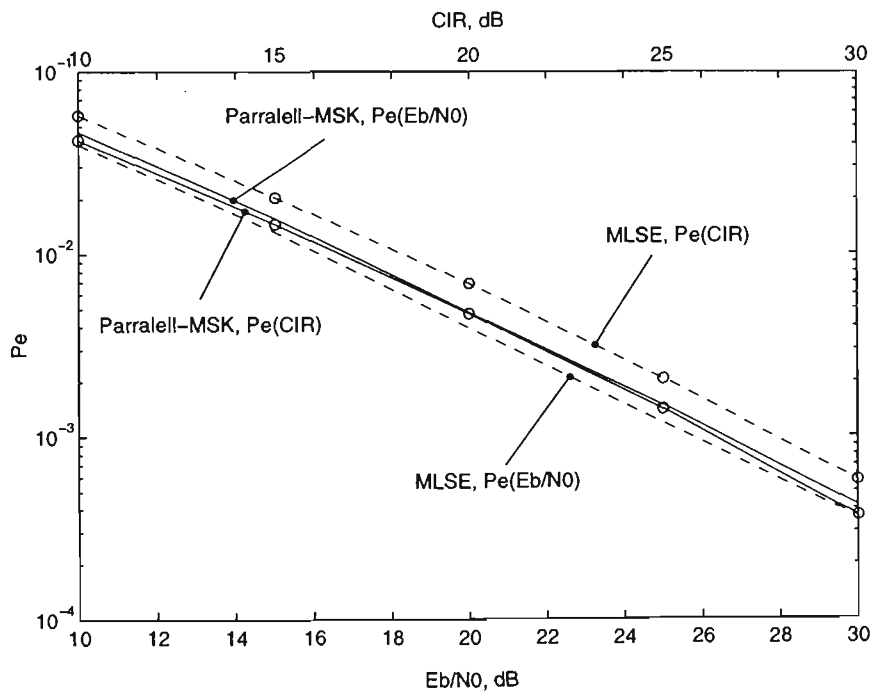

Fig. 2.11. BER performance of maximum likelihood and parallel MSK receivers in Rayleigh fading channel for GMSK BT=0.3 in AWGN and equivalent co-channel interference.

receiver, because of its better performance in the presence of a single interferer, has been selected as reference receiver.

2.6 Bit by Bit ICIC

The simplest detection strategy is to decide the data symbol on the information over one symbol period. The minimum value of the cost function is the criterion for the selection of the correct estimate from all the possible desired signal estimates. Once the correct estimate is selected, its corresponding data symbol will be released as output data. This detection strategy is called bit by bit indirect co-channel interference cancelling (BB-ICIC). In this section the BER performance of the BB-ICIC is investigated by Monte Carlo simulation for MSK, GMSK BT=0.5 and GMSK BT=0.3 modulation schemes in different channels.

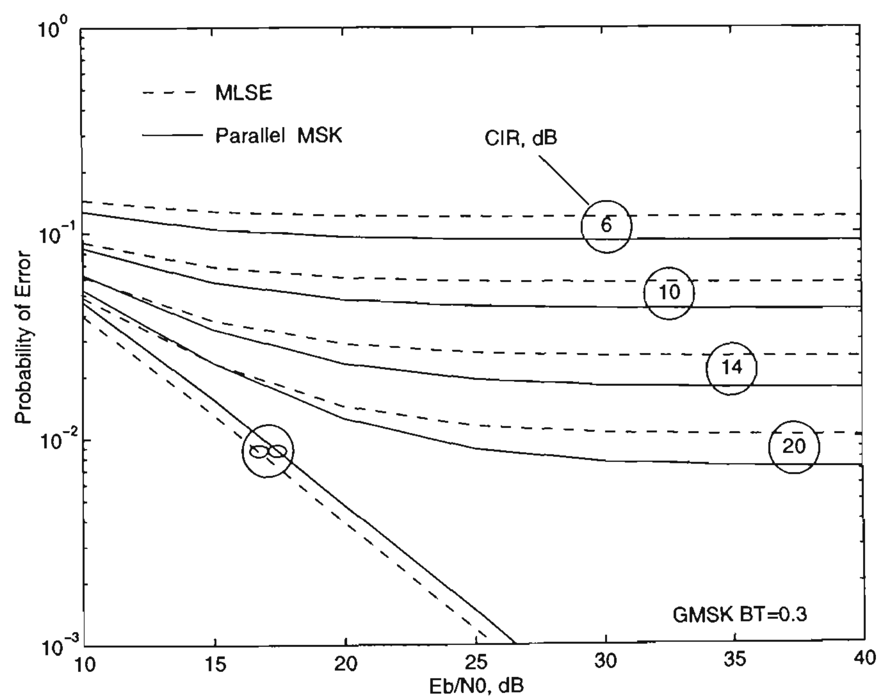

Fig. 2.12. BER performance of maximum likelihood and parallel MSK receivers in Rayleigh fading channel for GMSK BT=0.3 in AWGN and CCI.

2.6.1 Static Channel Performance

Fig. 2.13 shows BER performance of BB-ICIC in an AWGN channel. The BER performance of the Parallel MSK receiver is also shown in the same graph as a reference. This figure shows that the performance of the receiver is inferior to the performance of the Parallel MSK receiver, and also degrades with a reduction of the normalized bandwidth (BT) of the modulation scheme. The performance loss of the receiver increases from 2 to 5dB as the BT product is reduced from BT= ∞ to BT=0.3 ($P_e = 10^{-2}$).

2.6.2 Static Channel Performance with CCI

In Fig. 2.14, the BER performance of BB-ICIC in the presence of a single interferer is given for GMSK BT=0.3. The figure shows that the Parallel MSK receiver (conventional coherent receiver) outperforms the BB-ICIC when the CCI is weaker than the desired signal. However, when the CCI is stronger than the received signal, The BB-ICIC has a better BER performance. The BER performance of BB-ICIC shows an optimum point around CIR = -12dB. This behaviour indicates that the BER performance can only be improved if the desired signal falls *below* the interference level. This condition occasionally exists in a dynamic channel when the desired signal and interference fade independently (Fig. 2.15).

The good BER performance of the BB-ICIC with very large interference levels ($CIR \approx -10dB$) can be explained if ISI is neglected. Assume the received signal has the form of

$$r(k) = i(k) + n(k) + w(k) \tag{2.28}$$

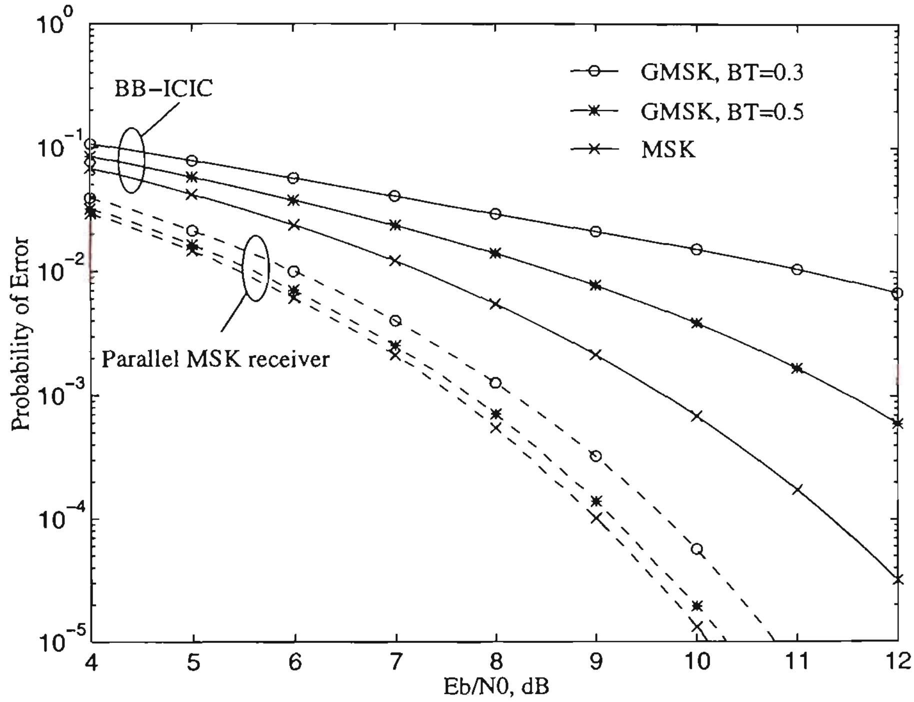

Fig. 2.13. Bit Error rate performance of BB-ICIC in AWGN channel.

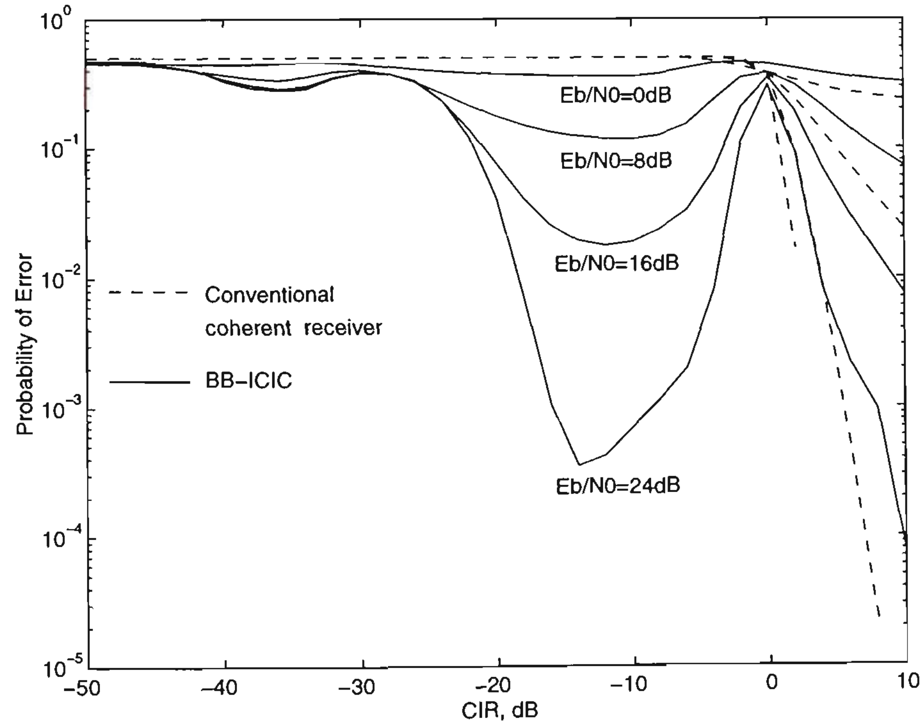

Fig. 2.14. Static channel performance of BB-ICIC in the presence of co-channel interference for GMSK BT=0.3 (I/Q lowpass filters are Maximally flat filter BT=0.6).

where i is interference, n is noise and w is the desired signal. Assume that the desired signal, w, can only take two values w_1 or w_2 (binary without ISI). If

$w = w_1$

$$r(k) = i(k) + n(k) + w_1(k) \tag{2.29}$$

The cost function of (2.5), gives the condition for correct decision as

$$\text{Cost function}\big|_{w_1} < \text{Cost function}\big|_{w_2} \Leftrightarrow L_1 < L_2 \tag{2.30}$$

substituting (2.28) into (2.30) gives

$$\sum_{k=0}^{m}\left\{[i(k)+n(k)]^2 - \overline{[i(k)+n(k)]^2}\right\}^2 < \sum_{k=0}^{m}\left\{[i(k)+n(k)+w_1(k)-w_2(k)]^2 - \overline{[i(k)+n(k)+w_1(k)-w_2(k)]^2}\right\}^2 \tag{2.31}$$

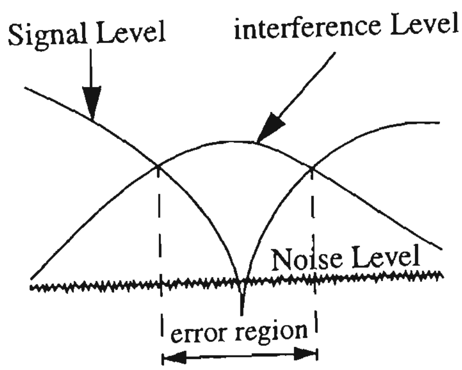

Fig. 2.15. Error event when the interference level exceeds desired signal.

Assuming that $i \gg n$, $i \gg w_1$, $i \gg w_2$ and the noise samples are uncorrelated (i.e. noise can be cancelled by time averaging) (2.31) is simplified to

$$\sum_{k=0}^{m}\left\{[i(k)+n(k)]^2-\overline{i^2}\right\}^2 < \sum_{k=0}^{m}\left\{[i(k)+n(k)+w_1(k)-w_2(k)]^2-\overline{i^2}\right\}^2 \qquad (2.32)$$

Further simplification of (2.32) can be done by considering that interference has a constant envelope (envelope fluctuation because of filtering is neglected). Hence $i^2(k)$ is constant for all k values (i.e. $i^2(k) = \overline{i^2}$, $k = 0, 1, \ldots, m$)

$$\sum_{k=0}^{m} 4\overline{i^2}n^2(k) < \sum_{k=0}^{m} 4\overline{i^2}[n(k)+w_1(k)-w_2(k)]^2 \qquad (2.33)$$

By dividing both sides of (2.33) by $4\overline{i^2}$; we have

$$\sum_{k=0}^{m} n^2(k) < \sum_{k=0}^{m} [n(k)+w_1(k)-w_2(k)]^2 \qquad (2.34)$$

Relation (2.34) is similar to the condition of correct decision for the maximum likelihood detection in the presence of only AWGN [26]. Interference is not present in the (2.34) and therefore, cannot cause any decision error. In practical situations the interference envelope fluctuations, caused by filtering, dominates all the other terms in the cost function. This deteriorates the BER performance, particularly at very high interference to signal ratios.

The reason why the BER has a maximum at $CIR = 0dB$ can be easily explained when both ISI and noise are neglected. When the bit timings for the desired signal and its interferer are the same (case of this simulation), with $CIR = 0dB$, interference can take either $w_1(k)$ or $w_2(k)$ waveforms. However, because of phase buildup from previous samples, a 180^o phase shift may exist such that the interference in fact becomes $-w_1(k)$ or $-w_2(k)$. Given this waveforms, the decision equations for $w = w_1$, in (2.31) takes the following forms

$$\sum_{k=0}^{m}\left\{w_1^2(k)-\overline{w_1^2(k)}\right\}^2 < \sum_{k=0}^{m}\left\{[2w_1(k)-w_2(k)]^2-\overline{[2w_1(k)-w_2(k)]^2}\right\}^2, i = w_1(k) \tag{2.35}$$

$$\sum_{k=0}^{m}\left\{w_1^2(k)-\overline{w_1^2(k)}\right\}^2 < \sum_{k=0}^{m}\left\{w_2^2(k)-\overline{w_2^2(k)}\right\}^2, i = -w_1(k) \tag{2.36}$$

$$\sum_{k=0}^{m}\left\{w_2^2(k)-\overline{w_2^2(k)}\right\}^2 < \sum_{k=0}^{m}\left\{w_1^2(k)-\overline{w_1^2(k)}\right\}^2, i = w_2(k) \tag{2.37}$$

$$\sum_{k=0}^{m}\left\{w_2^2(k)-\overline{w_2^2(k)}\right\}^2 < \sum_{k=0}^{m}\left\{[2w_2(k)-w_1(k)]^2-\overline{[2w_2(k)-w_1(k)]^2}\right\}^2, i = -w_2(k) \tag{2.38}$$

For constant envelope signals ($w_1(k)$ and $w_2(k)$) all the left hand sides of (2.35) to (2.38) are zero and the same for right hand sides of (2.36) and (2.37). As a result, the inequalities (2.36) and (2.37) can never hold and no valid decisions can be made in these cases. On the other hand, the inequalities in (2.35) and (2.38) hold as can be demonstrated using the waveforms in Table 5.1. This means that we have decision ambiguity in 50% of times. In the ambiguous situations decision is dominated by the additive noise as

$$\sum_{k=0}^{m} \{[n(k)-w_1(k)]-\overline{[n(k)-w_1(k)]}\}^2 < \sum_{k=0}^{m} \{[n(k)-w_2(k)]-\overline{[n(k)-w_2(k)]}\}^2, i = -w_1(k) \qquad (2.39)$$

$$\sum_{k=0}^{m} \{[n(k)+w_2(k)]-\overline{[n(k)+w_2(k)]}\}^2 < \sum_{k=0}^{m} \{[n(k)+w_2(k)]-\overline{[n(k)+w_2(k)]}\}^2, i = w_2(k) \qquad (2.40)$$

Due to the fact that noise is present in both sides of inequalities (2.39) and (2.40), $w_1(k)$ and $w_2(k)$ are equal energy waveforms, the decision made using these inequalities can be 50% in favour and 50% against the correct decision. This gives a 0.25 overall probability of error for a very low noise condition. However, presence of noise and ISI can increase this probability up to 0.50.

The worse performance of the BB-ICIC in $CIR > 0dB$ can be improved by eliminating unnecessary waveforms by a prediction algorithm (this will be discussed in Section 2.7.2).

2.6.3 Dynamic Channel Performance

The BER performance of BB-ICIC in a Rayleigh fading channel for GMSK BT=0.3 is shown in Fig. 2.16. Similar performances were observed for MSK and GMSK BT=0.5. In general, the performance improves with the increasing modulation BT product. For instance, the BER performance of MSK without interference is 1.3 dB and 1.9 dB better than GMSK BT=0.5 and GMSK BT=0.3 respectively. As can be seen from the figure, the BB-ICIC needs a minimum interference to noise ratio (INR) to outperform the reference receiver. The locus of the crossovers between CIR=6dB and CIR=24dB, is approximately a straight line (shown in Fig. 2.16). To the right of this line the BB-ICIC performs better than the reference receiver. The minimum INR (in this case is 10dB) can be found by subtracting the signal to noise ratio from CIR at the crossover point.

In the presence of co-channel interference, the rate of improvement depends on the amount of SNR. Fig. 2.17 shows the BER performance of BB-ICIC in a typical working condition ($E_b/N_0 = 30dB$). For voice communication where a $P_e = 10^{-2}$ is acceptable, the BB-ICIC receiver shows 1.8dB, 3.9dB and 5dB advantage over parallel-MSK receiver for GMSK BT=0.3, GMSK BT=0.5 and MSK respectively. In addition, the performance improvement at small CIRs is higher than at large CIRs as predicted from Fig. 2.14.

2.7 Waveform Reduction of GMSK

The complexity of the bit by bit detection can be further improved by reducing the number of estimates. This can be achieved by exploiting the MSK symmetry and considering it as an offset quadrature modulation scheme.

MSK is a binary modulation with a symbol interval T; but as a quadrature scheme, it

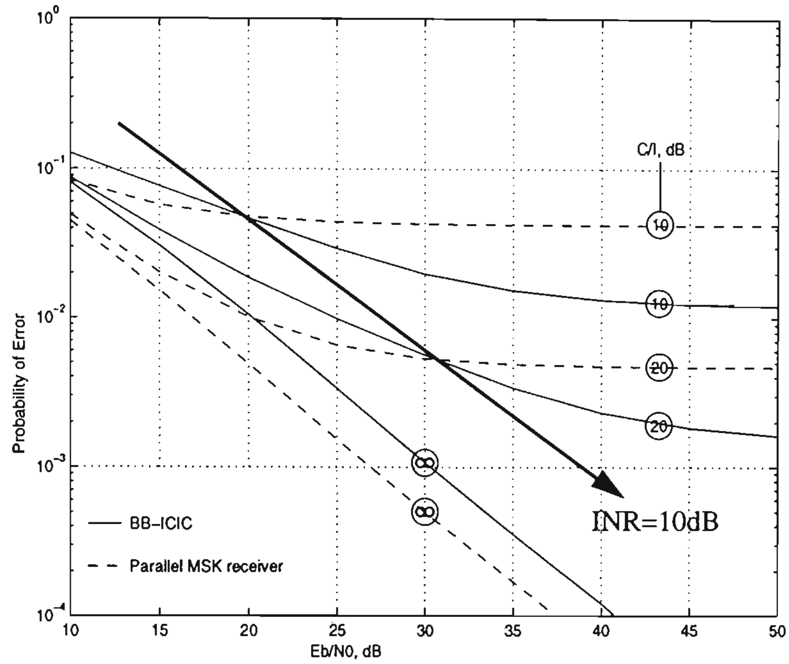

Fig. 2.16. BER performance of BB-ICIC for GMSK modulation scheme with BT=0.3.

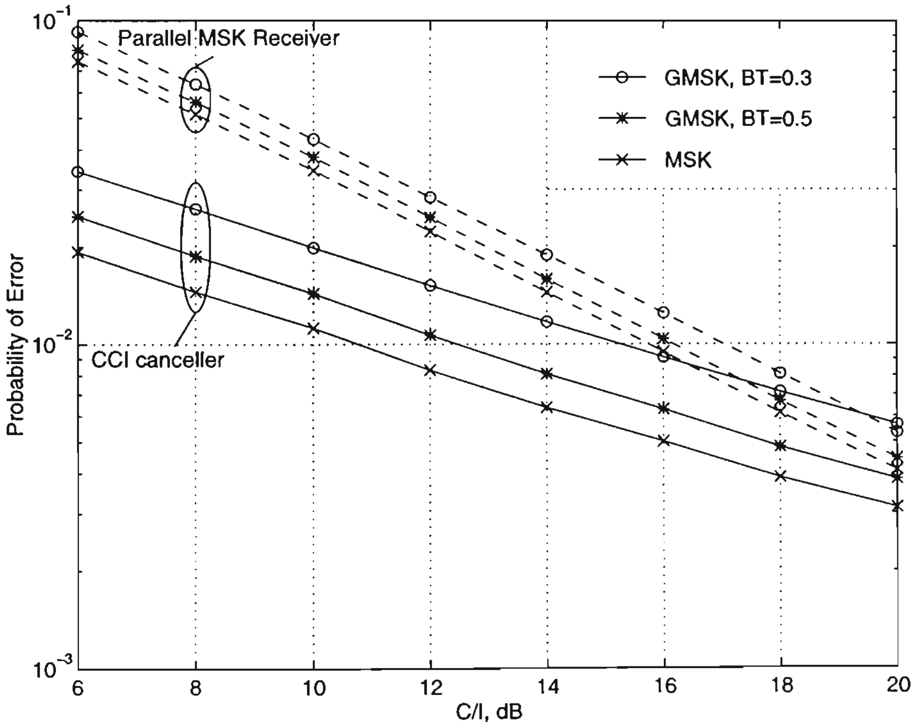

Fig. 2.17. BER performance of BB-ICIC for E_b/N_0=30dB in Rayleigh fading channel.

is a quaternary modulation over a double interval 2T. The binary differential encoded stream of data symbols $\{\alpha_n\}$ can be divided into even and odd symbols and creates I and Q pulse waveforms from two streams (see page 50 of reference [26])

for even n $S_i(t) = \alpha_n,\qquad (n-1)T \le t \le (n+1)T$

for odd n $S_q(t) = \alpha_n,\qquad (n-1)T \le t \le (n+1)T$

The MSK signal is then

$$R(t) = (2E_b/T)^{\frac{1}{2}}[S_i(t)\cos[(\pi t)/(2T)]\cos(2\pi f_c t) + \tag{2.41}$$

$$S_q(t)\sin[(\pi t)/(2T)]\sin(2\pi f_c t)]$$

In this case baseband in-phase and quadrature components of the MSK signal can be viewed as two BPSK signals with a symbol interval of *2T* and a time offset of *T*. The transmitter structure for such a modulator is given in Fig. 2.18. The GMSK modulation scheme can also be viewed as differentially encoded BPSK with ISI [132]. The ISI, in this case, comes from both I and Q data streams which complicates GMSK generation.

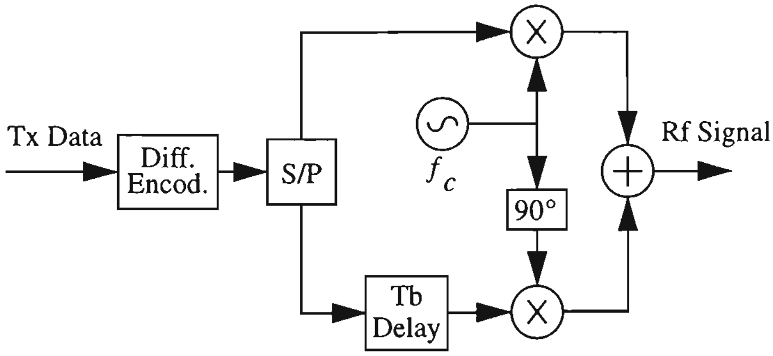

Fig. 2.18. Generation of MSK with differentially encoded BPSK.

The previous I/Q data symbols (S_i and S_q), can be obtained during bit by bit detection and used to reduce the number of possible waveforms. In Fig. 2.19 four situations are shown where the possible waveform estimates used for current timing interval are obtained based on the previous I/Q data bits (S_i and S_q). According to this figure, only four waveforms are required for GMSK BT=0.3 that originally needed 16 waveforms. The four complex envelope waveforms are tabulated in Table 2.2 for different values of (S_i and S_q). The table can be simplified to

$$W_{odd} = S_i \begin{bmatrix} w_{1i} \\ w_{2i} \\ w_{3i} \\ w_{4i} \end{bmatrix} + jS_q \begin{bmatrix} w_{1q} \\ w_{2q} \\ w_{3q} \\ w_{4q} \end{bmatrix} \tag{2.42}$$

By the same token the set of waveforms for the next time interval can be obtained by swapping the I and Q waveform estimates and multiplying them by the current bit I/Q symbols

$$W_{even} = S_i \begin{bmatrix} w_{1q} \\ w_{2q} \\ w_{3q} \\ w_{4q} \end{bmatrix} + jS_q \begin{bmatrix} w_{1i} \\ w_{2i} \\ w_{3i} \\ w_{4i} \end{bmatrix} \tag{2.43}$$

A block diagram of a system which can provide these waveforms is shown in Fig. 2.20. This type of waveform selection increases the minimum envelope distance of

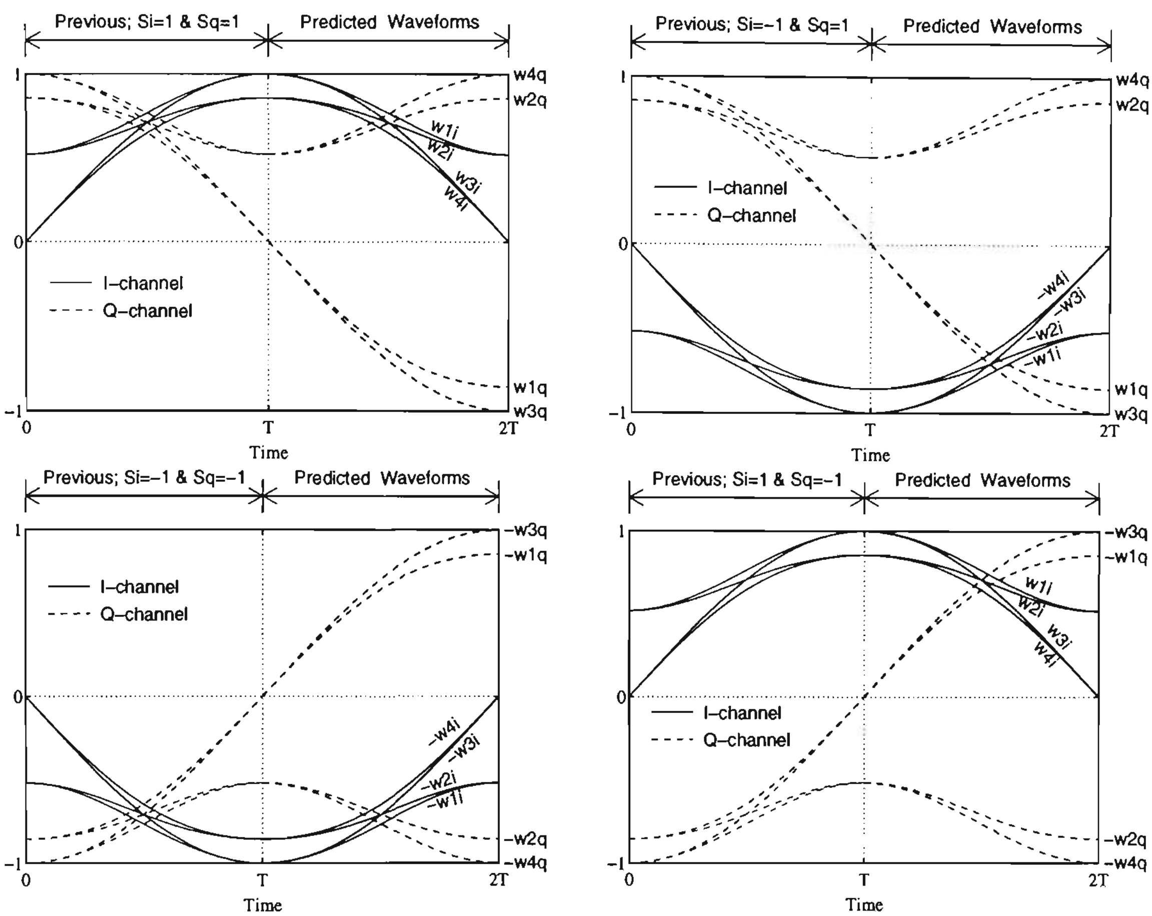

Fig. 2.19. Different GMSK wave shapes based on the previous decision. Solid line is selected to show the in-phase channel and dashed line is chosen for quadrature channel.

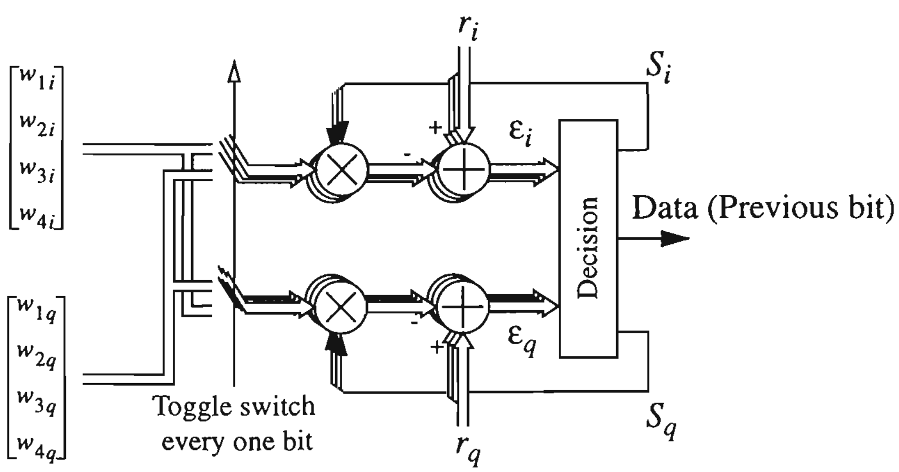

Fig. 2.20. Schematic circuit diagram for RWBB-CCI. S_i, S_q and toggle switch select the current set of waveform estimates to be subtracted from the complex input signal $r=r_i$-j. r_q.

Table 2.2. Possible complex envelopes of GMSK BT=0.3 in a bit time interval based on the I and Q channel symbols of the previous bit.

The previous bit I-channel symbol (s_i)	The previous bit Q-channel symbol (s_q)	Possible 4-tuple complex envelopes of GMSK BT=0.3 for the current bit.
1	1	$\begin{bmatrix} w_{1i}+jw_{1q} \\ w_{2i}+jw_{2q} \\ w_{3i}+jw_{3q} \\ w_{4i}+jw_{4q} \end{bmatrix}$
1	-1	$\begin{bmatrix} w_{1i}-jw_{1q} \\ w_{2i}-jw_{2q} \\ w_{3i}-jw_{3q} \\ w_{4i}-jw_{4q} \end{bmatrix}$
-1	1	$\begin{bmatrix} -w_{1i}+jw_{1q} \\ -w_{2i}+jw_{2q} \\ -w_{3i}+jw_{3q} \\ -w_{4i}+jw_{4q} \end{bmatrix}$
-1	-1	$\begin{bmatrix} -w_{1i}-jw_{1q} \\ -w_{2i}-jw_{2q} \\ -w_{3i}-jw_{3q} \\ -w_{4i}-jw_{4q} \end{bmatrix}$

the receiver [see chapter 5] because it eliminates redundant waveform estimates. The envelope distances of GMSK BT=0.3 for the selected waveforms (as in Fig. 2.19) are given in Tables I.1-I.4. These tables show that the minimum envelope distance (e_{min}) for GMSK modulation scheme has been increased by more than 100%[1]. However, there is a possibility of error propagation, but simulation shows that the reduced waveform bit-by-bit ICIC (RW-ICIC) receiver has a better performance than BB-ICIC.

2.7.1 Static Channel Performance Without Interference

The BER performance of RW-ICIC in AWGN channel is shown in Fig. 2.21. Comparing RW-ICIC and BB-ICIC shows that BER performance has been improved, which is expected from the higher minimum envelope distance. For instance, the improvement for MSK is about 1.8dB, but the result is still about 0.5dB worse than the parallel-MSK receiver.

2.7.2 Static Channel Performance with CCI

Fig. 2.22 shows the BER performance of RW-ICIC in the presence of CCI for GMSK BT=0.3. The shape of the BER curve is almost identical with the one obtained for BB-ICIC (Fig. 2.14). However, the BER generally improves, particularly at large CIRs (CIR>0dB).

2.7.3 Dynamic Channel Performance

Fig 2.23 presents the BER performance of RW-ICIC receiver in a Rayleigh fading channel in the presence of one co-channel interferer for GMSK BT=0.3. The

---

1.From the Table H.1 the minimum envelope distance is $e_{min} = 0.344$ while in Tables I.1-I.4, $e_{min} = 0.716$.

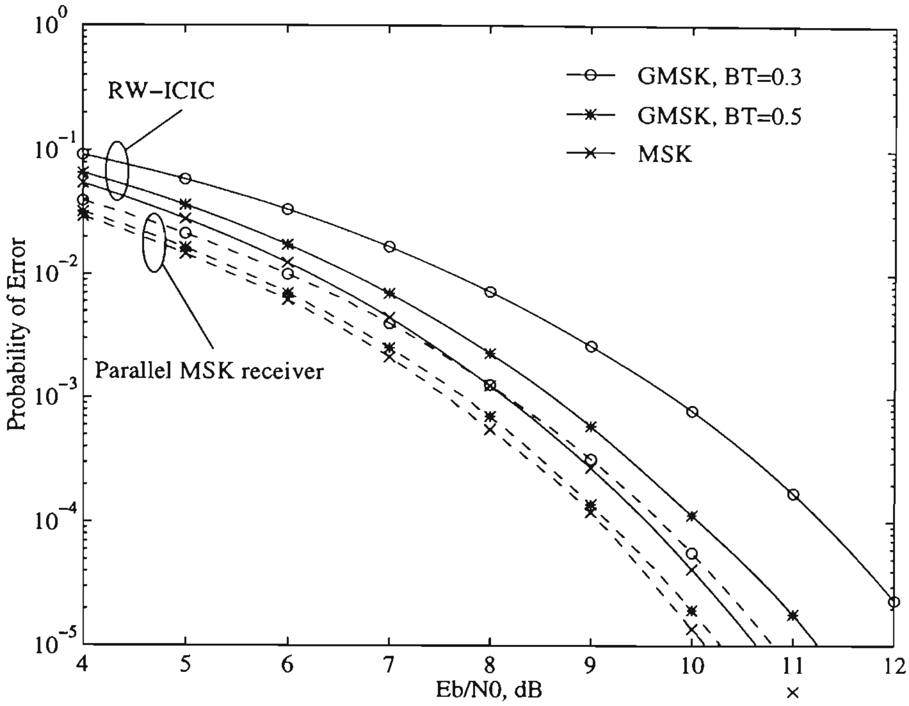

Fig. 2.21. BER performance of RW-ICIC in AWGN channel without co-channel interference.

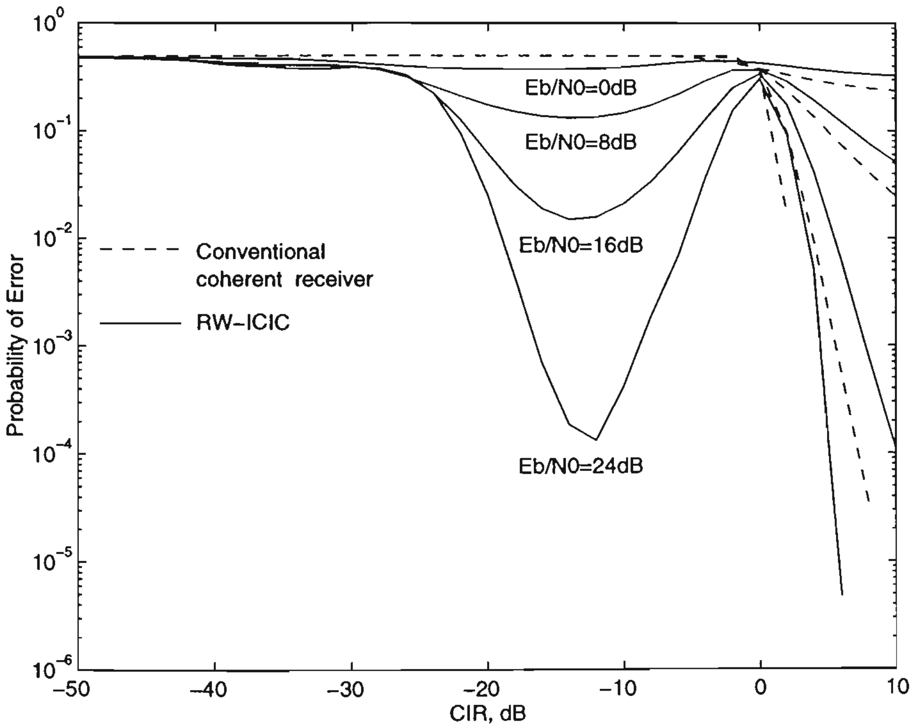

Fig. 2.22. Static channel performance of RW-ICIC in the presence of co-channel interference for GMSK BT=0.3 when I/Q lowpass filters are Maximally flat filter BT=0.6.

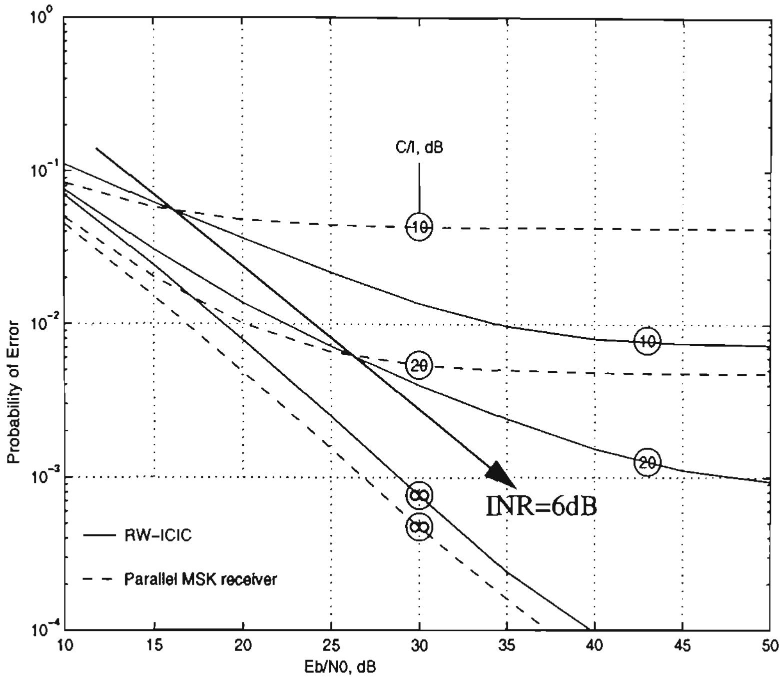

Fig. 2.23. BER performance of RW-ICIC for GMSK BT=0.3.

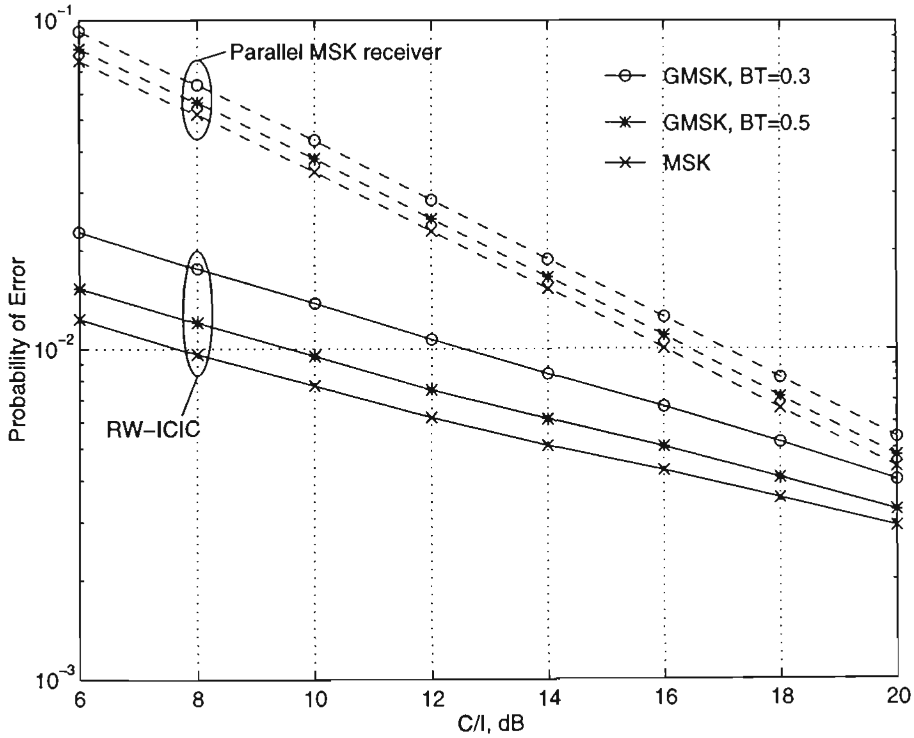

Fig. 2.24. BER performance of RW-ICIC canceller for E_b/N_0=30dB in Rayleigh fading channel.

RW-ICIC shows better BER performance than BB-ICIC. The minimum interference to noise ratio (INR) needed to outperform the parallel MSK has also been reduced by 4dB. Fig. 2.24 shows the performance in $E_b/N_0 = 30dB$. For an error rate of $P_e = 10^{-2}$, the RW-ICIC receiver shows 8.3dB, 6.9dB and 4.5 dB advantage over parallel MSK receiver for MSK, GMSK BT=0.5 and GMSK BT=0.3 respectively. This is approximately 3dB better than BB-ICIC. The performance improvement, as in BB-ICIC, in smaller CIRs is higher than the larger CIRs.

In conclusion, RW-ICIC, not only reduces the receiver complexity by eliminating many waveform comparisons, but also gives superior performance.

2.8 Detection Using Viterbi Algorithm

As shown in Section 5.5, minimum envelope distance of CPM modulation schemes can be increased by observing the signal over multiple bit intervals. To exploit this advantage, the signal has to be decoded with a sequential decoding algorithm.

One of the most popular algorithms that performs this task is the Viterbi Algorithm (VA) [145]. The VA calculates a metric (distance function or measure of similarity) between the received signal *r(t)* at the n^{th} symbol interval and all the trellis paths entering each state at this instant. In the event that more than one path enters a single state, only the one with the lowest metric (the survivor) is stored. The paths with larger metric are less likely, thus they are eliminated. The decoder continues in this way to advance deeper into the trellis eliminating the least likely paths. The VA can be applied to ICIC (VA-ICIC) where the cost function (2.6) is used as metric.

2.8.1 Static Channel Performance

Fig. 2.25 shows the BER performance of VA-ICIC receiver in the presence of

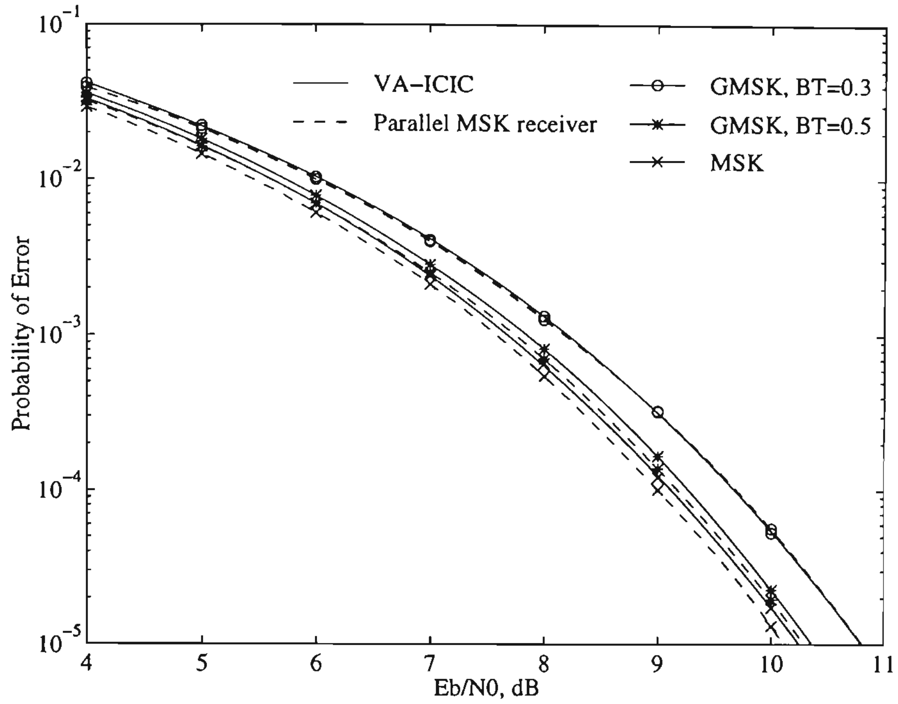

Fig. 2.25. BER performance of VA-ICIC in AWGN channel without co-channel interference.

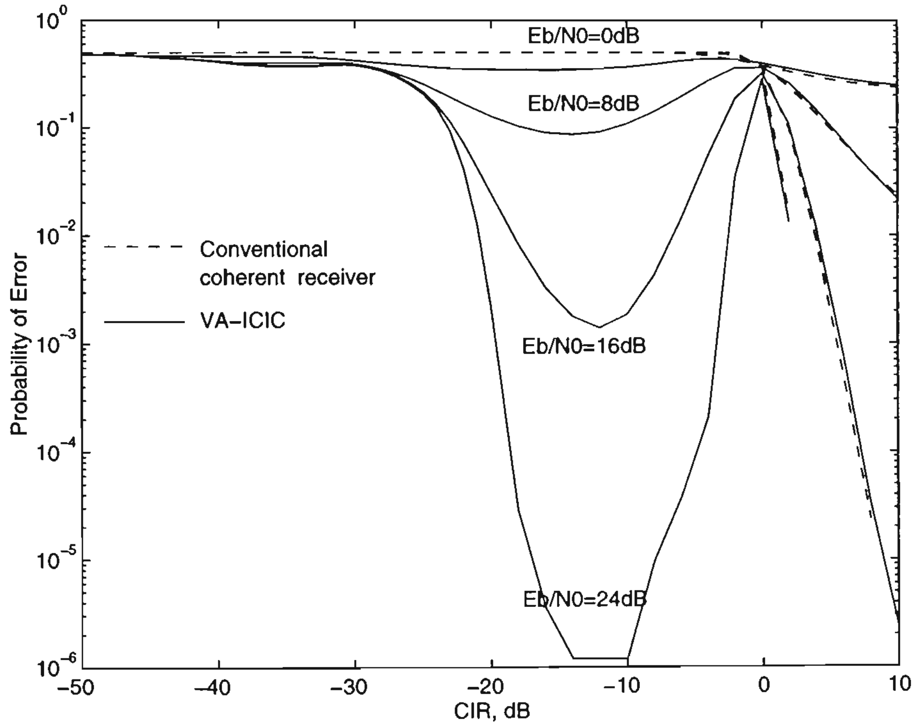

Fig. 2.26. Static channel performance of VA-ICIC in the presence of co-channel interference for GMSK BT=0.3 when I/Q lowpass filters are Maximally flat filter BT=0.6.

AWGN. As expected from the higher minimum envelope distance, the BER performance of VA-ICIC is better than both BB-ICIC and RW-ICIC and it is very close to that of the parallel MSK receiver.

2.8.2 Static Channel Performance with CCI

In Fig. 2.26 the performance of VA-ICIC in the presence of CCI is given for GMSK BT=0.3. As the figure indicates, when the CCI is weaker than the desired signal, both VA-ICIC and the parallel MSK receiver have almost similar performance. However, when the CCI is stronger than the received signal, the VA-ICIC shows a better BER performance which is generally better than the performance of BB-ICIC and RW-ICIC.

2.8.3 Dynamic Channel Performance

The BER performance of the VA-ICIC in a Rayleigh fading channel and in the presence of a co-channel interferer is shown in Fig. 2.27. In the absence of CCI, the BER performance of the VA-ICIC receiver is only 0.3dB worse than the parallel-MSK receiver. In general, the BER performance in the presence of CCI is better that the previously presented ICIC receivers. The minimum interference to noise ratio needed to outperform the reference receiver is about 1.5dB which is 4.5dB and 8.5dB less than RW-ICIC and BB-ICIC respectively. In the same channel as the RW-ICIC and BB-ICIC, (i.e. $E_b/N_0 = 30dB$ and a probability of error equal 10^{-2}) the VA-ICIC gives a large improvement (13dB) over the reference receiver (Fig. 2.28). This improvement is about 11dB and 8.5dB better that achieved by BB-ICIC and RW-ICIC respectively.

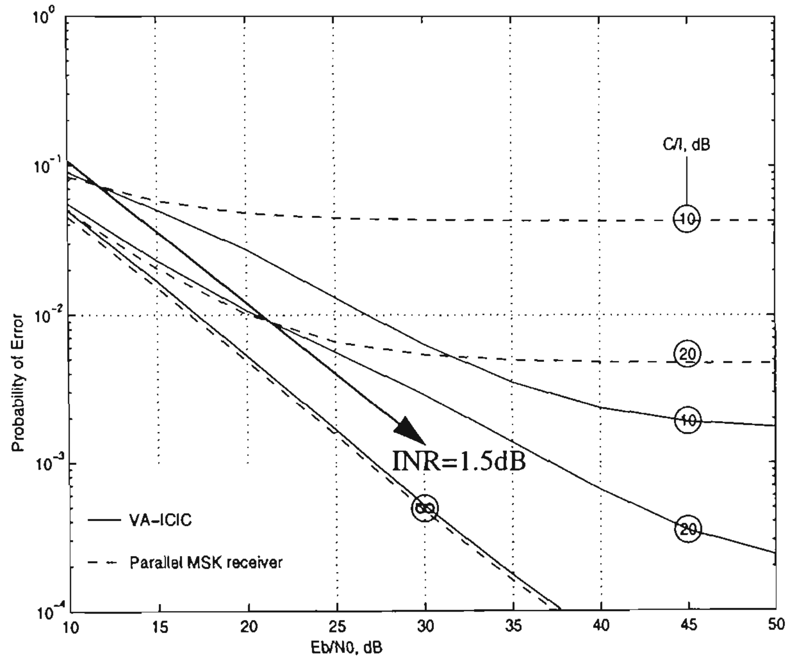

Fig. 2.27. BER performance of VA-ICIC for GMSK modulation scheme with BT=0.3.

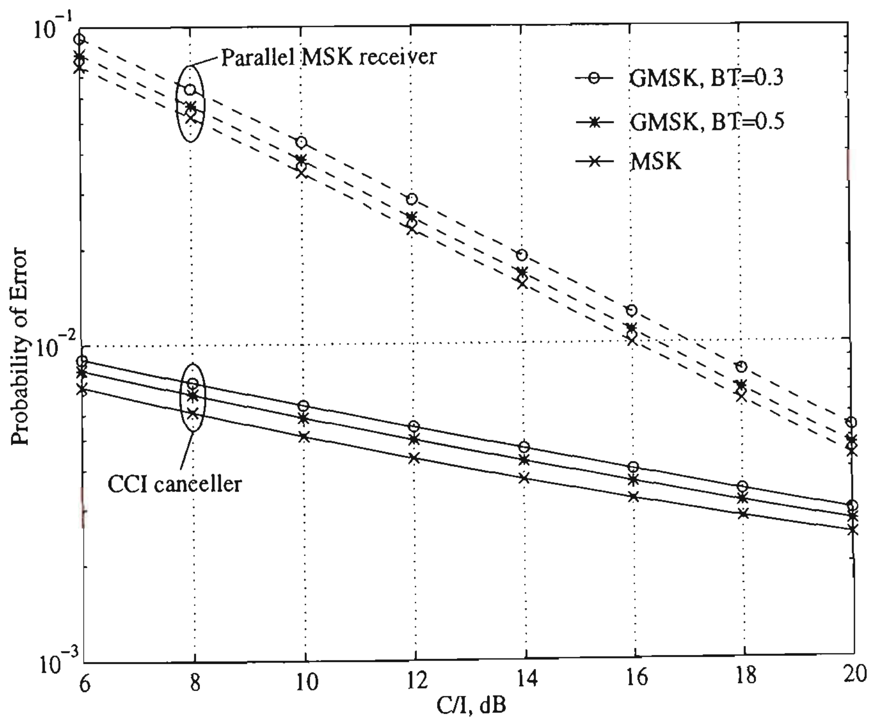

Fig. 2.28. BER performance of VA-ICIC for E_b/N_0=30dB in Rayleigh fading channel.

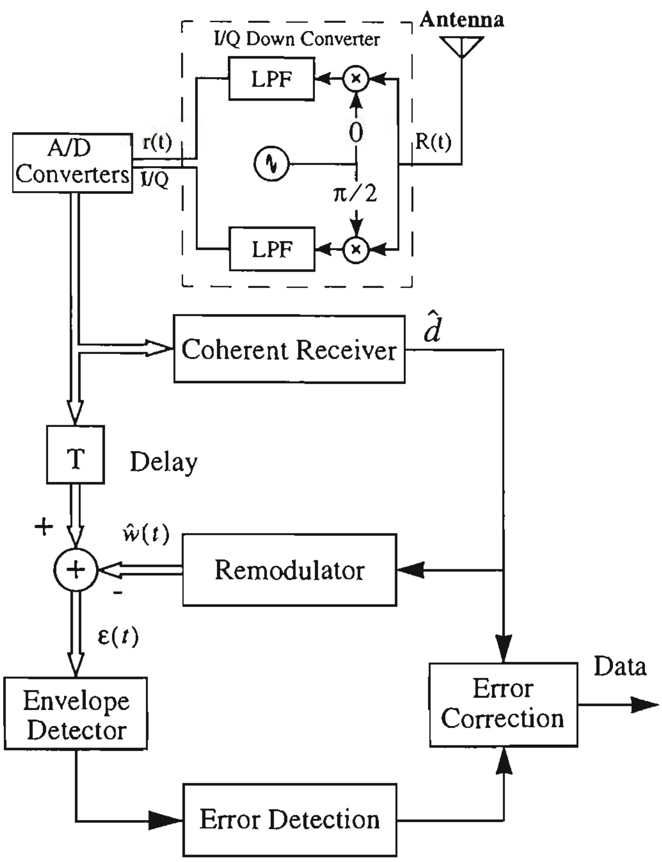

Fig. 2.29. Block diagram of ICIC error detection/correction receiver (EDC-ICIC).

2.9 Error Detection and Correction Receiver

In this section an error detection/correction scheme, similar to the one proposed by Gooch and Sublett [55], is presented. A block diagram of this scheme is shown in Fig. 2.29. It comprises of a conventional coherent receiver for predetection of data, a remodulator for regeneration of the desired signal, $\hat{w}(t)$, and an error detection/correction block. The delay, T, in the path of the received signal, $r(t)$, compensates for the processing time associated with the receiver and remodulator. The received signal, consists of the desired signal, $w(t)$, interference, $i(t)$, and noise, $n(t)$. The data output from the coherent receiver, is used to regenerate a replica of the desired signal, $\hat{w}(t)$ which is then subtracted from the received signal to form the residue signal, $\varepsilon(t) = r(t) - \hat{w}(t)$. If the decision and consequently regeneration are correct, the residue consists of only the constant envelope CCI. When there is an error, the regenerated signal, $\hat{w}(t)$, does not completely cancel out the desired signal, resulting in a non-constant residue. The error can be corrected after it is detected by comparing the envelope variation of the residue, as measured by metric (2.6), with a threshold level. The expected waveforms seen at the output of the envelope detector are derived in the next subsection.

2.9.1 Analysis (Full Response CPM)

Only full response CPM modulation schemes will be considered here. Partial response CPM would require the same procedure but becomes extremely laborious due to the inherent ISI it displays. The complex envelope of the residue signal can be expressed as

$$\varepsilon = \varepsilon_I - j\varepsilon_Q \tag{2.44}$$

where, using the notation used in (2.3), $\varepsilon_I = A\cos\Phi + B\cos\Theta - C\cos\Psi + n_i$, $\varepsilon_Q = A\sin\Phi + B\sin\Theta - C\sin\Psi + n_q$ and $\hat{w} = Ce^{j\Psi}$ is the regenerated desired signal. For a full response CPM modulation scheme, from (2.23) we can write

$$\begin{aligned}
\Phi &= \phi_n + \pi\alpha_n q(t) && \text{Phase of desired signal} \\
\Psi &= \psi_n + \pi\beta_n q(t) && \text{Phase of regenerated signal} \\
\Theta &= \theta_n + \pi\lambda_n q(t) && \text{Phase of CCI signal}
\end{aligned} \tag{2.45}$$

where ϕ_n, ψ_n and θ_n are phases at the beginning of the bit interval, *q(t)* is the phase pulse, and α_n, β_n and λ_n are data symbols.

With the complete knowledge of the desired signal amplitude ($C = A$), the residue power, M^2, can be calculated as follows

$$\begin{aligned} M^2 &= |\varepsilon|^2 \\ M^2 &= {\varepsilon_I}^2 + {\varepsilon_Q}^2 \\ M^2 &= P_s + P_n \end{aligned} \tag{2.46}$$

where

$$P_s = B^2 + 2A^2 + 2AB\cos(\Theta - \Phi) - 2AB\cos(\Theta - \Psi) - 2A^2\cos(\Phi - \Psi) \tag{2.47}$$

$$\begin{aligned} P_n = {} & n_i^2 + n_q^2 + 2B(n_i\cos\Theta + n_q\sin\Theta) + \\ & 2A(n_i\cos\Phi + n_q\sin\Phi) - 2A(n_i\cos\Psi + n_q\sin\Psi) \end{aligned} \tag{2.48}$$

P_s contains the desired signal as well as CCI information and P_n contains all the noise cross products. To simplify the analysis, P_n is ignored (i.e. channel without noise). The normalized power of the residue signal $(M^2/A^2 = P_s/A^2)$ is illustrated in Fig. 2.30 for MSK modulation scheme in a Rayleigh fading channel.

P_s, from (2.47), is now evaluated over a single bit period. The symbol boundaries are shown across the top of Fig. 2.30. The symbols with constant amplitude are marked C and these represent the correct decision estimate ($\hat{d}$). The residue power for the correct decision slowly changes with the fading on the CCI signal. There are two power levels associated with the correct decision. One of the levels (marked by P in the diagram) is caused by 180^0 phase shift in the regenerated signal which is due to phase build up from previous errors. Each error creates a 180^0 phase shift. Symbols marked E correspond to error in regeneration and result in a sine wave like shape of the residue power.

For simplicity, the analysis is done in two steps. In the first step, the CCI signal has no data transition over the evaluation bit period. In the second step, the data transition in the CCI is introduced. This models the timing offset between the desired and the co-channel signal.

Step 1:

At first let us consider the case of correct regeneration (Case C in Fig. 2.30) in which $\Psi = \Phi$ and hence:

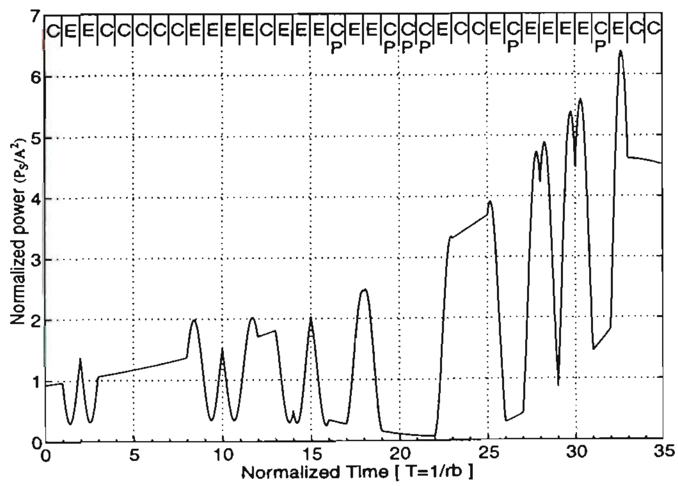

Fig. 2.30. Instantaneous power signal for MSK modulation scheme. The desired signal and CCI are synchronous. E: An error occurred in initial detection, C: No error in initial detection, C/P: no error in initial detection but a 180 degree phase shift is left from the error in the previous bit.

$$P_s = B^2 \tag{2.49}$$

This implies that P_s is a constant, independent of the phase and timing of the CCI.

Next, consider the 180^o phase error condition (i. e. $\Psi = \Phi \pm \pi$, Case CP in Fig. 2.30). from (2.47) we have:

$$P_s = B^2 + 4A^2 + 4AB\cos(\Theta - \Phi) \tag{2.50}$$

Substituting (2.45) into (2.50) yields

$$P_s = B^2 + 4A^2 + 4AB\cos[\pi(\lambda_n - \alpha_n)q(t) + \zeta] \tag{2.51}$$

Where $\zeta = (\theta_n - \phi_n)$. Equation (2.51) will have a constant value if $\alpha_n = \lambda_n$, which implies that no error exist.

In the event of error (i.e. $\beta_n = -\alpha_n$) the following four possible situations may exist:

1) $\alpha_n = \lambda_n$ (i.e. the desired and CCI data bits are the same) and $\psi_n = \phi_n$ (i.e. at the start of the bit period, the desired and the regenerated signals have the same phase)

$$\begin{aligned} \Phi &= \phi_n + \alpha_n q(t) \\ \Psi &= \phi_n - \alpha_n q(t) \\ \Theta &= \theta_n + \alpha_n q(t) \end{aligned} \tag{2.52}$$

2) $\alpha_n = -\lambda_n$ and $\psi_n = \phi_n$

$$\begin{aligned}\Phi &= \phi_n + \alpha_n q(t) \\ \Psi &= \phi_n - \alpha_n q(t) \\ \Theta &= \theta_n - \alpha_n q(t)\end{aligned} \tag{2.53}$$

3) $\alpha_n = \beta_n$ and $\psi_n = \phi_n \pm \pi$

$$\begin{aligned}\Phi &= \phi_n + \alpha_n q(t) \\ \Psi &= \phi_n \pm \pi - \alpha_n q(t) \\ \Theta &= \theta_n + \alpha_n q(t)\end{aligned} \tag{2.54}$$

4) $\alpha_n = -\beta_n$ and $\psi_n = \phi_n \pm \pi$

$$\begin{aligned}\Phi &= \phi_n + \alpha_n q(t) \\ \Psi &= \phi_n \pm \pi - \alpha_n q(t) \\ \Theta &= \theta_n - \alpha_n q(t)\end{aligned} \tag{2.55}$$

By substituting (2.52)-(2.55) into (2.47) the following equations are obtained respectively:

$$P_s = A^2 + \frac{X_1}{2A} - X_1 \cos[2\alpha_n q(t) - \gamma_1] \tag{2.56}$$

Where: $\gamma_1 = \operatorname{atan}\left(\frac{B\sin\zeta}{A + B\cos\zeta}\right)$, $X_1 = 2A(A^2 + B^2 + 2AB\cos\zeta)$

$$P_s = A^2 + \frac{X_2}{2A} + X_2\cos[2\alpha_n q(t) - \gamma_2] \tag{2.57}$$

Where: $\gamma_2 = \operatorname{atan}\left(\frac{B\sin\zeta}{A - B\cos\zeta}\right)$, $X_2 = 2A(A^2 + B^2 - 2AB\cos\zeta)$

$$P_s = A^2 + \frac{X_3}{2A} + X_3\cos[2\alpha_n q(t) - \gamma_3] \tag{2.58}$$

Where: $\gamma_3 = \operatorname{atan}\left(\frac{B\sin\zeta}{A + B\cos\zeta}\right)$, $X_3 = 2A(A^2 + B^2 + 2AB\cos\zeta)$

$$P_s = A^2 + \frac{X_4}{2A} + X_4\cos[2\alpha_n q(t) + \gamma_4] \tag{2.59}$$

where: $\gamma_4 = \operatorname{atan}\left(\frac{B\sin\zeta}{A + B\cos\zeta}\right)$, $X_4 = 2A(A^2 + B^2 + 2AB\cos\zeta)$.

Equations (2.56)-(2.59) show that the residue power, P_s, consists of a constant value ($A^2 + \frac{X_i}{2A}$, $i = 1, 2, 3, 4$) plus a cosine pulse of amplitude X_i. The latter accounts for the sinusoidal shape of the residue power under the error condition shown in Fig. 2.30.

Step2:

If there is a timing offset of T_1 (Fig. 2.31) and the CCI data symbol changes during

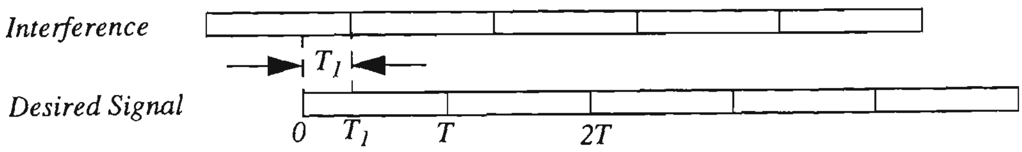

Fig. 2.31. The data bit timing offset of the desired and CCI signals.

the bit interval of the desired signal, (2.45) gives

$$\Theta = \begin{cases} \theta_n + \lambda_n q(t) & 0 < t < T1 \\ \theta_{n+1} - \lambda_n q(t) = \theta_n + \lambda_n \pi r_b T1 - \lambda_n q(t) & T1 < t < T \end{cases} \quad (2.60)$$

With an error in the estimate ($\beta_n = -\alpha_n$) and a 180° phase difference between the regenerated and desired signals (Case CP in Fig. 2.30), (2.51) indicates that P_s in one of the time intervals ([0,T1] or [T1,T]) is constant (Equation 2.51) and in another interval it is constant plus a fraction of a cosine shaped pulse (Equations (2.56)-(2.59)). The correct detection of data in this case, implies that α_n is equal to β_n in the bigger time interval. Thus, the cosine pulse portion of P_s is small and consequently harder to detect. The error correction might not take place.

When an error occurs in the regeneration of the desired signal, any change in the CCI data symbol swaps its phase (Ψ) from one of the situations shown in equations (2.52)-(2.55) into another one. In this case the power of the residue (P_s) has a constant component plus a cosine pulse which can be detected.

2.9.2 BER Performance

The system of Fig. 2.29 is simulated with a co-channel interferer and MSK modulation scheme in a Rayleigh fading channel with fd=100Hz. The baud rate of the data is 270 Kbits/s. The error detection process is a comparison between the value of metric (2.6) calculated in each bit interval and a threshold level. The threshold level is optimized to have a minimum error at $E_b/N_0 = 30dB$ and $CIR = 12dB$.

Fig. 2.32 shows the system BER performance for different signal to interference ratios (SIR) on the optimum threshold level. Fig. 2.33 shows the bit error rate performance of the system for three different threshold settings. The probability of error in low SNR with small threshold levels is higher than that in large SNRs with high threshold levels. An adaptive threshold can improve the system performance when the SNR changes.

EDC-ICIC faces difficulty from delay adjustment, and threshold setting. The threshold is dependent on noise, CCI and ISI levels. Adaptive threshold setting is a good solution to this problem, but at the cost of increased complexity. The ISI caused by filtering in the receiver smears any amplitude variation in the residue signal into the adjacent bit period, causing false error correction. Because of this, errors often occur in bursts. The same phenomena can happen in partial response CPM schemes because of the inherent ISI they display. Since the BER performance of this receiver is not satisfactory compared to the other proposed ICIC receivers, I have not proceeded further in the development of this scheme.

2.10 Comparison Between the Proposed ICIC receivers

Among the four proposed receivers, VA-ICIC has the best BER performance. Although the BER of RW-ICIC is superior to the BB-ICIC, its complexity reduction

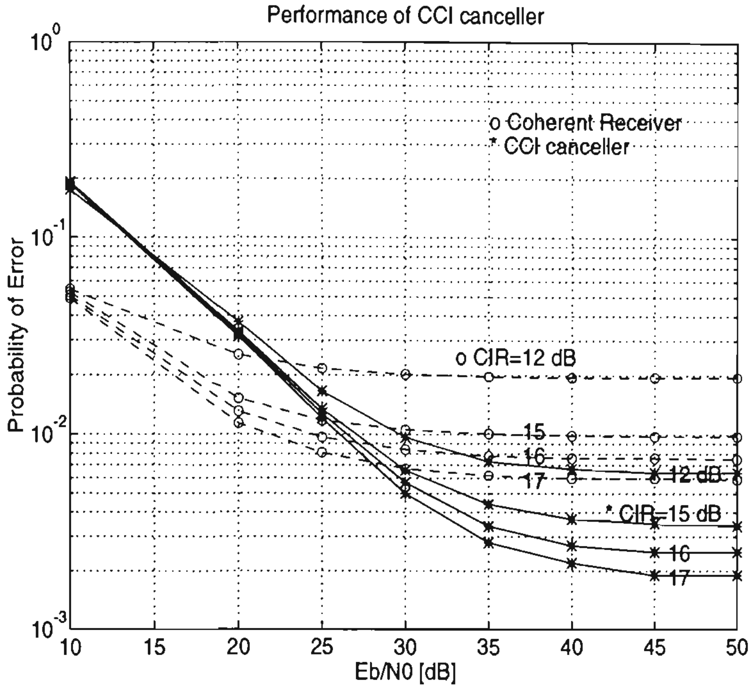

Fig. 2.32. BER performance of error detection/correction scheme for MSK modulation scheme in Rayleigh fading channel.

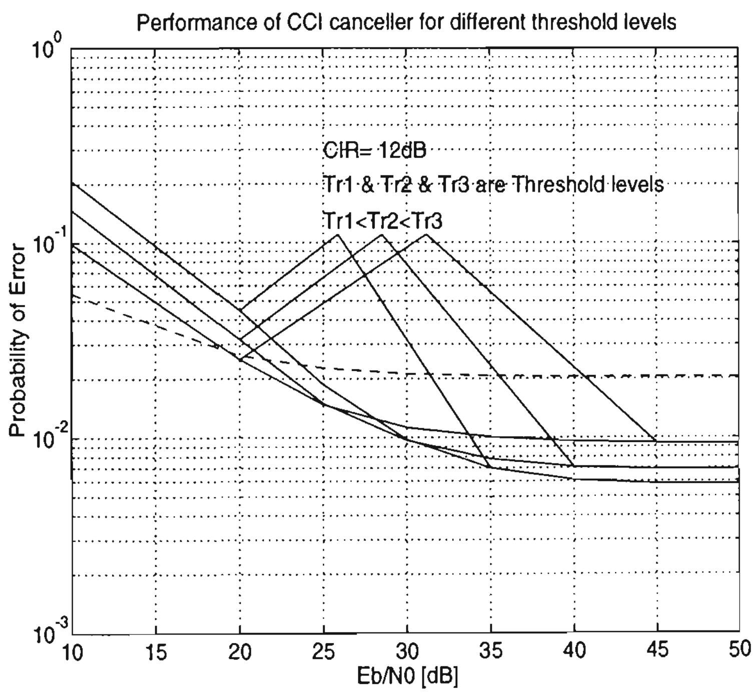

Fig. 2.33. BER performance in a error detection/correction scheme for MSK modulation scheme with different threshold levels. The dashed line shows the performance of the coherent receiver.

is not significant because of the complexity of waveform preparation. EDC-ICIC, compared to the other receivers, does not show a good BER performance. The receiver also experiences difficulty with delay adjustment and threshold setting. Performance of EDC-ICIC also largely deteriorates with ISI, such that the inherent ISI in partial response CPM schemes makes the EDC-ICIC inappropriate for these modulation schemes.

The practical implementation imperfections are addressed in the next chapter. The VA-ICIC scheme is selected for study due to its superior BER performance.

Chapter 3

Sensitivity Analysis of Indirect Co-channel Interference Canceller

Among the four proposed receivers introduced in the previous chapter, the VA-ICIC receiver has been selected for further study because of its good BER performance. This chapter investigates the range of different parameters affecting the performance of the VA-ICIC receiver. The results of this study increase the understanding of the design and hardware complexity of the VA-ICIC receiver. Some of the results, may be applied to other proposed receivers but they are not considered in these investigations.

3.1 Effect of Sampling Rate

In the metric (2.6), $\overline{M_i^2}$, the mean of complex residue envelope (M_i^2), is an estimate of cochannel interference. The quality of interference cancelling, which is carried out by subtracting $\overline{M_i^2}$ from M_i^2, depends on the accuracy of this estimate.

The *law of large numbers* [146] implies that the averaging can be improved by increasing the number of samples. In this particular case, increasing the number of samples can only be achieved by oversampling. However, the improvement in accuracy is limited by the increased correlation between adjacent samples. Additionally, oversampling requires increased complexity in the hardware. Initial investigations are carried out to observe the effect of the number of samples on the BER performance of the VA-ICIC. As indicated in Fig. 3.1, the 3-sample metric appears to be optimum it also demonstrates that increasing the number of samples ($m > 2$) deteriorates the BER performance. This can be better explained when the averaging is modelled as a lowpass filter. The impulse response of this filter (Fig. 3.2a) has the form

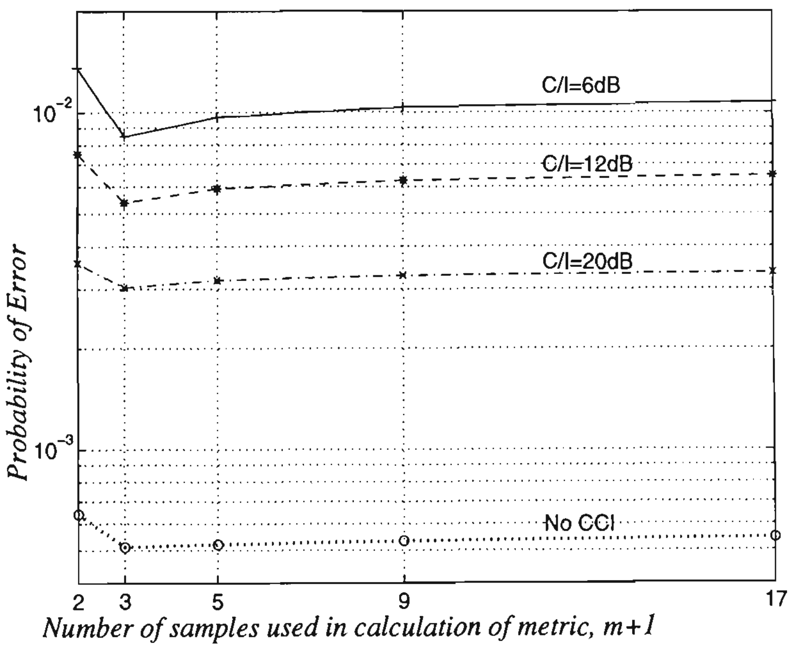

Fig. 3.1. BER performance of VA-ICIC for different sampling rates. The modulation is GMSK $BT = 0.3$ with a baud rate of 270kbits/s in a Rayleigh fading channel with a fading rate of 100Hz and $E_b/N_0 = 30dB$.

$$h(n) = \begin{cases} 1 & 0 \le n \le m \\ 0 & \text{elsewhere} \end{cases} \tag{3.1}$$

and its spectrum [147] can be expressed as

$$H(\omega) = \frac{\sin[\omega(m+1)/2]}{\sin(\omega/2)} e^{-j\omega m/2} \tag{3.2}$$

where $\omega = 2\pi f/f_s = 2\pi f T_b/m$. Fig. 3.2b shows the spectrum of this filter for different m values. As the figure indicates, increasing m increments the filter bandwidth which increases the noise and subsequently the estimation error. Therefore, the relatively poor performance for $m > 2$ is because of the wider filter bandwidth. The inferior performance with $m = 1$ is due to the small population size. As simulation shows these two contradicting factors are optimized at $m = 3$. From

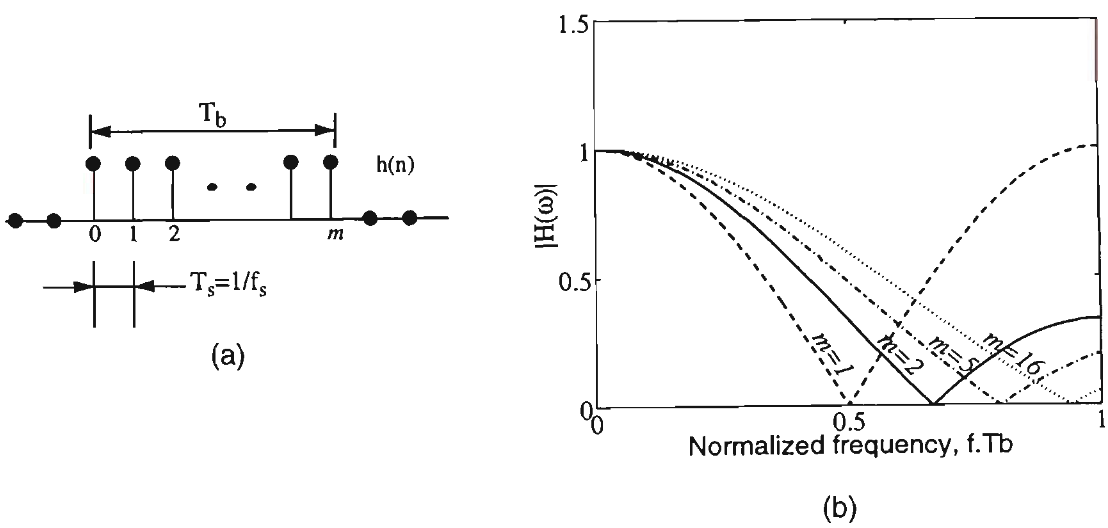

Fig. 3.2. (a) impulse response, (b) amplitude spectrum of a lowpass filter with an impulse response of: *h(n)=1, n=0,1,...,m; h (n)=0, elsewhere;* for different *m* values.

now on, the metric calculated with $m = 3$ is called 3-sample metric and $m = 2$ denoted 2-sample metric.

3.2 Effect of Quadrature Demodulator Filters

The reliance of ICIC on the constant envelope property of CCI, implies that any fluctuation in the envelope of CCI can degrade the BER performance of ICIC. One of the main causes of this envelope fluctuation is intersymbol interference (ISI) introduced by I/Q lowpass filters (Fig. 2.2). Fig. 3.3a shows the envelope eye diagram of a GMSK BT=0.3 signal, filtered with a Gaussian lowpass filter of normalized bandwidth $BT = 0.4$. If a lowpass filter with a wider bandwidth (Normalized bandwidth $BT = 0.6$) is used, the signal envelope fluctuations can be reduced (Fig. 3.3b). In Fig. 3.4 the envelope ripples of MSK, GMSK BT=0.3 and

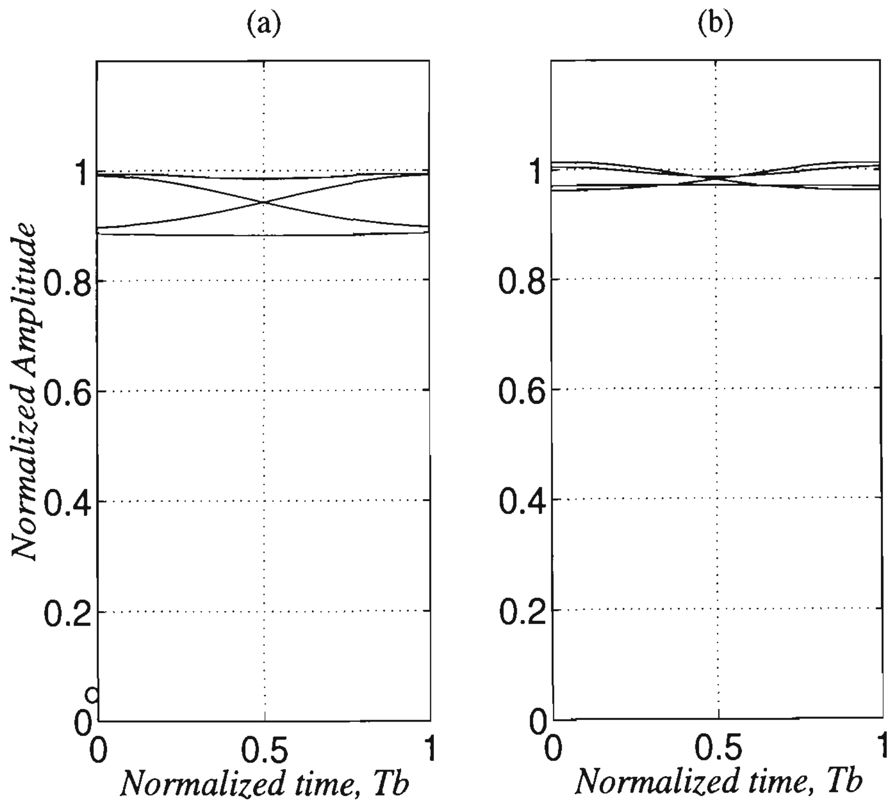

Fig. 3.3. The envelope eye diagram of GMSK3 BT=0.3 filtered with: (a) a Gaussian low pass filter with BT=0.4 (b) a maximally flat filter with BT= 0.6.

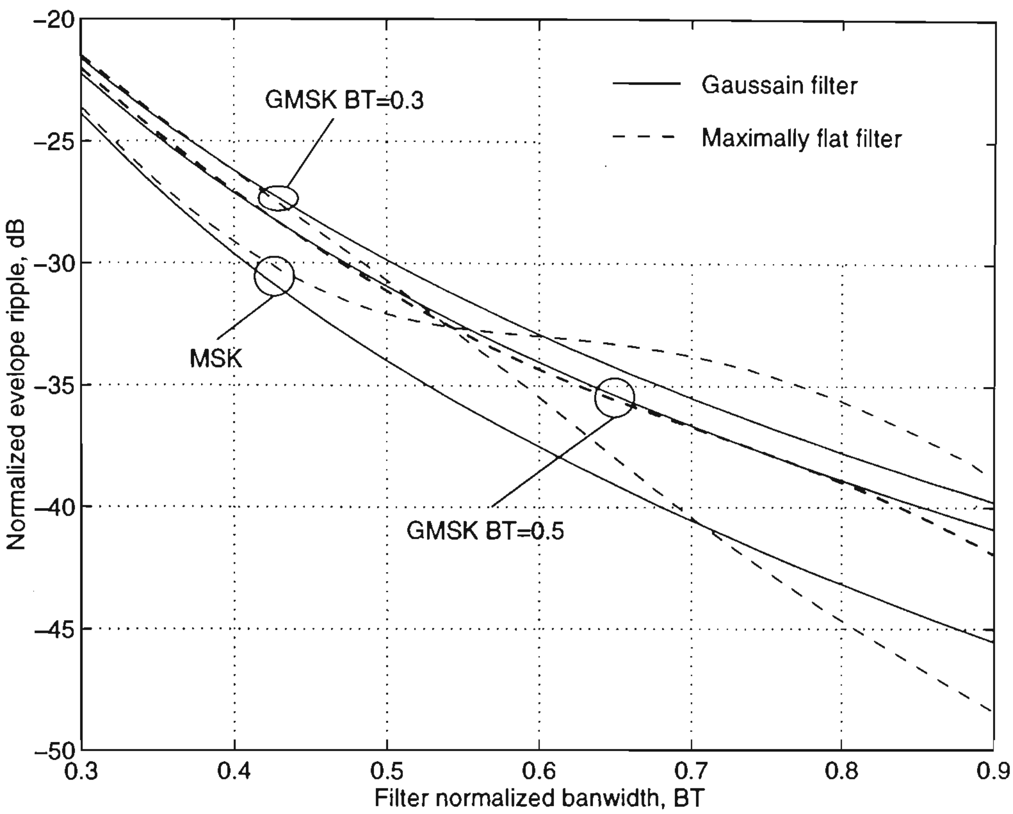

Fig. 3.4. The normalized envelop distortion of MSK, GMSK BT=0.5 and GMSK BT=0.3, filtered with Gaussian and Maximally flat lowpass filters.

GMSK BT=0.5 modulation schemes are depicted versus filter bandwidth with Gaussian and maximally flat filters. For MSK, the Gaussian filter always produces a better ripple reduction because of its larger transient band. For GMSK BT=0.5, both filters have similar performances, however, for GMSK BT=0.3, because of the concentration of energy in the lower frequencies, the maximally flat filter exhibits a better performance. While increasing the filter bandwidth reduces the envelope ripple, it can increase the noise and possibly adjacent channel interference. An optimum filter bandwidth can be found to jointly minimize the envelope distortion, noise and adjacent channel interference. Analysis of the simulation results shows that the optimum bandwidth is a function of interference to noise ratio (INR). Fig. 3.5 shows the 3dB normalized optimum bandwidth of a Gaussian filter for different INR. When the INR is reduced so that noise become dominant, e. g. 0dB, the optimum bandwidth is about BT=0.3 agrees with the optimum bandwidth (BT=0.315) found by Murota [27] using signal degradation in a static channel.

3.3 VA Truncation Depth

Truncation of survivors to some manageable length M [145] is necessary when the state sequences are very long or infinite in the Viterbi Algorithm. This will reduce the size of the required memory and hence complexity. Fig. 3.6 shows the probability of error for a VA-ICIC receiver with different CIR and CNRs for GMSK BT=0.3. It shows that a depth of $M=5$ can be accepted without any significant truncation cost. The same results are repeated for MSK and GMSK BT=0.5 modulation schemes.

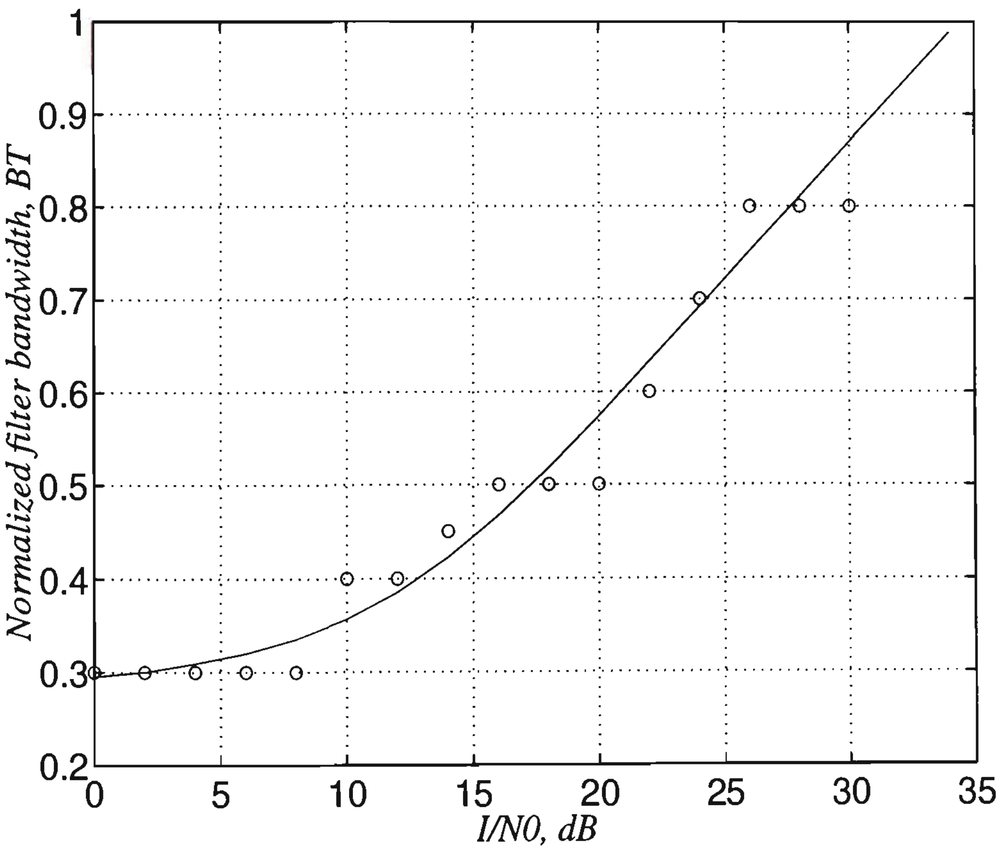

Fig. 3.5. The optimum 3dB normalized bandwidth of quadrature demodulator filters for GMSK BT=0.3.

3.4 Effect of Fading Rate

One of the main assumptions in ICIC is that the amplitude and phase of CCI is approximately constant over one bit interval which is not always applicable. For instance, in a fading channel, particularly in deep fades, the signal envelope may change rapidly over one bit interval. The severe envelope variation of CCI in deep fades is not very important because in these cases the CCI is weak and the probability of error is poor. However, the envelope variation of a powerful interferer cannot be neglected.

The envelope variation of co-channel interference not only depends on its fading

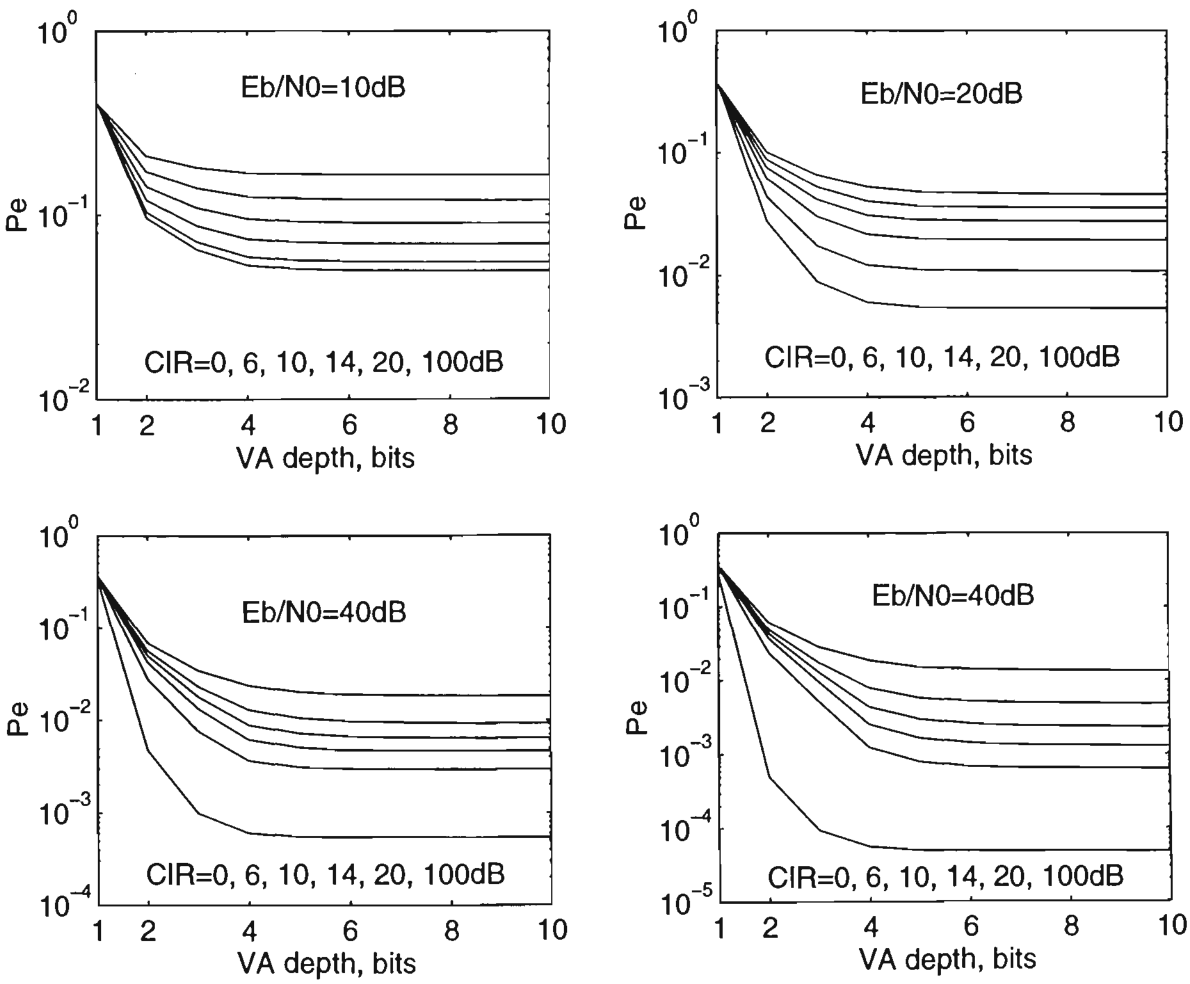

Fig. 3.6. BER performance of VA-ICIC receiver for GMSK BT=0.3 with different E_b/N_0 and VA depth.

channel but may also be dependent on the desired signal fading rate if the conventional fading cancellation method is applied (Fig. 3.7a, fading cancellation method-1). In the conventional fading cancellation method, the received signal, $r(t)$, is divided by the desired signal fading estimate, $\hat{c}(t)$, to obtain the unfaded desired signal as,

$$r'(t) = \frac{r(t)}{\hat{c}(t)} = \frac{c(t)}{\hat{c}(t)}w(t) + \frac{d(t)}{\hat{c}(t)}i(t) + \frac{n(t)}{\hat{c}(t)} \tag{3.3}$$

where $w(t)$ and $i(t)$ are the desired and interfering signals, $c(t)$ and $d(t)$ are their multiplicative fading respectively.

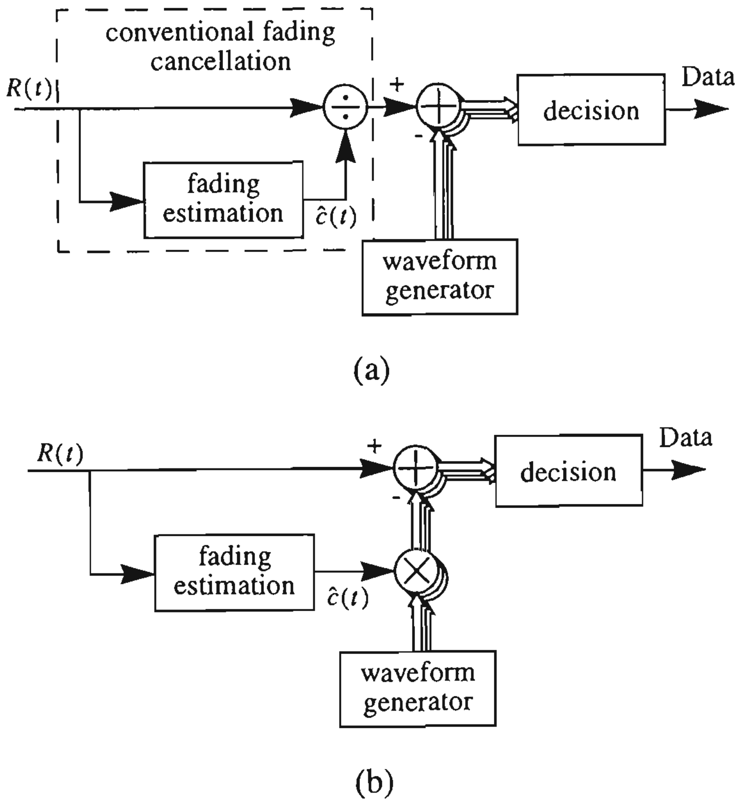

Fig. 3.7. ICIC with (a) conventional fading cancelling (method-1) (b) proposed fading cancelling (method-2).

With an ideal fading estimation (i.e. $\hat{c}(t) = c(t)$), (3.3) can be written as

$$r''(t) = w(t) + \frac{d(t)}{c(t)}i(t) + \frac{n(t)}{c(t)} \tag{3.4}$$

which results in complete fading cancellation from the desired signal. The interference canceller then subtracts the desired signal estimate to obtain the residue

$$\varepsilon(t) = [w(t) - \hat{w}(t)] + \frac{d(t)}{c(t)}i(t) + \frac{n(t)}{c(t)} \tag{3.5}$$

Equation (3.5) shows that with this method of fading cancellation, the interference is subject to both its own and the desired signal's channels. This may cause severe envelope variation of the interference. This method can also amplify the noise.

An alternative fading cancellation method, is proposed (Fig. 3.7b, fading cancellation method-2), where the cancellation is not performed in advance. Instead, the desired signal estimates are multiplied by the fading estimate and then subtracted from the received signal

$$\varepsilon(t) = r(t) - \hat{c}(t)\hat{w}(t) = [c(t)w(t) - \hat{c}(t)\hat{w}(t)] + d(t)i(t) + n(t) \tag{3.6}$$

A similar method was previously used in CDMA to cancel the effect of fading [149]. Equation (3.6) shows that the fading cancellation method-2, does not affect interference and noise.

As far as complexity is concerned there seem to be no significant difference. Method-2 requires several multipliers, however, method-1 requires a division operation (Fig. 3.7a).

Both fading cancellation methods are simulated for GMSK BT=0.3 modulation scheme. The fading rate is considered to be 100Hz. The signal bit rate is selected to give a normalized fading rate of 0.0125 to 3.7e-4.

Fig. 3.8 shows the bit error rate of the system with both fading cancellation methods for two values of f_dT. For small signal to noise ratios ($E_b/N_0 \leq 20dB$), the BER is insensitive to f_dT product and type of fading cancellation. However, the BER largely changes for large SNRs. Fig. 3.9 shows the BER with both fading cancellation methods for $E_b/N_0 = 30dB$ and $E_b/N_0 = 50dB$, versus f_dT. With method-2 for $E_b/N_0=30dB$, up to $f_dT = 0.003$, the probability of error is approximately constant and after that, it increases as f_dT increases. For $E_b/N_0 = 50dB$, except for a very small f_dT, the probability of error increases with increasing f_dT. These investigations indicate that fading cancellation method-2 is a more suitable scheme for ICIC receivers. If the minimum E_b/N_0 is limited to 30dB and a fading rate of 100Hz, the receiver using fading cancellation method-2 is able to work down to a data rate of 32kbits/s without any significant performance degradation.

3.5 Effect of The Second Interferer

Although the concept of ICIC has been defined for cancelling of only one interferer, it is still possible to cancel more than one co-channel interferer. This follows from the fact that, in fading channels, interferers fade independently and occasionally one is

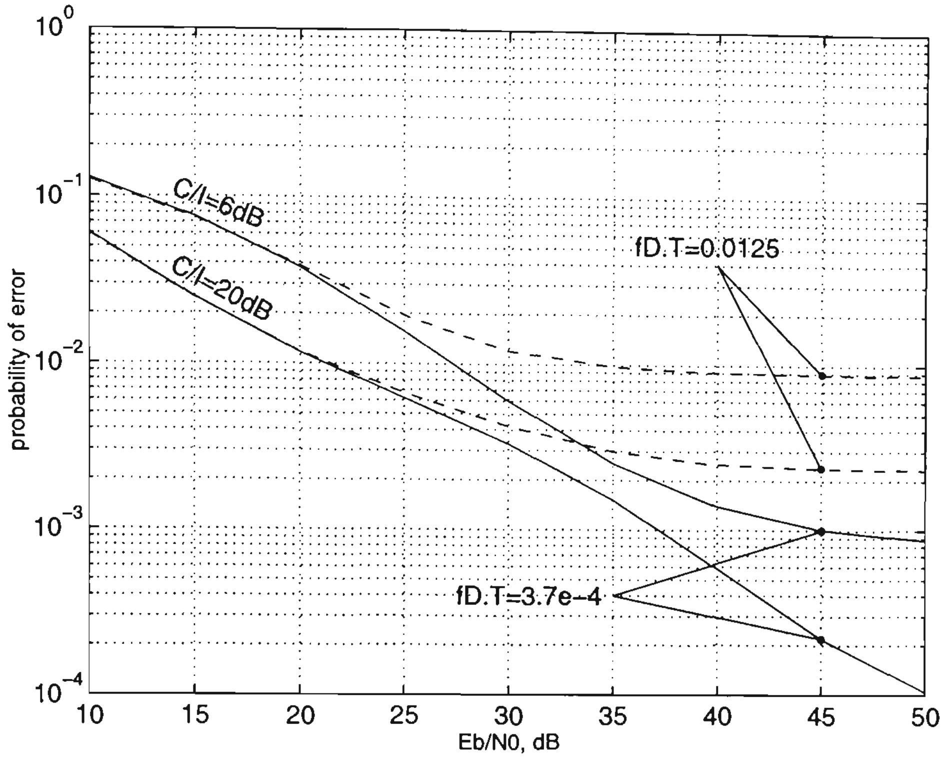

(a)

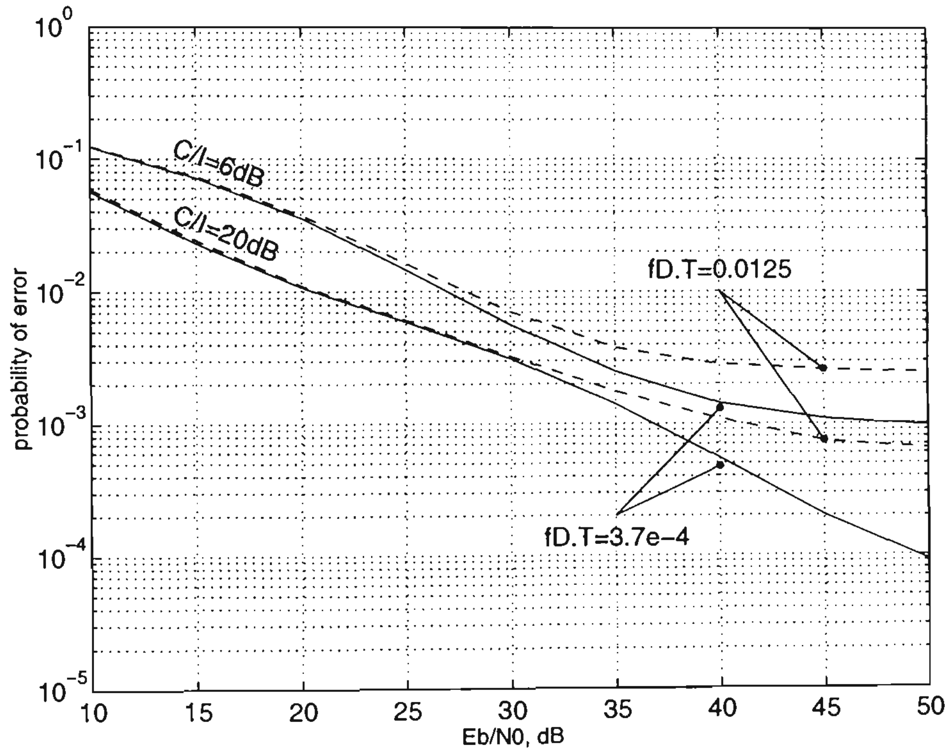

(b)

Fig. 3.8. BER performance of VA-ICIC for GMSK BT=0.3 for normalized fade frequencies of $f_dT = 0.0125$ and $f_dT = 0.00037$ (a) for fading cancellation method-1, (b) for fading cancellation method-2.

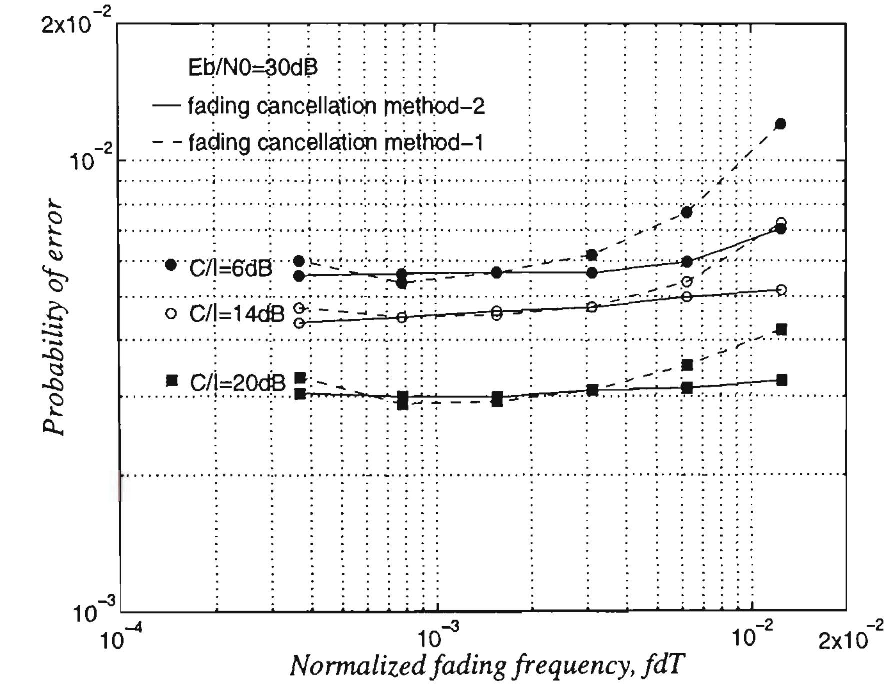

(a)

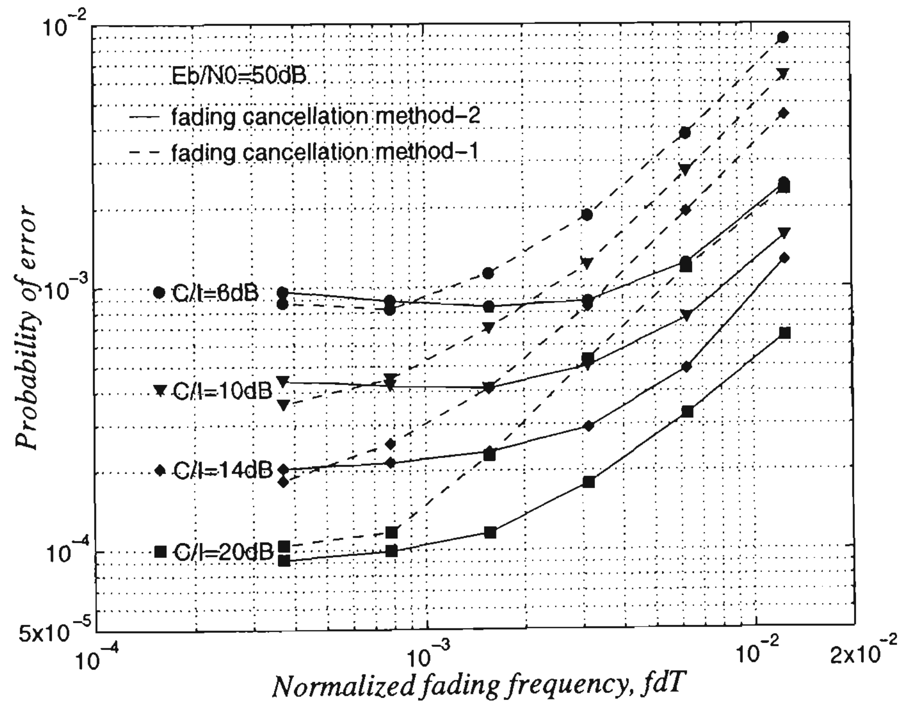

(b)

Fig. 3.9. BER performance of the VA-ICIC with different fading rates for GMSK BT=0.3 for (a) E_b/N_0=30dB and (b) E_b/N_0=50dB.

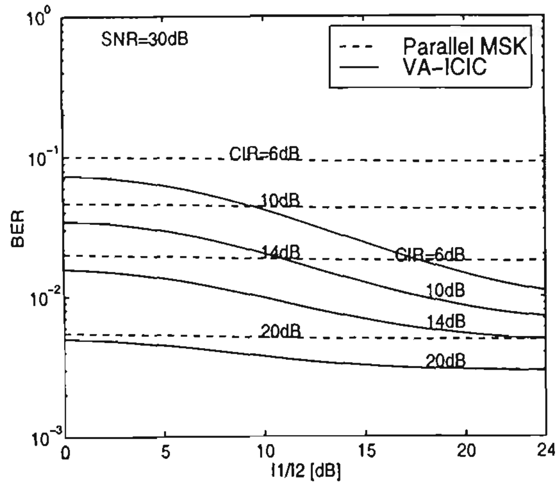

Fig. 3.10. BER performance of VA-ICIC in the presence of two interferers versus the ratio of first to second interferer (I1/I2) in a Rayleigh fading channel with SNR=30dB. Modulation is GMSK BT=0.3.

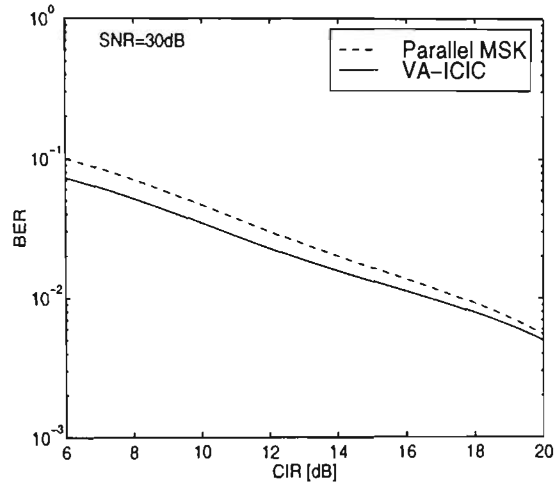

Fig. 3.11. BER performance of VA-ICIC in the presence of two equal power interferers versus signal to interference ratio in a Rayleigh fading channel with SNR=30dB. Modulation is GMSK BT=0.3.

dominant [40]. A simulation study was performed to investigate the effect of the second interferer. It is assumed that both interferers and the desired signal fade independently. In Fig. 3.10, the BER performance of VA-ICIC versus the first to second interferer ratio (I1/I2) for $E_b/N_0=30dB$ is depicted. Increasing I1/I2, which implies one interferer becomes dominant, improves the BER performance. In the worst case (i.e. I1/I2 = 0dB) and Pe=0.01, VA-ICIC still produces a 1dB better BER performance than the reference receiver (Fig. 3.11).

3.6 Effect of Delay Spread in Interference[1]

The performance of the ICIC receivers can be largely deteriorated by the envelope ripples caused by delay spread in interference. The extent of the performance degradation due to this problem, is investigated for the VA-ICIC in a channel given in Fig. 3.12. The interferer, its delay spread and the desired signal are subject to independent fading channels. In this investigation, the desired signal itself does not

1.The effects of delay spread on the desired signal and both desired and interference signals are topics of sections 4.5 and 4.6.

have any delay spread component ($W_d = 0$). The BER performance obtained under this condition, (Fig. 3.13) is nearly constant with small delay spreads (Td<0.2T). As the interference to delay spread power ratio (I/Id) increases, the BER performance improves due to the weaker envelope fluctuation. When the delay is small (less than T), the BER performance is better than in the presence of two independent interferers (Fig. 3.10). This is due to correlation between signal and its delay spread. As the delay spread increases beyond T (not shown) the overall BER performance approaches the BER performance obtained when two independent interferers are present. In contrast to VA-ICIC, the reference receiver does not show any significant sensitivity to delay spread. As discussed in section 2.5, this receiver is unaffected by the number of interferers. Therefore, zero delay conditions (where the interferer and its delay spread form a single interferer) or very long delay spreads (two independent interferers) do not affect the performance of the reference receiver.

3.7 Sensitivity to Desired Signal Pulse Shape Imperfections

In the ICIC technique any imperfection in the estimation of the desired signal can lead to a degraded performance. Some of these imperfections are: timing

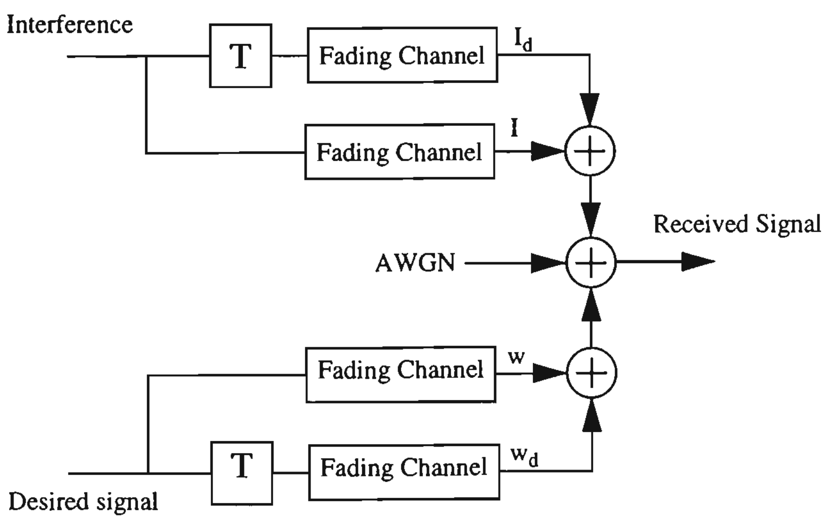

Fig. 3.12. The channel used in the study of delay spread.

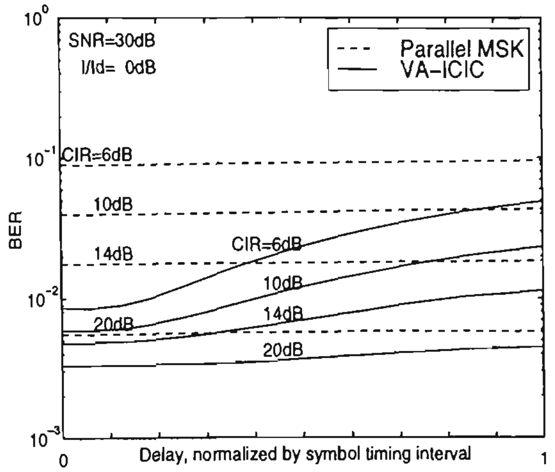

(a)

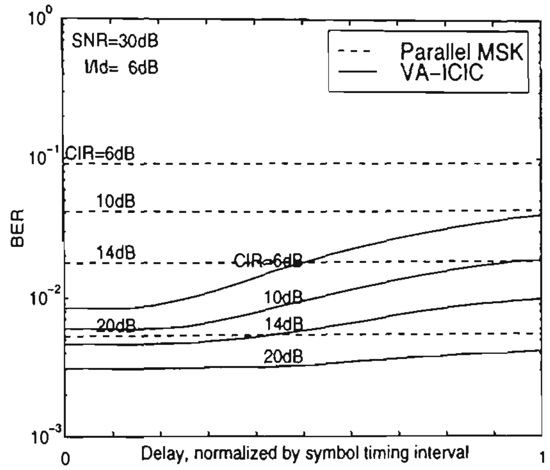

(b)

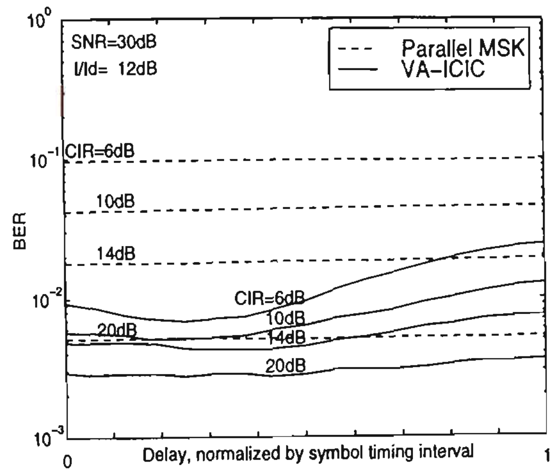

(c)

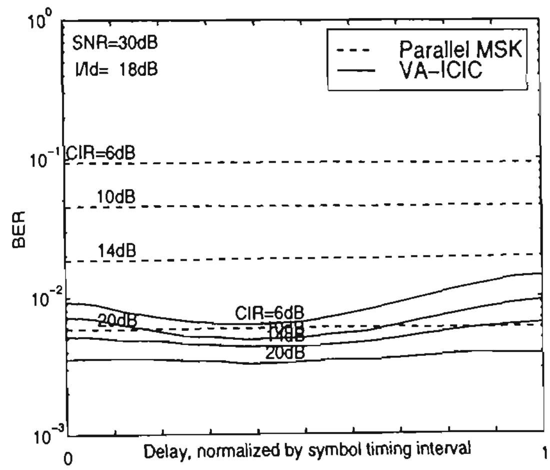

(d)

Fig. 3.13. BER performance of VA-ICIC in the presence of delay spread in interference (a) interferer to its delay spread ratio (I/Id) of 0dB, (b) 6dB, (c) 12dB and (d) 18dB.

misalignment of the received signal and its estimated pulse shapes, and phase and gain distortion of the desired signal due to channel fading. In the following sections, the sensitivity of the VA-ICIC to these imperfections is investigated by computer simulation.

3.7.1 Sensitivity to Timing Error

Timing recovery circuits usually synchronize the local clock to the received data signal with good accuracy even in poor signal to interference ratios [106]. However, because of the presence of noise, co-channel and adjacent channel interferences, will introduce jitter on the recovered timing clock. In ICIC, any timing misalignment of the regenerated waveforms with the desired signal may result in a residual unwanted signal that can be an extra source of error. This undesired jitter is usually limited, and may not be so critical to timing errors.

The BER performance of VA-ICIC receiver versus timing error is shown in Fig. 3.14.a. According to this figure timing error can substantially deteriorate the BER performance of the VA-ICIC receiver. Fortunately, for small timing errors, the degradation of the BER is not significant. To highlight this, the BER performance for

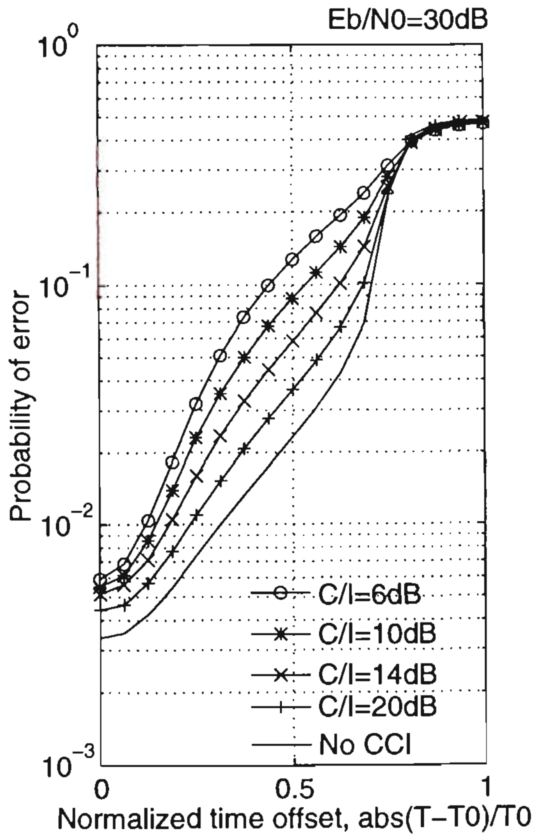

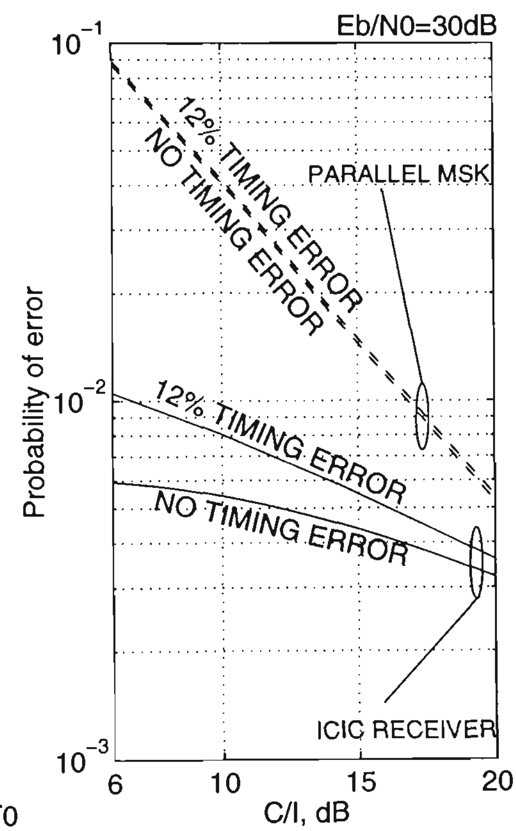

Fig. 3.14. (a) BER performance of VA-ICIC versus timing offset for GMSK BT=0.3 modulation scheme (b) probability of error versus carrier to interference ratio with zero and 12% timing offset in a Rayleigh fading channel with E_b/N_0=30dB.

12% timing error is depicted in Fig. 3.14.b which shows that the VA-ICIC receiver still gives 10dB better performance over the conventional coherent receiver.

3.7.2 Sensitivity to Channel Estimation Errors

The channel estimation error is one of the major impairments in the regeneration of the desired signal pulse shapes. In Chapter 4, the application of pilot symbol channel estimation of the VA-ICIC receiver will be discussed in detail. In this section, the problem is investigated with a different approach. The effect of phase and gain estimation errors on the BER performance of VA-ICIC are individually investigated.

3.7.2.1 Phase Error

The received signal complex envelope can be shown by $r(t) = c(t) \cdot w(t) + i(t) + n(t)$, where $w(t)$, $i(t)$ and $n(t)$ are the desired, interference and noise signals respectively. The complex desired signal channel can be shown by $c(t) = \Re e^{j\varnothing}$, where its amplitude and phase change with time, but for simplicity they are considered constant over one bit interval. The desired signal channel estimator estimates this channel and attempts to cancel it. Two solutions for fading cancellation are discussed in Section 3.4. In the first solution (i.e. conventional fading cancellation) the receiver divides the received signal by the estimated channel $\hat{c}(t) = \hat{\Re} e^{j\hat{\varnothing}}$

$$r'(t) = \left(\frac{\Re}{\hat{\Re}}\right) e^{j(\varnothing - \hat{\varnothing})} \cdot w(t) + [i(t) + n(t)] \cdot \left(\frac{1}{\hat{\Re}}\right) e^{-j\hat{\varnothing}} \tag{3.7}$$

The residual signal after the subtraction of the desired signal estimates is

$$\varepsilon(t) = \left(\frac{\Re}{\hat{\Re}}\right)e^{j(\varnothing - \hat{\varnothing})} \cdot w(t) - \hat{w}(t) + [i(t) + n(t)] \cdot \left(\frac{1}{\hat{\Re}}\right)e^{-j\hat{\varnothing}} \tag{3.8}$$

Assuming the gain estimation is correct it, (3.8) is simplified to

$$\varepsilon(t) = w(t) - \hat{w}(t) + [i(t) + n(t)] \cdot \left(\frac{1}{\Re}\right)e^{-j\hat{\varnothing}} + \zeta_1(t) \tag{3.9}$$

where $\zeta_1(t) = [e^{j(\varnothing - \hat{\varnothing})} - 1] \cdot w(t)$ is a residual signal which acts as a new interference source.

In the second solution, i.e. fading cancellation method-II, the residue will have the form of

$$\varepsilon(t) = [\Re e^{j\varnothing} w(t) - \hat{\Re} e^{j\hat{\varnothing}} \hat{w}(t)] + i(t) + n(t) \tag{3.10}$$

Equation (3.10) without gain error can be written as

$$\varepsilon(t) = \Re e^{j\varnothing}[w(t) - \hat{w}(t)] + i(t) + n(t) + \zeta_2(t) \tag{3.11}$$

Section 3.4 and (3.11) demonstrate that interference and noise energy are not affected by this fading cancellation method. Nevertheless, the phase error causes a residual interference source shown by $\zeta_2(t) = \Re\hat{w}(t)[e^{j\varnothing} - e^{j\hat{\varnothing}}]$.

Fig. 3.15 shows the BER performance of the GMSK BT=0.3 modulation scheme versus phase errors for $E_b/N_0=30dB$. The BER performance of the parallel-MSK receiver is also depicted in the same graph. These results show that the VA-ICIC receiver has similar sensitivity to phase error, for both fading cancellation methods and its sensitivity increases as the CIR is decreased.

3.7.2.2 Gain Error

When the phase estimation is correct, using conventional fading cancellation, (3.8) can be simplified to

$$\varepsilon(t) = w(t) - \hat{w}(t) + [i(t) + n(t)] \cdot \left(\frac{1}{\hat{\Re}}\right) e^{-j\varnothing} + \zeta_3(t) \tag{3.12}$$

where noise and interference powers are directly affected by the gain estimate. $\zeta_3(t) = \frac{\Re - \hat{\Re}}{\hat{\Re}} \hat{w}(t)$ is a residual interference which tends to zero as the gain estimation error decreases.

For fading cancellation method 2, equation (3.10) can be written as

$$\varepsilon(t) = [w(t) - \hat{w}(t)]\Re e^{j\varnothing} + i(t) + n(t) + \zeta_4(t) \tag{3.13}$$

where $\zeta_4(t) = (\Re - \hat{\Re})e^{j\varnothing}\hat{w}(t)$ is a residual signal which also tends to zero as the gain estimation error decreases. The BER of VA-ICIC versus the gain estimation error is given in Fig. 3.16. The modulation is GMSK BT=0.3 with $E_b/N_0 = 30dB$.

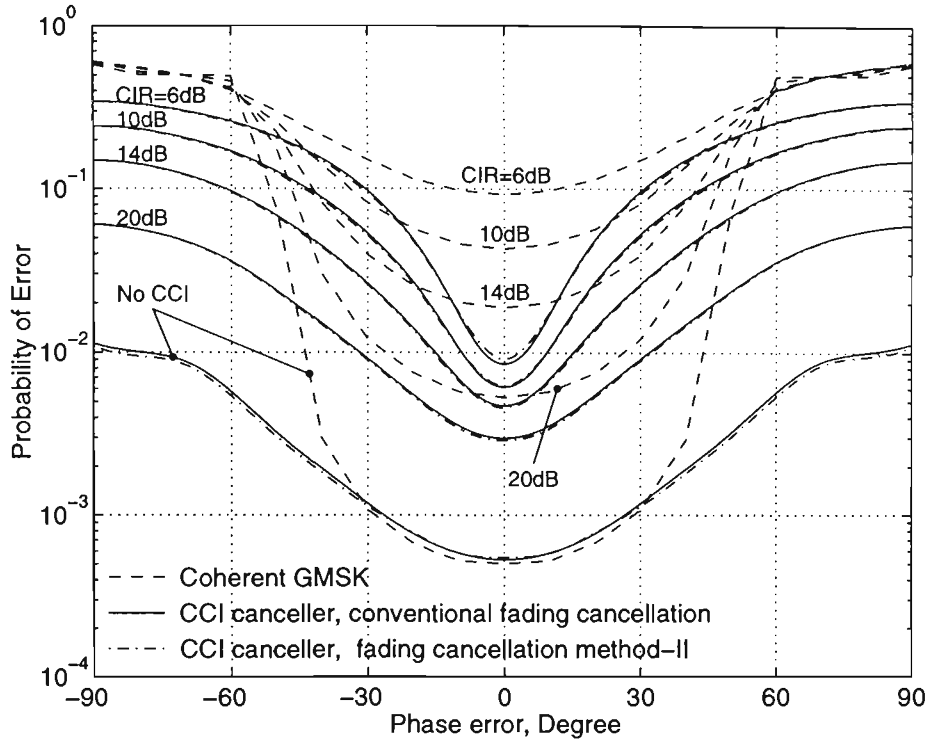

Fig. 3.15. BER performance of VA-ICIC versus phase estimation error. The modulation is GMSK in a Rayleigh fading channel with E_b/N_0=30dB.

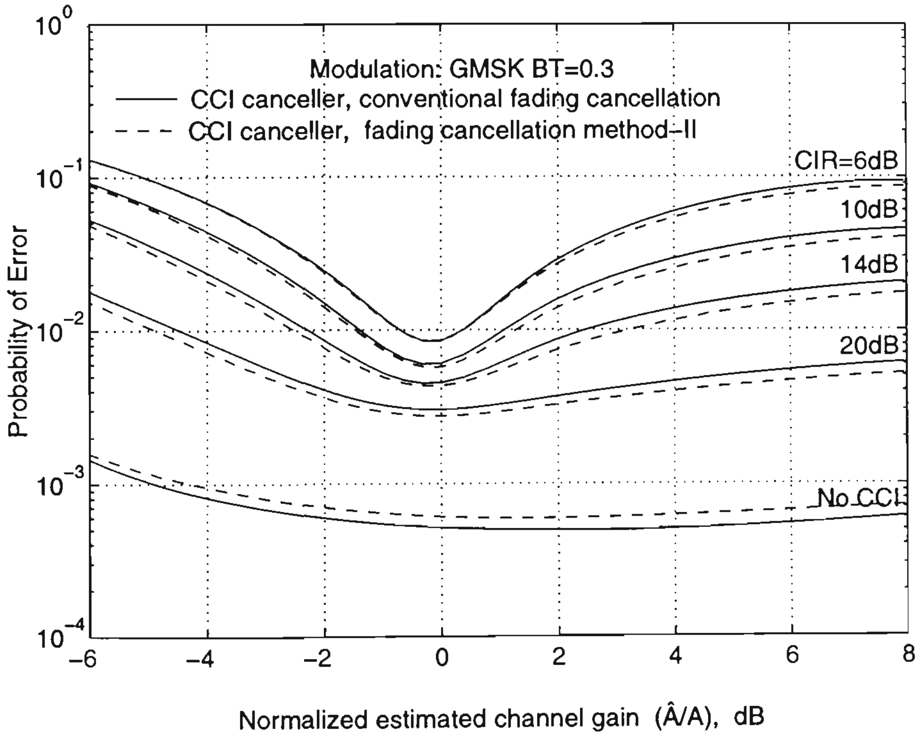

Fig. 3.16. BER performance of VA-ICIC versus amplitude estimation error. The modulation is GMSK in a Rayleigh fading channel with E_b/N_0=30dB.

These results show that the BER performance for both fading cancellation methods is similar and the sensitivity to gain error increases with decreasing CIR.

In conclusion, neither of the mentioned fading cancellation methods have any significant advantage in reducing the gain or phase estimation error.

3.8 Analog to Digital Convertor (ADC) Range

A distortion source in the digital signal processing (DSP) implementation of the ICIC receiver is the analog to digital convertor (ADC) peak power limitation. The ADC range must be adjusted to minimize the Hard-Limiting distortion on the varying power received signal. The distortion can be reduced by putting a lowpass filter after the ADC (as shown in Fig. 3.17). Fig. 3.18 shows the BER performance of the VA-ICIC receiver versus the normalized hard-limiting level. The BER, when the two lowpass filters are placed after ADC (Fig. 3.17), are shown in Fig. 3.19. The Hard-Limiter level is normalized by the desired signal rms level. In general, to avoid the BER performance degradation, the level of Hard-Limiter must be increased as the interference power is increased. The filtering increases ADC dynamic range by approximately 15dB.

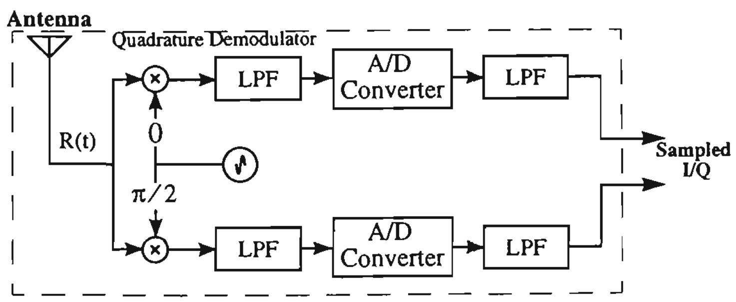

Fig. 3.17. Filtering after analog to digital convertors to reduce quantization noise and hard-limiting distortion.

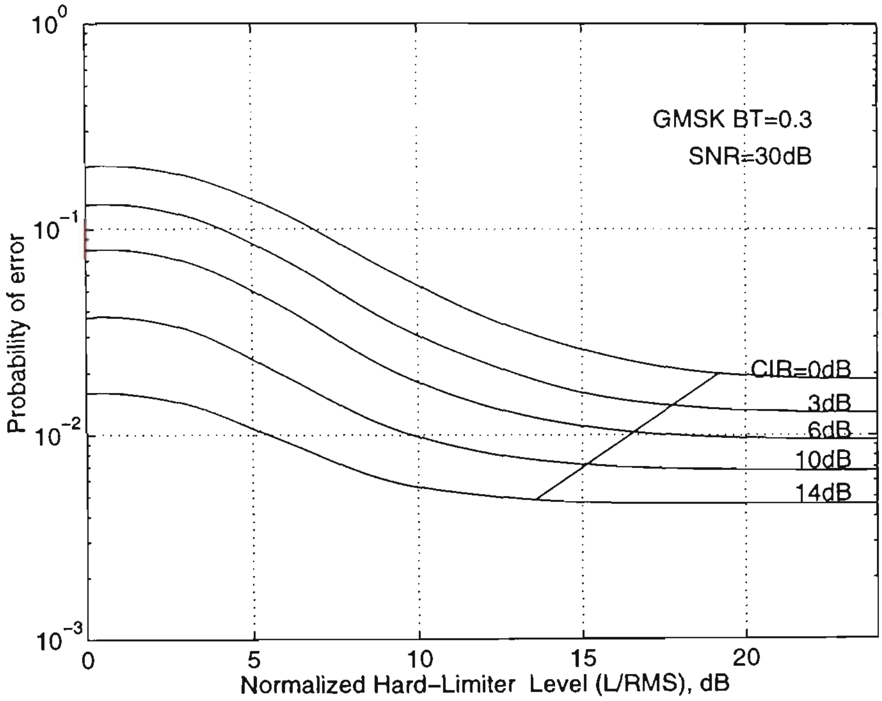

Fig. 3.18. The probability of error of VA-ICIC receiver versus Hard-Limiter normalized level without any filtering after Hard-Limiter in a Rayleigh fading channel with E_b/N_0=30dB and GMSK BT=0.3.

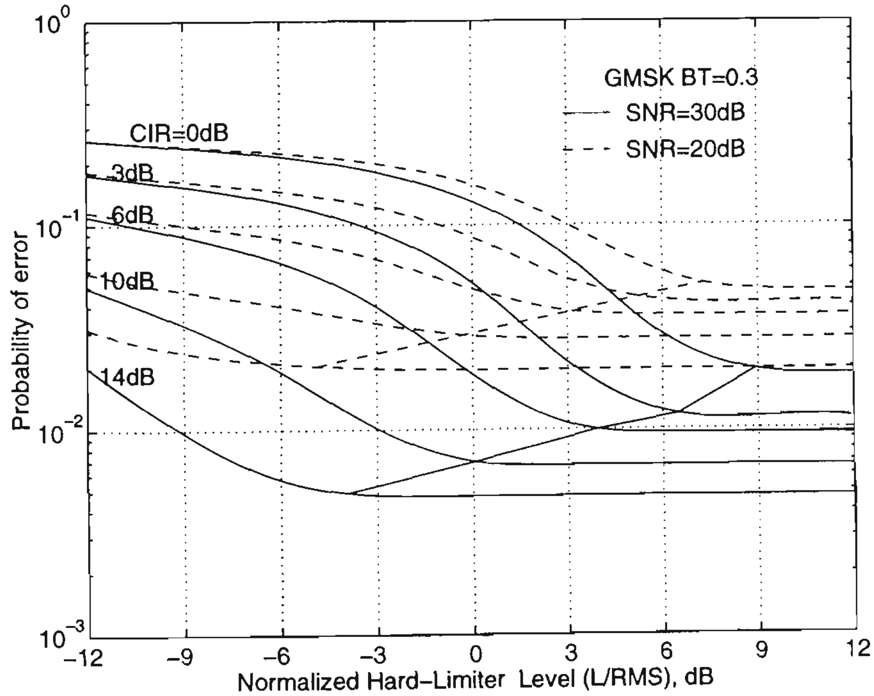

Fig. 3.19. The probability of error of VA-ICIC receiver versus Hard-Limiter normalized level in a Rayleigh fading channel with E_b/N_0=30dB and E_b/N_0=20dB for GMSK BT=0.3. The desired signal is filtered after Hard-Limiter.

3.9 Effect of Quantization

Since the ICIC receiver processes the sampled quantized signal, any quantization error can be a degrading factor. One of the most common quantizers is the linear quantizer. The quantization error due to this quantizer is discussed in this section. The step size of a linear quantizer is defined as

$$\Delta = \frac{V_q}{L_q} \tag{3.14}$$

where V_q is the dynamic range of quantizer and L_q is the number of quantization levels. The quantization error without overload distortion, is usually assumed uniformly distributed in $[[-\Delta/2, \Delta/2]]$. Under this assumption the mean squared quantization error is

$$Q = E\{q^2\} = \int_{-\Delta/2}^{\Delta/2} q^2\left(\frac{1}{\Delta}\right)dq = \frac{\Delta^2}{12} \tag{3.15}$$

The signal to quantization noise ratio can be defined as

$$SQNR = 10\log\frac{\sigma^2}{Q} \tag{3.16}$$

where σ^2 is the input signal variance. Fig. 3.20 shows the BER performance of VA-ICIC in a fading channel with different quantization levels. The quantizer is

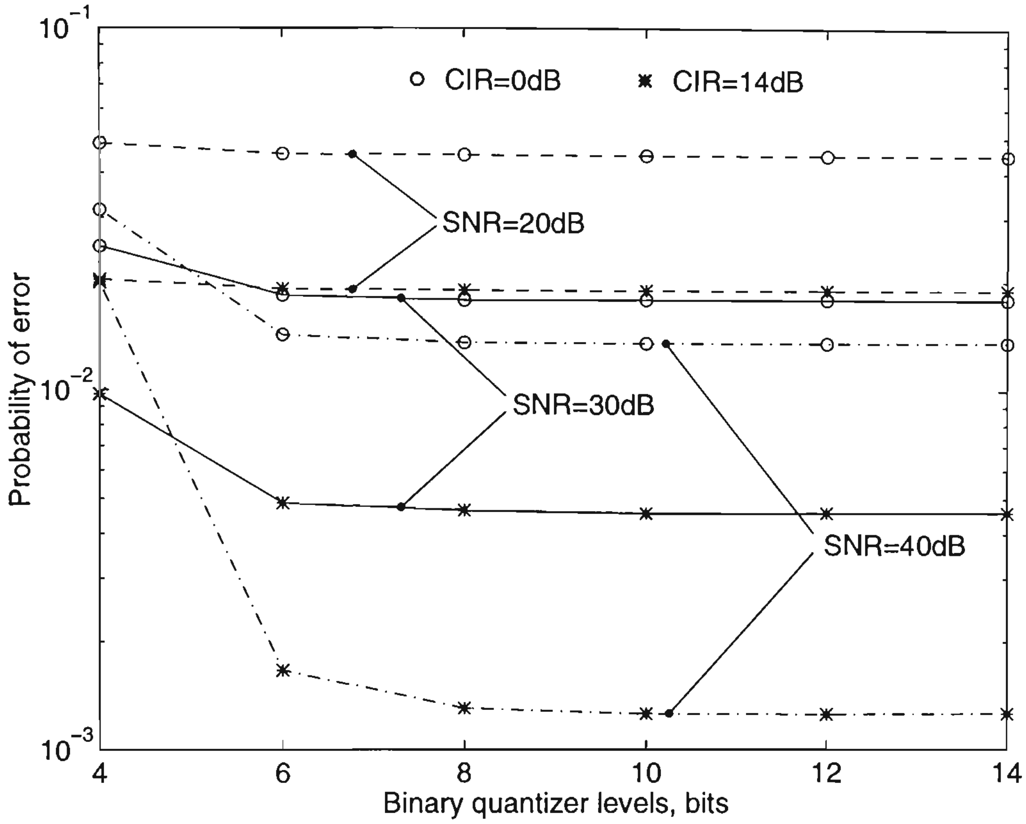

Fig. 3.20. BER performance of VA-ICIC receiver versus quantization levels for GMSK BT=0.3 in a Rayleigh fading channel.

followed by a lowpass filter (Fig. 3.17), to reduce the Hard-Limiting effect. This figure shows that a six bit quantizer is almost sufficient. Further simulations showed that in a circuit configuration without this lowpass filter, an eight-bit quantizer was necessary.

3.10 Effect of Timing offset between CCI and desired signal

Essentially, an ICIC receiver, is insensitive to co-channel interference timing because it uses the interference envelope. However, as indicated in Fig. 3.3, the envelope of CCI is not constant. Therefore, the data detection might be influenced by timing offset between desired signal and CCI. To address this problem, the BER performance of ICIC receiver is studied by Monte Carlo simulation both in static and Rayleigh fading channels. The simulation results did not indicate any sensitivity to the timing offset.

3.11 Conclusion

The effect of several important hardware implementation parameters on the performance of VA-ICIC was investigated. These parameters were: over sampling rate, filtering in the I/Q down converter, VA depth, fading rate, timing, phase and gain estimation errors, delay spread and quantization error. An optimum sampling rate (oversampling of 2 samples per data symbol) which minimizes the probability of error was found. In addition a fading cancellation method was proposed to provide a wider acceptable bit rate range for a given fading rate. These simulations showed that the ICIC schemes are highly sensitive to: timing error, channel estimation error, and delay spread.

In the next chapter, the performance of VA-ICIC with pilot symbol channel estimation will be investigated. The effect of delay spread on both the desired and interference signals will also be studied.

Chapter 4

Co-channel Interference Cancelling with Pilot Symbol Fading Cancellation

The need to have the knowledge of channel gain and phase for the desired signal was established in the previous chapters. In mobile communication channels the phase of the desired signal changes due to multipath fading, and its amplitude fluctuates owing to both path loss and multipath gain. To obtain the gain and phase of the desired signal, some types of channel estimation techniques must be utilized. Channel sounding [150]-[152], techniques such as pilot symbol assisted (PSA) and pilot tone assisted (PTA) methods are effective for precise estimation of the channel characteristics and consequent compensation of fading distortion. In PTA, a pilot tone is inserted in the transmitted spectrum. The receiver extracts the pilot and uses the result as a phase and gain reference. If the tone is placed at the channel edge it can suffer from distortion due to being close to the filter band edge and due to the adjacent channel interference [152]. If the tone is placed at the centre of the signal band, certain techniques must be used to provide a notch in the signal spectrum to prevent interference between pilot tone and the signal. These techniques include: (i) using an appropriate modulation scheme with a spectral notch at the location of pilot symbol, (ii) applying a spectral shaping code [132], and (iii) moving the signal frequency components by a Transparent Tone-in-Band (TTIB) scheme [150]. However, most of these methods need complicated transmitter/receiver structures. Another disadvantage of the PTA technique is that the pilot tone limits the spectral peak power and makes the envelope nonconstant [151]. This is destructive to the performance of ICIC receivers which are sensitive to envelope variation. On the other hand, pilot symbol aided fading cancelling [152], which does not have these disadvantages, can accomplish fade compensation for a wide range of Doppler Spread [153].

Pilot symbol aided channel estimation has been addressed by a number of authors. It was first proposed by Moher and Lodge [152] for 8-PSK and 16QAM in a Rician channel. Later, Sampei and Sunaga [154-155] applied PSA to the same modulation schemes but in a Rayleigh fading channel. Cavers analysed PSA in Rayleigh fading channels [153] with a delay spread [156]. The application of PSA to nonselective Rayleigh fading channels has been considered in [157]. A combination of PSA and Decision-Directed channel estimators on shadow fading channels has been reported by Irvine and McLane [158]. An application of PSA channel estimation to GMSK modulation scheme has been addressed by Leung [132]. PSA with co-channel interference has been investigated by Cavers and Varaldi [159]. Pilot and data symbol aided channel estimation in the presence of CCI and AWGN has been studied by Lau and Cheung [160]. They showed that using data symbols as well as pilot symbols can substantially improve BER performance.

In this chapter the PSA-GMSK developed in [132] is modified and employed to estimate the channel gain and phase of the desired signal. The obtained channel information is then used in VA-ICIC and its BER performance in AWGN and CCI is evaluated.

4.1 Pilot Symbol Aided Modulation Technique

A block diagram of the pilot symbol insertion method is shown in Fig. 4.1. In the PSA fading cancellation method, known pilot symbols are periodically inserted in the transmit data sequence (Fig. 4.2) to measure the channel distortion [152]-[132]. This is to generate a reference phase vector in the transmit signal (Fig. 4.3). The receiver derives the signal phase and amplitude from the samples of the received signal at the pilot symbol positions. Distortion in other symbols is compensated by interpolating

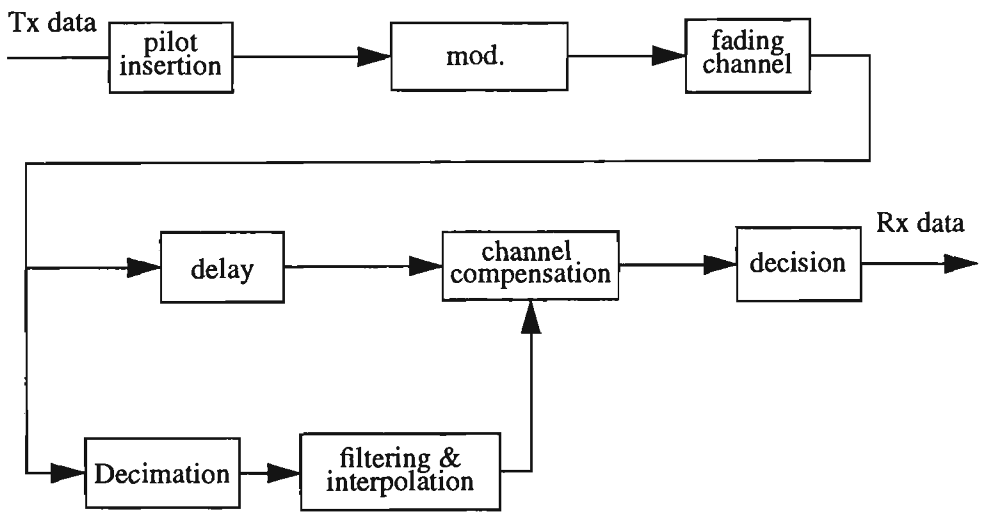

Fig. 4.1. Block diagram of a communication system with pilot symbol aided fading cancellation.

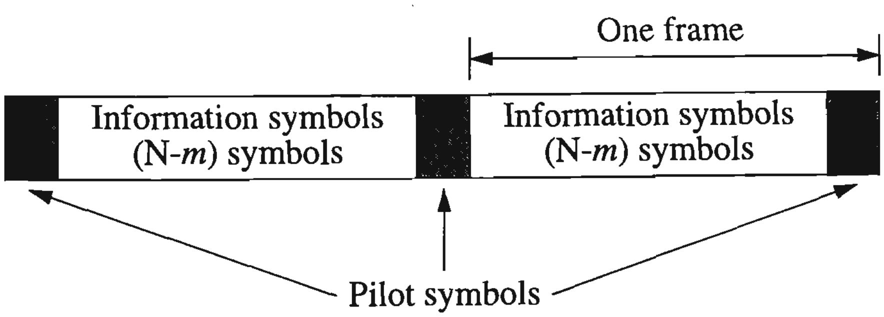

Fig. 4.2. Frame format of pilot symbol insertion method.

the sequence of the sampled vector. Since the sampled signal contains both channel phase and gain information it can be used to correct signal phase and gain.

In the frame format of PSK modulation schemes, a single pilot symbol is inserted for every $(N-1)$ information symbols. This method is not applicable for CPM modulation schemes, in which each pilot symbol may have intersymbol interference (ISI) from its adjacent symbols. The ISI changes the reference gain and phase randomly and prevents accurate channel estimation. Thus, for CPM schemes, additional symbols are required to remove ISI from pilot symbols. The frame size, N, is chosen considering the channel fading rate f_d and the system transmission efficiency. Large N is desirable for high transmission efficiency but it is detrimental to channel sounding accuracy. Pilot symbol power efficiency can be calculated by $10\log\left(\frac{N-m}{N}\right)\ dB$, where m is the number of pilot symbols in the frame.

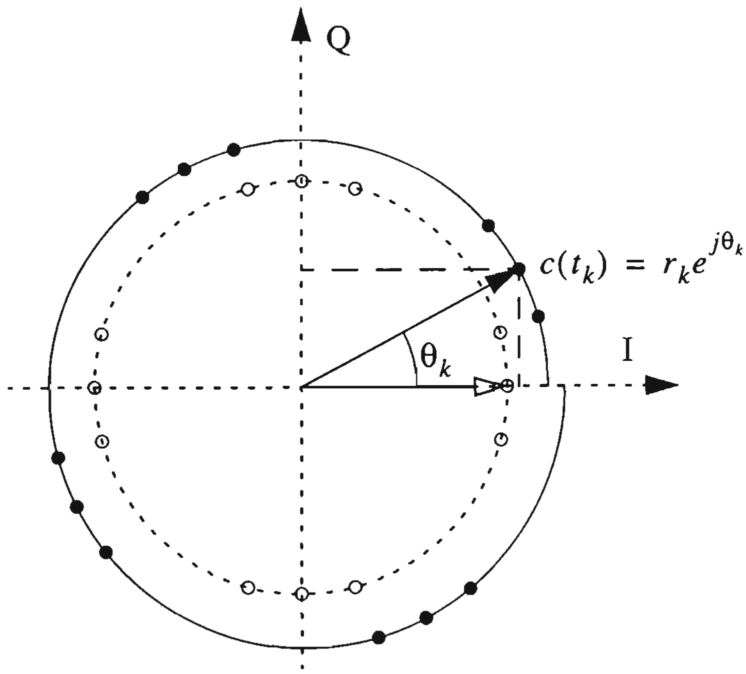

Fig. 4.3. An example of sampling event at the pilot symbol position in the receiver for GMSK modulation scheme. Solid line shows the faded signal trajectories and dashed line shows unfaded signal trajectories. The white and black circles show the signal constellation with and without fading, respectively.

A constant pilot sequence, however, results in spectral harmonics at multiples of the pilot rate. This spectral harmonics can be eliminated by inserting pilot symbols in a random manner with a sequence known at the receiver [152]. In long frame sizes (pilot rate is much smaller than the bit rate) however, most of the strong spectral harmonics fall inside the signal bandwidth and therefore randomization is not necessary.

A block diagram of a pilot symbol insertion method for GMSK modulation schemes is shown in Fig. 4.4. In this method, GMSK is considered as a partial response $\frac{\pi}{2}$-shift BPSK signalling with differential encoding (see Section 2.7). However the system in Fig. 4.4 is not a practical approach because of the complicated and nonlinear filter structure, but it is helpful to understand the PSA-GMSK scheme. In the PSA-GMSK scheme of Leung [132], for the k^{th} transmit frame, two pilot symbols, $P_i(k)$ and $P_q(k)$, are separately inserted in both the in-phase and the quadrature data streams (Fig. 4.5). The $P_i(k) = +1$ is always constant. The Q-channel pilot $P_q(k)$ is opposite of the last data symbol in the frame k, i.e. $P_q(k) = -S_q(k, N-1)$ where $S_q(k, N-1)$ is the last data symbol in the k^{th} frame in

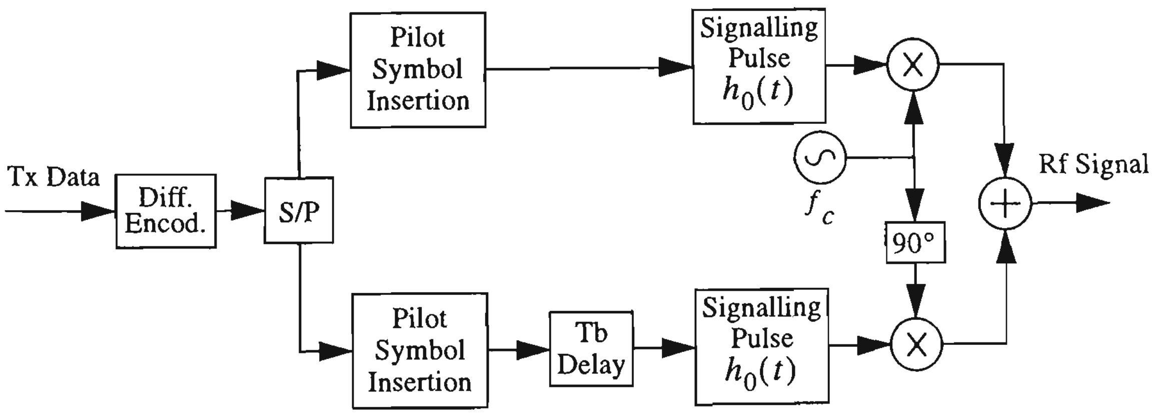

Fig. 4.4. The block diagram of the pilot symbol aided GMSK, proposed in [132]

Q-channel.

The above mentioned method of pilot symbol insertion is suitable only for the transmitter of Fig. 4.4. In the next subsection a modification will be introduced to this PSA-GMSK to make it appropriate to any GMSK transmitter.

4.2 Generalized Pilot Symbol Insertion

The main objective in general pilot insertion is to insert pilot symbols in the input data sequence before any further processing. This makes the transmitter structure independent from pilot symbol insertion. Consider I and Q channel symbols of a data frame of length N as shown in Fig. 4.5. According to the pilot symbol insertion method of [132] with even number of frame bits, the data symbols prior to serial to differential encoding (Fig. 4.4) will be

$$D(k-1, N) = -P_q(k-1)P_i(k-1) \qquad (4.1)$$

$$D(k, 1) = S_i(k, 1)P_q(k-1) \qquad (4.2)$$

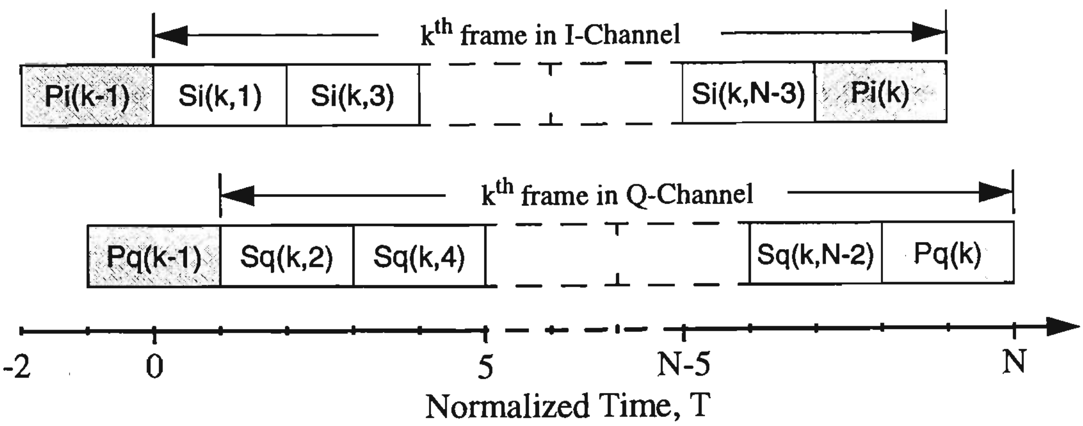

Fig. 4.5. Pilot symbol insertion in the PSA-GMSK modem.

$$D(k, 2) = -S_i(k, 1)S_q(k, 2) \tag{4.3}$$

$$D(k, 3) = S_q(k, 2)S_i(k, 3) \tag{4.4}$$

$$\ldots$$

$$D(k, N-2) = -S_i(k, N-3)S_q(k, N-2) \tag{4.5}$$

$$D(k, N-1) = S_q(k, N-2)P_i(k) \tag{4.6}$$

$$D(k, N) = -P_i(k)P_q(k) \tag{4.7}$$

By setting $P_i(k) = +1$ and $P_q(k) = -S_q(k, N-2)$ in (4.7), we have

$$D(k, N) = S_q(k, N-2)P_i(k) = D(k, N-1) \tag{4.8}$$

where $D(k, N-1)$ is to be found by equations (4.1)-(4.7) with successive substitution. Considering that each $S_i(k, \#)$ [1], $S_q(k, \#)$ and $D(k, \#)$ can only take ± 1 we have,

$$D(k, N-1) = D(k, N-2)D(k, N-3)\ldots D(k, 1)D(k-1, N) \tag{4.9}$$

1.# is a wild card for any number.

It is evident from (4.8) and (4.9) that the symbols $D(k, N)$ and $D(k, N-1)$ can be obtained from other data symbols in the frame. These two identical symbols are the pilot symbols which have to be added to the information symbols. The pilot symbol for data thus can be computed by multiplication of all information symbols and the pilot symbol of the previous frame

$$P(k) = D(k, N-2)D(k, N-3)\ldots D(k, 1)P(k-1) \tag{4.10}$$

As a result, the frame format for the data should follow Fig. 4.6. The number of symbols in a frame, *N*, should always be kept even to avoid alternating the position of pilot between I and Q channels, and also keeping the polarity of the pilot symbol fixed.

In the receiver, after quadrature demodulation, the received signal complex envelope (following the notation of Section 3.4) can be expressed as

$$r(t) = c(t)w(t) + d(t)i(t) + n(t) \tag{4.11}$$

The received signal samples $r(kN)$ corresponding to the I-channel pilot symbol in the k^{th} frame are given by,

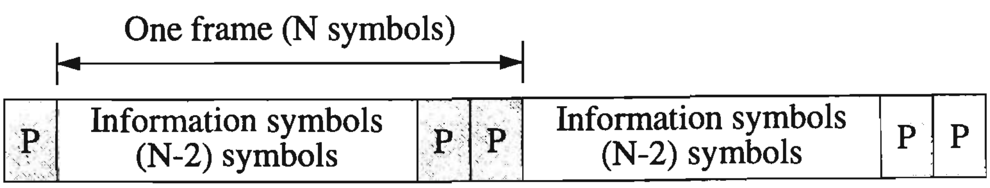

Fig. 4.6. Data frame format for GMSK3. P represents pilot symbol.

$$r(kN) = c(kN)P_i(k) + d(kN)i(kN) + n(kN) \tag{4.12}$$

The estimate of channel fading $\hat{c}(kN)$ at this sampling instant can thus be obtained by dividing $r(kN)$ by the known pilot symbol $P_i(k)$ as,

$$\hat{c}(kN) = \frac{r(kN)}{P_i(k)} = c(kN) + \frac{d(kN)i(kN) + n(kN)}{P_i(k)} \tag{4.13}$$

Interpolation can give prediction of the channel $\hat{c}(kN+m)$ at the m^{th} data position in the k^{th} frame from the channel samples $\hat{c}(kN)$. Consequently, these channel samples can be used to cancel channel effect for the desired signal employing the co-channel interference cancelling techniques described in Section 3.4.

4.3 Interpolation Techniques

The choice of interpolation technique has a serious impact on the performance of PSA-GMSK. It affects the accuracy of fade compensation as well as the processing delay. When designing an interpolator, the important factors that needed to be considered are: the processing delay, the computation cost, the minimum distortion, and the low overhead.

In the interpolation with integer factor N, $N-1$ zeros have to be inserted between two succeeding samples. The zero insertion repeats the spectrum of signal every Nf_s, where f_s is the sampling frequency. Thus, the interpolator has to be followed by a lowpass filter to attenuate the repeated version of the original spectrum. This filter should have specifications such as maximum attenuation in the stop band, linear phase response (to have a low estimation error) and a minimum computational load. Linear phase realization can be achieved by repeating the impulse response with its mirror image [146] at a cost of nearly doubling the processing overhead or using inherently symmetrical impulse response filter such as the even ordered Lagrange interpolator filter [161]. A practical interpolator response can be expressed as,

$$\hat{c}(n) = \sum_{k=-\frac{N-1}{2}}^{\frac{N-1}{2}} h(k)\hat{c}(nN-k) \tag{4.14}$$

where $h(n)$ is the impulse response of the interpolation filter. Selection of the filter type directly depends on the sampling rate of the channel signal, $c(k)$. At low sampling rates, a high stop band attenuation is required to reduce aliasing. On the other hand, at high sampling rates the filter type selection is more relaxed. Filtering, apart from attenuating the repeated versions of the signal spectrum, can reject a significant amount of decimated additive noise and CCI from channel samples arising from the smaller bandwidth of the fading process (compared with the signal; Fig. 4.7). However, including this task in the interpolating filter may increase the interpolation complexity. An alternative method which is proposed here is to filter the pilot symbol samples before interpolation (Fig. 4.8b). This will limit the total

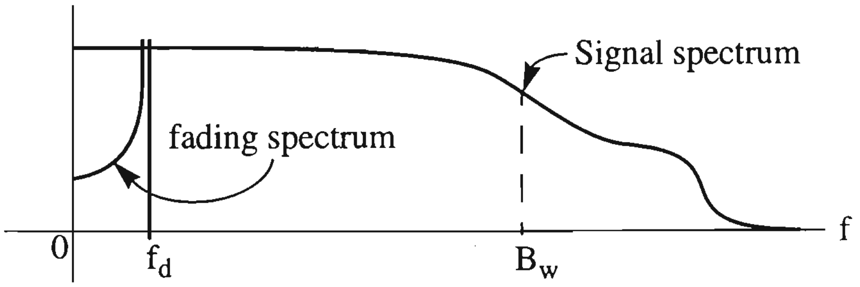

Fig. 4.7. A comparison between signal and fading power spectrum.

bandwidth to make it close to the fading rate rather than the signal spectrum. By using this technique, simple interpolators such as linear interpolation, can be applied without too much distortion [161]. The filtering-and-linear-interpolation (FALI) technique is suitable for applications in which the $f_d T$ product is small.

In both interpolation techniques, the filter type has a large impact on the bit error rate performance. Previous applications of PSA have used various interpolation filters, such as approximately Gaussian [155], Wiener [153] and 4th order Lagrange [132]. Since the channel information is limited to a bandwidth equal to the Doppler shift, the best filter might be a brickwall filter with a lowpass equivalent bandwidth equal to the fade frequency f_d. This brickwall filters impulse response can be written as

$$h(t) = 2B_w \mathrm{sinc}(2B_w t), \qquad -\infty \le t \le \infty \tag{4.15}$$

where $B_w = f_d$ is the filter bandwidth and $\mathrm{sinc}(x) = \dfrac{\sin(\pi x)}{\pi x}$.

As the brickwall filter is not a causal filter, it cannot be implemented in practice. The alternative is to truncate the infinite impulse response sequence [147] using a

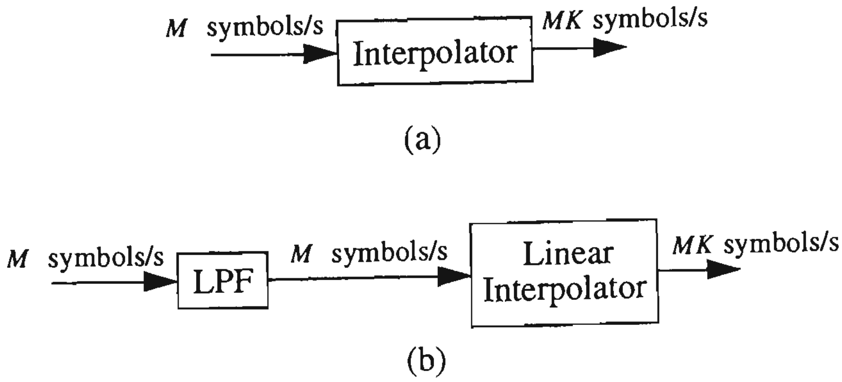

Fig. 4.8. (a) Conventional interpolation technique (b) filtering and linear interpolation technique.

window of N sample length. The resultant impulse response can then be written as

$$\begin{aligned} h(n) &= 2B_w \operatorname{sinc}(2B_w T_s n) w(n), & -(N-1)/2 \le n \le (N-1)/2 \quad & \text{odd } N \\ h(n) &= 2B_w \operatorname{sinc}[2B_w T_s (n+0.5)] w(n), & -(N/2) \le n \le (N/2)-1 \quad & \text{even } N \end{aligned} \tag{4.16}$$

where $w(n)$ is the window. To achieve a unit gain in the passband, $h(n)$ must be normalized by $\sum h(n)$. There are many window types with different properties for this truncation. A common feature of all windows is that their stopband attenuation is dependent on the shape of window, while the width of the transition region depends on the length of the window [147]. Therefore, there is a trade-off between the transient bandwidth and stop band attenuation. Increasing the transient bandwidth reduces the stop band attenuation and vice versa. To find the optimum window, we can use the amount of noise which can be attenuated by the filter as a figure of merit. The noise attenuation can be defined in dB by $NR = 10\log[(2B_N)/f_s]$ where B_N is the equivalent noise bandwidth of the filter and f_s is the sampling frequency. This noise attenuation can be obtained by different methods. One method is to obtain the filter spectrum and calculate the equivalent noise bandwidth. Another method is to filter an AWGN signal sampled with the sampling rate of f_s and measure the output to input power ratio. The noise attenuation of linear phase lowpass filters designed by Hanning and Rectangular windows for different sampling frequency to bandwidth ratio ($\alpha = f_s/B_w$) are shown in Fig. 4.9. The noise attenuations of the lowpass filters designed using other window types were also investigated but they are not shown in the figure. The rectangular window gives the sharpest increase in the noise attenuation for an increase in the filter length. However, because of the aliasing effect, it does not have a smooth roll-off after initial reduction. The other window types have a smoother noise reduction because of their less aliasing. By increasing the filter length the filters can reach the noise reduction limit (NRL) given by $NRL = 10\log[(2B_w)/f_s]$. Increasing the length of the filter beyond this cannot reduce noise any further. These confirm the simulation results, given in [153], that the probability of error, after initial reduction, remains constant with increasing filter length. This investigation also shows that a minimum length with a maximum noise reduction exists and the selection of an arbitrarily long filter length does not help improving the performance of PSA channel identification.

After filtering, channel estimates can be obtained using a linear interpolator

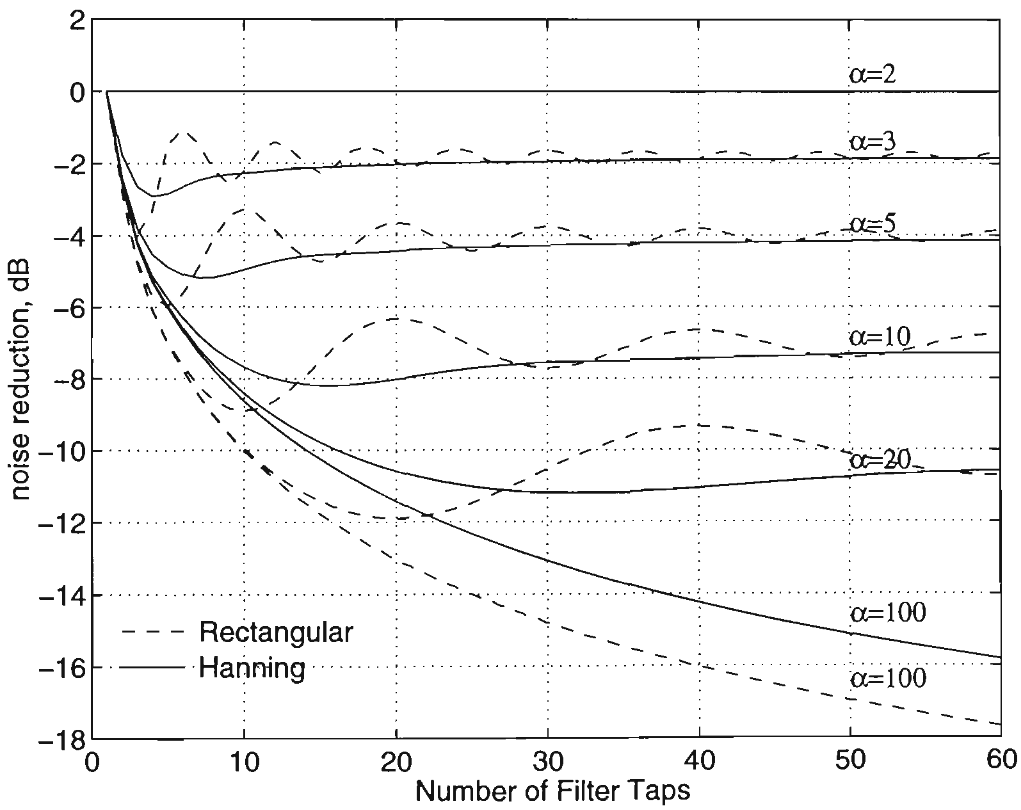

Fig. 4.9. Noise reduction of the linear phase lowpass filters designed by windowing method for different sampling frequency to bandwidth ratio $\alpha = \frac{f_s}{B_w} = \frac{Nr_b}{f_d} = \frac{N}{f_d T}$ using Hanning and Rectangular windows.

$$\hat{c}(kN+n) = c(kN)\left(1-\frac{n}{N}\right)+c([k+1]N)\left(\frac{n}{N}\right) \qquad 0 \le n \le L \tag{4.17}$$

For a linear interpolator, an equivalent FIR interpolation filter has a *(2N-1)* sample impulse response [161] in the form of

$$h(n) = 1-|n|/N, \qquad |n| < N \tag{4.18}$$

where $h(n)$ is the inverse Fourier transform of

$$H(e^{j\omega T}) = \frac{1}{N}\left\{\frac{\sin[\omega NT/2]}{\sin[\omega T/2]}\right\}^2 \tag{4.19}$$

4.3.1 Computational Complexity

Here, we compare the complexity of the FALI with the conventional interpolation in terms of the number of instructions they need in practical implementation. A pilot insertion period of N data symbols, an oversampling of K samples per data symbol and a filter impulse response length of L are assumed. Since DSP processors realize multiplication and addition in one instruction, L instructions are required for a convolution. Therefore, for the conventional interpolation technique, L instructions per sample are required. For the FALI, because of using convolution to filter out pilot symbol samples, the filtering needs L instructions per pilot symbol. Hence, the total number of instructions per sample is $\frac{L}{NK}$. In linear interpolation, two instructions per pilot symbol for the calculation of the gradient and one instruction per sample for the linear interpolation are necessary. Therefore the total number of operations per symbol is $1+\frac{L+2}{NK}$. Comparing this result with the conventional interpolation which needs L operation per symbol, the number of instructions necessary in FALI is substantially smaller. For example, for a frame length of 7 symbols, an oversampling rate of one and an interpolation length of 16, the conventional technique needs 7 operations while the FALI only needs 1.56 operations per symbol. The results for higher interpolation lengths are even better with the latter technique. For instance for the same condition but with an interpolation length of 37, the conventional technique needs 37 operations per symbol while FALI only needs 3.43 operations. If oversampling is taken into consideration, the FALI has even less complexity.

4.4 BER Performance of VA-ICIC with PSA Channel Estimation

The BER performances of VA-ICIC with PSA channel estimation in fast Rayleigh fading, AWGN and CCI environment have been investigated using Monte-Carlo simulations. A FALI which uses a filter with a Hanning impulse response of 37 samples has been adopted for this study. The data baud rate is 270kbits/sec with a pilot symbol insertion period $N = 16$ samples. With this arrangement, the total delay is 1.1ms. Both fading cancellation methods, described in Section 3.4, are used. The similarity between results confirms the sensitivity analysis of Section 3.7.2.

Fig. 4.10 shows the BER performance of GMSK BT=0.3 in CCI and AWGN. Comparison of these results shows the degradation in the BER performance with regard to the ideal channel estimation. For instance, for $E_b/N_0 = 30dB$ and $P_e = 10^{-2}$ the amount of degradation is about 8dB. However VA-ICIC can still give a 4dB better tolerance to co-channel interference. The rationale behind this

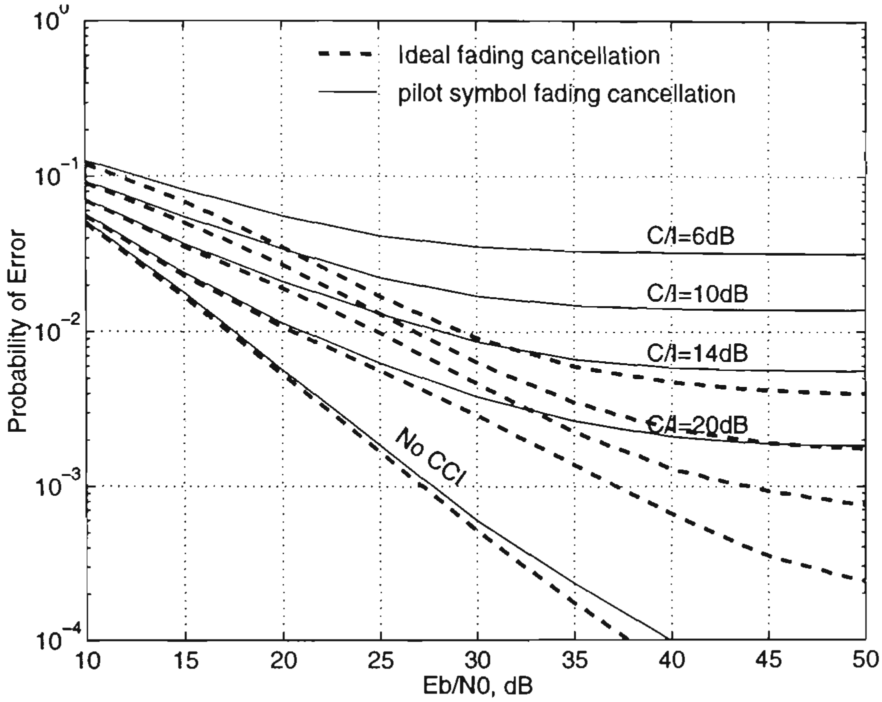

Fig. 4.10. BER performance of VA-ICIC with ideal and PSA-GMSK channel estimation ($f_dT=0.00037$).

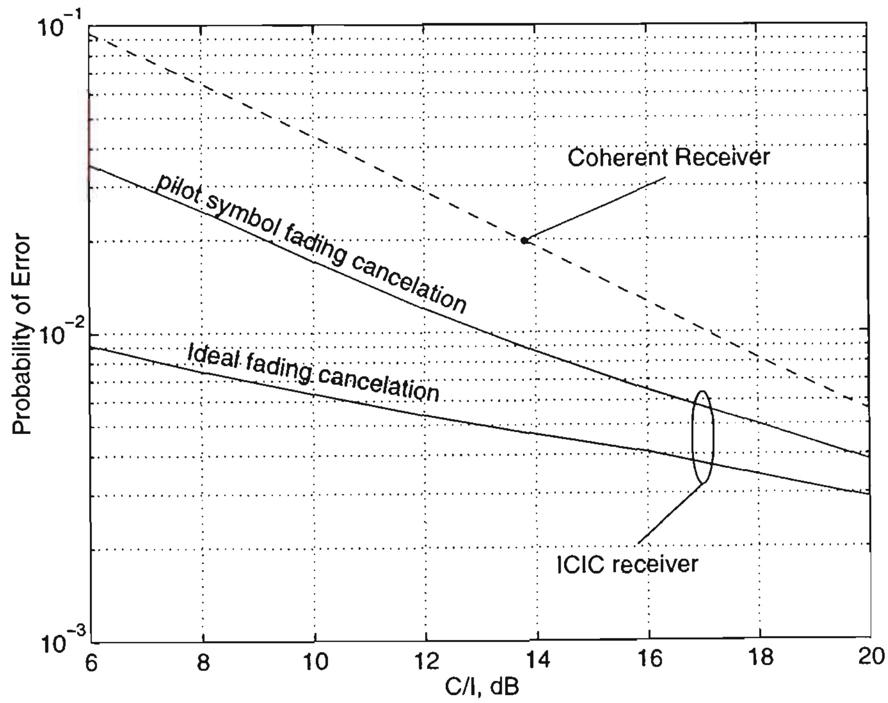

Fig. 4.11. BER performance of VA-ICIC with PSA-GMSK channel estimation for $E_b/N_0=30dB$.

performance degradation is that CCI cancellation is mainly performed when the desired signal power is smaller than the co-channel interference. The presence of a strong CCI in this period causes a severe channel estimation error which in turn degrades the BER performance. This can be easily seen from the fact that in the absence of CCI, the performance degradation is very small. The result of this study shows that ICIC receivers need high quality channel estimation techniques to maintain their good BER performance which in turn increases their complexity.

4.5 Effect of Delay Spread in Desired Signal

The performance of VA-ICIC with delay spread in the interfering signal was studied in section 3.6. In this section the effect of delay spread in the desired signal is investigated with a two-ray model (as depicted in Fig. 3.12, when I_d=0) and PSA channel estimation. For very small delays, the delay spread can help detection by boosting the power of the desired signal. However, for large delays, the delayed signal behaves as an extra interference and thus degrades the BER performance. Apart from that, the presence of the delayed signal can degrade the performance of the pilot symbol channel estimator, causing further performance degradation. The BER performance of VA-ICIC for GMSK BT=0.3 in a Rayleigh fading channel with an $E_b/N_0 = 30dB$ is plotted in Fig. 4.12. These results indicate that the BER performance of VA-ICIC dramatically degrades with increasing the delay spread, particularly when the ratio of the desired signal to its delayed path (W/W_d), is small. Considering the fact that the delayed version of signals usually attenuate with increasing delay [162], the performance degradation of VA-ICIC should be smaller than what appears in Fig. 4.12.

4.6 Effect of Delay Spread in Both Desired and CCI Signals

The BER performance of VA-ICIC for small delay spreads ($T_d = 0.2T$) for GMSK BT=0.3 at a SNR=30dB when both desired and interference signals are subject to delay spread is shown in Fig. 4.13. The gains of each signal and its delayed version are similar (worst case). As expected, the impact of delay spread in interference on the BER performance is negligible. Furthermore, it appears that the proposed

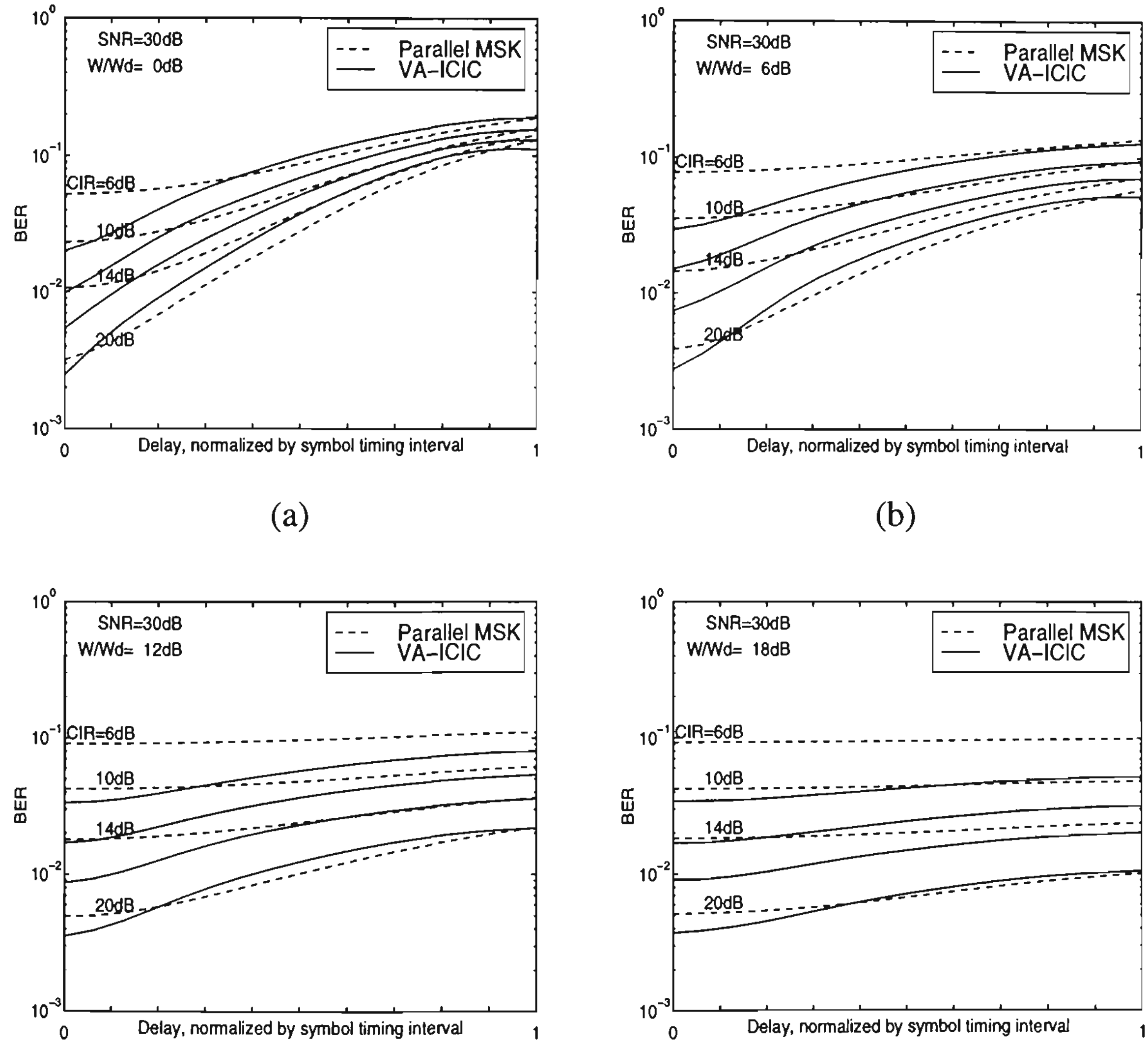

(a) (b)

(c) (d)

Fig. 4.12. BER performance of VA-ICIC in the presence of delay spread in desired signal, a) desired signal to its delay spread ratio (C/Cd) of 0dB, b) 6dB, c) 12dB and d) 18dB.

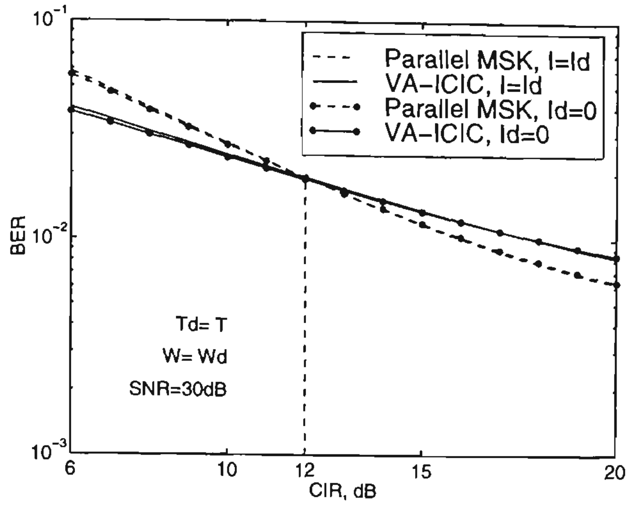

Fig. 4.13. The BER performance of VA-ICIC with delay spread in both desired and interference signals with pilot symbol aided channel estimation.

interference canceller can only improve the BER performance in poor carrier to interference ratios (CIR<12dB).

4.7 Conclusion

A general method of pilot symbol insertion technique is presented. It is shown that for a GMSK modulation technique at least 2 pilot symbols per frame are necessary. It is also shown that an optimum interpolation filter length exists for any selected frame length. The comparison of conventional interpolation with filtering and linear interpolation shows that the latter is superior at higher bit rates. The BER performance of VA-ICIC with PSA-GMSK shows a significant performance degradation compared with an ideal channel estimation. However, VA-ICIC outperforms the conventional coherent receiver by about 4dB CIR. The method used here is only a conventional PSA channel estimation and correction technique. Therefore, a better BER performance can be obtained if more sophisticated channel phase and gain estimation techniques, such as the one introduced in [157], are applied.

Further study of delay spread effect on the performance of VA-ICIC has been carried out in this chapter. The presence of delay spread affects both detection process and channel estimation. It is shown that the BER performance of VA-ICIC can be severely degraded by strong and long delay spreads. These investigations show that the ICIC scheme is suitable only in environments where the delay spread is small and the carrier to interference ratio is poor.

Chapter 5

Probability of Error Analysis of BB-ICIC Receiver in a Static AWGN Channel

This chapter analysis the BER performance of the BB-ICIC receiver in AWGN. The analysis was limited to static AWGN channel because of the time constraint. The BB-ICIC was selected because of its simple structure, while an AWGN channel was chosen because of its relative simplicity compared with the channels with interference. This analysis highlights the parameters that affect the BER performance of the BB-ICIC and confirms the results obtained by simulations. Error analysis in ICIC receivers, is somewhat more difficult compared with conventional linear receivers due to their nonlinear structures. Therefore, in certain conditions, a solution can only be obtained by statistical simulation.

Analysis begins with the definition of the probability of error followed by the derivation of probability density functions (PDFs). The required PDFs will be derived based on the cost function of (2.6). Only the 3-sample metric, which is shown to give an optimum BER performance, is considered (similar PDFs with simpler expressions, derived for 2-sample metric, are given in Appendix F).

An open form expression is given for the average probability of error and the computer simulation results are compared with the numerically calculated BER performances. Finally, a novel concept for signal distance, envelope distance, is defined based on the cost function of (2.6) to qualitatively explain the BER performance.

5.1 Introduction

A model of a communication system with an AWGN channel is shown in Fig. 5.1. Here, one waveform of the discrete set of specified waveforms $\{w_i(t)\}$, $i = 1, 2, \ldots, N$, is transmitted over a channel disturbed by AWGN. The received is defined as

$$r(t) = w(t) + n(t) \tag{5.1}$$

The waveform transmitted depends on the random message input, α. For example, when $\alpha = \alpha_i$, the transmitted signal is $w_i(t)$. Therefore, the following expression,

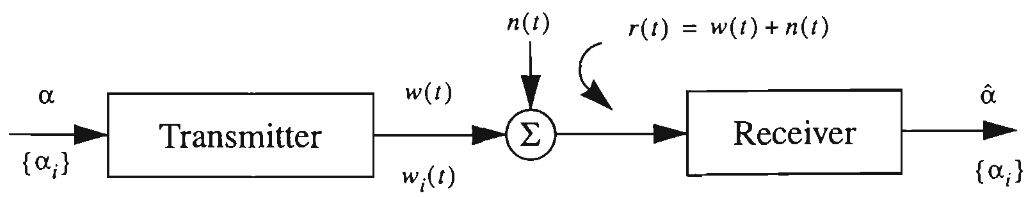

Fig. 5.1. A model of a communication system with AWGN channel.

$$\alpha = \alpha_i \Leftrightarrow w(t) = w_i(t) \tag{5.2}$$

defines the transmitter. The receiver produces an estimate, $\hat{\alpha}$, of the transmitted input α. The probability of error can be defined as

$$P[\varepsilon] = P[\hat{\alpha} \neq \alpha] \tag{5.3}$$

When CPM is used, the transmitted waveform not only depends on the current data symbol but also on from the previous symbols. Following the notation used in Chapter 2, the relationships for a sampled CPM modulated signal can be rewritten as

$$\delta = \delta_i \Leftrightarrow w(k) = w_i(k) \tag{5.4}$$

where $w_i(k)$ is a possible waveform of the desired signal. Also, $\delta = \{\theta_n, \ldots, \alpha_{n-1}, \alpha_n, \alpha_{n+1}, \ldots\}$, where α_n represents the transmitted symbol and θ_n the phase state in the n^{th} timing interval.

For binary signalling, α_n can be either zero or one. Therefore, half of the possible waveforms represent one and the other half represent zero. For instance, for MSK modulation scheme, there are eight possible waveforms, depending on the initial phase at the beginning of bit timing interval, Θ_n, there are a pair of waveforms for the data symbols 0 and 1. These waveforms in complex form are shown in Table 5.1.

Table 5.1. Different MSK waveforms. m is the oversampling rate.

Θ_n	Data symbol 1	Data symbol 0
0	$w_1(k) = \sqrt{\frac{E_b}{T}}\left[\cos\left(\frac{\pi k}{2m}\right)+j\sin\left(\frac{\pi k}{2m}\right)\right]$	$w_2(k) = \sqrt{\frac{E_b}{T}}\left[\cos\left(\frac{\pi k}{2m}\right)-j\sin\left(\frac{\pi k}{2m}\right)\right]$
$\pi/2$	$w_1(k) = \sqrt{\frac{E_b}{T}}\left[\sin\left(\frac{\pi k}{2m}\right)+j\cos\left(\frac{\pi k}{2m}\right)\right]$	$w_2(k) = \sqrt{\frac{E_b}{T}}\left[\sin\left(\frac{\pi k}{2m}\right)-j\cos\left(\frac{\pi k}{2m}\right)\right]$
π	$w_1(k) = \sqrt{\frac{E_b}{T}}\left[-\cos\left(\frac{\pi k}{2m}\right)-j\sin\left(\frac{\pi k}{2m}\right)\right]$	$w_2(k) = \sqrt{\frac{E_b}{T}}\left[-\cos\left(\frac{\pi k}{2m}\right)+j\sin\left(\frac{\pi k}{2m}\right)\right]$
$3\pi/2$	$w_1(k) = \sqrt{\frac{E_b}{T}}\left[-\sin\left(\frac{\pi k}{2m}\right)-j\cos\left(\frac{\pi k}{2m}\right)\right]$	$w_2(k) = \sqrt{\frac{E_b}{T}}\left[-\sin\left(\frac{\pi k}{2m}\right)+j\cos\left(\frac{\pi k}{2m}\right)\right]$

In BB-ICIC, all the possible waveforms of the received signal, $w_i(k)$, are generated and the metric (2.6) is calculated for each of them. Decision on the correct waveform is based on the minimum value of the metric. Once the correct waveform is selected the corresponding data symbol will be released as the output data.

The metric (2.6) normalized with factor, $\frac{T}{m+1}$, to simplify the derivation and is shown below

$$L_i = \frac{T}{m+1}\sum_{k=0}^{m}\left|M^2{}_i(k)-\overline{M^2{}_i(k)}\right| \tag{5.5}$$

and

$$M^2{}_i(k) = \left|r(k)-w_i(k)\right|^2 \tag{5.6}$$

where T is the symbol timing period, m is the number of samples per bit, and $w_i(k)$ is the i^{th} waveform among the N possible signal pulse shapes. $\overline{M^2{}_i(k)}$, the average of $M^2{}_i(k)$ during one symbol interval, is

$$\overline{M^2{}_i(k)} = \frac{1}{m+1}\sum_{k=0}^{m} M^2{}_i(k) \tag{5.7}$$

Assume that the received information signal $w(k) = w_r(k)$, $r = 1, \ldots, N$ where $w_r(k)$ has the following complex envelope

$$w_r(k) = Real\{w_r(k)\} + jImag\{w_r(k)\} \tag{5.8}$$

$Real\{w_r(k)\}$ and $Imag\{w_r(k)\}$ represent in-phase and quadrature waveforms in a bit timing interval. Thus, the received signal in an AWGN channel can be expressed as

$$r(k) = [Real\{w_r(k)\} + n_i(k)] + j[Imag\{w_r(k)\} + n_q(k)] \tag{5.9}$$

$n_i(k)$ and $n_q(k)$ are time sampled in-phase and quadrature components of the band limited Gaussian noise with zero mean and a variance of $\sigma^2{}_n$. Substituting (5.9) into (5.5) gives

$$L_{ri} = \frac{T}{m+1}\sum_{k=0}^{m}\left|[n_i(k)+p(k)]^2+[n_q(k)+q(k)]^2 - \frac{1}{m+1}\sum_{k=0}^{m}\{[n_i(k)+p(k)]^2+[n_q(k)+q(k)]^2\}\right| \tag{5.10}$$

where $p(k)$ and $q(k)$ are the in-phase and quadrature components of $w_r(k) - w_i(k)$ defined as

$$\begin{cases} p(k) = Real\{w_r(k) - w_i(k)\} \\ q(k) = Imag\{w_r(k) - w_i(k)\} \end{cases} \tag{5.11}$$

From (5.11) we have

$$p(k)^2 + q(k)^2 = |w_r(k) - w_i(k)|^2 \tag{5.12}$$

If $w_i(k) = w_r(k)$, (5.10) will become

$$L_{rr} = \frac{T}{m+1}\sum_{k=0}^{m}\left|n_i^2(k)+n_q^2(k) - \frac{1}{m+1}\sum_{k=0}^{m}[n_i^2(k)+n_q^2(k)]\right| \tag{5.13}$$

From the structure of the receiver, the correct decision can be made if

$$\{L_{rr} < L_{ri} | (i \neq r)\} \tag{5.14}$$

Additional conditions for a correct decision are required because half of the waveforms ($w_i(k)$) represent zero and the other half one. These conditions are

$$\{L_{rj} < L_{ri} | (j \neq i, \alpha_j = \alpha_r)\} \tag{5.15}$$

The relation (5.14) is a special case of (5.15). From (5.15), the conditional probability of a correct decision can be defined as

$$P[C|w_r(k)] = \sum_{j=1}^{N} \sum_{i=1}^{N} P[\{L_{rj} < L_{ri} | (j \neq i, \alpha_j = \alpha_r)\}] \tag{5.16}$$

The unconditional probability of error will be

$$P(C) = \sum_{r=1}^{N} P[C|w_r(k)]P[w_r(k)] \tag{5.17}$$

Assuming equal probabilities for all $w_r(k)$, simplifies (5.17) to

$$P(C) = \frac{1}{N} \sum_{r=1}^{N} P[C|w_r(k)] \tag{5.18}$$

Thus, the probability of error (i.e. bit error rate) can be stated as

$$P(E) = 1 - P(C) \tag{5.19}$$

To calculate the BER of BB-ICIC from (5.19), the PDFs of L_{rr} and L_{ri} must be obtained.

5.2 PDF of L_{rr}

Substituting $v(k) = n_i^2(k) + n_q^2(k)$ into (5.13) gives

$$L_{rr} = \frac{T}{m+1}\sum_{k=0}^{m}\left|v(k) - \frac{1}{m+1}\sum_{i=0}^{m} v(i)\right| \tag{5.20}$$

Relation (5.20) can be simplified as

$$L_{rr} = \frac{T}{m+1}\sum_{k=0}^{m}\left|\left(\frac{m}{m+1}\right)v(k) - \frac{1}{m+1}\sum_{i=0, i\neq k}^{m} v(i)\right| \tag{5.21}$$

Since L_{rr} is a function of $v(k)$, the PDF of $v(k)$ has to be found.

PDF of $v(k)$

$v(k)$ is a sum of squared independent identically distributed (IID) Gaussian processes (i.e. $n_i(k)$ and $n_q(k)$) with zero mean and a variance of σ^2_n. The PDF of $v(k)$ is exponential [146] with an average of $E[v] = 2\sigma_n^2$. This PDF can be written as

$$f_v(v) = \alpha e^{-\alpha v} U(v), \qquad \alpha = 1/(2\sigma^2) \tag{5.22}$$

where $U(v)$ is the unit step. To proceed with the analysis, the correlation between samples of v must be known. The autocovariance of v can be defined by

$$C_{vv}(t_1, t_2) = E\{v(t_1)v(t_2)\} - \bar{v}^2 \tag{5.23}$$

Two samples of v separated by T_s are said to be uncorrelated if the autocovariance of v at the time T_s is sufficiently small.

The autocovariance of v, given by equation (Appendix E.4), calculated for three different filter bandwidths, is shown in Fig. 5.2. As can be seen in the figure, the autocovariance is comparatively small for a one bit timing interval (T). This indicates that two samples separated by a symbol interval, can be assumed to be uncorrelated. It can also be noted that the correlation reduces as the filter bandwidth increases. Furthermore, when the sampling rate is increased, the correlation between samples increases. As shown in section 3.1, the best bit error rate performance can be obtained with a sampling rate of 2 samples per symbol which results in a separation of $T/2$. For this sampling rate, samples are correlated. However, the correlation factor is sufficiently small for an engineering solution. The accuracy of this assumption improves with increasing filter bandwidth.

PDF of L_{rr} with 3-Sample metric

In a 3-sample metric, L_{rr} can be written as

$$L_{rr} = \frac{T}{3}\{|2\nu(0) - [\nu(1) + \nu(2)]| + |2\nu(1) - [\nu(0) + \nu(2)]| + |2\nu(2) - [\nu(1) + \nu(0)]|\} \tag{5.24}$$

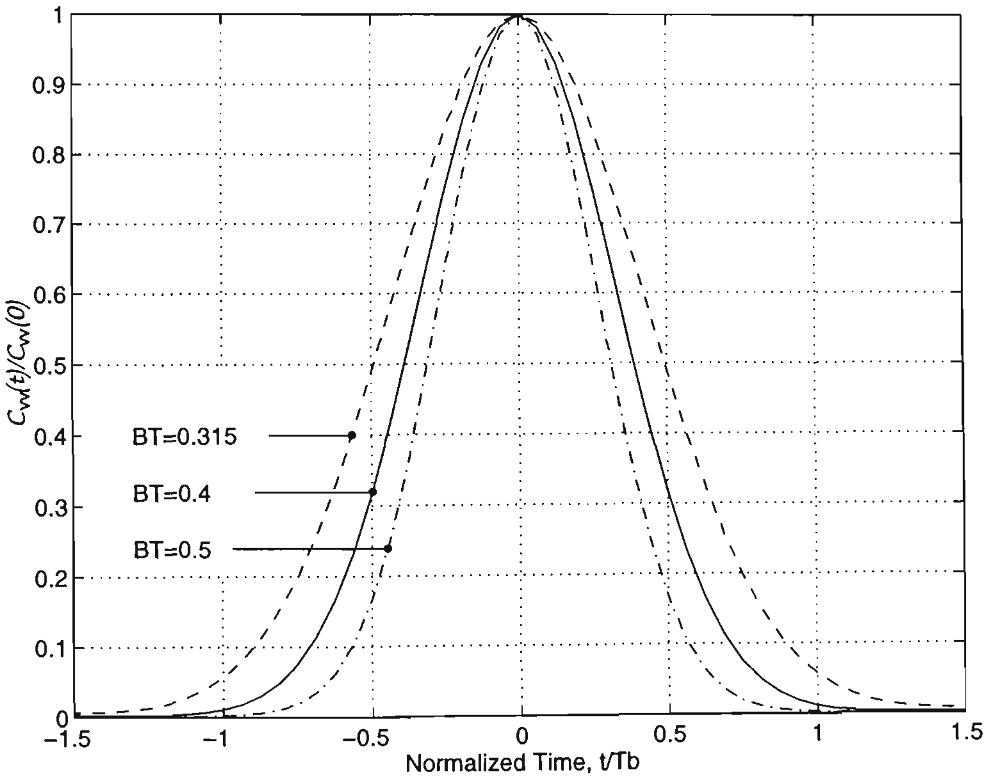

Fig. 5.2. Normalized autocovariance of ν when the AWGN is filtered with a Gaussian filter with *BT=0.315*, *BT=0.4* and *BT=0.5*.

To simplify (5.24) we define

$$\begin{cases} R_1 = 2v(0) - [v(1) + v(2)] \\ R_2 = 2v(1) - [v(0) + v(2)] \\ R_3 = 2v(2) - [v(1) + v(0)] \end{cases} \tag{5.25}$$

Substituting of (5.25) into (5.24) gives

$$L_{rr} = \frac{T}{3}\{|R_1| + |R_2| + |R_3|\} \tag{5.26}$$

The values of L_{rr} for different combinations of R_1, R_2 and R_3 are shown in Table 5.2. From the set of equations (5.25) we can write

$$R_1 + R_2 + R_3 = 0 \tag{5.27}$$

Relation (5.27) shows that R_1, R_2 and R_3 are not mutually independent. As a result, the conditions C_1-C_8 (Table 5.2) are not mutually exclusive. Therefore, an explicit relation between L_{rr} and the samples of v cannot be found. An alternative approach is to find a stochastic solution based on the hypothesis that L_{rr} follows a particular probability distribution. The statistical data can be obtained by computer simulation of L_{rr}. The parameters of the hypothesized distribution can be adjusted to fit the PDF obtained through simulation. A goodness-of-fit test procedure based on the

Table 5.2. Values of L_{rr} for different signs of R_1, R_2 and R_3

condition	R_3	R_2	R_1	L_{rr}
C_1	+	+	+	Not defined
C_2	+	+	-	$\frac{2T}{3}\{[v(1)+v(2)]-2v(0)\}>0$
C_3	+	-	+	$\frac{2T}{3}\{[v(0)+v(2)]-2v(1)\}>0$
C_4	+	-	-	$\frac{2T}{3}\{2v(2)-[v(0)+v(1)]\}>0$
C_5	-	+	+	$\frac{2T}{3}\{[v(1)+v(0)]-2v(2)\}>0$
C_6	-	+	-	$\frac{2T}{3}\{2v(1)-[v(0)+v(2)]\}>0$
C_7	-	-	+	$\frac{2T}{3}\{2v(0)-[v(1)+v(2)]\}>0$
C_8	-	-	-	Not defined

Kolmogorov-Smirnov [163] approach can be employed for this purpose. Based on this approach, parameters of the hypothesized distribution are adjusted to minimize the maximum difference (or distance) between the simulated and the hypothetical cumulative distribution functions (CDF) as

$$D = \sup|F_n(x) - F(x)| \tag{5.28}$$

The first step in the estimation of the PDF is to find a PDF similar to the one obtained by simulation. It is observed that the PDF of L_{rr} has a shape similar to a Gamma distribution. The Gamma distribution function has the form of

$$f_x(x) = \frac{\beta(\beta x)^{n-1}}{\Gamma(n)} e^{-\beta x} U(x) \tag{5.29}$$

where $\Gamma(n)$ is the well-known Gamma function which is defined as $\Gamma(n) = (n-1)!$ for an integer n. The PDF and CDF of the non-normalized metric, $W_{rr} = \frac{3}{T} L_{rr}$, for an I/Q Gaussian lowpass filter with a normalized bandwidth of BT=0.5 was estimated by stochastic simulation and the results are shown in Fig. 5.3. The simulated PDFs and CDFs are fitted with a Gamma distribution.

The fitting error was measured by a Kolmogorov-Smirnov test and the parameters of the fitted Gamma distribution for various filter bandwidths obtained. These results are shown in Table 5.3. The variances in the parameters are a direct result of the

Table 5.3. Parameters of fitted Gamma distribution in different I/Q lowpass filter bandwidth.

Filter type	Gaussian			Maximally flat		
Filter normalized bandwidth [BT]	0.4	0.5	0.6	0.4	0.5	0.6
Filtered noise variance σ_n	0.2054	0.2309	0.2535	0.2025	0.2244	0.2446
β	13.15	10.11	8.29	13.98	10.85	8.97
n	1.71	1.77	1.80	1.69	1.71	1.76
Approximation error%	0.59	0.54	0.60	0.49	0.56	0.52

correlation between adjacent samples of v and due to its filtering. The small error (about 0.6%) confirms that the Gamma distribution describes the statistical properties of W_{rr}. The parameters of fitted Gamma distributions for maximally flat filters are also given in the same table.

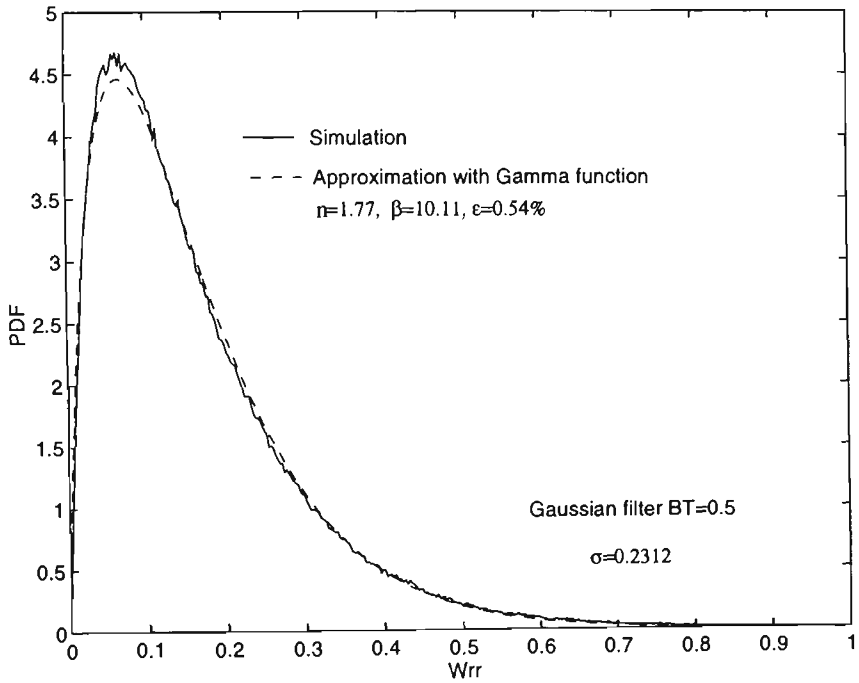

(a)

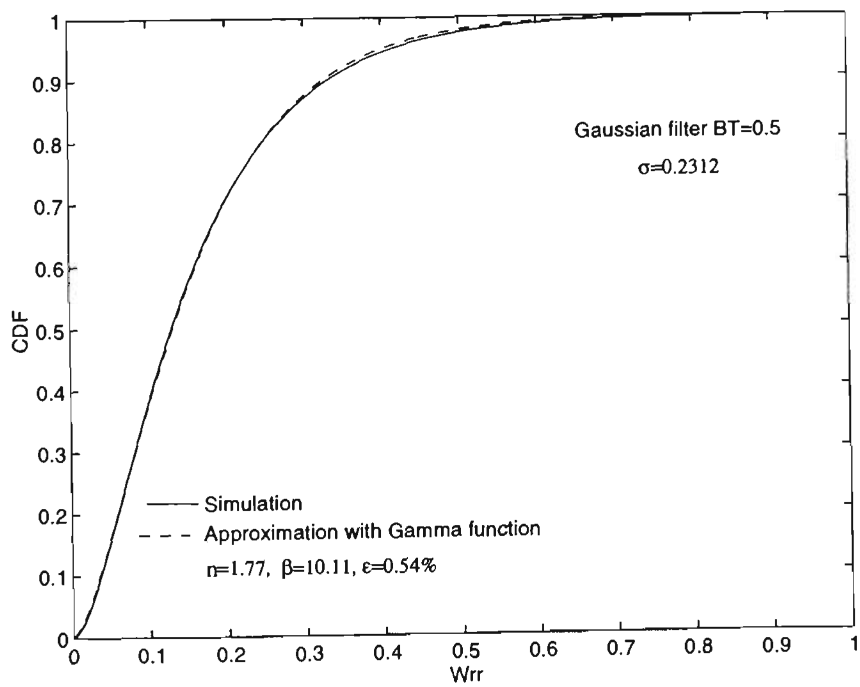

(b)

Fig. 5.3. The simulated PDF and CDF of W_{rr} and their approximation to the Gamma distribution.

An empirical formula is found to describe the PDF of W_{rr} in the given filter range. This expression is

$$f_{W_{rr}}(W_{rr}) = \frac{1.1\alpha(1.1\alpha W_{rr})^{n-1}}{\Gamma(n)} e^{-1.1\alpha W_{rr}} U(W_{rr}) \tag{5.30}$$

where $n = 1.53 + 0.42B_T$ and B_T is the normalized bandwidth of the filter. The PDF of the normalized metric can be written as

$$f_{L_{rr}}(L_{rr}) = \frac{1.1\frac{3\alpha}{T}\left[1.1\frac{3\alpha}{T}L_{rr}\right]^{n-1}}{\Gamma(1.53 + 0.42B_T')} e^{-1.1\frac{3\alpha}{T}L_{rr}} U(L_{rr}) \tag{5.31}$$

Substituting $\alpha = 1/(2\sigma_n^2)$ into (5.31) and taking σ_n^2 from (F.10) in Appendix F gives

$$f_{L_{rr}}(L_{rr}) = \frac{\frac{1.65}{N_0 k_b B_T}\left[\frac{1.65}{N_0 k_b B_T}L_{rr}\right]^{(0.53 + 0.42B_T)}}{\Gamma(1.53 + 0.42B_T)} e^{-\frac{1.65}{N_0 k_b B_T}L_{rr}} U(L_{rr}) \tag{5.32}$$

A normalized variable, which will be later used in the calculation of the bit error rate, defined as $\Lambda_{rr} = L_{rr}/N_0$ can be substituted into (5.32) to give

$$f_{\Lambda_{rr}}(\Lambda_{rr}) = \frac{\frac{1.65}{k_b B_T}\left[\frac{1.65}{k_b B_T}\Lambda_{rr}\right]^{(0.53 + 0.42B_T)}}{\Gamma(1.53 + 0.42B_T)} e^{-\frac{1.65}{k_b B_T}\Lambda_{rr}} U(\Lambda_{rr}) \tag{5.33}$$

5.3 PDF of L_{ri}

Starting from (5.10), $u(k)$ can be defined as

$$u(k) = [n_i(k) + p(k)]^2 + [n_q(k) + q(k)]^2 \tag{5.34}$$

PDF of $u(k)$

Since n_i and n_q are band limited Gaussian processes with zero mean and a variance of σ_n, the PDF of $u(k)$ is a noncenteral chi-square [164] with two degrees of freedom

$$f_u(u) = \frac{1}{2\sigma_n^2} e^{-\frac{u + p^2 + q^2}{2\sigma_n^2}} I_0\left(\frac{\sqrt{u(p^2 + q^2)}}{\sigma_n^2}\right) \tag{5.35}$$

where $I_0(x)$ is a zero order modified Bessel function of the first kind. Substituting (5.12) into (5.35) gives

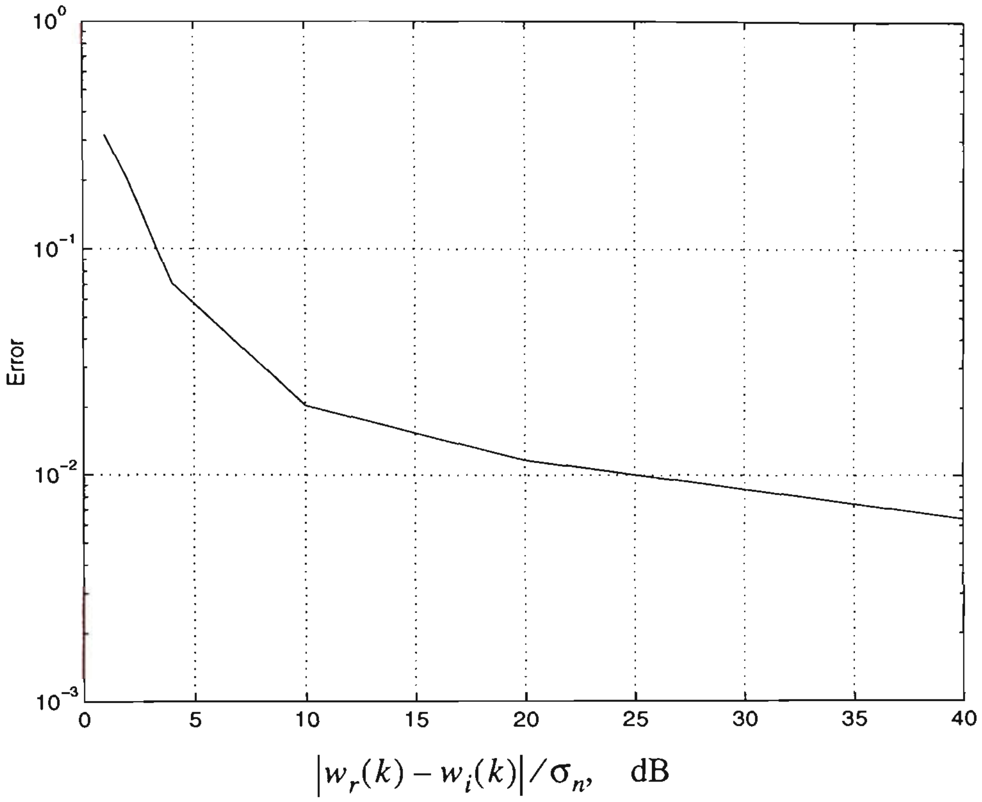

Fig. 5.4. Approximation error of (5.37) using normal distribution.

$$f_u(u) = \frac{1}{2\sigma_n^2} e^{-\frac{u + |w_r(k) - w_i(k)|^2}{2\sigma_n^2}} I_0\left(\frac{\sqrt{u|w_r(k) - w_i(k)|^2}}{\sigma_n^2}\right) \tag{5.36}$$

If $|w_r(k) - w_i(k)| \gg \sigma_n$, (5.36) can be approximated by a normal distribution

$$f_u(u) \approx \frac{1}{\xi\sqrt{2\pi}} e^{-\frac{[u - |w_r(k) - w_i(k)|^2]^2}{2\xi^2}} U(u) \tag{5.37}$$

where $\xi = 2\sigma_n|w_r(k) - w_i(k)|$. The error of this approximation based on a Kolmogorov-Smirnov test is shown in Fig. 5.4 which implies that for small noise levels, a Gaussian distribution can be used. This approximation will assist in estimating the PDF of L_{ri}.

PDF of L_{ri} with a 3-Sample Metric

Using a 3-sample metric, The relation of L_{ri} is similar to (5.24), the only difference is that the random variable $u(k)$ has a different PDF. As discussed in Section 5.2, the analytical solution of (5.24) is difficult. On the other hand, a numerical approach can simplify the analysis and give a tractable solution.

In our numerical study, MSK, GMSK BT=0.3 and GMSK BT=0.5 are used and the PDF of the non-normalized metric W_{ri} is determined. The simulation is carried out with a large number of data samples to reduce the error in the PDF estimation. Simulations have been performed for different signal to noise ratios and different signal powers.

The PDFs of non-normalized metric W_{ri}, obtained by simulation, are shown in Fig. 5.5. When the signal to noise ratio is high, these PDFs can be approximated with a normal distribution, truncated to positive values. Despite a larger error, the same approximation can still be used for the low SNRs. The approximate PDF of W_{ri} based on the truncated-normal distribution (see equation (D.10) in Appendix D) can be stated as

$$f_{W_{ri}}(W_{ri}) \approx \frac{1}{\sigma_W\left[0.5 + erf\left(\frac{\mu_W}{\sigma_W}\right)\right]\sqrt{2\pi}} e^{\frac{-(W_{ri}-\mu_W)^2}{2\sigma_W^2}} U(W_{ri}) \tag{5.38}$$

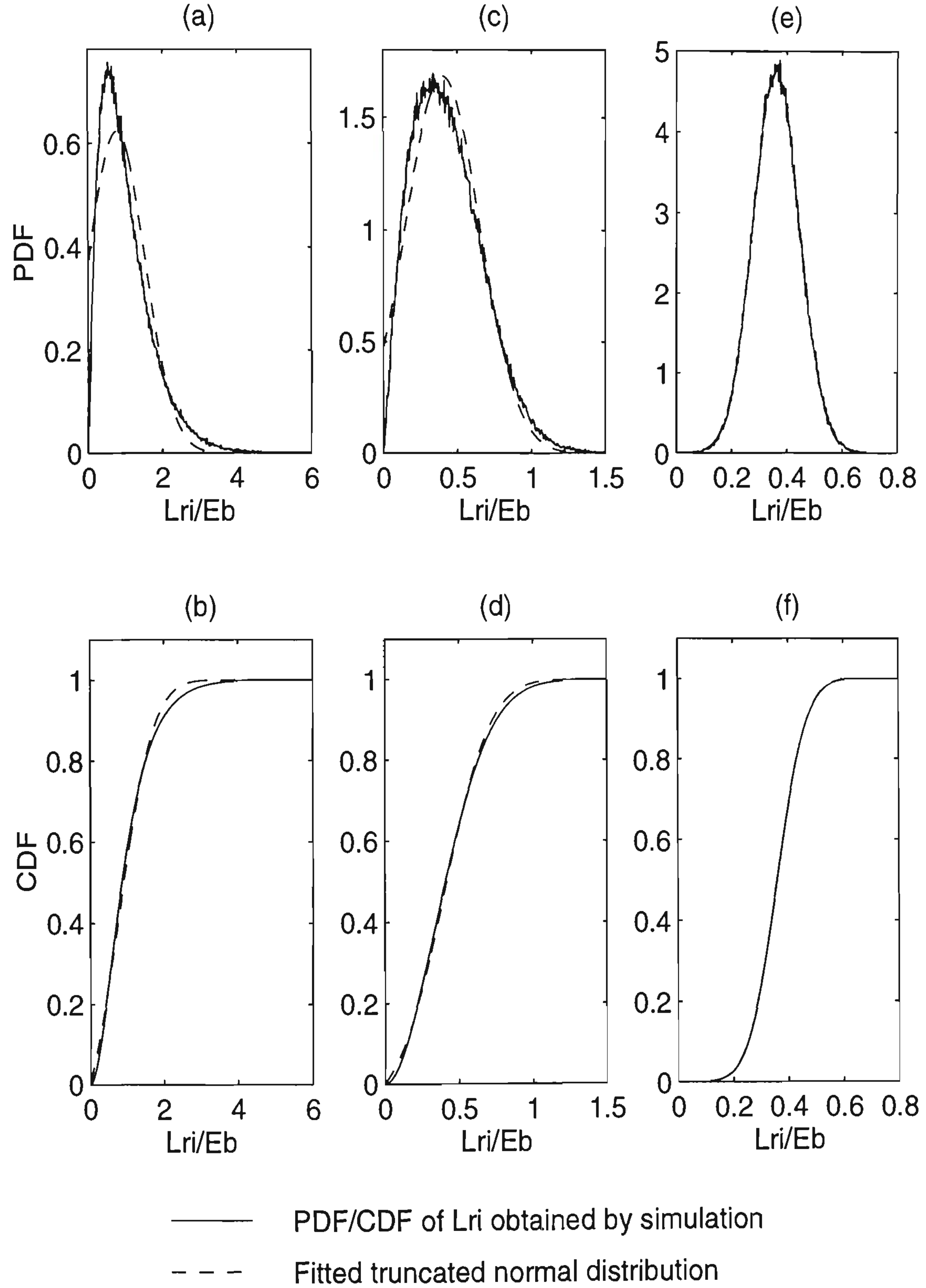

Fig. 5.5. PDF and CDF of L_{ri} for (a, b) SNR=0dB, (c, d) SNR=10dB and (e, f) SNR=20dB for GMSK modulation scheme and e_{ri}=0.344.

where $erf(x) = \frac{1}{\sqrt{2\pi}} \int_{-\infty}^{x} e^{-\lambda^2} d\lambda$.

The parameters of the fitted truncated-normal distribution, μ_W and σ_W, determined for GMSK BT=0.3, GMSK BT=0.5 and MSK modulation schemes are summarized in Tables G.1-G.36 in Appendix G. Empirical formulas have been found to obtain μ_W and σ_W based on the main channel parameters (i.e. noise variance σ_n, signal energy per bit E_b, the I/Q filter normalized bandwidth B_T, the Euclidean distances between $w_r(k)$ and $w_i(k)$, and a new parameter, E_{ri}, denoted the envelope distance between $w_r(k)$ and $w_i(k)$ as defined in equation 5.69). These formulas are

$$\mu_W \approx 3\sigma_n^2 + E_{ri} \tag{5.39}$$

$$\sigma_w \approx \frac{3\sigma_n D_{ri}}{\sqrt{2T}} \tag{5.40}$$

Here, E_{ri} is the envelope distance determined as

$$E_{ri} = 3\frac{E_b}{T}e_{ri} \tag{5.41}$$

where, e_{ri} is the normalized envelope distance (equation 5.70), and D_{ri} is the Euclidean distance (equation 5.67) between $w_r(k)$ and $w_i(k)$ determined as

$$D_{ri}^2 = \frac{T}{3}\sum_{k=0}^{2} \left|w_r(k) - w_i(k)\right|^2 \tag{5.42}$$

The squared Euclidean distance normalized by the bit energy [139] is

$$d_{ri}^2 = \frac{D_{ri}^2}{2E_b} \tag{5.43}$$

Substituting (5.41) into (5.39) and (5.43) into (5.40) gives

$$\mu_W \approx 3\left(\sigma_n^2 + \frac{E_b}{T}e_{ri}\right) \tag{5.44}$$

$$\sigma_W \approx 3\sigma_n d_{ri}\sqrt{\frac{E_b}{T}} \tag{5.45}$$

The empirical formulas, (5.44) and (5.45) summarize the results of the Tables G.1-G.36 in Appendix G with good accuracy.

The PDF of the normalized metric, $L_{ri} = \frac{T}{3}W_{ri}$, can thus be approximated by

$$f_{L_{ri}}(L_{ri}) \approx \frac{1}{\frac{T}{3}\sigma_W\left[0.5 + erf\left(\frac{\mu_W}{\sigma_W}\right)\right]\sqrt{2\pi}} e^{\frac{-\left(L_{ri} - \frac{T}{3}\mu_W\right)^2}{2\frac{T^2}{9}\sigma_W^2}} U(L_{ri}) \tag{5.46}$$

Substituting (5.44) and (5.45) into (5.46) gives

$$f_{L_{ri}}(L_{ri}) \approx \frac{1}{\sigma_n d_{ri}\sqrt{2\pi T E_b}\left[0.5 + erf\left(\frac{\sigma_n^2 T + E_b e_{ri}}{\sigma_n d_{ri}\sqrt{T E_b}}\right)\right]} e^{\frac{-[L_{ri} - (\sigma_n^2 T + E_b e_{ri})]^2}{2\sigma_n^2 T d_{ri}^2 E_b}} U(L_{ri}) \tag{5.47}$$

Inserting equation (F.10), in Appendix F, into (5.47) yields

$$f_{L_{ri}}(L_{ri}) \approx \frac{1}{d_{ri}\sqrt{2\pi N_0 E_b k_b B_T}\left[0.5 + erf\left(\frac{N_0 k_b B_T + E_b e_{ri}}{d_{ri}\sqrt{N_0 E_b k_b B_T}}\right)\right]} \tag{5.48}$$

$$e^{\frac{-[L_{ri} - (N_0 k_b B_T + E_b e_{ri})]^2}{2N_0 k_b B_T d_{ri}^2 E_b}} U(L_{ri})$$

To describe the above PDF with only one parameter $\eta = \frac{E_b}{N_0}$, we can define a new variable $\Lambda_{ri} = L_{ri}/N_0$. Thus the PDF of Λ_{ri} will be

$$f_{\Lambda_{ri}}(\Lambda_{ri}) \approx \frac{1}{d_{ri}\sqrt{2\pi k_b B_T \eta}\left[0.5 + erf\left(\frac{k_b B_T + e_{ri}\eta}{d_{ri}\sqrt{k_b B_T \eta}}\right)\right]} e^{\frac{-[\Lambda_{ri} - (k_b B_T + e_{ri}\eta)]^2}{2k_b B_T d_{ri}^2 \eta}} U(\Lambda_{ri}) \quad (5.49)$$

5.4 Bit Error Rate

The probability of correct decision conditioned on reception of waveform $w_r(t)$, can be found from (5.16). In (5.16), the variables $\{L_{ri}\}$ can be substituted by their normalized values: $\{\Lambda_{ri}\} = \{L_{ri}/N_0\}$, $N_0 \neq 0$ to yield

$$P[C|w_r(k)] = \sum_{j=1}^{N} \sum_{i=1}^{N} P[\{\Lambda_{rj} < \Lambda_{ri} | j \neq i, a_j = a_r\}] \quad (5.50)$$

In (5.50), $P[\{\Lambda_{rj} < L_{ri} | j \neq i, a_j = a_r\}]$ can be described by

$$P_{rj} = P[\{\Lambda_{rj} < \Lambda_{ri} | j \neq i, a_j = a_r\}] = \quad (5.51)$$

$$\int_0^{\infty} d\Lambda_{rj} \int_{\Lambda_{rj}}^{\infty} \cdots \int_{\Lambda_{rj}}^{\infty} f(\Lambda_{rj}, \{\Lambda_{ri}, (i = 1, \ldots, N), (i \neq j)\}) \prod_{i=1, i \neq j}^{N} d\Lambda_{ri} \qquad a_j = a_r$$

where $f(\Lambda_{rj}, \{\Lambda_{ri}, (i = 1, \ldots, N), (i \neq j)\})$ is the joint probability density function of the variables $\{\Lambda_{ri}\}$. Since the variables $\{\Lambda_{ri}\}$ are positive, the limits of the first integral are between zero and infinity.

$f(\Lambda_{rj}, \{\Lambda_{ri}, (i = 1, \ldots, N), (i \neq j)\})$ can be further simplified if any of the random variables $\{\Lambda_{ri}\}$, $(i = 1, \ldots, N)$ are independent of others. For instance, if Λ_{rj} is independent of all others, we can write

$$f(\Lambda_{rj}, \{\Lambda_{ri}, (i = 1, \ldots, N), (i \neq j)\}) = \\ f(\Lambda_{rj}) f(\{\Lambda_{ri}, (i = 1, \ldots, N), (i \neq j)\}) \tag{5.52}$$

PDF of $\{\Lambda_{ri}\}$ can be found with several constraints. One of these constraints is to solve (5.51) in a high signal to noise ratio condition in which the truncated normal PDFs of $\{\Lambda_{ri}\}$ are almost normal. In this case any two Λ_{ri} can be considered independent [146]. The correlation coefficients of $\{\Lambda_{ri}\}$ are shown in Tables J.1-J.4 in Appendix J. The tables show that most of the Λ_{ri} can be roughly considered either mutually uncorrelated or fully correlated. The ambiguity caused by a small number of Λ_{ri} with correlation coefficients around 0.5 can be eliminated by assuming that those $\{\Lambda_{ri}\}$ with correlation coefficients below 0.5 are uncorrelated and above this limit are fully correlated, This assumption introduces a deliberate error into the solution. However, the error is not so crucial owing to a small number of Λ_{ri} with this condition. Those fully correlated $\{\Lambda_{ri}\}$ with negligible differences in their mean and variance, (as they are originated from one set of noise samples) are identical and thus, can be considered as a single variable. (Tables G.1-G.36 give all the possible values of mean and variances of $\{W_{ij}\}$. The mean and variance of Λ_{ri} can be obtained from those of $\{W_{ij}\}$ by multiplying them by $\frac{T}{3N_0}$). For large SNR, (large

(large η) and two fully correlated Λ_{ri} (x and y) with different mean values, we can write

$$\mu_x < \mu_y \Rightarrow x < y \tag{5.53}$$

Provided that their standard deviations are much smaller than the difference between their mean values ($\eta > 20dB$). This produces the following expression where z is smaller than x and y

$$P[z < x, y] = P[z < x] \qquad \mu_x < \mu_y \tag{5.54}$$

(5.54) implies that between two fully correlated Λ_{ri}, the one with the larger mean value can be ignored. The above assumptions simplifies (5.51) to

$$P_{cj} = \int_0^{\infty} f_{\Lambda_{rj}}(\Lambda_{rj})d\Lambda_{rj} \prod_{i \neq j}^{N} \int_{\Lambda_{rj}}^{\infty} f_{\Lambda_{ri}}(\Lambda_{ri})d\Lambda_{ri} \qquad \begin{cases} a_j = a_r \\ \{\Lambda_{ri}, i \neq j\} \quad \text{uncorrelated} \end{cases} \tag{5.55}$$

In (5.55), only mutually uncorrelated $\{\Lambda_{ri}\}$ are considered. Between those $\{\Lambda_{ri}\}$ which are mutually fully correlated, the one with the larger mean value is eliminated.

Due to different PDFs for Λ_{rr} and $\{\Lambda_{rj} | j \neq r\}$, (5.55) can be separated into the following equations

$$P_{rr} = \int_0^{\infty} f_{\Lambda_{rr}}(\Lambda_{rr})d\Lambda_{rr}\prod_{i \neq r}^{N}\int_{\Lambda_{rr}}^{\infty} f_{\Lambda_{ri}}(\Lambda_{ri})d\Lambda_{ri} \qquad \begin{cases} a_j = a_r \\ \{\Lambda_{rj}, i \neq r\} & \text{uncorrelated} \end{cases} \tag{5.56}$$

$$P_{rj} = \int_0^{\infty} f_{\Lambda_{rj}}(\Lambda_{rj})d\Lambda_{rj}\prod_{i \neq j}^{N}\int_{\Lambda_{rj}}^{\infty} f_{\Lambda_{ri}}(\Lambda_{ri})d\Lambda_{ri} \qquad \begin{cases} a_j = a_r \\ \{\Lambda_{rj}, i \neq j\} & \text{uncorrelated} \end{cases} \tag{5.57}$$

Substituting of (5.33) and (5.49) into (5.56) and (5.57) results in

$$P_{rr} = \frac{\left(\frac{1.65}{B_T}\right)^{(1.53 + 0.42B_T)}}{\Gamma(1.53 + 0.42B_T)}\int_0^{\infty}\lambda^{(0.53 + 0.42B_T)}e^{-\frac{1.65}{B_T}\lambda}\left(\prod_{i \neq r}^{N}\frac{\int_{\lambda}^{\infty} e^{\frac{-[\Lambda_{ri} - (B_T + e_{ri}\eta)]^2}{2B_T d_{ri}^2\eta}}d\Lambda_{ri}}{d_{ri}\sqrt{2\pi B_T\eta}\left[0.5 + erf\left(\frac{B_T + e_{ri}\eta}{d_{ri}\sqrt{B_T\eta}}\right)\right]}\right)d\lambda \tag{5.58}$$

$$P_{rj} = \frac{1}{d_{rj}\sqrt{2\pi B_T\eta}\left[0.5 + erf\left(\frac{B_T + e_{rj}\eta}{d_{rj}\sqrt{B_T\eta}}\right)\right]} \tag{5.59}$$

$$\int_0^\infty e^{\frac{-[\Lambda_{rj} - (B_T + e_{rj}\eta)]^2}{2B_T d_{rj}^2\eta}} \left(\prod_{i \neq r, j}^{N} \frac{\int_{\Lambda_{rj}}^{\infty} e^{\frac{-[\Lambda_{ri} - (B_T + e_{ri}\eta)]^2}{2B_T d_{ri}^2\eta}} d\Lambda_{ri}}{d_{ri}\sqrt{2\pi B_T\eta}\left[0.5 + erf\left(\frac{B_T + e_{ri}\eta}{d_{ri}\sqrt{B_T\eta}}\right)\right]} \right)$$

$$\left(\frac{\left(\frac{1.65}{B_T}\right)^{(1.53 + 0.42B_T)}}{\Gamma(1.53 + 0.42B_T)} \int_{\Lambda_{rj}}^{\infty} \lambda^{(0.53 + 0.42B_T)} e^{-\frac{1.65}{B_T}\lambda} d\lambda \right) d\Lambda_{rj}$$

Substituting $\frac{1}{\sqrt{2\pi}}\int_x^\infty e^{\frac{-[\alpha - \mu]^2}{2\sigma^2}} d\alpha = Q\left(\frac{x-\mu}{\sigma}\right) = 0.5 - erf\left(\frac{x-\mu}{\sigma}\right)$ into (5.58) and (5.59)

results in

$$P_{rr} = \frac{\left(\frac{1.65}{B_T}\right)^{(1.53 + 0.42B_T)}}{\Gamma(1.53 + 0.42B_T)} \int_0^\infty \lambda^{(0.53 + 0.42B_T)} e^{-\frac{1.65}{B_T}\lambda} \tag{5.60}$$

$$\left(\prod_{i \neq r}^{N} \frac{1}{d_{ri}\sqrt{2\pi B_T\eta}} \frac{\left[0.5 - erf\left(\frac{\lambda - (B_T + e_{ri}\eta)}{d_{ri}\sqrt{B_T\eta}}\right)\right]}{\left[0.5 + erf\left(\frac{B_T + e_{ri}\eta}{d_{ri}\sqrt{B_T\eta}}\right)\right]} \right) d\lambda$$

$$P_{rj} = \frac{1}{d_{rj}\sqrt{2\pi B_T\eta}\left[0.5 + erf\left(\frac{B_T + e_{rj}\eta}{d_{rj}\sqrt{B_T\eta}}\right)\right]} \tag{5.61}$$

$$\int_0^{\infty} e^{\frac{-[\Lambda_{rj} - (B_T + e_{rj}\eta)]^2}{4B_T d_{rj}^2\eta}} \left(\prod_{i \neq r, j}^{N} \frac{1}{d_{ri}\sqrt{2\pi B_T\eta}} \frac{\left[0.5 - erf\left(\frac{\lambda - (B_T + e_{ri}\eta)}{d_{ri}\sqrt{B_T\eta}}\right)\right]}{\left[0.5 + erf\left(\frac{B_T + e_{ri}\eta}{d_{ri}\sqrt{B_T\eta}}\right)\right]} \right)$$

$$\left(\frac{\left(\frac{1.65}{B_T}\right)^{(1.53 + 0.42B_T)}}{\Gamma(1.53 + 0.42B_T)} \int_{\Lambda_{rj}}^{\infty} \lambda^{(0.53 + 0.42B_T)} e^{-\frac{1.65}{B_T}\lambda} d\lambda \right) d\Lambda_{rj}$$

Relations (5.60) and (5.61) cannot be further simplified and must be solved numerically. Substituting (5.60) and (5.61) into (5.16) gives the probability of a correct decision conditioned on waveform $w_r(k)$ as

$$P(C|w_r(k)) = \sum_{i=1}^{N} P_{ri}, \quad a_i = a_r \tag{5.62}$$

Since this probability is not uniform for all $\{w_r(k)\}$, the average probability of correct decision can be found by averaging (5.62) over all possible waveforms as

$$P(C) = \frac{1}{N}\sum_{r=1}^{N}\sum_{i=1}^{N} P_{ri}, \quad a_i = a_r \tag{5.63}$$

The probability of error can thus be found from

$$P(E) = 1 - P(C) = 1 - \frac{1}{N}\sum_{r=1}^{N}\sum_{i=1}^{N} P_{ri}, \quad a_i = a_r \tag{5.64}$$

An algorithm is written to solve (5.64) numerically. For a given η, the algorithm calculates (5.60) and (5.61) for a given waveform, $w_r(k)$, and adds all the obtained P_{cr} and P_{cr} to find $P(C|w_r(k))$. It then continues this procedure for all waveforms and finally gives the average of the obtained $P(C|w_r(k))$ value as the probability of correct decision. Finally, the probability of error is calculated as in (5.64). The most time consuming part of this algorithm is the calculation of correlation coefficient which is needed to cancel out one of the mutually correlated Λ_{ij}.

Analytical and simulated BER performance of the BB-ICIC receiver for different η are compared in Fig. 5.6. For large η (i.e. $\eta > 10dB$), analytical and simulated results are very close. When small values of η are used the analytical results deviate from the simulation due to the inaccuracy of the empirical formulas for the parameters of the truncated normal distribution and the error of the fitted distribution. In addition most of the assumptions made to find the BER are not correct under these conditions.

In the next subsection the concept of envelope distance is defined. It is shown that the minimum envelope distance (e_{min}) can qualitatively describe the BER performance of ICIC receivers.

5.5 Signal Space and Envelope Distance

The idea of visualising transmitted signals geometrically (i.e. signal space diagram which is often called signal constellation) is of fundamental importance. This signal representation simplifies analysis of communication systems in AWGN. In this representation, the transmitted signal, $w(t)$, is approximated by a weighted linear combination of a set of orthonormal functions $\{ \varphi_k(t), k = 1, ..., N \}$ i.e.

$$w(t) \approx \sum_{k=1}^{N} w_k \varphi_k(t) \tag{5.65}$$

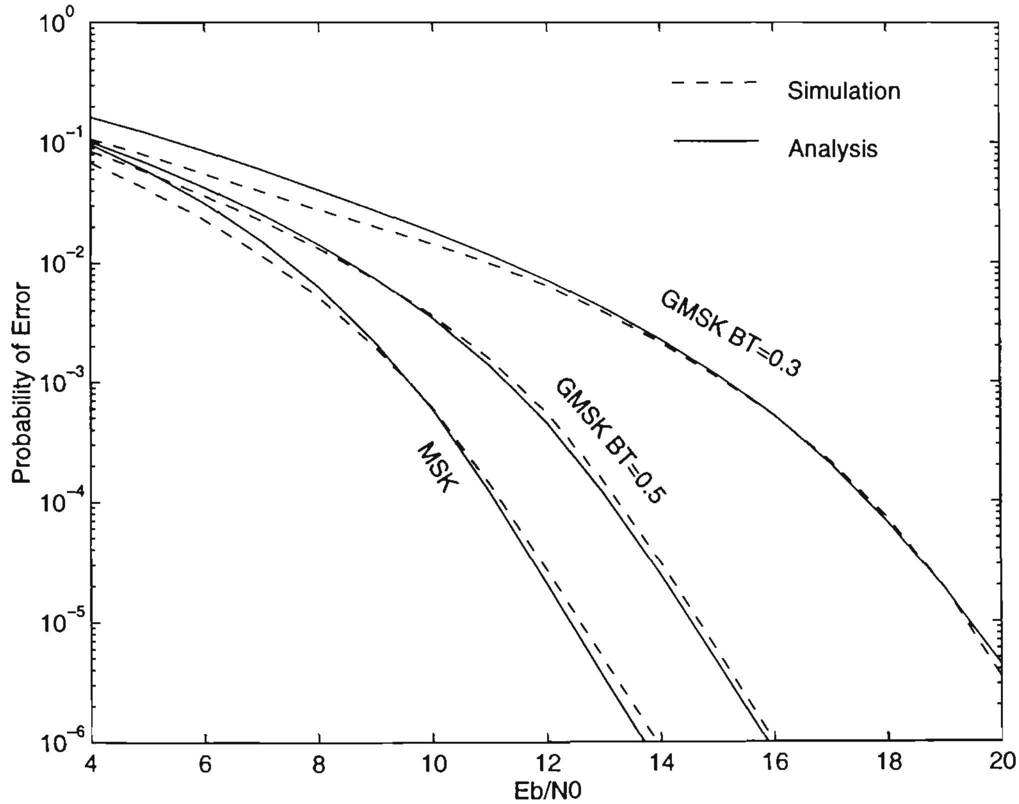

Fig. 5.6. Analytical and simulation results of bit by bit ICIC receiver in AWGN channel for GMSK BT=0.3, GMSK BT=0.5 and MSK modulation schemes.

where the orthonormality of the set $\{ \varphi_k(t) \}$ is defined by

$$\int_0^T \varphi_i(t)\varphi_j(t) = \begin{cases} 0, & i \neq j \\ 1, & i = j \end{cases} \tag{5.66}$$

The process of projecting the finite energy waveforms on to these orthonormal axes is called the Gram-Schmidt orthogonalization procedure which has been well documented in [165]. In fact many signals in today's communication systems can be expressed in only two dimensions [165] which is analogous with two-dimensional space. For instance, QPSK signal space $\{ \varphi_k(t) \}$ is defined with two quadrature tones at the same frequencies (i.e. $\sqrt{2/T}\cos[2\pi f_c t]$, $\sqrt{2/T}\sin[2\pi f_c t]$). QPSK, PAM and QAM can be shown by discrete points in this space. The CPM modulation schemes can be projected on the same signal space by various paths or trajectories from one phase state to another, rather than discrete points. This is due to the time variant phase of CPM. For a constant amplitude CPM signal, various trajectories form a circle (Fig. 5.7). In a special case of CPM, i.e. MSK, there are two cosine tones at two coherently orthogonal frequencies over [0,T] (i.e. $\sqrt{2/T}\cos[2\pi(f_c - 1/(4T))t]$ and $\sqrt{2/T}\cos[2\pi(f_c + 1/(4T))t]$) which can be used as basic signals [166] for the signal space. The signal constellation for an MSK modulation scheme in this space is shown in Fig. 5.8. Since this signal space can only show two frequency components, it is not appropriate for Gaussian noise signals which contain a range of frequency components. However, some researchers use this signal space to describe some attractive features of MSK [166]. In this thesis we use this signal space representation to show some basic differences between ICIC and maximum likelihood detection

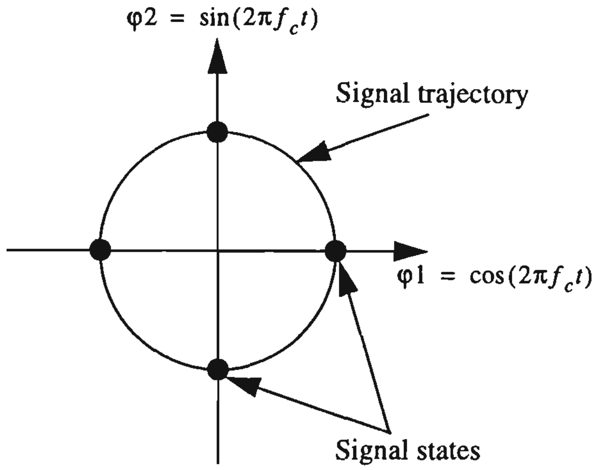

Fig. 5.7. MSK signal trajectories in signal space.

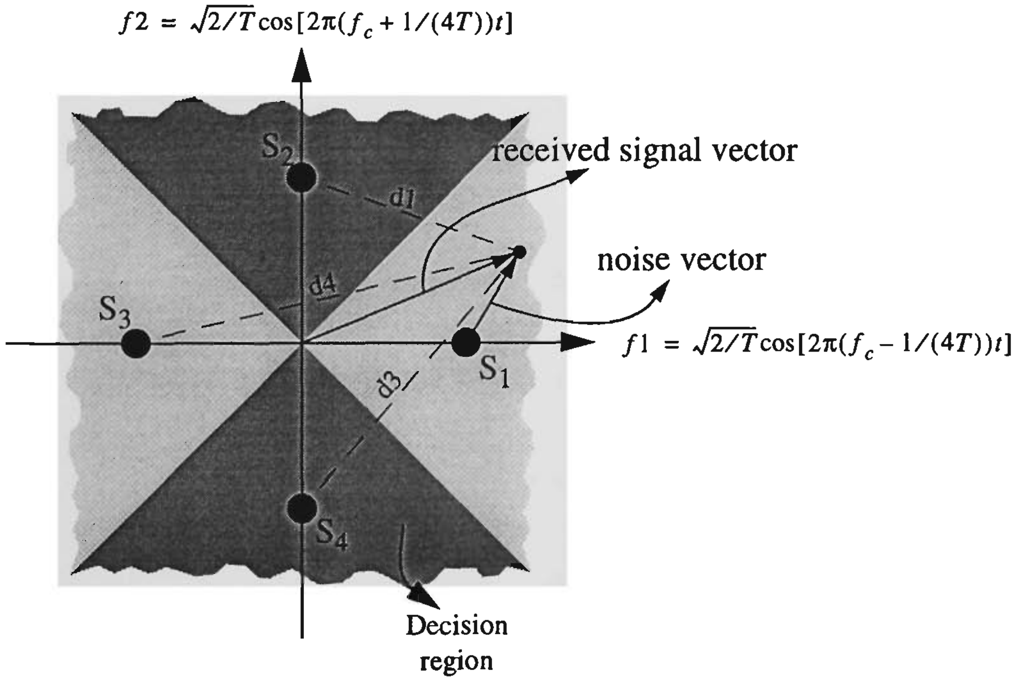

Fig. 5.8. Received signals and decision regions in the signal space of MSK.

schemes. Both maximum likelihood detection and ICIC detection calculate metrics and decide on the signal symbol based on the minimum metric value. In maximum likelihood detection, the metric is the Euclidean distance between the received signal and the hypothesised signal constellation point. Using the analogy of maximum likelihood and ICIC detection schemes, the value of the metric in (2.6) can be denoted by the envelope distance.

If we consider only two components of additive noise at frequencies $f1 = \sqrt{2/T}\cos[2\pi(f_c - 1/(4T))t]$, and $f2 = \sqrt{2/T}\cos[2\pi(f_c + 1/(4T))t]$, the received MSK signal with noise can be illustrated by a single point in the signal space (Fig. 5.8). Envelope distances and Euclidean distances of different signal space points from the signal constellation point S1 are shown in Fig. 5.9.

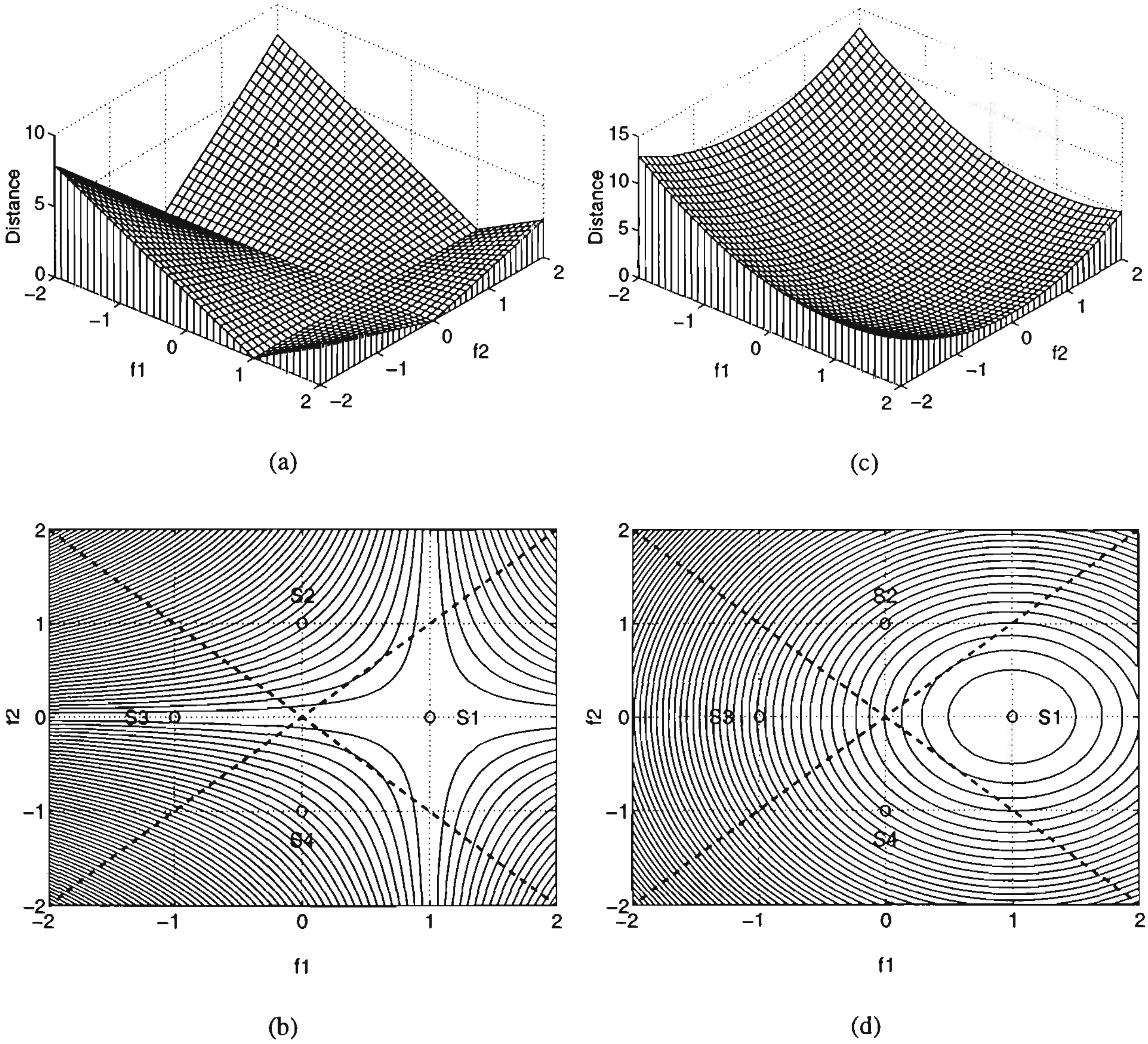

Fig. 5.9. Envelope and Euclidean distance profiles of MSK modulation scheme in MSK signal space. (a) Envelope distance profile, (b) contour and decision regions, (c) Euclidean distance profile and (d) contours and decision regions. Signal constellation points are labelled by S1, S2, S3 and S4.

As can be seen from Figs. 5.9c and 5.9d, the minimum value of the Euclidean distance is located in the signal constellation point. On the contrary, the minimum value of the envelope distance, Figs. 5.9a and 5.9b, is situated along two perpendicular lines crossing at S1. If we assume decision boundaries as in the figure, the minimum envelope distance lines cross all the decision boundaries. This can cause an error if the received signal point falls on the minimum line inside the decision regions S2 or S4 which have different data symbols from the region S1. However, for the decision region S3, because of its identical data symbol with decision region S1 this will not cause any error. This example demonstrates the reason why ICIC is not an optimum detection scheme.

5.5.1 Envelope Distance

In maximum likelihood detection, Euclidean distance directly determines the probability of error [26]. The squared Euclidean distance, $D^2_{i,\,j}$, between two signals $w_j(t)$ and $w_j(t)$ is defined as

$$D^2_{i,\,j} = \int_{t1}^{t2} |w_i(t) - w_j(t)|^2 dt \qquad (5.67)$$

Using the integration method as shown in Appendix D.1, $D^2_{i,\,j}$ can be calculated from the sampled signals, $w_i(k)$ and $w_j(k)$

$$D^2_{i,\,j} = \frac{T}{m+1} \sum_{k=0}^{m} |w_i(k) - w_j(k)|^2 \qquad (5.68)$$

The minimum value of $D^2_{i,j}$ for two signals with different symbols, denoted as minimum Euclidean distance, is generally used as an indication of the BER performance.

The distance between two signals, referred as the envelope distance, can be defined using the metric of (2.6). As shown in Section 5.3, the BER of ICIC receiver can be described based on this parameter. The envelope distance between two signals $w_i(k)$ and $w_j(k)$ can be defined as

$$E_{ij} = \sum_{k=0}^{m} \left| |w_i(k) - w_j(k)|^2 - \frac{1}{m+1} \sum_{k=0}^{m} |w_i(k) - w_j(k)|^2 \right| \tag{5.69}$$

5.5.1.1 Normalization of envelope distance

The dimension of E_{ij} can be changed from power to energy by multiplying it by bit period T. In addition, to make the magnitude of the envelope distance independent from the variation of signal energy, it can be normalized by the signal energy per bit (E_b). It can also be made independent from the number of the samples if it is normalized by $m+1$. Including all these normalization gives

$$e_{ij} = \frac{T}{m+1} \cdot \frac{E_{ij}}{E_b} = \frac{1}{m+1} \sum_{k=0}^{m} \left| \left| \sqrt{\frac{T}{E_b}} w_i(k) - \sqrt{\frac{T}{E_b}} w_j(k) \right|^2 \right. \tag{5.70}$$
$$\left. - \frac{1}{m+1} \sum_{k=0}^{m} \left| \sqrt{\frac{T}{E_b}} w_i(k) - \sqrt{\frac{T}{E_b}} w_j(k) \right|^2 \right|$$

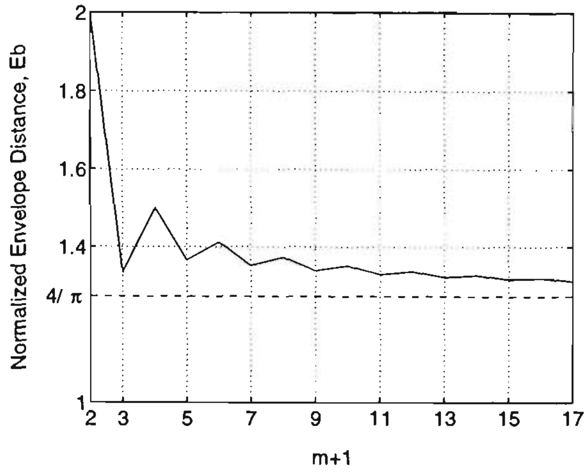

Fig. 5.10. Normalised envelope distance of mark and space MSK signals versus the number of samples used in the metric.

where $\sqrt{\frac{T}{E_b}}w_i(k)$ and $\sqrt{\frac{T}{E_b}}w_j(k)$ are normalized wave shapes. This normalization does not give a monotonic value for different m. For instance, the MSK modulation scheme with signals defined by,

$$\begin{aligned} w_i(t) &= \sqrt{\frac{E_b}{T}}\left[\cos\left(\frac{\pi t}{2T}\right) + j\sin\left(\frac{\pi t}{2T}\right)\right] \\ w_j(t) &= \sqrt{\frac{E_b}{T}}\left[-\cos\left(\frac{\pi t}{2T}\right) + j\sin\left(\frac{\pi t}{2T}\right)\right] \end{aligned} \tag{5.71}$$

produces a normalized envelope distance (NED) of

$$e_{ij} = \frac{1}{m+1}\sum_{k=0}^{m}\left|4\cos^2\left(\frac{\pi k}{2m}\right) - 2\right| \tag{5.72}$$

The NED versus $m + 1$ is shown in Fig. 5.10. The reason behind the large difference in the envelope distance for $m = 1$ and $m = 2$ is that the middle sample in $m = 2$ is zero (Fig. 5.11). Thus, (2.6) is identical for both $m = 1$ and $m = 2$, while the normalization factors are different. Similar results can be repeated with the GMSK modulation scheme. The normalized envelope distances between the phase trellis of GMSK BT=0.3 calculated for *one bit timing interval*, are given in Tables H.1-H.18 in Appendix H. The trellises are numbered, according to the numbering in the Table 2.1.

The envelope distance can be calculated either in a period of one bit interval (for bit by bit detection) or in a period of multiple bit intervals (for sequence estimation). For more than one bit interval, the ICIC receiver calculates the metric for a signal trajectory in a bit time interval and accumulates it for each signal path.

5.5.2 Minimum Envelope Distance

For convenience, the minimum envelope distance (e_{min}) is defined as the value of NED between two signal pulses with different data symbols. This can be used to indicate the performance of the ICIC receiver in AWGN. To observe the effect of different parameters on e_{min}, several numerical computations have been carried out.

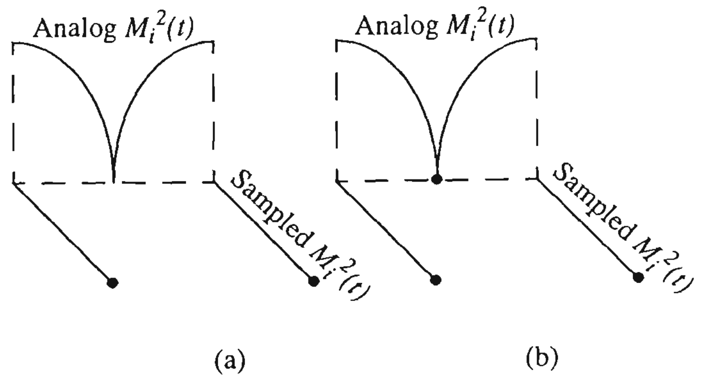

Fig. 5.11. Position of samples on $M_i^2(t)$ for MSK modulation scheme (a) 2 samples (b) 3 samples per bit.

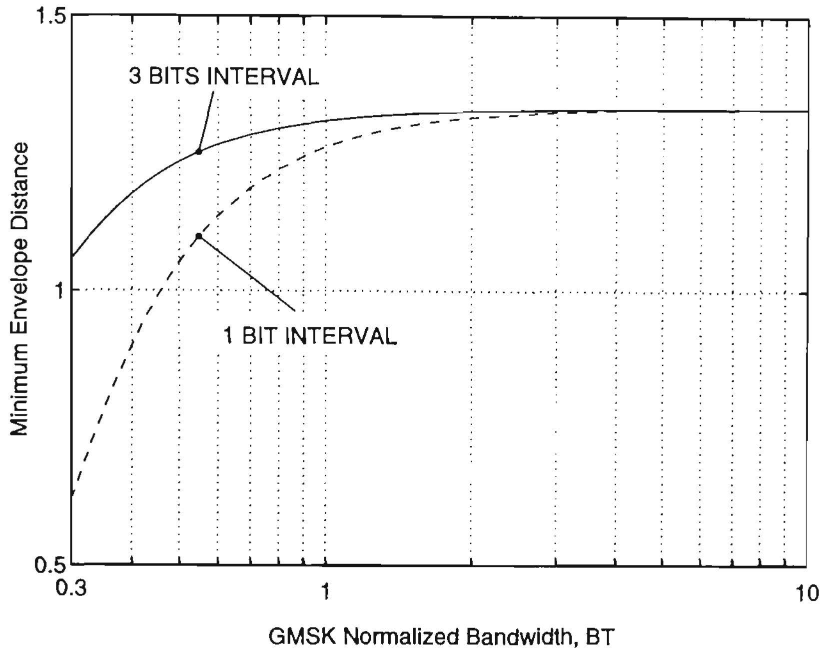

Fig. 5.12. Minimum envelope distance of GMSK modulation scheme for 1 bit and 3 bits observation intervals. Number of samples in the calculation of metric in each bit interval is selected *m=3*.

modulation bandwidth. Figs. 5.13 and 5.14 present e_{min} for different quadrature demodulator filter bandwidths. These results show that sequential estimation has a larger e_{min} than bit by bit detection which gives a better BER performance. Increasing the modulation bandwidth of GMSK increases the e_{min}. Furthermore, increasing the filter bandwidth increases the e_{min} and improves the BER performance, however this improvement (as discussed in Section 3.2) is limited by the increase in the amount of noise. Between the Gaussian and the maximally flat filters (Appendix C), the maximally flat filter produces a higher e_{min} which implies that giving a better BER performance will result. This demonstrates that the lower frequency components of the signal have a significant impact on e_{min}.

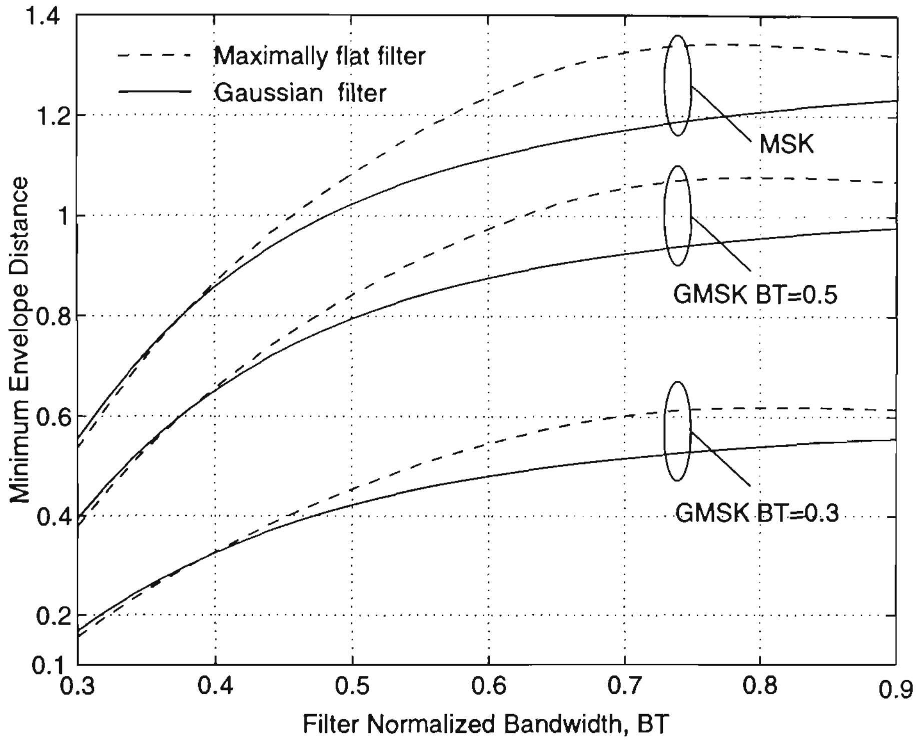

Fig. 5.13. Minimum envelope distance of filtered GMSK, versus filter normalized bandwidth for a single bit observation interval.

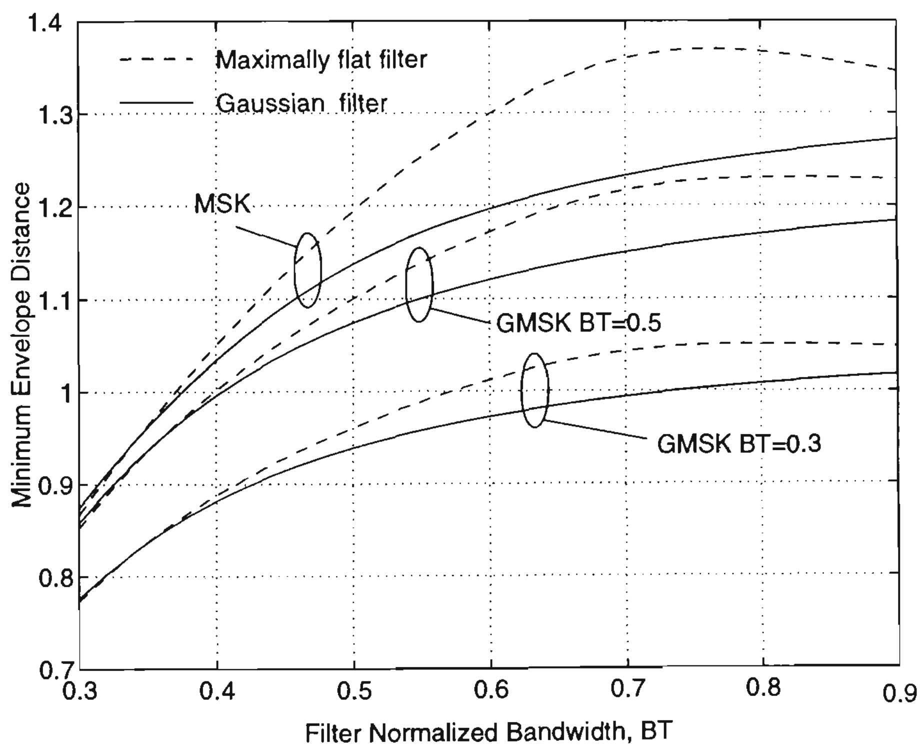

Fig. 5.14. Minimum envelope distance of filtered GMSK versus filter normalized bandwidth for multiple bits observation time.

5.6 Conclusion

The bit error rate performance of the BB-ICIC receiver was analysed and compared with Monte Carlo simulation results. For a 2-sample metric relatively simple analytical PDFs have derived. However, for a 3-sample metric, an explicit probability space was not found and hence, a numerical approach was adopted. Two different hypothesis distributions (i.e. Gamma and truncated normal) were fitted with the simulated PDFs based on minimization of the Kolmogorov-Smirnov distance. Several empirical formulas were found to describe the parameters of the fitted distributions based on the input parameters, $\eta = E_b/N_0$, the filter normalized bandwidth (B_T) and the signal envelope distance. The obtained PDFs were used to find the BER performance of the BB-ICIC receiver. Several assumptions were made to simplify the numerical calculation of the BER performance. For large η values, the analytical BER closely matches with the Monte Carlo simulation results as seen from Chapter 2. For small η values, analytical and simulated BER performances are different because the empirical formulas for the parameters of two fitted distributions are inaccurate and also the assumptions made to simplify the analytical solution are not valid under these conditions.

The envelope distance was defined to simplify the analysis. It was shown that the minimum envelope distance can qualitatively explain BER performance of BB-ICIC. A large e_{min} implies better BER performance. Additionally, the effects of I/Q filters, GMSK modulation bandwidth and multiple observation time on e_{min} were investigated. It was shown that increasing the I/Q filter bandwidth, GMSK modulation bandwidth and the observation interval increases e_{min} and subsequently improves the BER performance.

Chapter 6

Conclusions and further research

6.1 Summary of Results

The primary objective of this investigation is to propose a low complexity receiver structure for cellular mobile communication systems subjected to co-channel interference. To achieve this goal, a new concept of co-channel interference cancelling is proposed. The main idea behind this concept is to exploit envelope fluctuation of constant envelope modulation schemes for signal detection in the presence of co-channel interference.

Four different receiver structures: bit-by-bit, reduced waveform bit-by-bit, sequential estimation based on Viterbi algorithm, and an error detection/correction scheme are proposed. The BER performance of the proposed receivers have been investigated with computer simulation. The static channel performances of the proposed receivers show that they outperform conventional receivers under very low carrier to interference ratios. This condition can occasionally happen in TDMA cellular radio systems when the desired signal power is smaller than the interference power (i.e. a deep fade). The simulation results in a Rayleigh fading channel show that the ICIC receiver can give a remarkable performance improvement over conventional coherent receivers. Amongst the above mentioned receiver structures, ICIC with Viterbi algorithm has the best BER performance.

The effects of different implementation imperfections on the performance of the VA-ICIC were studied. Sensitivity studies of the VA-ICIC receiver shows its high sensitivity to channel and timing errors. Two fading cancellation techniques were studied and it can be seen that one of them can reduce the sensitivity of VA-ICIC to the fading rate. The VA-ICIC with pilot symbol aided channel estimation were investigated. During this study a general pilot symbol aided GMSK was proposed. The BER performance of VA-ICIC with channel estimation shows that it needs a very accurate channel estimation technique. The BER of VA-ICIC has also been investigated in a delay spread channel. It was shown that the BER performance of VA-ICIC severely degrades in delay spread. This makes VA-ICIC suitable for only low delay spread channels.

The BER performance of BB-ICIC receiver was theoretically analysed and compared with the simulation results. Due to nonlinearities of the receiver, it was difficult to find the required probability density functions. For instance, relatively simple analytical PDF was derived for a 2-sample metric, however, for the 3-sample metric, an explicit probability space was not found and hence a numerical approach was adopted. Two different hypothesized distributions (i.e. gamma and truncated normal) were fitted with the simulated PDFs based on the Kolmogorov-Smirnov test. Several empirical formulas were obtained for the parameters of the fitted distributions based on the input parameters (i.e. $\eta = E_b/N_0$, filter normalized bandwidth, B_T, and envelope distance). The obtained PDFs were used to find the BER performance of the BB-ICIC receiver with some constraints. For large η values, analytical BERs agree well with Monte Carlo simulation results but for small η values, the analytical and simulated BER performances differ. The reason for this is that the empirical formulas are not sufficiently accurate and also the assumptions are not applicable to these conditions.

Using the analogy with the Euclidean distance, the envelope distance was defined to simplify the analysis. The minimum value of envelope distance, e_{min}, can qualitatively reflect the BER performance of BB-ICIC. A large e_{min} implies a better BER performance. The effects of I/Q down convertor filters, GMSK modulation bandwidth and multiple observation time on e_{min} distance were also investigated. It was shown that on increasing the I/Q filter bandwidth or GMSK modulation bandwidth and observation interval increases e_{min} and subsequently improves BER performance.

6.2 Future Research

Indirect co-channel interference cancelling (ICIC), because of its novelty, can open a large area of research. Some examples of further studies on this interference cancelling technique are:

(i) Different investigations throughout this thesis show that I/Q lowpass filters have a large impact on reduction of envelope distortion and subsequently the performance of ICIC receivers. Finding an appropriate filter type to minimize envelope fluctuations was attempted in this thesis. It was found that the a maximally flat filter performs better than a Gaussian filter. However, further research is necessary to find an optimum filter type for this purpose.

(ii) The main advantage of ICIC over conventional receivers appears under small carrier to interference ratios. One possibility of exploiting this advantage is to switch on the ICIC when the desired signal is sufficiently weaker than interference. For the remaining periods, a better performing conventional receiver can be used. The main difficulty in this case is the separation of these two conditions. The combination of ICIC with other interference cancelling techniques in order to reduce their complexity is worth investigation in the further.

(iii) To further improve the BER performance, an enhanced channel estimation technique than the one currently employed, provided that the the receiver design complexity is kept relatively low.

(iv) In the BER rate analysis of this thesis certain assumptions were made which can be avoided. The probability of error analysis of different ICIC receivers can be proceeded by analysing them in different multipath scenarios with co-channel interference. Nevertheless, this will be a laborious and long procedure.

(v) Application of ICIC on constant modulus schemes other than CPM may also be of interest. For instance, ICIC can be easily applied on BPSK and QPSK modulation schemes. Some of the secondary results of this research, such as filtering strategy, may attract interest in other applications of constant modulation schemes.

(vi) Finally, ICIC receivers can be applied in various mobile communication environments with limited number of interferers. Some examples of such environments are: smart antennas, sectorized cells and cross-coupled polarized communications. The high sensitivity of ICIC receivers to delay spread limits their application to low delay spread scenarios. A possible application can be orthogonal frequency multiplex (OFDM) systems which inherently have low bit rates.

Bibliography

[1] V. H. Mac Donald, "Advanced mobile phone service: the cellular concept," *The bell System Technical Journal,* vol. 58, No. 1, pp. 15-41, Jan. 1979.

[2] F. H. Blecher, "Advanced mobile phone services," *IEEE Transaction on Vehicular Technology,* vol. 29, pp. 238-244, May, 1980.

[3] J. J. Chang, R. A. Miska and R. Anthony Shober, "Wireless systems and technologies: an overview," *AT&T Technical Journal*, pp. 11-18, July/August 1993.

[4] D. C. Cox, "Wireless personal communications: what is it?," *IEEE Personal Communications*, pp. 20-35, April 1995.

[5] D. J. Goodman, "Second generation wireless information networks," *IEEE Transaction on Vehicular Technology,* vol. VT-40, pp. 366-374, May 1991.

[6] J. M. Nijihof, I. S. Dewantara and R. Prasad, "Base station system configurations," *Proc. of 43rd IEEE Vehicular Technology Conference*, NJ, USA, pp. 621-624, May 1993.

[7] D. L. Schilling, "Wireless Communication going into the 21st century," *IEEE Transaction on Vehicular Technology,* vol. 43, pp. 645-651, Aug. 1994.

[8] R. Steele, "The evolution of personal communications," *IEEE Personal communications*, pp. 6-11, Second Quarter 1994.

[9] A. J. Viterbi, "The evolution of digital wireless technology from space exploration to personal communication services," *IEEE Transaction on Vehicular Technology,* vol. 43, pp. 638-644, Aug. 1994.

[10] W. C. Y. Lee, *Mobile cellular telecommunications systems*, New York: McGraw-Hill 1989.

[11] A. S. Rosenbaum, "PSK error performance with Gaussian noise and interference," *Bell Sys. Tech. J.*, vol. 48, no. 2, pp. 413-442, Feb. 1969.

[12] A. S. Rosenbaum, "Binary PSK error probabilities with multiple cochannel interference," *IEEE Trans. Commu. Tech.*, vol. COM-18, pp. 241-253, June 1970.

[13] V. K. Prabhu, "Error rate considerations for coherent phase-shift keyed systems with co-channel interference," *Bell Sys. Tech. J.*, vol. 48, no. 3, pp. 743-767, March 1969.

[14] V. K. Prabhu, "Error probability upper bound for coherently PSK signals with co-channel interference," *Electronic Lett.*, vol. 5, no. 16, Aug. 1969.

[15] Goldman, J. "Multiple error performance of PSK systems with cochannel interference and noise," *IEEE Trans. on Commu.*, vol. COM-18, pp. 420-430, Aug. 1971.

[16] O. Shimbo and R. Fang, "Effect of cochannel interference and Gaussian noise in M-array PSK systems," *COMSAT Tech. Rev.*, vol. 3, no. 1, 1973.

[17] A. S. Rosenbaum and F. E. Glave "An Error-probability upper bound for phase-shift keying with interference," *IEEE Trans. Commu. Tech.*, vol. COM-22, pp. 6-16, Jan. 1974.

[18] A. S. Rosenbaum, "An Upper bound analysis for coherent phase shift keying with interference," *Proc. of IEEE Int. Conf. Communications*, pp. 18.10-18.16, 1973.

[19] A. S. Rosenbaum, "An upper bound analysis for coherent phase-shift keying with cochannel, Adjacent-Channel, and Intersymbol Interference," *IEEE Trans. Commu. Tech.*, vol. COM-23, pp. 586-597, June 1975.

[20] S. Benedetto, E. Bigleri and V. Castellani, "Combined effect of intersymbol, interchannel and co-channel interference in M-ary CPSK systems," *IEEE Trans. on Commu.*, vol. COM-21, pp. 997-1008, Sept. 1973.

[21] P. Stravroulakis, Ed., *Interference analysis of communication systems*, IEEE Press: New Yourk, 1980.

[22] Y. Guo and K. Feher, "Performance evaluation of differential π/4-QPSK system in a Rayleigh fading/delay spread/CCI/AWGN environment," *Proc.. of IEEE 40th Veh. Tech. Conference*, Orlando, FL, USA, May 1990, PP 420-424.

[23] M. T. Le and A. U. Sheikh, "Performance of π/4-QPSK in A Rayleigh/lognormal/delay Spread/AWGN/cochannel interference environment," *Proc. of IEEE 42nd Veh. Tech. Conference*, Denver, USA, May

1992, PP 147-150.

[24] N. C. Beaulieu and A. A. Abu-Dayya, "Nyquist shaped QPSK in cochannel interference and fading," *Proc. of IEEE Global communication Conf. (GLOBCOM 93),* Houston, Tx, USA, pp. 1419-1423, Nov. 1993.

[25] F. Adachi and M. Sawashi, "Error rate analysis of MDPSK/CPSK with diversity reception under very slow Rayleigh fading and cochannel interference," *IEEE Transaction on Vehicular Technology,* vol. 43, pp. 252-263, May 1994.

[26] J. B. Anderson, Tor Aulin and C. E. Sundberg, *Digital phase modulation*, New York: Plenum Press, 1989.

[27] K. Murota and K. Hirad, "GMSK modulation for digital mobile radio telephony," *IEEE Trans. on Commu.*, vol. 29, Jul. 1981, pp. 1044-1050.

[28] M. Mouly and M. B. Pautet, *The GSM system for mobile communications*, France: Mouly, 49 rue Louis Brunea F-91120 Palaiseau, 1992.

[29] H. Ochsner, "Digital European cordless telecommunications," *Proc. of 39th IEEE Vehicular Technology Conference*, pp. 718-721, May 1989.

[30] R. B. Rhodes, S. G. Wilson and A. Svensson, "MSK-type reception of continuous phase modulation: cochannel and adjacent channel interference," *IEEE Transaction on Commu.*, vol. COM-35, pp. 185-193, Feb. 1987.

[31] N. A. B. Svensson, "Error probability analysis for CPM with linear detection on Gaussian and Rayleigh fading channels with multiple signal interference," *IEE Proc., Pt. F, Commu., Radar, Sig. Process.*, vol. 134, no. 7, pp. 695-705, Dec. 1987.

[32] P. P. S. Carter and A. M. D. Turkamani, "Performance evaluation of Rayleigh and log-normal GMSK signals in the presence of cochannel interference," *IEE Proceedings-I*, vol. 139, No 2, April 1992.

[33] S. W. Wales, "Performance of continuous phase modulations in the presence of cochannel interference," *Electronic Lett.*, vol. 24, No. 3, pp. 186-187, Feb. 1988.

[34] N. A. B. Svensson, "Error probability analysis for continuous phase modulation with Viterbi detection on a Gaussian channel with multiple single interference," *IEEE Transaction on commu.*, vol. 37, pp. 230-237, March 1989.

[35] O. Andrisano, G. Corazza and G. Immovilli, "Adjacent channel and cochannel interference in CPFSK with nonlinear transmitters and Limiter-discriminator

detection," *IEEE Trans. on Commu.*, vol. 36, pp. 544-552, May 1988.

[36] I. Korn, "GMSK with frequency-selective rayleigh fading and cochannel interference," *IEEE Journal on Selected Areas in Commu.*, vol. 10, pp. 506-515, May 1994.

[37] S. S. Shin and P. T. Mathiopoulos, "Differentially detected GMSK signals in CCI channels for mobile cellular telecommunication systems," *IEEE Transaction on Vehicular Technology,* vol. 42, pp. 289-293, Aug. 1993.

[38] C. Tellambura and V. K. Bharagava, "Performance of GMSK in frequency selective Rayleigh fading and multiple cochannel interferers," *Proc. of 45th IEEE Vehicular Technology Conference*, Chicago, USA, pp. 211-215, May 1995.

[39] D. Yu, D. D. Falconer and H. M. Hafez, "Interference characteristics of TDMA in-building wireless systems," *The Third Annual International Conference on Universal Personal Communications*, San Diego, CA, USA, pp. 99-103, 1994.

[40] P. Bo Hagerman, "Downlink relative co-channel interference powers in cellular radio systems," *IEEE 45th Veh. Tech. Conference*, Chicago, Illinois, July 1995, pp 366-370.

[41] T. S. Sundresh, F. A. Cassara and H. Schachter, "Maximum a posteriori estimator for suppression of interchannel interference in FM receivers," *IEEE Transaction on commu.,* vol. COM-25, pp. 1480-1485, March 1977.

[42] W. L. Aranguren and R. E. Langseth, "Evaluation of a method for interference control in analog FM systems," *IEEE Transaction on commu.,* vol. COM-27, pp. 762-767, April 1979.

[43] Y. Bar-Ness and H. Bunin, "Co-channel interference suppression and signal separation method," *Proc. of IEEE International Conference on communications*, 1988, pp. 1077-1081.

[44] Y. Bar-Ness and H. Bunin, "Adaptive co-channel interference cancellation and signal separation method," *Proc. of IEEE International Conference on communications*, 1989, pp. 825-830.

[45] M. L. Welborne and J. H. Reed, "Co-channel interference rejection using a model-based demodulator for AMPS and NAMPS," *IEEE 46th Veh. Tech. Conference*, Atlanta, Georgia, USA, May 1996, pp. 1312-1316.

[46] S. Haykin, Ed., *Array signal processing*, Prentice-Hall: Englewood Cliffs, NJ,

1985.

[47] K. Girindhar, S. Chari, J. J. Shynk and R. P. Gooch, "Joint demodulation of cochannel signals using MLSE and MAPSD algorithms," *IEEE International Conference on Acoustics, Speech, and Signal Processing*, Minneapolis, Minnesota, U.S.A., April 1993, pp. IV-(160-163).

[48] K. Girindhar, S. Chari, J. J. Shynk, R. P. Gooch and D. J. Artman, "Joint estimation algorithms for cochannel signal demodulation," *IEEE International Conference on Communications*, Geneva, Switzerland, May1993, pp. 1497-1501.

[49] P. A. Ranta, Z. Honkasalo and J. Tapaninen, "TDMA cellular network application of an interference cancellation technique," *IEEE 45th Veh. Tech. Conference*, Chicago, Illinois, July 1995, pp 296-300.

[50] S. W. Wales, "Technique for cochannel interference suppression in TDMA mobile radio system," *IEE Proc. communication*, vol. 43, No. 3, pp. 638-644, Aug. 1994.

[51] P. A. Ranta, A. Hottinen and Z. Honkasalo, "Co-channel interference cancelling for TDMA mobile systems," *IEEE International Conference on Communications*, Seattle, Wasington, June 1995, pp. 17-21.

[52] S. Heidari and C. L. Nikias, "A new method for the design of high performance receivers in the presence of co-channel interference," *Proc. of International Symposium on Time -Frequency and Time-Scale Analysis*, Philadelphia, PA, USA, Oct. 1994, pp 496-499.

[53] H. Yoshino, K. Fukawa and H. Suzuki, "Interference cancelling equalizer (ICE) for mobile radio communications," *IEEE International Conference on Communications*, New Orleans, U.S.A., May 1994, pp. 1427-1432.

[54] M. Uesugi, S. Futagi and K. Homma, "Interference cancellation method using DFE," *IEEE 46th Veh. Tech. Conference*, Atlanta, Georgia, USA, May 1996, pp. 1190-1194.

[55] R. P. Gooch and B. J. Sublett, "Demodulation of cochannel QAM signals," *IEEE International conference on Acoustic, speech & signal processing*, vol. 3, May 1989, pp. 1392-1395.

[56] H. Matsue and T. Murase, "Vector correlation type interference canceller," *Proc. of IEEE Global communication Conf. (GLOBCOM' 87)*, pp. 1233-1238, May 1987.

[57] H. Matsue and T. Murase, "Digitized cross-polarization interference canceller for multilevel digital radio," *IEEE Journal on Selected Areas in Commu.*, vol. SAC-5, April 1987, pp. 493-501.

[58] H. V. Poor and S. Verdu, "Single-user detectors for multiuser channels," *IEEE Trans. Commu.*, vol. COM-36, pp. 50-60, Jan. 1988.

[59] R. Kohno, M. Hotari and H. Imai, "Cancellation techniques of cochannel interference in asynchronous spread spectrum multiple access systems," *Electronic and Commu.*, vol. 66-A, no. 5, pp. 20-29, 1983.

[60] K. S. Schneider, "Optimum detection of code division multiplexed signals," *IEEE Trans. Aerosp. Electron. Syst.*, vol. AES-15, pp. 181-185, Jan. 1979.

[61] K. S. Schneider, "Crosstalk resistant receiver for M-ary multiplexed communications," *IEEE Trans. Aerosp. Electron. Syst.*, vol. AES-16, July 1980.

[62] S. Verdu, "Minimum probability of error for asynchronous Gaussian multiple-access channels," *IEEE Transaction on Information Theory,* vol. IT-32, pp. 85-96, Jan. 1986.

[63] S. Verdu, "Optimum multiuser asymptotic efficiency," *IEEE Transaction on commu.,* vol. COM-34, pp. 890-897, Sept. 1986.

[64] A. Duel-Hallen, "Decorrelating decision-feedback multiuser detector for synchronous code-division multiple-access channel," *IEEE Trans. on Commu.*, vol. COM-41, pp. 285-290, Feb. 1993.

[65] A. Duel-Hallen, "A family of multiuser decision-feedback detectors for asynchronous code-division multiple-access channels," *IEEE Trans. on Commu.*, vol. COM-43, pp. 421-434, Feb./March/April 1995.

[66] R. Lupas and S. Verdu, "Near far resistance of multiuser detectors in asynchronous channels," *IEEE Transaction on Commu.,* vol. COM-38, pp. 496-508, April 1990.

[67] T. K. Moon, Z. Xie, C. K. Rushforth and R. T. Short, "Parameter estimation in a multi-user communication system," *IEEE Trans. on Commu.*, vol. COM-42, Aug. 1994, pp. 2553-2560.

[68] P. Patel and J. Holtzman, "Analysis of a simple successive interference cancellation scheme in a DS/CDMA system," *IEEE Journal on Selected Areas In Commu.,* vol. SAC-12, pp. 796-807, May 1994.

[69] M. K. Varanasi and A. Azhang, "Multistage detection in asynchronous code-division multiple access communications," *IEEE Trans. Commu.*, vol. COM-38, pp. 509-519, April 1990.

[70] M. K. Varanasi and A. Azhang, "Near-optimum detection in synchronous code-division multiple-access systems," *IEEE Trans. Commu.*, vol. COM-39, pp. 725-736, May 1991.

[71] Z. Xie, R. T. Short and C. K. Rushforth, "A family of suboptimum detectors for coherent multiuser communications," *IEEE Journal on Selected Areas In Commu.,* vol. SAC-8, pp. 683-690, May 1990.

[72] Z. Xie, C. K. Rushforth and R. T. Short and T. K. Moon, "Joint signal detection and parameter estimation in multiuser communications," *IEEE Trans. Commu.*, vol. COM-41, pp. 1208-1216, April 1993.

[73] T. K. Moon, Z. Xie, C. K. Rushforth and R. T. Short, "Parameter estimation in a multi-user communication system," *IEEE Trans. on Commu.*, vol. COM-42, Aug. 1994, pp. 2553-2560.

[74] M. K. Varanasi and S. Vasudevan, "Multiuser detectors for synchronous CDMA Communication over non-selective Rician fading channels," *IEEE Trans. Commu.*, vol. COM-42, pp. 711-22, Feb./March/April 1994.

[75] M. K. Varanasi and S. Vasudevan, "Optimum diversity combiner based multiuser detection for time-dispersive Rician fading CDMA channels," *IEEE Journal on Selected Areas In Commu.,* vol. 12, pp. 580-592, May 1994.

[76] Z. Zvonar and D. Brady, "Multiuser detection in single-path fading channels," *IEEE Trans. Commu.*, vol. COM-42, pp. 1729-1739, Feb./March/April 1994.

[77] Z. Zvonar and D. Brady, "Suboptimal multiuser detector for frequency selective Rayleigh fading synchronous CDMA channels," *IEEE Trans. Commu.*, vol. COM-43, pp. 154-157, Feb./March/April 1995.

[78] J. Holtzman, "DS/CDMA successive interference cancellation," *In code Division Multiple Access Communication*, S. G. Glisic and P. A. Leppanen, Ed. Kluer Academic Publishers, pp. 161-180, 1995.

[79] A. L. Johnsson and A. Svensson, "Successive interference cancellation in multiple data rate DS/CDMA systems," *IEEE 45th Veh. Tech. Conference*, Chicago, Illinois, USA, July 1995, pp. 704-708.

[80] A. L. Johnsson and A. Svensson, "multistage interference cancellation with

decision directed channel estimation in multirate DS/CDMA on a mobile radio channel," *IEEE 46th Veh. Tech. Conference*, Atlanta, Georgia, USA, May 1996, pp. 331-335.

[81] K. I. Pedersen, T. E. Kolding, I. Seskar and J. M. Holtzman, "Practical implementation of successive interference cancellation in DS/CDMA systems," *IEEE 46th Veh. Tech. Conference*, Atlanta, Georgia, USA, May 1996, pp. 321-325.

[82] S. R. Kim, J. G. Lee and H. Lee, "Interference cancellation scheme with simple structure and better performance," *Electronic Lett.*, vol. 32, no. 23, pp. 2115-2117, Nov. 1996.

[83] P. Bo Hagerman, "On the detection of antipodal Rayleigh fading signals in severe co-channel interference," *IEEE 44th Veh. Tech. Conference*, Stockholm, Sweden, June 1994, PP 1259-1262.

[84] W. A. Gardner, "Measurement of spectral correlation," *IEEE Trans. on Acoustic, Speech, and Signal Processing*, vol. ASSP-34, pp. 1111-1123, Oct. 1986.

[85] W. A. Gardner, "Spectral correlation of modulated signals: part I-analog modulation," *IEEE Trans. on Commu.*, vol. COM-35, pp. 584-594, June 1987.

[86] W. A. Gardner, W. A. Brown and C. K. Chen, "Spectral correlation of modulated signals: part II-digital modulation," *IEEE Trans. on Commu.*, vol. COM-35, pp. 595-601, June 1987.

[87] W. A. Gardner and W. A. Brown, "Frequency-shift filtering theory for adaptive co-channel interference removal," *Proc. of IEEE 23rd Asilomar Conference on Signals, Systems & Computers*, Los Angeles, California, U.S.A., Nov. 1989, pp. 562-567.

[88] W. A. Gardner and S. Venkataraman, "Performance of optimum and adaptive frequency-shift filters for co-channel interference and fading," *Proc. of IEEE 24th Asilomar Conference on Signals, Systems & Computers*, Pacific Grove, California, U.S.A., Nov. 1990, pp. 243-247.

[89] W. A. Gardner, "Cyclic Wiener filtering: theory and method," *IEEE Trans. on Commu.*, vol. 41, pp. 151-163, Jan. 1993.

[90] P. Monsen, "MMSE equalisation of interference on fading diversity channels," *IEEE Transaction on Commu.*, vol. COM-34, pp. 5-12, Jan. 1984.

[91] J. H. Winters, "Optimum combining in digital mobile radio with cochannel interference," *IEEE Journal on Selected Areas In Commu.,* vol. SAC-2, pp. 528-539, June 1973.

[92] S. Anderson, M. Millnert, M. Viberg and B. Wahlberg, "An adaptive array for mobile communication systems," *IEEE Transaction on Vehicular Technology,* vol. 40, pp. 230-236, Feb. 1991.

[93] R. L. Riegler and R. T. Compton, Jr., "An adaptive array for interference rejection," *Proc. of the IEEE,* vol. 61, pp. 748-758, June 1973.

[94] B. Widrow, P. E. Mantey, L. J. Griffiths and B. B. Goode, "Adaptive antenna systems," *Proc. of the IEEE,* vol. 55, pp. 2143-2159, Dec. 1967.

[95] J. H. Winters, "Optimum combining in digital mobile radio with cochannel interference," *IEEE Journal on Selected Areas In Commu.,* vol. SAC-2, pp. 528-539, June 1973.

[96] J. H. Winters, "Optimum combining for indoor radio systems with multiple users," *IEEE Trans. Commu.*, vol. COM-35, pp. 1222-1230, Nov. 1987.

[97] R. T. Compton, Jr., *Adaptive antennas: concept and performance*, Englewood Cliffs: Prentice-Hall Inc., 1988.

[98] R. A. Monzingo and T. W. Miller, *Introduction to adaptive antenna array*, New York: John Wiley and Sons, 1980.

[99] M. Barret and R. Arnott, "Adaptive antennas for mobile communications," IEE Electron. & communication Journal, pp. 203-214, Aug. 1994.

[100] D. W. Tufts and A. A. Shah, "Rapid interference suppression and channel identification for digital, multipath wireless Channels," *Proc. of 44th IEEE Vehicular Technology Conference,* Stockholm, Sweden, June 1994, pp. 1241-1244.

[101] T. Ohgane, T. Shimura, N. Mutsuzawa and H. Sasaoka, "An implementation of a CMA adaptive array for high speed GMSK Transmission in Mobile Communications," *IEEE Transaction on Vehicular Technology,* vol. 42, pp. 282-288, Aug. 1993.

[102] J. R. Treichler and B. G. Agee, "A new approach to multipath correction of constant modulus signals," *IEEE Trans. on Acoustic, Speech, and Signal Processing*, vol. ASSP-31, pp. 459-472, April 1983.

[103] Y. C. Pati, G. G. Rayleigh and A. Paulraj, "Estimation of cochannel FM signals with multitarget adaptive phase-locked loops and antenna arrays," *IEEE International Conference on Acoustics, Speech, and Signal Processing*, Detroit, MI, U.S.A., May 1995, pp. 1741-1744.

[104] S. V. Schell and W. A. Gardner, "Blind adaptive arrays for increased capacity in cellular communications," *Wireless Personal Communications; Trends and Challenges*, Ed. T. S. Rappaport, *et al*, Boston: Keuer Academic, 1994, pp. 16-26.

[105] J. B. Carruthers, D. D. Falconer, H. M. Sandler and L. Strawczynski, "Bit synchronisation in the presence of co-channel interference," *Proc. of Canadian Conf. on Elec. and Comp. Eng.*, pp. 411-417, Ottawa, ON, 1990.

[106] D. W. Paranchych and N. C. Beaulieu, "Digital symbol synchronizer performance in the presence of multiple cochannel interferer," *Proceeding of 7th Canadian Conference on Electrical and Computer Engineering*, Halifax, NS, CANADA, 25-28 Sept. 1994, pp 284-287.

[107] D. W. Paranchych and N. C. Beaulieu, "Markov modelling of a digital symbol synchronizer in cochannel interference," *IEEE International Conference on Communications*, Seattle, Wasington, June 1995, pp. 1800-1804.

[108] A. E. Payzin, "Analysis of a digital bit synchronizer," *IEEE Trans. Commu.*, vol. COM-31, pp. 199-209, April 1983.

[109] D. C. Cox, "Cochannel interference consideration in frequency reuse small-coverage-area radio systems," *IEEE Trans. Commu.*, vol. COM-30, pp. 135-142, Jan. 1982.

[110] W. C. Y. Lee, *Mobile communication design fundamental*, Indianapolis: Howard W. Sams, 1986.

[111] F. Adachi and K. Ohno, "Block error probability for noncoherent FSK with diversity reception in mobile radio," *Elect. Lett.*, vol. 24, pp. 1523-1525, 1988.

[112] R. J. C. Bultitude and G. K. Bedal, "Propagation characteristics on microcellular urban mobile radio channels at 910 MHz," *IEEE J. Select. Areas Commu.*, vol. 7, pp. 31-39, Jan. 1989.

[113] M. Nakagami, "The m-distribution - a general formula of intensity distribution of rapid fading," *Statistical Methods of Radio Wave Propagation*, W. C. Hoffman, Ed. Oxford, England: Pergamon, 1960, pp. 3-36.

[114] U. Charash, "Reception through Nakagami fading multipath channels with random delays," *IEEE Trans. Commu.*, vol. COM-27, pp. 657-670, April 1979.

[115] H. Suzuki, "A statistical model for urban radio propagation," *IEEE Trans. Commu.*, vol. COM-25, pp. 673-680, July 1977.

[116] A. Wonjar, "Unknown bounds on performance in Nakagami channels," *IEEE Trans. Commu.*, vol. COM-34, pp. 22-24, Jan. 1986.

[117] R. C. French, "The effect of fading and shadowing on channel reuse in mobile radio," *IEEE Transaction on Veh. Tech.*, vol. VT-28, pp. 171-181, 1979.

[118] Y. S. Yeh and S. C. Schwartz, "Outage probability in mobile telephony due to multiple log-normal interferers," *IEEE Trans. on Commu.*, vol. COM-32, pp. 380-387, April 1984.

[119] A. Safak, "Optimal channel reuse in cellular radio systems with correlated log-normal interferers," *IEEE Transaction on Vehicular Technology,* vol. 43, pp. 304-312, May 1994.

[120] R. Muammar and S. C. Gupta, "Cochannel interference in high capacity mobile radio systems," *IEEE Transaction on Commu.,* vol. COM-30, pp. 1973-1982, Aug. 1982.

[121] K. W. Sowerby and A. G. Williamson, "Outage probability calculations for mobile radio systems with multiple interferers," *Elect. Lett.*, vol. 24, pp. 1073-1075, Aug. 1988.

[122] A. G. Williamson and J. D. Parsons, "Outage probability in a mobile radio system subject to fading and shadowing," *Elect. Lett.*, vol. 21, pp. 622-623, 1985.

[123] K. W. Sowerby and A. G. Williamson, "Outage probability calculations for a mobile radio system having multiple Rayleigh interferers," *Elect. Lett.*, vol. 23, pp. 600-601, 1987.

[124] K. W. Sowerby and A. G. Williamson, "Outage probability calculations for multiple cochannel interferers in cellular mobile radio systems," *IEE Proc.*, pt. F. vol. 135, no. 3, pp. 208-215, June 1988.

[125] Y. D. Yao and A. U. H. Sheikh, "Outage probability analysis for microcell mobile radio systems with cochannel interferers in Rician/Rayleigh fading environment," *Elect. Lett.*, vol. 26, pp. 864-866, June 1990.

[126] R. Prasad and A. Kegel, "Spectrum efficiency of Microcellular systems," *41st IEEE Vehicular Technology Conference*, pp. 357-361, June 1991.

[127] A. A. Abu-Dayya and N. C. Beaulieu, "Outage probabilities of cellular mobile radio systems with multiple Nakagami interferers," *IEEE Transaction on Vehicular Technology*, vol. 40, pp. 757-768, Nov. 1991.

[128] Y. D. Yao and A. U. H. Sheikh, "Investigation into cochannel interference in microcellular mobile radio systems," *IEEE Transaction on Vehicular Technology*, vol. 41, pp. 114-123, May 1992.

[129] C. Tellambura and V. K. Bharagava, "Outage probability analysis for cellular mobile radio with multiple, arbitrary Nakagami interferers," *Proc. of 45th IEEE Vehicular Technology Conference*, Chicago, USA, pp. 384-388, May 1995.

[130] F. D. Jager and C. D. Dekker, "Tamed frequency modulation, a novel method to achieve spectrum economy in digital transmission," *IEEE Transaction on commu.*, vol. COM-26, pp. 534-542, May 1978.

[131] P. S. K. Leung, "Asymmetric raised cosine frequency shift keying (ARC-FSK) - a new anti-multipath modulation for mobile and personal communication systems," *Proc. of IEEE 4th International Conference on Universal Communications*, Tokyo, Japan, Nov. 1995.

[132] P. S. K. Leung, *GMSK and F-QPSK for high capacity cellular mobile radio and microcellular personal communication Systems*, PhD. Thesis, The University of California Davis, 1994.

[133] R. P. Gooch and J. Lundell, "The CM array: an adative beamformer for constant modulus signals," *Proc. ICASSP'86*, Tokyo, Japan, April 1986, pp. 2523-2526.

[134] S. Lang, *Linear algebra*, Addison-Wesley Publishing Company, 1972.

[135] P. J. McLane, "A residual intersymbol interference error bound for truncated-state viterbi detectors," *IEEE Transaction on Information Theory*, vol. IT-26, pp. 549-553, Sept. 1980.

[136] W. C. Jakes, *Microwave mobile communications*, New York: John Wiley & Sons, 1974.

[137] I. B. Ball, "A Real time fading simulator for mobile radio," *The Radio Electronic Engineer*, vol. 52, No. 10, pp. 457-478, Oct. 1982.

[138] W. P. Osborn and M. B. Luntz, "Coherent and noncoherent detection of

CPFSK," *IEEE Transaction on commu.*, vol. COM-22, pp. 1023-1036, Aug. 1974.

[139] Tor Aulin and C. E. W. Sundberg, "Continuous phase Modulation-Part I: Full response rignaling," *IEEE Transaction on commu.*, vol. COM-29, pp. 196-209, March 1981.

[140] Tor Aulin and C. E. W. Sundberg, "Continuous phase Modulation-Part II: Partial response signaling," *IEEE Transaction on commu.*, vol. COM-29, pp. 210-226, March 1981.

[141] F. Amoroso and A. Kivett, "Simplified MSK signaling Techniques," *IEEE Trans. on Commu.*, vol. COM-25, pp. 433-441, April 1977.

[142] R. E. Ziemer, C. R. Ryan and J. H. Stilwell, "Conversion and Mached Filter Approximation for serial minimum-shift keyed modulation," *IEEE Trans. on Commu.*, vol. COM-30, pp. 495-509, March 1982.

[143] R. Buda, "Coherent demodulation of Frequency-Shift Keying with low deviation ratio," *IEEE Trans. Commu*, pp. 429-435, June 1972.

[144] N. A. B. Svensson and C. E. Sundberg, "Optimum MSK-Type receivers for CPM on Gaussian and Rayleigh fading channels," *IEE Proc., Pt. F, Commu., Radar, Sig. Process.*, vol. 131, pp. 480-490, May 1987.

[145] G. D. Forney, "The Viterbi algorithm," *Proc. of the IEEE*, vol. 61, pp. 268-278, March 1973.

[146] A. Papoulis, *Probability, random variables, and stochastic processes*, New York: McGraw-Hill, 1965.

[147] A. V. Oppenheim and R. W. Schafer, *Digital signal processing*, New Jersey: Prentice-Hall, New Jersy, 1975.

[148] B.E. Rimioldi, "A decomposition approach to CPM," *IEEE Transaction on Information Theory*, vol. 34, pp. 260-270, March 1988.

[149] R. Prasad, *CDMA for wireless personal communications*, Boston: Artech House, 1996.

[150] J. P. McGeehan and A. J. Bateman, "Phase-locked transparent tone-in-band (TTIB): a new spectrum configuration particularly suited to the transmission of data over SSB mobile radio networks," *IEEE Transaction on Commu.*, vol. 32, pp. 81-87, Jan. 1984.

[151] J. K. Cavers, "Performance of tone calibration with frequency offset and imperfect pilot filter," *IEEE Transaction on Vehicular Technology,* vol. 40, pp. 426-434, May, 1991.

[152] M. L. Moher and J. H. Lodge, "TCMP-a modulation and coding strategy for rician fading channels," *IEEE Journal on Selected Areas in Commu.*, vol. 7, pp. 1347-1355, Dec. 1989.

[153] J. K. Cavers, "An analysis of pilot symbol assisted modulation for Rayleigh fading channels," *IEEE Transaction on Vehicular Technology,* vol. 40, pp. 686-693, Nov. 1991.

[154] S. Sampei and T. Sunaga, "Rayleigh fading compensation method for 16QAM in digital land mobile radio channels," *39th IEEE Vehicular Technology Conference,* pp. 640-649, 1989.

[155] S. Sampei and T. Sunaga, "Rayleigh Fading Compensation Method for QAM in Land Mobile Radio Communications," *IEEE Transaction on Vehicular Technology,* vol. 42, pp. 137-147, May. 1993.

[156] J. K. Cavers, "Pilot symbol assisted modulation in fading and delay spread," *Proc. of 43rd IEEE Vehicular Technology Conference*, NJ, USA, pp. 641-644, May 1993.

[157] A. N. D'Andrea, A. Diglio and U. Mengali, "Symbol-aided channel estimation with nonselective Rayleigh fading channels," *IEEE Transaction on Vehicular Technology,* vol. 44, pp. 41-49, Feb. 1995.

[158] G. T. Irvine and P. J. McLane, "Symbol-Aided Plus Decision-Directed Reception for PSK/TCM Modulation on Shadowed Mobile Satellite Fading Channels," *IEEE Journal on Selected Areas in Commu.*, vol. 10, pp. 1289-1299, Oct. 1992.

[159] J. K. Cavers and J. Varaldi, "Cochannel interference and pilot Symbol Assisted Modulation," *IEEE Transaction on Vehicular Technology,* vol. 42, pp. 407-413, Nov. 1993.

[160] H. K. Lau and S. W. Cheung, "Performance of a pilot symbol-aided technique in frequency-selective Rayleigh fading channels corrupted by co-channel interference and Gaussian noise," *IEEE 46th Veh. Tech. Conference*, Atlanta, Georgia, USA, May 1996, pp. 1008-1012.

[161] R. Shafer and L. Rabiner, "A digital signal processing approach to interpolation," *Proc. of IEEE*, vol. 61, pp. 692-702, June 1973.

[162] M. Wittmann, J. Marti and T. Kurner, "Impact of the power delay profile shape on the bit error rate in mobile radio systems," *IEEE Transaction on Vehicular Technology*, vol. 46, pp. 329-339, May 1997.

[163] R. J. Serfling, Approximation Theorms of Mathematical Statistics, John Wiley & Sons: New York, 1980.

[164] A. Stuart and K. Ord, *Advanced theory of statistcs*, Volume 2, New York: Oxford University Press, 1991.

[165] J. D. Gibson, *Principals of digital and analog communications*, New York: Macmillan Publishing Company, 1993.

[166] H. Leib and S. Pasupathy, "Error-control properties of minimum shift keying,", *IEEE communication Magazine*, pp. 52-61, Jan. 1993.

[167] I. S. Gradshtein and I.M. Ryzhik, *Table of integrals, series, and products*, Boston: Academic Press, 1994.

Appendices

APPENDIX A

SIMILARITIES BETWEEN COST FUNCTIONS (2.5) AND (2.6)

To show the resemblance between metric (2.5) and (2.6), a statistical study has been performed. These metrics are calculated for a number of sets of $m+1$ normal random numbers. Their comparison in Fig. A.1 shows that for a small m two metrics are highly correlated. As m increases, the correlation between them remains good but decreases.

To further investigate the resemblance between (2.5) and (2.6), Monte Carlo simulation is performed on the BB-ICIC receiver (see section 2.6). The BER

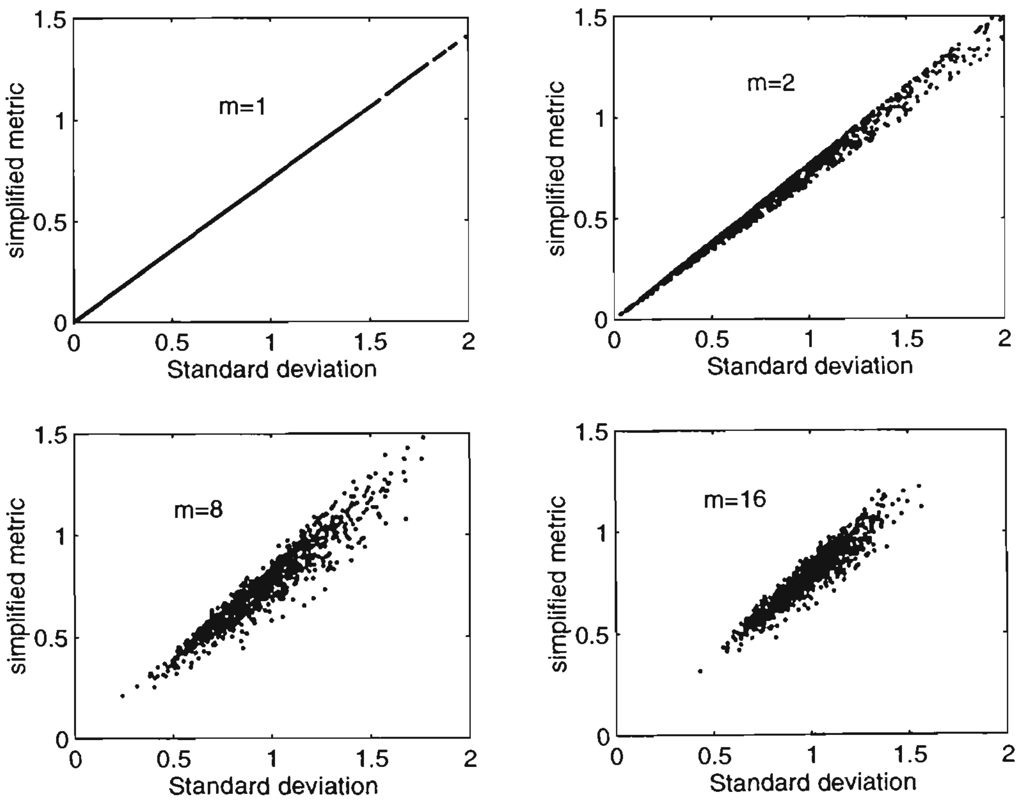

Fig. A.1. Simplified metric (2.6) values versus corresponding standard deviation for 1000 sets of *m+1* random numbers.

performance in AWGN channel, presented in Fig. A.2, shows no significant difference between two metrics. A similar results was obtained in Rayleigh fading channel with CCI (Fig. A.3).

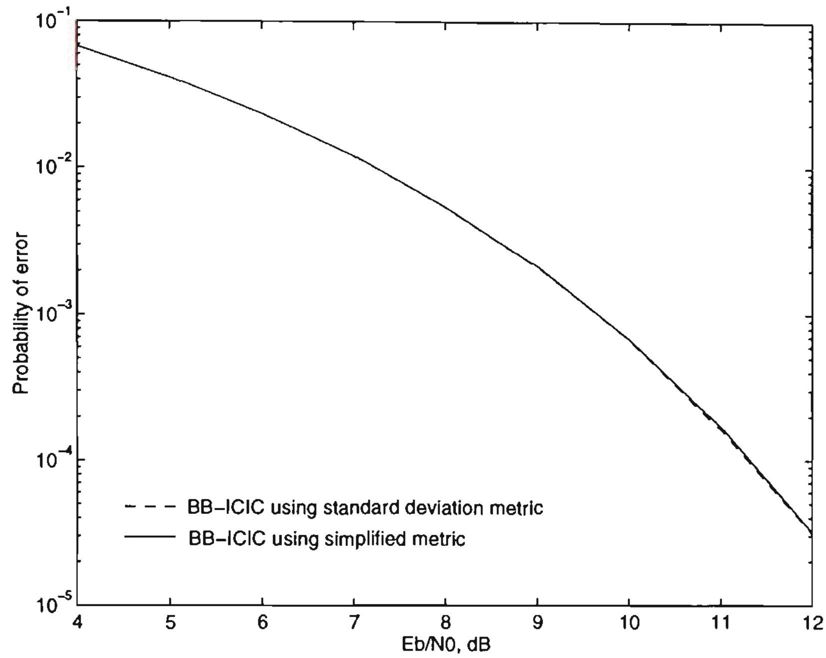

Fig. A.2. BER performance of BB-ICIC for MSK in AWGN .

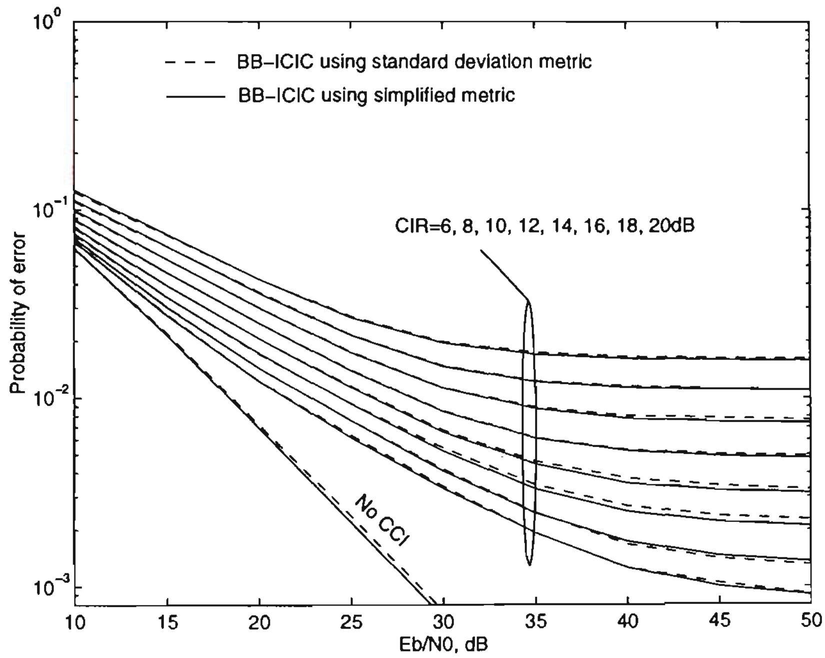

Fig. A.3. BER performance of BB-ICIC for MSK in Rayleigh fading channel with CCI.

APPENDIX B

Table B.1. List of famous CPM modulation schemes and their frequency pulses (from [26] and [131]).

LRC (raised cosine)	$g(t) = \begin{cases} \frac{1}{2LT}\left[1-\cos\left(\frac{2\pi t}{LT}\right)\right], & 0 \le t \le LT \\ 0 & otherwise \end{cases}$
LSRC (spectral raised cosine)	$g(t) = \frac{1}{LT}\left\{\frac{\sin\left(\frac{2\pi t}{LT}\right)\cos\left(\beta\frac{2\pi t}{LT}\right)}{\frac{2\pi t}{LT}\left[1-\left(\frac{4\beta}{LT}t\right)^2\right]}\right\}, \quad 0 \le \beta \le 1$
ARC-FSK (asymmetric raised cosine)	$g(t) = \begin{cases} \frac{1}{4T}\left[1+\cos\left(\frac{2\pi t}{T}\right)\right] - \frac{A}{4T}\left[1-\cos\left(\frac{2\pi t}{T}\right)\right]?\mathrm{sgn}?(t), & -T \le t \le T \\ 0 & otherwise \end{cases}$ $0 \le A < 1, \quad ?\mathrm{sgn}?(t) = \begin{cases} 1 & t \ge 0 \\ -1 & t < 0 \end{cases}$
LREC (rectangular frequency pulse)	$g(t) = \begin{cases} \frac{1}{LT}, & 0 \le t \le LT \\ 0 & otherwise \end{cases}$
TFM (tamed FM)	$g(t) = \frac{1}{8}[g_0(t-T) + 2g_0(t) + g_0(t+T)]$ $g_0(t) = \frac{1}{T}\left[\frac{\sin\left(\frac{\pi t}{T}\right)}{\frac{\pi t}{T}} - \left(\frac{\pi^2}{24}\right)\frac{2\sin\left(\frac{\pi t}{T}\right) - \frac{2\pi t}{T}\cos\left(\frac{\pi t}{T}\right) - \left(\frac{\pi t}{T}\right)^2\sin\left(\frac{\pi t}{T}\right)}{\left(\frac{\pi t}{T}\right)^3}\right]$
GMSK (Gaussian-shaped MSK)	$g(t) = \frac{1}{2T}\left\{Q\left[2\pi B_b\frac{t-\frac{T}{2}}{(\ln 2)^{1/2}}\right] - Q\left[2\pi B_b\frac{t+\frac{T}{2}}{(\ln 2)^{1/2}}\right]\right\}$ $Q(t) = \int_t^{\infty}\frac{1}{(2\pi)^{1/2}}e^{-\tau^2/2}d\tau$

APPENDIX C

FREQUENCY RESPONSE OF GAUSSIAN AND MAXIMALLY FLAT LOWPASS FILTERS

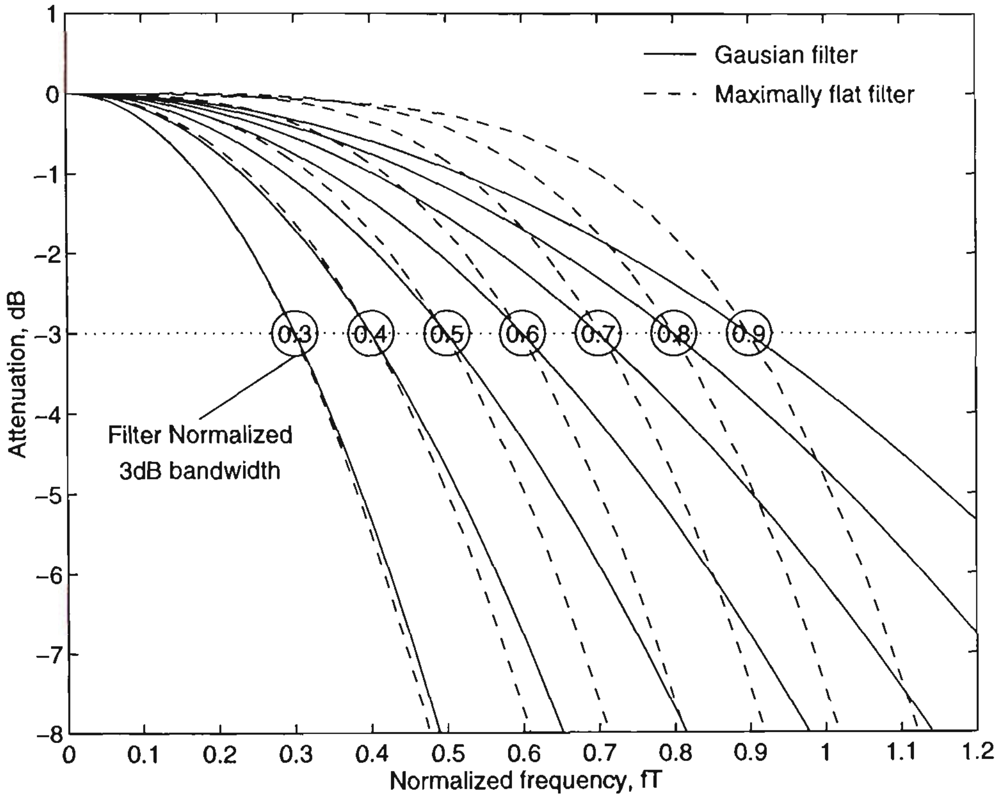

Fig. C.1. Frequency response of 36 taps FIR Gaussian and Maximally flat FIR filters designed with Frequency Sampling Design method [146] and Hanning window. Sampling rate for both filters is $f_s = 16 \cdot r_b$.

APPENDIX D

D.1 Calculation of Integral using sampled analog signal with An extra sample

Consider integral $A = \int_{t_0}^{(t_0+T)} f(t)dt$ has to be calculated using the samples of integrand $f(t)$. There are many numerical algorithms which can be used to calculate this integral. However, for normalization of (2.6) only those algorithms which can be explained in terms of summation of consecutive samples of $f(t)$ are of interest. Perhaps, the simplest algorithm is to estimate the integral by adding the areas of rectangles which their widths are equal to the sampling period T_s and their heights are taken from the samples of integrand (Fig. D.1.a). Such approximation can be defined as

$$A \approx T_s \sum_{k=0}^{m-1} f(t_0 + kT_s) \qquad 0 \le kT_s \le T \tag{D.1}$$

If the sampling rate, as in (2.6), is integer multiple of $1/T$ and the samples start from the beginning of integration period, total number of samples are $m+1$. To include the extra sample into this summation, number of rectangles must be increased by one and their width must be reduced by a factor of $m/(m+1)$ (Fig. D.1.b). In this case approximated area will be

$$A \approx \frac{mT_s}{m+1} \sum_{k=0}^{m} f(t_0 + kT_s) \tag{D.2}$$

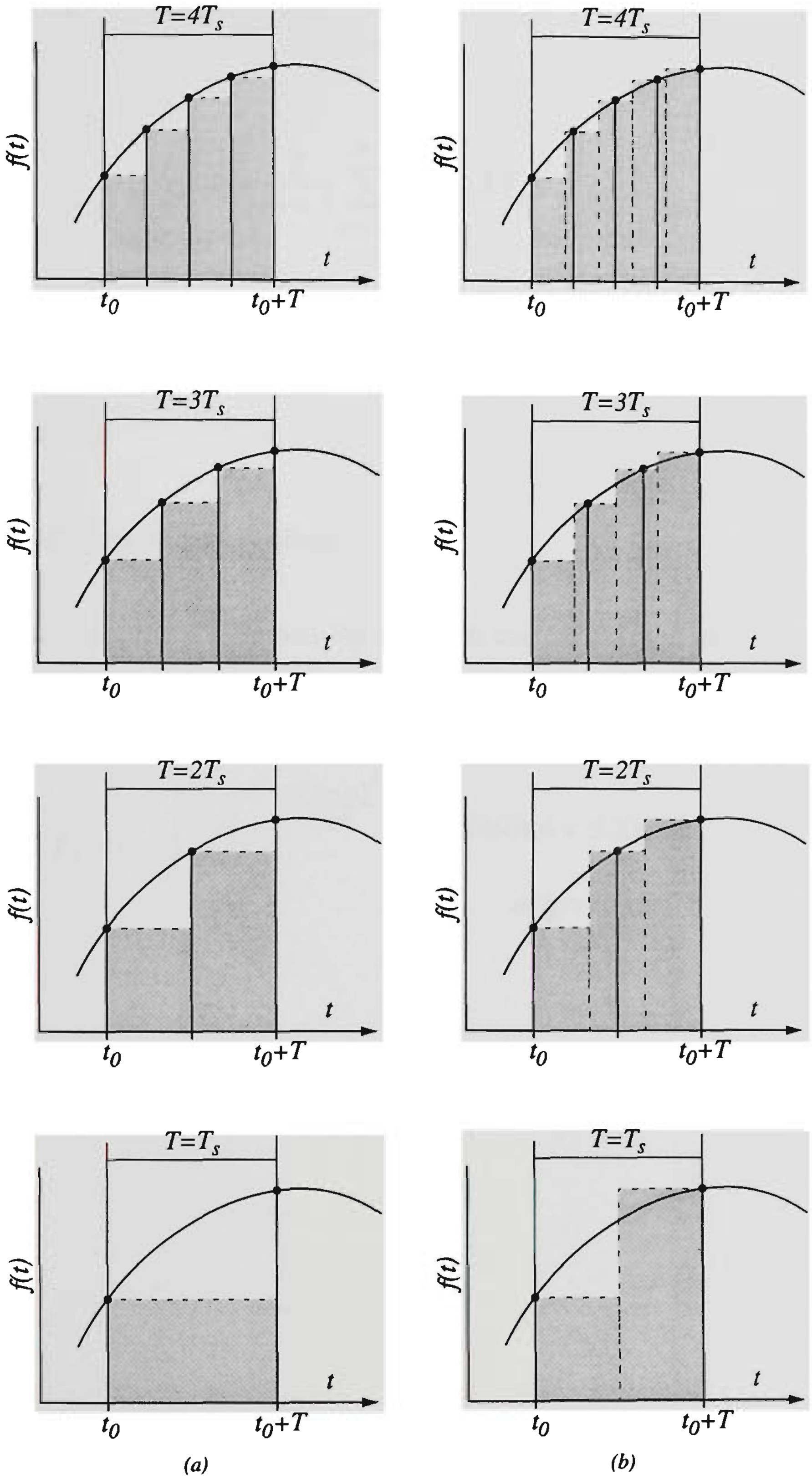

Fig. D.1. Calculation of area under $f(t)$ in $t_0 \leq t \leq t_0+T$ using (a) m out of $m+1$ samples (b) $m+1$ out of $m+1$ samples

Substituting $mT_s = T$ into (D.2) gives

$$A \approx \frac{T}{m+1}\sum_{k=0}^{m} f(t_0 + kT_s) \tag{D.3}$$

As shown by the examples of Fig. D.1. this algorithm increases the accuracy of integral estimation.

D.2 Truncated normal distribution

Truncated Gaussian probability density function can be defined as

$$f_x(x) = \begin{cases} \dfrac{K}{\sigma\sqrt{2\pi}} e^{\frac{-(x-\mu)^2}{2\sigma^2}} & Xmin \le x \le Xmax \\ 0 & otherwise \end{cases} \tag{D.4}$$

where K is the normalization constant such that

$$\int_{X_{min}}^{X_{max}} f_x(x)dx = 1 \tag{D.5}$$

It can be easily shown that

$$\frac{1}{\sigma\sqrt{2\pi}}\int_{X_{min}}^{X_{max}} e^{\frac{-(x-\mu)^2}{2\sigma^2}}dx = erf\frac{X_{max}-\mu}{\sigma} - erf\frac{X_{min}-\mu}{\sigma} \tag{D.6}$$

where erf is error function defined as

$$erf(x) = \frac{1}{\sqrt{2\pi}}\int_0^x e^{-\lambda^2/2}d\lambda \tag{D.7}$$

Hence

$$K = \left[erf\frac{X_{max}-\mu}{\sigma} - erf\frac{X_{min}-\mu}{\sigma}\right]^{-1} \tag{D.8}$$

For $0 < x < \infty$ we have

$$K = \left[0.5 - erf\left(\frac{-\mu}{\sigma}\right)\right]^{-1} = \left[0.5 + erf\left(\frac{\mu}{\sigma}\right)\right]^{-1} \tag{D.9}$$

As a result, (D.4) can be written as

$$f_x(x) = \frac{1}{\left[0.5 + erf\left(\frac{\mu}{\sigma}\right)\right]\sigma\sqrt{2\pi}} e^{\frac{-(x-\mu)^2}{2\sigma^2}} U(x) \tag{D.10}$$

Random variable x for $0 < x < \infty$ has an average of

$$E\{x\} = \frac{\sigma_x}{\left[0.5 + erf\left(\frac{\mu}{\sigma}\right)\right]\sqrt{2\pi}} + \frac{\mu}{2\left[0.5 + erf\left(\frac{\mu}{\sigma}\right)\right]} \tag{D.11}$$

and a variance of

$$\sigma_x^2 = \frac{1}{\left[0.5 + erf\left(\frac{\mu}{\sigma}\right)\right]\sqrt{2\pi}}[\sqrt{2}\Gamma(3/2)\sigma^2 + \mu^2\sqrt{\pi/2} + 2\mu\sigma] - \left\{\frac{\sigma}{\left[0.5 + erf\left(\frac{\mu}{\sigma}\right)\right]\sqrt{2\pi}} + \frac{\mu}{2\left[0.5 + erf\left(\frac{\mu}{\sigma}\right)\right]}\right\}^2 \tag{D.12}$$

APPENDIX E

AUTOCORRELATION OF AWGN FILTERED WITH A GAUSSIAN FILTER

The autocorrelation function of an additive white Gaussian noise filtered with a Gaussian filter can be written as

$$\mathcal{R}_{xx}(\tau) = \mathcal{F}^{-1}[G(j\omega)] \tag{E.1}$$

where the operator $\mathcal{F}^{-1}$ is the inverse Fourier Transform and $G(j\omega)$ is the power spectral density of the filter defined by

$$G(j\omega) = |H(j\omega)|^2 \tag{E.2}$$

where for the Gaussian filter $|H(j\omega)|$ is

$$|H(j\omega)| = \exp\left[-\frac{\ln(2)}{2}\left(\frac{\omega}{\omega_c}\right)^2\right] \tag{E.3}$$

In (E.3), $\omega_c = 2\pi B$ and B is the filter bandwidth. Substituting (E.3) into (E.1) gives

$$\mathcal{R}_{xx}(\tau) = \mathcal{F}^{-1}\left\{\exp\left[-\ln(2)\left(\frac{\omega}{\omega_c}\right)^2\right]\right\} = \sqrt{\frac{\pi}{\ln(2)}}B\exp\left[-\frac{\pi^2}{\ln(2)}(Bt)^2\right] \tag{E.4}$$

APPENDIX F

THE REQUIRED PDFS FOR 2-SAMPLE METRIC

F.1 PDF of L_{rr} with 2-Sample metric

From (5.21) for 2-samples metric L_{rr} can be written as

$$L_{rr} = \frac{T}{2}\left[\left|\frac{1}{2}v(0)-\frac{1}{2}v(1)\right| + \left|\frac{1}{2}v(0)-\frac{1}{2}v(1)\right|\right] = \frac{T}{2}|v(0)-v(1)| \tag{F.1}$$

where $v(0)$ and $v(1)$ are samples taken from the beginning and the end of bit time interval. The PDF of $x = -v(1)$ using (5.22) can be written as

$$f_x(x) = \alpha e^{\alpha x}U(-x) \tag{F.2}$$

Denoting $y = v(0)$, with the assumption of the independence of $v(0)$ and $v(1)$, the PDF of $z = x + y$ can be defined by the convolution of their PDFs

$$f_z(z) = \int_{-\infty}^{\infty} f_y(y)f_x(z-y)dy \tag{F.3}$$

Substituting (5.22) and (F.2) into (F.3) results in

$$f_z(z) = \begin{cases} \int_z^{\infty} \alpha^2 e^{\alpha(z-y)} e^{-\alpha y} dy & z > 0 \\ \int_0^{\infty} \alpha^2 e^{\alpha(z-y)} e^{-\alpha y} dy & z < 0 \end{cases} \tag{F.4}$$

From (F.4) we have

$$f_z(z) = \frac{\alpha}{2} e^{-\alpha|z|} \tag{F.5}$$

From (F.5) and considering that $L_{rr} = \frac{T}{2}|z|$, the PDF of L_{rr} is as follows

$$f_{L_{rr}}(L_{rr}) = \frac{2\alpha}{T} e^{-\frac{2\alpha L_{rr}}{T}} U(L_{rr}) \tag{F.6}$$

Substituting $\alpha = 1/(2\sigma_n^2)$ into (F.6) results

$$f_{L_{rr}}(L_{rr}) = \frac{1}{\sigma_n^2 T} e^{-\frac{L_{rr}}{\sigma_n^2 T}} U(L_{rr}) \tag{F.7}$$

The variance of noise can be shown by

$$\sigma_n^2 = N_0 B_N \tag{F.8}$$

where N_0 is one sided noise power spectral density and B_N is filter lowpass noise equivalent bandwidth. For most of the filters, B_N and 3dB bandwidth are proportional such that we can write

$$B_N = k_b \frac{B_T}{T} \tag{F.9}$$

where B_T is the filter normalized 3dB bandwidth and k_b is a factor which is usually close to one. Substituting (F.9) into (F.8) gives

$$\sigma_n^2 = \frac{N_0 k_b B_T}{T} \tag{F.10}$$

Insertion of (F.10) into (F.7) yields

$$f_{L_{rr}}(L_{rr}) = \frac{1}{k_b B_T N_0} e^{-\frac{L_{rr}}{k_b B_T N_0}} U(L_{rr}) \tag{F.11}$$

Fig. F.1 shows the numerical values of (F.11) and the PDFs obtained from simulation. The analytical PDF fully overlaps the simulated PDF which proves this assumption that the samples of v are independent.

F.2 PDF of L_{ri} with 2-Samples Metric

With 2-samples metric, L_{ri} has a relation similar to (F.1) as

$$L_{ri} = \frac{T}{2}|v(0)-v(1)| \tag{F.12}$$

PDF of $x = v(0)-v(1)$ is convolution of PDFs of $v(0)$ and $-v(1)$ given as

$$f_x(x) = \begin{cases} \int_x^{\infty} f_{v(0)}(\lambda) f_{v(1)}(\lambda - x) d\lambda & x > 0 \\ \int_0^{\infty} f_{v(0)}(\lambda) f_{v(1)}(\lambda - x) d\lambda & x < 0 \end{cases} \tag{F.13}$$

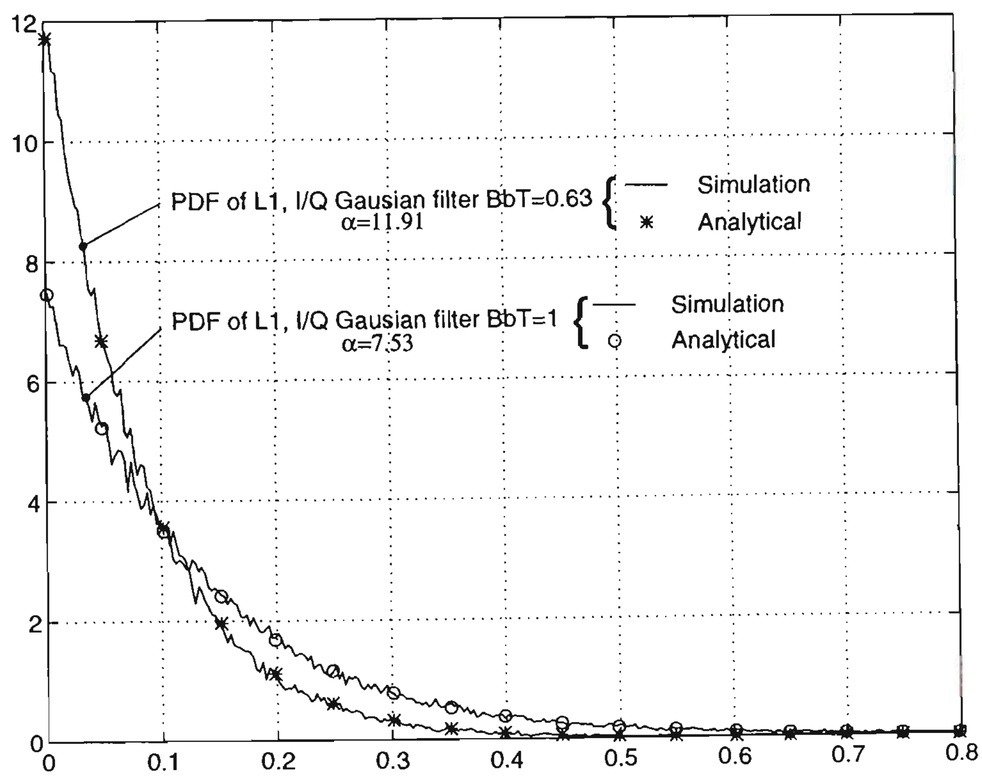

Fig. F.1. The PDF of L_{rr} for selection of 2 samples per symbol.

Substituting (5.35) into (F.13) yields

$$f_x(x) = \begin{cases} \left(\dfrac{1}{2\sigma_n^2}\right)^2 \displaystyle\int_x^{\infty} \left\{ e^{-\frac{\lambda + |w_r(0) - w_i(0)|^2}{2\sigma_n^2}} I_0\left(\dfrac{\sqrt{\lambda}|w_r(0) - w_i(0)|^2}{\sigma_n^2}\right) \right. \\ \left. e^{-\frac{x - \lambda + |w_r(1) - w_i(1)|^2}{2\sigma_n^2}} I_0\left(\dfrac{\sqrt{(\lambda - x)}|w_r(1) - w_i(1)|^2}{\sigma_n^2}\right)\right\} d\lambda & x > 0 \\ \\ \left(\dfrac{1}{2\sigma_n^2}\right)^2 \displaystyle\int_0^{\infty} \left\{ e^{-\frac{\lambda + |w_r(0) - w_i(0)|^2}{2\sigma_n^2}} I_0\left(\dfrac{\sqrt{\lambda}|w_r(0) - w_i(0)|^2}{\sigma_n^2}\right) \right. \\ \left. e^{-\frac{x - \lambda + |w_r(1) - w_i(1)|^2}{2\sigma_n^2}} I_0\left(\dfrac{\sqrt{(\lambda - x)}|w_r(1) - w_i(1)|^2}{\sigma_n^2}\right)\right\} d\lambda & x < 0 \end{cases} \tag{F.14}$$

The PDF of $W_i = |x|$ in this case is

$$f_{W_i}(W_i) = \left(\frac{1}{2\sigma_n^{\ 2}}\right)^2 \int_{W_i}^{\infty} \left\{ e^{-\frac{\lambda + |w_r(0) - w_i(0)|^2}{2\sigma_n^{\ 2}}} I_0\left(\frac{\sqrt{\lambda |w_r(0) - w_i(0)|^2}}{\sigma_n^{\ 2}}\right) \right.$$

$$\left. e^{-\frac{W_i - \lambda + |w_r(1) - w_i(1)|^2}{2\sigma_n^{\ 2}}} I_0\left(\frac{\sqrt{(\lambda - W_i)|w_r(1) - w_i(1)|^2}}{\sigma_n^{\ 2}}\right)\right\} d\lambda \tag{F.15}$$

$$+ \left(\frac{1}{2\sigma_n^{\ 2}}\right)^2 \int_{0}^{\infty} \left\{ e^{-\frac{\lambda + |w_r(0) - w_i(0)|^2}{2\sigma_n^{\ 2}}} I_0\left(\frac{\sqrt{\lambda |w_r(0) - w_i(0)|^2}}{\sigma_n^{\ 2}}\right) \right.$$

$$\left. e^{-\frac{-W_i - \lambda + |w_r(1) - w_i(1)|^2}{2\sigma_n^{\ 2}}} I_0\left(\frac{\sqrt{(\lambda + W_i)|w_r(1) - w_i(1)|^2}}{\sigma_n^{\ 2}}\right)\right\} d\lambda$$

Analytical solutions of integrals in (F.15) is very difficult. Alternative methods are numerical solution or using the approximation of (5.37). If the approximation of (5.37) is used, $v(0)$ has approximately a normal PDF with an average of $|w_r(0) - w_i(0)|^2$ and a standard deviation of $\xi = 2\sigma_n|w_r(0) - w_i(0)|$. Moreover, $v(1)$ has the same distribution with an average of $|w_r(1) - w_i(1)|^2$ and a standard deviation of $\xi = 2\sigma_n|w_r(1) - w_i(1)|$. The PDF of $-v(1)$ is also normal with an average of $-|w_r(1) - w_i(1)|^2$ and the same standard deviation as $v(1)$. THe PDF of $x = v(0) - v(1)$ can be obtained using a general rule that addition of two normal distribution with averages of μ_1, μ_2 and standard deviations of σ_1 and σ_2 is also normal with an average of $\mu_x = \mu_1 + \mu_2$ and a standard deviation of $\sigma_x = \sqrt{\sigma_1^2 + \sigma_2^2}$.

Hence

$$f_x(x) \approx \frac{1}{\sigma_x\sqrt{2\pi}} e^{-\frac{[v-\mu_x]^2}{2\sigma_x^2}} \tag{F.16}$$

where $\sigma_x = 2\sigma_n\sqrt{|w_r(0)-w_i(0)|^2+|w_r(1)-w_i(1)|^2} = 2\sigma_n\sqrt{\sum_{k=0}^{1}|w_r(k)-w_i(k)|^2}$

and $\mu_x = |w_r(0)-w_i(0)|^2-|w_r(1)-w_i(1)|^2$. The PDF of $W_{ri} = |x|$ in this situation will be

$$f_{W_{ri}}(W_{ri}) \approx \left[\frac{1}{\sigma_x\sqrt{2\pi}} e^{-\frac{[W_{ri}-|\mu_x|]^2}{2\sigma_x^2}} + \frac{1}{\sigma_x\sqrt{2\pi}} e^{-\frac{[W_{ri}+|\mu_x|]^2}{2\sigma_x^2}}\right] U(W_{ri}) \tag{F.17}$$

If $\mu_x \gg \sigma_x$ (F.17) can be approximated as

$$f_{W_{ri}}(W_{ri}) \approx \left[\frac{1}{\sigma_x\sqrt{2\pi}} e^{-\frac{[W_{ri}-|\mu_x|]^2}{2\sigma_x^2}}\right] U(W_{ri}) \tag{F.18}$$

The PDF of $L_{ri} = \frac{T}{2}W_{ri}$ will be

$$f_{L_{ri}}(L_{ri}) \approx \left[\frac{1}{\frac{\sigma_x T}{2}\sqrt{2\pi}} e^{-\frac{\left[L_{ri} - \frac{T}{2}|\mu_x|\right]^2}{2\left(\frac{\sigma_x T}{2}\right)^2}} \right] U(L_{ri}) \qquad \text{(F.19)}$$

$\mu_L = \frac{T}{2}|\mu_x|$ is the value of metric without noise which can be defined as envelope distance between $w_r(k)$ and $w_i(k)$. This definition will be discussed in detail in Section 5.5.

APPENDIX G

G.1 Parameters of truncated normal distribution, fitted to PDF of L_{ij}

Table G.1. Parameters of fitted truncated normal distribution for W_{ij}, $a_i \neq a_j$ with Gaussian I/Q lowpass filters BT=0.4, $E_b = 1$ and GMSK BT=0.3

e_{ij}	d_{ij}	$E_b/N_0 = 0dB$ σ_n=0.6528			$E_b/N_0 = 4dB$ σ_n=0.4123			$E_b/N_0 = 6dB$ σ_n=0.327		
		σ_W	μ_W	error [%]	σ_W	μ_W	error [%]	σ_W	μ_W	error [%]
0.3443	1.3998	2.2577	2.3242	3.25	1.3376	1.6592	3.08	1.0817	1.4385	2.81
0.5697	1.5317	2.5667	2.7080	3.22	1.6141	2.1255	2.68	1.3330	1.9854	2.14
0.6057	1.5076	2.5440	2.6992	3.27	1.6314	2.1362	2.78	1.3440	2.0010	2.19
0.7163	1.2076	2.5405	2.3213	2.85	1.4845	2.3164	2.04	1.1397	2.3018	1.72
0.7983	1.0944	2.6304	2.4839	2.68	1.4693	2.6582	2.16	1.1128	2.6475	2.07
0.9150	1.3311	2.8400	2.9604	2.74	1.6778	3.0454	1.86	1.2930	3.0249	1.77
0.9223	1.3234	2.8474	2.9937	2.73	1.6813	3.0664	1.90	1.3001	3.0454	1.77
0.9467	1.3490	2.8506	3.0239	2.68	1.6590	3.0835	1.91	1.2732	3.0552	1.73
1.0383	1.2423	2.9087	3.3110	2.54	1.6268	3.4634	2.18	1.2477	3.4141	1.91
1.0683	1.2229	2.9203	3.2725	2.59	1.6339	3.4512	2.28	1.2576	3.4116	2.00

e_{ij}	d_{ij}	$E_b/N_0 = 10dB$ σ_n=0.2055			$E_b/N_0 = 20dB$ σ_n=0.0628			$E_b/N_0 = 30dB$ σ_n=0.0205		
		σ_W	μ_W	error [%]	σ_W	μ_W	error [%]	σ_W	μ_W	error [%]
0.3443	1.3998	0.7500	1.2051	1.76	0.2533	1.0859	0.20	0.0809	1.0444	0.27
0.5697	1.5317	0.8905	1.8877	0.78	0.2802	1.7549	0.33	0.0911	1.7153	0.32
0.6057	1.5076	0.9029	1.9155	0.90	0.2954	1.8232	0.36	0.0947	1.8179	0.14
0.7163	1.2076	0.6887	2.2378	1.23	0.2087	2.1528	0.45	0.0653	2.1494	0.14
0.7983	1.0944	0.6749	2.5596	1.51	0.2073	2.4395	0.54	0.0646	2.4019	0.31
0.9150	1.3311	0.7921	2.9341	1.35	0.2462	2.8057	0.65	0.0781	2.7622	0.47
0.9223	1.3234	0.7900	2.9556	1.32	0.2487	2.8188	0.70	0.0809	2.7769	0.55
0.9467	1.3490	0.7761	2.9609	1.21	0.2342	2.8506	0.42	0.0734	2.8398	0.21
1.0383	1.2423	0.7705	3.3096	1.34	0.2423	3.1709	0.58	0.0777	3.1260	0.47
1.0683	1.2229	0.7850	3.3154	1.44	0.2582	3.2100	0.69	0.0841	3.2046	0.19

Table G.2. Parameters of fitted truncated normal distribution for W_{ij}, $a_i \neq a_j$ with Gaussian I/Q lowpass filters BT=0.5, $E_b = 1$ and GMSK BT=0.3.

e_{ij}	d_{ij}	$E_b/N_0 = 0dB$, σ_n= 0.7181			$E_b/N_0 = 4dB$, σ_n= 0.4663			$E_b/N_0 = 6dB$, σ_n= 0.365		
		σ_W	μ_W	error [%]	σ_W	μ_W	error [%]	σ_W	μ_W	error [%]
0.4350	1.4047	2.8382	2.9980	3.12	1.6180	2.1484	2.90	1.3110	1.8691	2.59
0.7070	1.5436	3.1894	3.5029	3.10	1.9585	2.7290	2.61	1.6020	2.5386	2.12
0.7087	1.5120	3.1310	3.4219	3.21	1.9302	2.6538	2.64	1.5875	2.4575	2.22
0.7853	1.2378	3.0506	2.9033	3.06	1.7578	2.6763	2.32	1.3620	2.6255	1.82
0.8717	1.1435	3.1384	2.9468	2.84	1.7649	2.9575	2.33	1.3103	2.9346	2.18
0.9893	1.3584	3.3876	3.5244	2.84	1.9911	3.4224	2.09	1.5422	3.3696	1.84
0.9950	1.3535	3.4043	3.5269	2.95	1.9907	3.4287	2.17	1.5334	3.3779	1.94
1.0403	1.3877	3.4315	3.6519	2.87	1.9978	3.5425	2.08	1.5312	3.4800	1.91
1.1127	1.2690	3.4754	3.6978	2.72	1.9571	3.7686	2.37	1.4831	3.7207	2.26
1.1330	1.3004	3.4655	3.8311	2.68	1.9575	3.8696	2.21	1.4852	3.8198	2.18

e_{ij}	d_{ij}	$E_b/N_0 = 10dB$, σ_n= 0.2278			$E_b/N_0 = 20dB$, σ_n= 0.0733			$E_b/N_0 = 30dB$, σ_n= 0.023		
		σ_W	μ_W	error [%]	σ_W	μ_W	error [%]	σ_W	μ_W	error [%]
0.4350	1.4047	0.9004	1.5728	1.58	0.2986	1.3799	0.39	0.0961	1.3203	0.30
0.7070	1.5436	1.0555	2.3667	0.96	0.3379	2.1733	0.47	0.1135	2.1230	0.43
0.7087	1.5120	1.0615	2.2939	1.04	0.3496	2.1401	0.47	0.1145	2.1260	0.15
0.7853	1.2378	0.8179	2.5132	1.37	0.2430	2.3701	0.37	0.0759	2.3564	0.10
0.8717	1.1435	0.7846	2.8164	1.68	0.2370	2.6592	0.71	0.0724	2.6172	0.27
0.9893	1.3584	0.9362	3.2344	1.49	0.2912	3.0508	0.83	0.0929	2.9912	0.70
0.9950	1.3535	0.9358	3.2524	1.47	0.2922	3.0596	0.87	0.0950	3.0020	0.79
1.0403	1.3877	0.9298	3.3423	1.34	0.2784	3.1597	0.55	0.0848	3.1230	0.25
1.1127	1.2690	0.9167	3.5801	1.73	0.3000	3.4150	0.96	0.1032	3.3882	0.28
1.1330	1.3004	0.9121	3.6650	1.62	0.2837	3.4819	0.80	0.0908	3.4204	0.66

Table G.3. Parameters of fitted truncated normal distribution for W_{ij}, $a_i \neq a_j$ with Gaussian I/Q lowpass filters BT=0.6, $E_b = 1$ and GMSK BT=0.3.

e_{ij}	d_{ij}	$E_b/N_0 = 0dB$ σ_n= 0.7982			$E_b/N_0 = 4dB$ σ_n= 0.5082			$E_b/N_0 = 6dB$ σ_n= 0.3977		
		σ_W	μ_W	error [%]	σ_W	μ_W	error [%]	σ_W	μ_W	error [%]
0.4890	1.4075	3.3285	3.5703	3.10	1.8906	2.5361	2.82	1.4969	2.1958	2.59
0.7923	1.5147	3.6793	4.0259	3.17	2.1879	3.0669	2.71	1.7691	2.8027	2.33
0.7710	1.5511	3.7388	4.1318	3.16	2.2233	3.1812	2.67	1.8116	2.9390	2.12
0.8263	1.2552	3.5073	3.3818	3.11	2.0042	2.9619	2.43	1.5337	2.8604	2.04
0.9143	1.1712	3.5834	3.3311	3.01	2.0006	3.1816	2.40	1.5008	3.1338	2.37
1.0330	1.3743	3.8443	4.0093	2.98	2.2336	3.6948	2.38	1.7288	3.6045	2.05
1.0377	1.3711	3.8935	3.9922	2.93	2.2438	3.7046	2.35	1.7394	3.6118	2.09
1.0970	1.4104	3.9572	4.1616	2.91	2.2821	3.8721	2.25	1.7422	3.7744	2.05
1.1893	1.2954	3.9438	4.0376	2.94	2.2166	3.9917	2.45	1.6764	3.9287	2.41
1.1637	1.3337	3.9986	4.2520	2.84	2.2297	4.1670	2.37	1.6937	4.0894	2.38

e_{ij}	d_{ij}	$E_b/N_0 = 10dB$ σ_n= 0.2510			$E_b/N_0 = 20dB$ σ_n= 0.0798			$E_b/N_0 = 30dB$ σ_n= 0.0252		
		σ_W	μ_W	error [%]	σ_W	μ_W	error [%]	σ_W	μ_W	error [%]
0.4890	1.4075	1.0116	1.8271	1.61	0.3354	1.5649	0.46	0.1074	1.4893	0.41
0.7923	1.5147	1.1833	2.5562	1.24	0.3910	2.3389	0.70	0.1315	2.3135	0.13
0.7710	1.5511	1.1939	2.6958	1.08	0.3846	2.4385	0.63	0.1312	2.3794	0.34
0.8263	1.2552	0.9248	2.6968	1.52	0.2713	2.5049	0.53	0.0830	2.4795	0.23
0.9143	1.1712	0.8831	2.9834	1.98	0.2611	2.7905	0.91	0.0773	2.7451	0.28
1.0330	1.3743	1.0551	3.4365	1.68	0.3276	3.2051	0.98	0.1046	3.1294	0.90
1.0377	1.3711	1.0533	3.4458	1.72	0.3301	3.2119	1.11	0.1060	3.1382	0.92
1.0970	1.4104	1.0579	3.5933	1.58	0.3184	3.3589	0.82	0.0947	3.2964	0.25
1.1893	1.2954	1.0282	3.7554	2.02	0.3347	3.5444	1.34	0.1173	3.4932	0.66
1.1637	1.3337	1.0264	3.9038	1.89	0.3195	3.6729	1.18	0.1014	3.5991	0.94

Table G.4. Parameters of fitted truncated normal distribution for W_{ij}, $a_i \neq a_j$ with I/Q maximally flat lowpass filters BT=0.4, $E_b = 1$ and GMSK BT=0.3.

e_{ij}	d_{ij}	$E_b/N_0 = 0dB$ σ_n= 0.6436			$E_b/N_0 = 4dB$ σ_n= 0.4058			$E_b/N_0 = 6dB$ σ_n= 0.3224		
		σ_W	μ_W	error [%]	σ_W	μ_W	error [%]	σ_W	μ_W	error [%]
0.3420	1.4024	2.2750	2.1187	3.36	1.3567	1.5708	3.18	1.0767	1.3652	3.03
0.5587	1.5338	2.5143	2.4795	3.41	1.6003	2.0303	2.77	1.3408	1.9102	2.10
0.6017	1.5104	2.5256	2.5161	3.45	1.6484	2.0278	2.83	1.3641	1.9316	2.10
0.7200	1.2122	2.5734	2.1826	2.93	1.4834	2.2681	2.16	1.1599	2.3018	1.88
0.8100	1.1025	2.6591	2.4692	2.72	1.4725	2.7246	2.35	1.1047	2.6899	2.11
0.9220	1.3357	2.9097	2.7891	2.58	1.6689	3.0571	2.04	1.3072	3.0693	1.95
0.9290	1.3282	2.9048	2.8535	2.61	1.7036	3.0566	1.95	1.2792	3.0532	1.75
0.9497	1.3530	2.8573	2.8999	2.63	1.6459	3.0649	2.07	1.2732	3.0610	1.88
1.0483	1.2497	2.9352	3.3389	2.59	1.6289	3.5239	2.30	1.2548	3.4502	2.01
1.0837	1.2309	2.9310	3.3164	2.53	1.6339	3.5269	2.23	1.2813	3.4570	2.08

e_{ij}	d_{ij}	$E_b/N_0 = 10dB$ σ_n= 0.2021			$E_b/N_0 = 20dB$ σ_n= 0.0644			$E_b/N_0 = 30dB$ σ_n= 0.0201		
		σ_W	μ_W	error [%]	σ_W	μ_W	error [%]	σ_W	μ_W	error [%]
0.3420	1.4024	0.7528	1.1533	1.84	0.2512	1.0610	0.37	0.0805	1.0298	0.24
0.5587	1.5338	0.8951	1.8364	0.74	0.2781	1.7095	0.34	0.0890	1.6797	0.30
0.6017	1.5104	0.9248	1.8945	1.00	0.2929	1.8086	0.42	0.0911	1.8062	0.26
0.7200	1.2122	0.6930	2.2417	1.33	0.2076	2.1631	0.42	0.0646	2.1606	0.23
0.8100	1.1025	0.6922	2.5781	1.25	0.2104	2.4746	0.57	0.0642	2.4390	0.45
0.9220	1.3357	0.7956	2.9263	1.42	0.2476	2.8159	0.74	0.0777	2.7783	0.50
0.9290	1.3282	0.8069	2.9658	1.58	0.2473	2.8276	0.61	0.0798	2.7930	0.43
0.9497	1.3530	0.7857	2.9434	1.02	0.2328	2.8545	0.59	0.0724	2.8496	0.31
1.0483	1.2497	0.7981	3.3247	1.22	0.2423	3.2007	0.62	0.0752	3.1567	0.34
1.0837	1.2309	0.8091	3.3389	1.36	0.2551	3.2549	0.61	0.0812	3.2520	0.27

Table G.5. Parameters of fitted truncated normal distribution for W_{ij}, $a_i \neq a_j$ with I/Q maximally flat lowpass filters BT=0.5, $E_b = 1$ and GMSK BT=0.3.

e_{ij}	d_{ij}	$E_b/N_0 = 0dB$ σ_n= 0.7081			$E_b/N_0 = 4dB$ σ_n= 0.4440			$E_b/N_0 = 6dB$ σ_n= 0.3561		
		σ_W	μ_W	error [%]	σ_W	μ_W	error [%]	σ_W	μ_W	error [%]
0.4533	1.4024	2.7674	2.6943	3.22	1.6573	2.0098	3.01	1.3426	1.7681	2.82
0.7203	1.5338	3.0878	3.1558	3.38	1.9461	2.6040	2.60	1.6297	2.4878	1.98
0.7267	1.5104	3.1108	3.0879	3.26	1.9783	2.5122	2.74	1.6052	2.3960	2.18
0.8060	1.2122	3.0750	2.6851	3.13	1.7741	2.6201	2.31	1.4020	2.6479	1.96
0.9060	1.1025	3.1738	2.9224	2.88	1.7359	3.0815	2.45	1.3110	3.0332	2.16
1.0173	1.3357	3.4128	3.3276	2.83	1.9922	3.4478	2.14	1.5500	3.4399	2.01
1.0220	1.3282	3.3809	3.3418	2.79	2.0240	3.4312	2.17	1.5259	3.4390	1.88
1.0657	1.3530	3.4160	3.4819	2.66	2.0095	3.5581	2.23	1.5348	3.5171	1.94
1.1683	1.2497	3.4967	3.6851	2.62	1.9483	3.9189	2.34	1.5033	3.8296	2.30
1.1670	1.2309	3.5045	3.8604	2.70	1.9451	4.0049	2.40	1.4905	3.9199	2.20

e_{ij}	d_{ij}	$E_b/N_0 = 10dB$ σ_n= 0.2220			$E_b/N_0 = 20dB$ σ_n= 0.0714			$E_b/N_0 = 30dB$ σ_n= 0.0223		
		σ_W	μ_W	error [%]	σ_W	μ_W	error [%]	σ_W	μ_W	error [%]
0.4533	1.4024	0.9153	1.5366	1.62	0.3004	1.3999	0.43	0.0979	1.3633	0.29
0.7203	1.5338	1.0714	2.3481	0.84	0.3372	2.1865	0.41	0.1103	2.1616	0.28
0.7267	1.5104	1.1001	2.3169	1.17	0.3496	2.1851	0.45	0.1099	2.1797	0.25
0.8060	1.2122	0.8328	2.5674	1.51	0.2462	2.4287	0.47	0.0756	2.4185	0.21
0.9060	1.1025	0.8115	2.8975	1.44	0.2420	2.7568	0.68	0.0734	2.7202	0.43
1.0173	1.3357	0.9500	3.2803	1.66	0.2940	3.1157	0.88	0.0929	3.0654	0.60
1.0220	1.3282	0.9457	3.2998	1.62	0.2922	3.1226	0.67	0.0947	3.0752	0.58
1.0657	1.3530	0.9393	3.3628	1.11	0.2788	3.2227	0.68	0.0844	3.1973	0.34
1.1683	1.2497	0.9436	3.6553	1.46	0.2965	3.5215	0.85	0.0979	3.5015	0.28
1.1670	1.2309	0.9354	3.7520	1.35	0.2841	3.5884	0.64	0.0873	3.5308	0.39

Table G.6. Parameters of fitted truncated normal distribution for W_{ij}, $a_i \neq a_j$ with I/Q maximally flat lowpass filters BT=0.6, $E_b = 1$ and GMSK BT=0.3.

e_{ij}	d_{ij}	$E_b/N_0 = 0dB$ σ_n= 0.7687			$E_b/N_0 = 4dB$ σ_n=0.4889			$E_b/N_0 = 6dB$ σ_n=03900		
		σ_W	μ_W	error [%]	σ_W	μ_W	error [%]	σ_W	μ_W	error [%]
0.5377	1.4146	3.2319	3.2637	3.19	1.9136	2.4077	2.93	1.5631	2.1357	2.65
0.8473	1.5220	3.6464	3.6528	3.24	2.2527	2.9561	2.78	1.8052	2.7939	2.27
0.8220	1.5605	3.6365	3.8174	3.44	2.2562	3.1094	2.51	1.8824	2.9771	2.11
0.8680	1.2775	3.5979	3.1128	3.23	2.0307	2.9507	2.54	1.6265	2.9316	2.08
0.9727	1.2080	3.6917	3.2798	2.94	1.9822	3.3613	2.55	1.5075	3.3081	2.29
1.0863	1.3955	3.9197	3.8125	2.99	2.2828	3.7930	2.32	1.7688	3.7305	2.06
1.0897	1.3942	3.8553	3.8218	2.91	2.3040	3.7290	2.28	1.7486	3.7427	2.10
1.1503	1.4357	4.0068	4.0166	2.75	2.3490	3.9526	2.36	1.7702	3.8950	2.01
1.2573	1.3312	3.9767	4.0542	2.72	2.2378	4.2119	2.44	1.7086	4.1323	2.51
1.2223	1.3734	4.0386	4.3296	2.76	2.2523	4.3940	2.56	1.7111	4.2925	2.32

e_{ij}	d_{ij}	$E_b/N_0 = 10dB$ σ_n= 0.2451			$E_b/N_0 = 20dB$ σ_n= 0.0771			$E_b/N_0 = 30dB$ σ_n= 0.0244		
		σ_W	μ_W	error [%]	σ_W	μ_W	error [%]	σ_W	μ_W	error [%]
0.5377	1.4146	1.0459	1.8496	1.60	0.3436	1.6641	0.51	0.1131	1.6172	0.32
0.8473	1.5220	1.2477	2.6533	1.35	0.4013	2.4751	0.51	0.1273	2.4658	0.21
0.8220	1.5605	1.2300	2.7729	1.00	0.3921	2.5659	0.49	0.1297	2.5425	0.22
0.8680	1.2775	0.9631	2.8213	1.70	0.2805	2.6260	0.50	0.0848	2.6040	0.29
0.9727	1.2080	0.9160	3.1401	1.62	0.2685	2.9570	0.73	0.0809	2.9189	0.40
1.0863	1.3955	1.0824	3.5513	1.73	0.3347	3.3384	1.05	0.1067	3.2754	0.78
1.0897	1.3942	1.0746	3.5586	1.72	0.3329	3.3423	0.81	0.1085	3.2817	0.72
1.1503	1.4357	1.0806	3.7153	1.27	0.3230	3.5083	0.83	0.0958	3.4551	0.33
1.2573	1.3312	1.0657	3.8906	1.68	0.3322	3.7139	1.07	0.1120	3.6689	0.55
1.2223	1.3734	1.0661	4.0781	1.52	0.3223	3.8716	0.78	0.0979	3.8018	0.51

Table G.7. Parameters of fitted truncated normal distribution for W_{ij}, $a_i \neq a_j$ with Gaussian I/Q lowpass filters BT=0.4, $E_b = 1$ and GMSK BT=0.5.

e_{ij}	d_{ij}	$E_b/N_0 = 0dB$ σ_n=0.6528			$E_b/N_0 = 4dB$ σ_n=0.4123			$E_b/N_0 = 6dB$ σ_n=0.327		
		σ_W	μ_W	error [%]	σ_W	μ_W	error [%]	σ_W	μ_W	error [%]
0.6568	1.3716	2.9117	2.2341	3.65	1.6314	2.1975	2.36	1.3006	2.1617	1.64
0.7354	1.4091	2.6970	2.6293	3.02	1.6988	2.3989	2.18	1.3715	2.3876	1.54
0.7998	1.4190	2.7726	2.7350	2.96	1.7430	2.5537	2.17	1.4101	2.5441	1.55
0.8908	1.2553	2.8400	2.7169	2.62	1.5902	2.9088	1.99	1.2132	2.8964	1.84
0.9541	1.1963	2.8930	2.9693	2.49	1.5699	3.1784	2.10	1.2059	3.1458	2.02
0.9570	1.2949	2.9691	2.9184	2.51	1.6445	3.1501	2.04	1.2516	3.1333	1.83
0.9963	1.3070	2.9562	3.0768	2.52	1.6934	3.2857	1.97	1.2903	3.2560	1.95
0.9971	1.3060	2.9507	3.0879	2.56	1.6810	3.2853	1.99	1.2932	3.2631	1.93
1.0225	1.2369	2.9258	3.2534	2.39	1.6223	3.4275	2.16	1.2445	3.3822	1.99
1.0861	1.2495	2.9924	3.4012	2.46	1.6595	3.5637	2.17	1.2808	3.5202	2.01

e_{ij}	d_{ij}	$E_b/N_0 = 10dB$ σ_n=0.2055			$E_b/N_0 = 20dB$ σ_n=0.0628			$E_b/N_0 = 30dB$ σ_n=0.0205		
		σ_W	μ_W	error [%]	σ_W	μ_W	error [%]	σ_W	μ_W	error [%]
0.6568	1.3716	0.8218	2.1088	0.91	0.2623	1.9907	0.48	0.0869	1.9706	0.28
0.7354	1.4091	0.8466	2.3336	0.93	0.2751	2.2202	0.45	0.0903	2.2061	0.17
0.7998	1.4190	0.8715	2.4904	1.03	0.2883	2.3977	0.37	0.0929	2.3992	0.16
0.8908	1.2553	0.7391	2.8029	1.29	0.2235	2.6906	0.49	0.0691	2.6728	0.14
0.9541	1.1963	0.7393	3.0407	1.43	0.2265	2.9125	0.47	0.0713	2.8698	0.25
0.9570	1.2949	0.7699	3.0277	1.30	0.2333	2.9052	0.61	0.0709	2.8730	0.15
0.9963	1.3070	0.7952	3.1545	1.43	0.2534	3.0279	0.71	0.0841	2.9920	0.41
0.9971	1.3060	0.7948	3.1551	1.44	0.2529	3.0289	0.75	0.0844	2.9940	0.45
1.0225	1.2369	0.7652	3.2706	1.37	0.2400	3.1335	0.60	0.0755	3.0857	0.31
1.0861	1.2495	0.7905	3.4027	1.40	0.2558	3.2797	0.66	0.0848	3.2580	0.25

Table G.8. Parameters of fitted truncated normal distribution for W_{ij}, $a_i \neq a_j$ with Gaussian I/Q lowpass filters BT=0.5, W_{ij}, $a_i \neq a_j$ and GMSK BT=0.5.

e_{ij}	d_{ij}	$E_b/N_0 = 0dB$ σ_n= 0.7181			$E_b/N_0 = 4dB$ σ_n= 0.4663			$E_b/N_0 = 6dB$ σ_n= 0.365		
		σ_W	μ_W	error [%]	σ_W	μ_W	error [%]	σ_W	μ_W	error [%]
0.7960	1.3844	3.4106	3.0643	3.29	1.9640	2.7811	2.40	1.5492	2.7074	1.78
0.8959	1.4252	3.5464	3.2516	3.27	2.0460	3.0327	2.30	1.6268	2.9747	1.72
0.9321	1.4281	3.4595	3.3768	2.96	2.0598	3.1114	2.34	1.6540	3.0627	1.80
0.9866	1.2954	3.3788	3.3217	2.74	1.9092	3.3462	2.15	1.4599	3.3130	2.04
1.0473	1.2534	3.4161	3.4712	2.65	1.8801	3.5594	2.23	1.4381	3.5221	2.20
1.0616	1.3384	3.5340	3.5479	2.68	1.9920	3.6345	2.20	1.5096	3.5866	2.04
1.0890	1.3421	3.5073	3.6383	2.71	2.0248	3.6964	2.12	1.5355	3.6451	2.12
1.0894	1.3416	3.6634	3.5429	2.91	1.9982	3.6981	2.16	1.5386	3.6525	2.09
1.1229	1.2973	3.5285	3.7506	2.56	1.9523	3.8565	2.28	1.4944	3.8025	2.20
1.1586	1.3011	3.5628	3.8213	2.60	1.9764	3.9294	2.28	1.5106	3.8664	2.21

e_{ij}	d_{ij}	$E_b/N_0 = 10dB$ σ_n= 0.2278			$E_b/N_0 = 20dB$ σ_n= 0.0733			$E_b/N_0 = 30dB$ σ_n= 0.023		
		σ_W	μ_W	error [%]	σ_W	μ_W	error [%]	σ_W	μ_W	error [%]
0.7960	1.3844	0.9688	2.6015	1.16	0.3126	2.4258	0.70	0.1056	2.3884	0.32
0.8959	1.4252	1.0083	2.8746	1.17	0.3322	2.7082	0.68	0.1113	2.6874	0.20
0.9321	1.4281	1.0251	2.9572	1.27	0.3433	2.8044	0.65	0.1129	2.7959	0.22
0.9866	1.2954	0.8818	3.1688	1.51	0.2660	3.0014	0.63	0.0800	2.9623	0.18
1.0473	1.2534	0.8708	3.3703	1.63	0.2617	3.1979	0.62	0.0802	3.1469	0.23
1.0616	1.3384	0.9265	3.4446	1.58	0.2841	3.2597	0.86	0.0869	3.2030	0.46
1.0890	1.3421	0.9420	3.5045	1.67	0.3015	3.3263	0.94	0.1006	3.2735	0.66
1.0894	1.3416	0.9415	3.5056	1.65	0.3000	3.3255	0.97	0.1010	3.2743	0.68
1.1229	1.2973	0.9058	3.6460	1.64	0.2826	3.4587	0.79	0.0888	3.3966	0.57
1.1586	1.3011	0.9300	3.7052	1.64	0.2974	3.5294	1.01	0.1006	3.4790	0.56

Table G.9. Parameters of fitted truncated normal distribution for W_{ij}, $a_i \neq a_j$ with Gaussian I/Q lowpass filters BT=0.6, $E_b = 1$ and GMSK BT=0.5.

e_{ij}	d_{ij}	$E_b/N_0 = 0dB$ σ_n= 0.7982			$E_b/N_0 = 4dB$ σ_n= 0.5082			$E_b/N_0 = 6dB$ σ_n= 0.3977		
		σ_W	μ_W	error [%]	σ_W	μ_W	error [%]	σ_W	μ_W	error [%]
0.8765	1.3926	4.1457	3.4502	3.75	2.2096	3.2052	2.55	1.7430	3.0704	1.96
0.9925	1.4360	4.1839	3.7946	3.44	2.3240	3.4869	2.43	1.8335	3.3929	1.97
1.0097	1.4344	3.8901	3.9796	3.09	2.3358	3.5013	2.47	1.8500	3.4063	1.98
1.0440	1.3187	3.8848	3.8185	2.85	2.1672	3.6604	2.27	1.6591	3.5910	2.18
1.1017	1.2855	4.3587	3.5683	3.42	2.1504	3.8378	2.32	1.6171	3.7722	2.34
1.1256	1.3642	4.6073	3.6924	3.60	2.2680	3.9679	2.30	1.7339	3.8885	2.29
1.1424	1.3628	4.0481	4.0783	2.82	2.2999	3.9890	2.32	1.7268	3.9140	2.28
1.1427	1.3625	4.0202	4.0711	2.89	2.3061	3.9881	2.40	1.7361	3.9189	2.32
1.1828	1.3318	4.5582	3.8339	3.41	2.2506	4.1679	2.41	1.6967	4.0737	2.40
1.1996	1.3304	4.0392	4.1839	2.71	2.2546	4.1707	2.42	1.7045	4.0876	2.38

e_{ij}	d_{ij}	$E_b/N_0 = 10dB$ σ_n= 0.2510			$E_b/N_0 = 20dB$ σ_n= 0.0798			$E_b/N_0 = 30dB$ σ_n= 0.0252		
		σ_W	μ_W	error [%]	σ_W	μ_W	error [%]	σ_W	μ_W	error [%]
0.8765	1.3926	1.2654	2.9342	3.92	0.3496	2.6891	0.90	0.1203	2.6320	0.54
0.9925	1.4360	1.1343	3.2324	1.41	0.3759	3.82	0.92	0.1292	2.9772	0.21
1.97	1.4344	1.1462	3.2549	1.48	0.3838	3.0485	0.93	0.1300	3.0283	0.16
1.0440	1.3187	0.9994	3.4167	1.76	0.2986	3.1955	0.97	0.0878	3.1366	0.30
1.1017	1.2855	0.9802	3.5771	1.86	0.2923	3.3684	0.88	0.0861	3.3094	0.31
1.1256	1.3642	1.0525	3.7232	1.78	0.3244	3.4863	1.20	0.1023	3.4106	0.90
1.1424	1.3628	1.0581	3.7300	1.86	0.3358	3.5063	1.19	0.1132	3.4398	0.95
1.1427	1.3625	1.0591	3.7336	1.84	0.3348	3.5088	1.23	0.1129	3.4397	0.94
1.1828	1.3318	1.0326	3.8918	1.74	0.3195	3.6594	1.20	0.0998	3.5835	0.94
1.1996	1.3304	1.0388	3.9138	1.95	0.3284	3.6795	1.19	0.1103	3.6111	0.98

Table G.10. Parameters of fitted truncated normal distribution for W_{ij}, $a_i \neq a_j$ with I/Q maximally flat lowpass filters BT=0.4, $E_b = 1$ and GMSK BT=0.5.

e_{ij}	$\frac{S_i}{E_b/T}$	$E_b/N_0 = 0dB$ σ_n= 0.6436			$E_b/N_0 = 4dB$ σ_n= 0.4058			$E_b/N_0 = 6dB$ σ_n= 0.3224		
		σ_W	μ_W	error [%]	σ_W	μ_W	error [%]	σ_W	μ_W	error [%]
0.6535	1.3742	2.8400	1.9861	3.62	1.6848	2.0375	2.60	1.2872	2.0699	1.54
0.7262	1.4110	2.6631	2.3826	3.04	1.6563	2.2905	2.12	1.3368	2.2945	1.35
0.7981	1.4223	2.8202	2.4745	3.27	1.9532	2.3681	3.00	1.3811	2.4576	1.34
0.8922	1.2598	2.7703	2.6209	2.45	1.5362	2.8806	1.91	1.1837	2.8867	1.83
0.9577	1.2988	2.8471	2.8489	2.38	1.5986	3.1028	1.93	1.2288	3.0929	1.84
0.9681	1.2050	2.7854	2.9971	2.43	1.5359	3.2069	2.18	1.1761	3.1693	1.90
1.0057	1.3121	2.8944	2.9906	2.39	1.6453	3.2646	1.96	1.2546	3.2400	1.83
1.0063	1.3112	2.9739	2.9639	2.49	1.7022	3.2559	2.32	1.2578	3.2480	1.76
1.0333	1.2450	2.8755	3.2298	2.32	1.5813	3.4279	2.11	1.2166	3.3909	1.79
1.1027	1.2589	2.9059	3.3970	2.35	1.6144	3.5881	2.11	1.2559	3.5563	1.98

e_{ij}	d_{ij}	$E_b/N_0 = 10dB$ σ_n= 0.2021			$E_b/N_0 = 20dB$ σ_n= 0.0644			$E_b/N_0 = 30dB$ σ_n= 0.0201		
		σ_W	μ_W	error [%]	σ_W	μ_W	error [%]	σ_W	μ_W	error [%]
0.6535	1.3742	0.8050	2.0506	0.76	0.2606	1.9666	0.46	0.0840	1.9602	0.20
0.7262	1.4110	0.8300	2.2682	1.04	0.2698	2.1826	0.34	0.0859	2.1783	0.17
0.7981	1.4223	0.8663	2.4539	0.98	0.2808	2.3931	0.32	0.0892	2.3942	0.22
0.8922	1.2598	0.7240	2.7960	1.29	0.2206	2.6977	0.53	0.0683	2.6765	0.18
0.9577	1.2988	0.7458	3.0055	1.33	0.2287	2.9006	0.58	0.0702	2.8749	0.18
0.9681	1.2050	0.7262	3.0650	1.31	0.2243	2.9501	0.42	0.0706	2.9110	0.25
1.0057	1.3121	0.7767	3.1535	1.35	0.2477	3.0447	0.72	0.0833	3.0178	0.30
1.0063	1.3112	0.7814	3.1611	1.33	0.2486	3.0446	0.62	0.0833	3.0195	0.35
1.0333	1.2450	0.7508	3.2841	1.21	0.2342	3.1633	0.48	0.0730	3.1185	0.21
1.1027	1.2589	0.7788	3.4410	1.29	0.2483	3.3240	0.60	0.0823	3.3081	0.15

Table G.11. Parameters of fitted truncated normal distribution for W_{ij}, $a_i \neq a_j$ with I/Q maximally flat lowpass filters BT=0.5, $E_b = 1$ and GMSK BT=0.5.

e_{ij}	d_{ij}	$E_b/N_0 = 0dB$ $\sigma_n = 0.7081$			$E_b/N_0 = 4dB$ $\sigma_n = 0.4440$			$E_b/N_0 = 6dB$ $\sigma_n = 0.3561$		
		σ_W	μ_W	error [%]	σ_W	μ_W	error [%]	σ_W	μ_W	error [%]
0.8291	1.3916	3.1891	2.8276	3.08	2.1684	2.5898	3.08	1.5583	2.6510	1.58
0.9219	1.4317	3.2681	3.0699	2.93	2.0139	2.9478	2.09	1.6200	2.9395	1.47
0.9649	1.4354	3.4018	3.1054	3.19	2.0579	3.0239	2.15	1.6410	3.0163	1.52
1.0096	1.3109	3.5741	3.0044	2.94	1.8601	3.3524	2.00	1.4302	3.3470	1.93
1.0857	1.3533	3.4466	3.4224	2.57	1.9458	3.6298	2.04	1.4879	3.5991	1.93
1.0900	1.2787	3.3506	3.4702	2.49	1.8340	3.6627	2.27	1.3938	3.6055	1.98
1.1282	1.3573	3.4587	3.4849	2.51	1.9556	3.7192	1.98	1.5030	3.6859	1.96
1.1284	1.3573	3.4939	3.4692	2.60	1.9809	3.7068	2.03	1.5126	3.6901	1.89
1.1653	1.3221	3.4535	3.7365	2.40	1.8904	3.9273	2.17	1.4481	3.8749	1.94
1.2020	1.3262	3.4709	3.8178	2.39	1.9151	4.0076	2.21	1.4686	3.9637	2.08

e_{ij}	d_{ij}	$E_b/N_0 = 10dB$ $\sigma_n = 0.2220$			$E_b/N_0 = 20dB$ $\sigma_n = 0.0714$			$E_b/N_0 = 30dB$ $\sigma_n = 0.0223$		
		σ_W	μ_W	error [%]	σ_W	μ_W	error [%]	σ_W	μ_W	error [%]
0.8291	1.3916	0.9710	2.6134	1.08	0.3168	2.4930	0.48	0.1027	2.4871	0.20
0.9219	1.4317	0.9970	2.8726	1.20	0.3293	2.7676	0.40	0.1054	2.7652	0.18
0.9649	1.4354	1.0276	2.9835	1.16	0.3378	2.8931	0.35	0.1072	2.8942	0.15
1.0096	1.3109	0.8739	3.2255	1.42	0.2665	3.0800	0.61	0.0814	3.0351	0.26
1.0857	1.3533	0.9043	3.4798	1.46	0.2818	3.3308	0.74	0.0884	3.2811	0.48
1.0900	1.2787	0.8540	3.4726	1.44	0.2609	3.3198	0.51	0.0810	3.2742	0.25
1.1282	1.3573	0.9264	3.5653	1.46	0.2976	3.4175	0.83	0.1014	3.3854	0.31
1.1284	1.3573	0.9246	3.5690	1.46	0.2981	3.4173	0.76	0.1013	3.3856	0.35
1.1653	1.3221	0.8874	3.7342	1.37	0.2763	3.5725	0.63	0.0853	3.5156	0.30
1.2020	1.3262	0.9094	3.8177	1.40	0.2865	3.6516	0.73	0.0972	3.6082	0.35

Table G.12. Parameters of fitted truncated normal distribution for W_{ij}, $a_i \neq a_j$ with I/Q maximally flat lowpass filters BT=0.5, $E_b = 1$ and GMSK BT=0.5.

e_{ij}	d_{ij}	$E_b/N_0 = 0dB$, σ_n= 0.7687			$E_b/N_0 = 4dB$, σ_n= 0.4889			$E_b/N_0 = 6dB$, σ_n= 0.3900		
		σ_W	μ_W	error [%]	σ_W	μ_W	error [%]	σ_W	μ_W	error [%]
0.9618	1.4058	3.7075	3.4564	3.08	2.2368	3.1800	2.25	1.7928	3.1285	1.74
1.0730	1.4489	3.9074	3.6368	3.07	2.3726	3.4781	2.13	1.8679	3.4482	1.65
1.0916	1.4469	3.9871	3.6446	3.18	2.3631	3.5056	2.21	1.8690	3.4713	1.75
1.0958	1.3470	4.2222	3.4162	3.22	2.1808	3.7421	2.14	1.6575	3.7051	2.03
1.1759	1.3281	3.8964	3.8828	2.51	2.1167	3.9981	2.25	1.6018	3.9389	2.13
1.1999	1.3924	3.9803	3.9786	2.64	2.2562	4.0491	2.19	1.7105	4.0197	2.07
1.2182	1.3902	4.2729	3.8057	3.05	2.2879	4.0928	2.17	1.7264	4.0337	2.08
1.2183	1.3898	4.4784	3.6061	3.25	2.2535	4.0648	2.20	1.7348	4.0380	2.00
1.2593	1.3744	3.9572	4.1981	2.60	2.1896	4.3108	2.25	1.6597	4.2534	2.21
1.2710	1.3717	3.9607	4.2453	2.56	2.1996	4.3371	2.26	1.6720	4.2677	2.22

e_{ij}	d_{ij}	$E_b/N_0 = 10dB$, σ_n= 0.2451			$E_b/N_0 = 20dB$, σ_n= 0.0771			$E_b/N_0 = 30dB$, σ_n= 0.0244		
		σ_W	μ_W	error [%]	σ_W	μ_W	error [%]	σ_W	μ_W	error [%]
0.9618	1.4058	1.1086	3.0483	1.29	0.3658	2.8929	0.65	0.1200	2.8850	0.19
1.0730	1.4489	1.1607	3.3685	1.42	0.3852	3.2217	0.59	0.1245	3.2191	0.16
1.0916	1.4469	1.1605	3.3992	1.31	0.3925	3.2736	0.48	0.1249	3.2743	0.14
1.0958	1.3470	0.9975	3.5636	1.56	0.3092	3.3710	0.85	0.0954	3.3077	0.47
1.1759	1.3281	0.9721	3.7815	1.59	0.2950	3.5859	0.64	0.0895	3.5307	0.20
1.1999	1.3924	1.0558	3.8626	1.53	0.3335	3.6671	0.99	0.1100	3.6084	0.70
1.2182	1.3902	1.0619	3.8839	1.59	0.3455	3.6964	1.02	0.1188	3.6558	0.40
1.2183	1.3898	1.0661	3.8858	1.67	0.3435	3.6986	0.90	0.1186	3.6558	0.46
1.2593	1.3744	1.0200	4.0775	1.57	0.3133	3.8694	0.73	0.0975	3.8018	0.50
1.2710	1.3717	1.0285	4.0990	1.65	0.3237	3.8910	0.92	0.1062	3.8263	0.71

Table G.13. Parameters of fitted truncated normal distribution for W_{ij}, $a_i \neq a_j$ with I/Q Gaussian filter BT=0.4, $E_b = 1$ and MSK.

e_{ij}	d_{ij}	$E_b/N_0 = 0dB$ σ_n= 0.6528			$E_b/N_0 = 4dB$ σ_n=0.4123			$E_b/N_0 = 6dB$ σ_n=0.327		
		σ_W	μ_W	error [%]	σ_W	μ_W	error [%]	σ_W	μ_W	error [%]
0.8577	1.3299	2.8703	2.6474	2.84	1.7277	2.7356	1.85	1.3287	2.7436	1.60
0.9218	1.3480	3.0950	2.6915	3.07	1.7470	2.9071	1.85	1.3706	2.9086	1.53
0.9700	1.2644	2.9496	2.9667	2.42	1.6363	3.2189	2.07	1.2499	3.2007	1.94
1.0177	1.2353	2.9201	3.2206	2.45	1.6277	3.4057	2.15	1.2453	3.3787	1.96
1.0341	1.2835	3.0084	3.1197	2.43	1.6680	3.3809	2.15	1.2778	3.3538	1.98
1.0817	1.2548	2.9682	3.4060	2.37	1.6471	3.5711	2.12	1.2798	3.5360	2.00

e_{ij}	d_{ij}	$E_b/N_0 = 10dB$ σ_n= 0.2055			$E_b/N_0 = 20dB$ σ_n= 0.0628			$E_b/N_0 = 30dB$ σ_n= 0.0.205		
		σ_W	μ_W	error [%]	σ_W	μ_W	error [%]	σ_W	μ_W	error [%]
0.8577	1.3299	0.8143	2.6797	1.21	0.2684	2.5778	0.51	0.0874	2.5727	0.25
0.9218	1.3480	0.8416	2.8448	1.27	0.2813	2.7654	0.40	0.0893	2.7653	0.21
0.9700	1.2644	0.7633	3.0969	1.38	0.2369	2.9723	0.69	0.0748	2.9294	0.45
1.0177	1.2353	0.7708	3.2553	1.36	0.2386	3.1235	0.57	0.0749	3.0752	0.30
1.0341	1.2835	0.7891	3.2503	1.49	0.2550	3.1276	0.75	0.0861	3.1021	0.34
1.0817	1.2548	0.7906	3.4079	1.34	0.2511	3.2771	0.64	0.0844	3.2456	0.23

Table G.14. Parameters of fitted truncated normal distribution for W_{ij}, $a_i \neq a_j$ with Gaussian I/Q lowpass filters BT=0.5, $E_b = 1$ and MSK.

e_{ij}	d_{ij}	$E_b/N_0 = 0dB$ σ_n=0.7181			$E_b/N_0 = 4dB$ σ_n=0.4663			$E_b/N_0 = 6dB$ σ_n=0.365		
		σ_W	μ_W	error [%]	σ_W	μ_W	error [%]	σ_W	μ_W	error [%]
1.0224	1.3528	3.6591	3.3054	3.1000	2.0613	3.3911	2.0900	1.5753	3.3666	1.9700
1.0663	1.3650	3.5639	3.4783	2.7900	2.0619	3.5030	2.1100	1.6073	3.4689	1.8800
1.0938	1.3126	3.5431	3.5818	2.6300	1.9829	3.7196	2.2100	1.5046	3.6769	2.1300
1.1212	1.2968	3.5210	3.7379	2.5900	1.9592	3.8411	2.2800	1.4918	3.8021	2.1900
1.1377	1.3251	3.5787	3.6756	2.6500	1.9981	3.8256	2.3000	1.5269	3.7789	2.2000
1.1651	1.3095	3.5642	3.8529	2.5300	1.9639	3.9532	2.2500	1.5211	3.9133	2.2400

e_{ij}	d_{ij}	$E_b/N_0 = 10dB$ σ_n=0.2278			$E_b/N_0 = 20dB$ σ_n=0.0733			$E_b/N_0 = 30dB$ σ_n=0.0230		
		σ_W	μ_W	error [%]	σ_W	μ_W	error [%]	σ_W	μ_W	error [%]
1.0224	1.3528	0.9667	3.2466	1.5300	0.3200	3.0853	0.8300	0.1083	3.0665	0.2600
1.0663	1.3650	0.9872	3.3549	1.5800	0.3331	3.2084	0.7500	0.1095	3.1989	0.2300
1.0938	1.3126	0.9174	3.5292	1.6300	0.2871	3.3535	0.9900	0.0940	3.2957	0.7600
1.1212	1.2968	0.9123	3.6349	1.6100	0.2821	3.4578	0.8700	0.0885	3.3938	0.5600
1.1377	1.3251	0.9383	3.6344	1.7100	0.3025	3.4586	1.0300	0.1040	3.4143	0.5500
1.1651	1.3095	0.9317	3.7414	1.6300	0.2930	3.5582	0.9100	0.0987	3.5021	0.5800

Table G.15. Parameters of fitted truncated normal distribution for W_{ij}, $a_i \neq a_j$ with Gaussian I/Q lowpass filters BT=0.6, $E_b = 1$ and MSK.

e_{ij}	d_{ij}	$E_b/N_0 = 0dB$ σ_n= 0.7982			$E_b/N_0 = 4dB$ σ_n= 0.5082			$E_b/N_0 = 6dB$ σ_n= 0.3977		
		σ_W	μ_W	error [%]	σ_W	μ_W	error [%]	σ_W	μ_W	error [%]
1.1155	1.3687	4.0658	3.9559	2.9300	2.3284	3.8295	2.2900	1.7650	3.7751	2.2600
1.1471	1.3773	4.1588	3.9603	3.0200	2.3159	3.9124	2.3200	1.8002	3.8427	2.1600
1.1646	1.3415	4.0566	4.0552	2.7500	2.2756	4.0609	2.3900	1.7104	3.9918	2.3500
1.1822	1.3316	4.0502	4.1485	2.7100	2.2432	4.1369	2.4100	1.7009	4.0834	2.4100
1.1963	1.3503	4.0691	4.1358	2.8000	2.2737	4.1259	2.4500	1.7286	4.0632	2.4400
1.2138	1.3405	4.0689	4.2518	2.7400	2.2424	4.2243	2.4000	1.7258	4.1674	2.4400

e_{ij}	d_{ij}	$E_b/N_0 = 10dB$ σ_n= 0.2510			$E_b/N_0 = 20dB$ σ_n= 0.0798			$E_b/N_0 = 30dB$ σ_n= 0.0252		
		σ_W	μ_W	error [%]	σ_W	μ_W	error [%]	σ_W	μ_W	error [%]
1.1155	1.3687	1.0805	3.6048	1.8100	0.3568	3.3876	1.1700	0.1249	3.3466	0.4000
1.1471	1.3773	1.0987	3.6815	1.8300	0.3669	3.4722	1.1200	0.1270	3.4416	0.3000
1.1646	1.3415	1.0386	3.8063	1.8900	0.3259	3.5841	1.2300	0.1071	3.5129	1.0700
1.1822	1.3316	1.0326	3.8796	1.9100	0.3184	3.6603	1.1400	0.0999	3.5829	0.8700
1.1963	1.3503	1.0569	3.8819	1.9400	0.3385	3.6591	1.3300	0.1164	3.5950	0.9600
1.2138	1.3405	1.0487	3.9575	1.8900	0.3284	3.7303	1.2500	0.1089	3.6573	0.9500

Table G.16. Parameters of fitted truncated normal distribution for W_{ij}, $a_i \neq a_j$ with I/Q maximally flat lowpass filters BT=0.4, $E_b = 1$ and MSK.

e_{ij}	d_{ij}	$E_b/N_0 = 0dB$ σ_n= 0.6436			$E_b/N_0 = 4dB$ σ_n= 0.4058			$E_b/N_0 = 6dB$ σ_n= 0.3224		
		σ_W	μ_W	error [%]	σ_W	μ_W	error [%]	σ_W	μ_W	error [%]
0.8602	1.3326	3.0319	2.2480	3.1700	1.7039	2.6310	1.7800	1.3192	2.6625	1.4400
0.9303	1.3523	2.8743	2.6092	2.7900	1.7286	2.8300	1.7700	1.3597	2.8600	1.4000
0.9800	1.2687	2.8776	2.8966	2.4300	1.5929	3.2070	1.9600	1.2116	3.1782	1.7500
1.0326	1.2445	3.0846	3.1290	2.8400	1.5813	3.4362	2.1800	1.2192	3.3935	1.9400
1.0502	1.2894	2.9213	3.0773	2.4200	1.6360	3.3758	2.1000	1.2537	3.3533	1.8900
1.0997	1.2656	2.9174	3.4058	2.3300	1.6255	3.6128	2.0800	1.2574	3.5612	1.9700

e_{ij}	d_{ij}	$E_b/N_0 = 10dB$ σ_n= 0.2021			$E_b/N_0 = 20dB$ σ_n= 0.0644			$E_b/N_0 = 30dB$ σ_n= 0.0201		
		σ_W	μ_W	error [%]	σ_W	μ_W	error [%]	σ_W	μ_W	error [%]
0.8602	1.3326	0.8122	2.6391	1.1700	0.2660	2.5808	0.2800	0.0842	2.5797	0.1100
0.9303	1.3523	0.8446	2.8209	1.1600	0.2764	2.7895	0.3200	0.0868	2.7908	0.1400
0.9800	1.2687	0.7535	3.0927	1.3500	0.2375	2.9779	0.6200	0.0769	2.9451	0.4100
1.0326	1.2445	0.7497	3.2884	1.2000	0.2344	3.1581	0.5500	0.0735	3.1147	0.2500
1.0502	1.2894	0.7804	3.2609	1.3500	0.2553	3.1607	0.6900	0.0838	3.1501	0.2000
1.0997	1.2656	0.7760	3.4499	1.2600	0.2460	3.3257	0.5500	0.0813	3.2998	0.2300

Table G.17. Parameters of fitted truncated normal distribution for W_{ij}, $a_i \neq a_j$ with I/Q maximally flat lowpass filters BT=0.5, $E_b = 1$ and MSK.

e_{ij}	d_{ij}	$E_b/N_0 = 0dB$ σ_n= 0.7081			$E_b/N_0 = 4dB$ σ_n= 0.4440			$E_b/N_0 = 6dB$ σ_n= 0.3561		
		σ_W	μ_W	error [%]	σ_W	μ_W	error [%]	σ_W	μ_W	error [%]
1.0761	1.3621	3.4353	3.1351	2.7700	2.0547	3.3393	1.9200	1.5782	3.3584	1.7000
1.1252	1.3756	3.6230	3.1892	2.9300	2.0719	3.4816	1.9400	1.6165	3.5001	1.6500
1.1452	1.3292	3.7544	3.3163	2.9300	1.9340	3.7617	2.0800	1.4715	3.7274	1.8700
1.1684	1.3239	3.4309	3.8010	2.4300	1.8923	3.9527	2.2500	1.4567	3.8956	2.0700
1.1943	1.3431	3.4730	3.6318	2.5800	1.9732	3.8882	2.1900	1.5072	3.8538	2.0100
1.2141	1.3378	3.4951	3.8738	2.4100	1.9255	4.0757	2.2200	1.4818	4.0091	2.1100

e_{ij}	d_{ij}	$E_b/N_0 = 10dB$ σ_n= 0.2220			$E_b/N_0 = 20dB$ σ_n= 0.0714			$E_b/N_0 = 30dB$ σ_n= 0.0223		
		σ_W	μ_W	error [%]	σ_W	μ_W	error [%]	σ_W	μ_W	error [%]
1.0761	1.3621	0.9805	3.3051	1.3600	0.3274	3.2278	0.3300	0.1037	3.2273	0.1500
1.1252	1.3756	1.0068	3.4257	1.3600	0.3358	3.3741	0.3700	0.1053	3.3752	0.1500
1.1452	1.3292	0.9136	3.6087	1.5000	0.2962	3.4630	0.7700	0.0995	3.4354	0.2500
1.1684	1.3239	0.8907	3.7530	1.3300	0.2772	3.5844	0.6500	0.0864	3.5277	0.3200
1.1943	1.3431	0.9357	3.7286	1.5100	0.3102	3.5956	0.7700	0.1026	3.5827	0.1800
1.2141	1.3378	0.9122	3.8674	1.3900	0.2873	3.6972	0.6800	0.0949	3.6488	0.4600

Table G.18. Parameters of fitted truncated normal distribution for W_{ij}, $a_i \neq a_j$ with I/Q maximally flat lowpass filters BT=0.6, $E_b = 1$ and MSK.

e_{ij}	d_{ij}	$E_b/N_0 = 0dB$ σ_n= 0.7687			$E_b/N_0 = 4dB$ σ_n=0.4889			$E_b/N_0 = 6dB$ σ_n=03900		
		σ_W	μ_W	error [%]	σ_W	μ_W	error [%]	σ_W	μ_W	error [%]
1.2341	1.3873	4.0158	3.7495	2.8400	2.3661	3.8954	2.1300	1.8104	3.8992	1.9800
1.2644	1.3772	4.0590	3.8577	2.5600	2.3747	4.0051	2.3000	1.8423	3.9951	2.2400
1.2658	1.3728	4.0062	4.0149	2.6600	2.2475	4.2021	2.1900	1.7104	4.1572	2.0200
1.2678	1.3966	3.9575	4.2701	2.8200	2.1934	4.3515	2.1500	1.6857	4.2831	1.8900
1.2965	1.3866	4.0151	4.1047	2.4700	2.2792	4.2936	2.3300	1.7354	4.2501	2.2300
1.2996	1.3822	4.0527	4.2787	2.6800	2.2212	4.4344	2.2900	1.6936	4.3570	2.2000

e_{ij}	d_{ij}	$E_b/N_0 = 10dB$ σ_n= 0.2451			$E_b/N_0 = 20dB$ σ_n= 0.0771			$E_b/N_0 = 30dB$ σ_n= 0.0244		
		σ_W	μ_W	error [%]	σ_W	μ_W	error [%]	σ_W	μ_W	error [%]
1.2341	1.3873	1.1266	3.8102	1.5600	0.3840	3.7023	0.4400	0.1222	3.7013	0.1600
1.2644	1.3772	1.1497	3.8896	1.5300	0.3916	3.8019	0.8300	0.1232	3.8029	0.4800
1.2658	1.3728	1.0589	4.0081	1.6800	0.3490	3.8250	0.9700	0.1186	3.7970	0.2100
1.2678	1.3966	1.0215	4.1012	1.5800	0.3177	3.8942	0.4300	0.0990	3.8243	0.1700
1.2965	1.3866	1.0740	4.0900	1.6000	0.3594	3.9170	0.8500	0.1209	3.8985	0.7500
1.2996	1.3822	1.0398	4.1836	1.6700	0.3251	3.9713	0.9500	0.1062	3.9053	0.1900

Table G.19. Parameters of fitted truncated normal distribution for W_{ij}, $a_i = a_j$ with Gaussian I/Q lowpass filters BT=0.4, $E_b = 1$ and GMSK BT=0.3

e_{ij}	d_{ij}	Eb/N0=0dB σ=0.6528			Eb/N0=4dB σ=0.4123			Eb/N0=6dB σ=0.327		
		σ_W	μ_W	error [%]	σ_W	μ_W	error [%]	σ_W	μ_W	error [%]
0.1319	0.5354	1.581	0.934	3.20	0.7583	0.6498	3.14	0.5459	0.5811	3.23
0.156	0.4967	1.629	0.9276	3.15	0.8054	0.6701	3.25	0.5556	0.6386	2.87
0.1571	0.3617	1.479	0.7432	3.24	0.779	0.3461	3.36	0.5975	0.2966	3.21
0.1643	0.3686	1.498	0.7315	3.23	0.8044	0.331	3.25	0.6057	0.3143	3.25
0.0198	1.757	2.579	3.355	2.93	1.479	2.161	2.51	1.154	1.728	2.39
0.0614	1.783	2.573	3.218	2.87	1.468	2.098	2.54	1.139	1.676	2.43
0.127	1.805	2.579	3.131	2.90	1.458	2.051	2.60	1.136	1.657	2.49
0.1388	1.804	2.556	3.163	2.91	1.461	2.061	2.57	1.132	1.667	2.45
0.2334	1.882	2.864	3.256	3.52	1.572	2.205	2.75	1.435	1.717	3.69
0.2677	1.897	2.662	3.249	3.00	1.57	2.129	2.76	1.25	1.754	2.67

e_{ij}	d_{ij}	Eb/N0=10dB σ=0.2055			Eb/N0=20dB σ=0.0628			Eb/N0=30dB σ=0.0205		
		σ_W	μ_W	error [%]	σ_W	μ_W	error [%]	σ_W	μ_W	error [%]
0.1319	0.5354	0.2698	0.5046	3.07	0.0618	0.3987	0.85	0.0188	0.3958	0.31
0.156	0.4967	0.2765	0.5619	2.75	0.0675	0.4683	0.78	0.0212	0.4678	0.29
0.1571	0.3617	0.3559	0.3941	2.37	0.0994	0.468	1.13	0.0314	0.471	0.45
0.1643	0.3686	0.3897	0.4051	2.78	0.1017	0.4904	1.08	0.0320	0.4928	0.46
0.0198	1.757	0.7054	1.096	2.28	0.223	0.3521	2.07	0.0723	0.1227	1.80
0.0614	1.783	0.8456	1.025	3.86	0.225	0.3831	1.75	0.0750	0.2114	0.65
0.127	1.805	0.692	1.09	2.19	0.2279	0.4953	1.10	0.0725	0.3842	0.25
0.1388	1.804	0.7032	1.101	2.16	0.2268	0.5227	0.94	0.0723	0.4181	0.30
0.2334	1.882	0.8383	1.219	2.47	0.3435	0.7841	0.48	0.1097	0.7229	0.12
0.2677	1.897	0.8399	1.209	2.47	0.3394	0.8298	0.43	0.111	0.8035	0.10

Table G.20. Parameters of fitted truncated normal distribution for W_{ij}, $a_i = a_j$ with Gaussian I/Q lowpass filters BT=0.5, $E_b = 1$ and GMSK BT=0.3.

e_{ij}	d_{ij}	Eb/N0=0dB σ=0.7181			Eb/N0=4dB σ=0.4663			Eb/N0=6dB σ=0.365		
		σ_W	μ_W	error [%]	σ_W	μ_W	error [%]	σ_W	μ_W	error [%]
0.1286	0.5083	1.943	1.218	3.25	0.9335	0.7044	3.25	0.6705	0.5951	3.11
0.1491	0.4784	2.026	1.128	3.29	0.9423	0.7257	3.11	0.7053	0.599	3.31
0.1481	0.3465	1.815	1.039	3.30	0.8905	0.4585	3.29	0.6569	0.3483	3.41
0.153	0.3515	1.985	0.8565	3.60	0.9059	0.4595	3.25	0.6747	0.3449	3.25
0.0117	1.839	3.212	4.179	2.76	2.155	2.564	3.97	1.403	2.142	2.31
0.0641	1.847	3.205	4.111	2.83	1.805	2.651	2.44	1.397	2.12	2.35
0.1213	1.853	3.439	3.908	3.47	1.79	2.602	2.44	1.366	2.095	2.37
0.132	1.853	3.19	4.007	2.79	1.811	2.612	2.51	1.391	2.109	2.28
0.172	1.921	3.303	4.235	2.80	1.888	2.731	2.50	1.458	2.2	2.42
0.2248	1.923	3.293	4.116	2.93	1.874	2.702	2.48	1.478	2.174	2.39

e_{ij}	d_{ij}	Eb/N0=10dB σ=0.2278			Eb/N0=20dB σ=0.0733			Eb/N0=30dB σ=0.023		
		σ_W	μ_W	error [%]	σ_W	μ_W	error [%]	σ_W	μ_W	error [%]
0.1286	0.5083	0.3345	0.5059	2.76	0.0758	0.3904	0.92	0.0231	0.3856	0.31
0.1491	0.4784	0.3404	0.546	2.67	0.0791	0.4487	0.95	0.0244	0.447	0.40
0.1481	0.3465	0.4059	0.333	2.85	0.1106	0.4414	1.30	0.0349	0.444	0.39
0.153	0.3515	0.4058	0.3534	2.82	0.1124	0.4564	1.23	0.0354	0.4587	0.45
0.0117	1.839	0.8584	1.369	2.14	0.2668	0.4332	1.94	0.0858	0.1403	1.88
0.0641	1.847	0.8546	1.349	2.12	0.2778	0.463	1.86	0.1027	0.243	0.79
0.1213	1.853	0.859	1.356	2.13	0.2861	0.5332	1.36	0.0993	0.3738	0.36
0.132	1.853	0.8565	1.358	2.06	0.2901	0.5558	1.25	0.1001	0.4029	0.30
0.172	1.921	0.9281	1.424	2.26	0.3704	0.6487	1.53	0.1294	0.5475	0.21
0.2248	1.923	0.9316	1.441	2.26	0.3882	0.7448	1.15	0.132	0.677	0.15

Table G.21. Parameters of fitted truncated normal distribution for W_{ij}, $a_i = a_j$ with Gaussian I/Q lowpass filters BT=0.6, $E_b = 1$ and GMSK BT=0.3.

e_{ij}	d_{ij}	Eb/N0=0dB σ=0.7982			Eb/N0=4dB σ=0.5082			Eb/N0=6dB σ=0.3977		
		σ_W	μ_W	error [%]	σ_W	μ_W	error [%]	σ_W	μ_W	error [%]
0.1257	0.4919	2.366	1.416	3.20	1.087	0.7834	3.15	0.7948	0.6184	3.39
0.1439	0.4672	2.303	1.47	3.23	1.081	0.7814	3.23	0.7628	0.6473	3.09
0.1423	0.3374	2.195	1.279	3.34	1.02	0.5614	3.34	0.7534	0.3812	3.50
0.1459	0.3411	2.178	1.306	3.3	1.02	0.5703	3.30	0.7384	0.4104	3.31
0.0075	1.886	3.831	4.884	2.90	2.133	3.171	2.41	1.629	2.527	2.32
0.0791	1.884	3.794	4.852	2.82	2.118	3.123	2.46	1.634	2.502	2.36
0.1181	1.88	3.769	4.802	2.88	2.442	2.964	3.77	1.617	2.463	2.31
0.1286	1.882	4.265	4.56	3.81	2.483	2.971	3.93	1.626	2.483	2.24
0.1297	1.944	3.833	4.963	2.84	2.176	3.212	2.47	1.692	2.57	2.30
0.1976	1.938	4.48	4.575	3.88	2.156	3.207	2.45	1.928	2.486	3.60

e_{ij}	d_{ij}	Eb/N0=10dB σ=0.251			Eb/N0=20dB σ=0.0798			Eb/N0=30dB σ=0.0252		
		σ_W	μ_W	error [%]	σ_W	μ_W	error [%]	σ_W	μ_W	error [%]
0.1257	0.4919	0.3878	0.5086	2.79	0.0901	0.3847	0.92	0.0272	0.3768	0.22
0.1439	0.4672	0.4585	0.5087	3.80	0.0887	0.4348	1.14	0.0269	0.4315	0.39
0.1423	0.3374	0.4509	0.2966	3.18	0.12	0.4229	1.56	0.0382	0.4265	0.65
0.1459	0.3411	0.4554	0.3072	3.21	0.1221	0.4345	1.58	0.0384	0.4369	0.52
0.0075	1.886	1.004	1.61	2.05	0.3112	0.509	1.97	0.0981	0.1616	1.88
0.0791	1.884	0.9954	1.601	2.09	0.3248	0.5417	1.84	0.1416	0.2756	2.49
0.1181	1.88	0.9943	1.586	2.08	0.3338	0.5842	1.58	0.1222	0.3704	0.44
0.1286	1.882	0.9948	1.597	2.11	0.3352	0.6037	1.53	0.1232	0.3992	0.42
0.1297	1.944	1.036	1.649	2.11	0.377	0.6173	1.89	0.1457	0.4316	0.23
0.1976	1.938	1.053	1.667	2.13	0.4063	0.7226	1.44	0.1479	0.6007	0.17

Table G.22. Parameters of fitted truncated normal distribution for W_{ij}, $a_i = a_j$ with I/Q maximally flat lowpass filters BT=0.4, $E_b = 1$ and GMSK BT=0.3.

e_{ij}	d_{ij}	Eb/N0=0dB σ=0.6436			Eb/N0=4dB σ=0.4058			Eb/N0=6dB σ=0.3224		
		σ_W	μ_W	error [%]	σ_W	μ_W	error [%]	σ_W	μ_W	error [%]
0.1344	0.5373	1.538	0.8389	3.06	0.7836	0.5904	3.57	0.5132	0.5866	3.11
0.1594	0.5002	1.795	0.6037	3.67	0.7581	0.6895	3.02	0.528	0.6543	2.86
0.1595	0.3635	1.464	0.5781	3.14	0.7844	0.2788	3.24	0.5901	0.2828	3.13
0.1669	0.3706	1.493	0.5623	3.11	0.7734	0.3242	3.30	0.6037	0.2958	3.11
0.0151	1.767	2.518	3.206	2.88	1.444	2.068	2.59	1.123	1.656	2.43
0.0633	1.791	2.474	3.058	3.01	1.425	1.985	2.56	1.097	1.593	2.48
0.1255	1.811	2.813	2.73	3.81	1.409	1.932	2.70	1.09	1.557	2.55
0.137	1.811	2.454	2.943	3.02	1.4	1.937	2.64	1.088	1.572	2.56
0.2603	1.889	2.584	3.132	3.09	1.541	2.063	2.76	1.244	1.696	2.78
0.2778	1.902	2.608	2.982	3.06	1.532	1.992	2.84	1.233	1.629	2.72

e_{ij}	d_{ij}	Eb/N0=10dB σ=0.2021			Eb/N0=20dB σ=0.0644			Eb/N0=30dB σ=0.0201		
		σ_W	μ_W	error [%]	σ_W	μ_W	error [%]	σ_W	μ_W	error [%]
0.1344	0.5373	0.2516	0.5076	3.23	0.0563	0.4048	0.93	0.0172	0.4031	0.35
0.1594	0.5002	0.2647	0.5718	2.71	0.0655	0.4782	0.71	0.0206	0.4779	0.24
0.1595	0.3635	0.3496	0.4049	2.25	0.0971	0.4763	1.02	0.0307	0.478	0.42
0.1669	0.3706	0.3795	0.4212	2.52	0.0998	0.4976	1.03	0.0315	0.5002	0.41
0.0151	1.767	0.687	1.044	2.38	0.2156	0.3367	2.23	0.0693	0.1135	2.02
0.0633	1.791	0.6833	1.016	2.36	0.2255	0.3699	2.10	0.0686	0.2109	0.56
0.1255	1.811	0.6756	1.029	2.22	0.2409	0.4839	3.39	0.0640	0.3793	0.21
0.137	1.811	0.676	1.045	2.19	0.2103	0.5108	1.07	0.0641	0.4128	0.21
0.2603	1.889	0.8441	1.182	2.62	0.3382	0.8498	0.28	0.1063	0.7959	0.15
0.2778	1.902	0.8331	1.154	2.53	0.3626	0.8528	1.82	0.1076	0.8332	0.16

Table G.23. Parameters of fitted truncated normal distribution for W_{ij}, $a_i = a_j$ with I/Q maximally flat lowpass filters BT=0.5, $E_b = 1$ and GMSK BT=0.3.

e_{ij}	d_{ij}	Eb/N0=0dB σ=0.7081			Eb/N0=4dB σ=0.444			Eb/N0=6dB σ=0.3561		
		σ_W	μ_W	error [%]	σ_W	μ_W	error [%]	σ_W	μ_W	error [%]
0.1311	0.5056	1.808	1.073	3.25	0.8795	0.6584	3.18	0.6088	0.5899	3.16
0.1523	0.4807	1.868	1.037	3.13	0.8915	0.6981	3.07	0.6372	0.6208	3.05
0.1497	0.3465	1.736	0.8384	3.23	0.8459	0.3962	3.32	0.6399	0.3058	3.31
0.1542	0.3512	1.758	0.8092	3.26	0.8737	0.3848	3.28	0.6536	0.3131	3.24
0.0021	1.871	3.014	3.936	2.86	1.74	2.555	2.43	1.341	2.026	2.31
0.0628	1.873	3.049	3.804	2.96	1.74	2.471	2.45	1.324	1.978	2.46
0.1149	1.872	2.988	3.719	2.93	1.688	2.4	2.57	1.314	1.934	2.43
0.1247	1.873	2.998	3.686	2.95	1.71	2.398	2.62	1.315	1.94	2.44
0.2017	1.939	3.124	3.871	2.89	1.794	2.529	2.73	1.412	2.03	2.56
0.2292	1.936	3.085	3.778	2.92	1.799	2.474	2.71	1.406	1.998	2.68

e_{ij}	d_{ij}	Eb/N0=10dB σ=0.222			Eb/N0=20dB σ=0.0714			Eb/N0=30dB σ=0.0223		
		σ_W	μ_W	error [%]	σ_W	μ_W	error [%]	σ_W	μ_W	error [%]
0.1311	0.5056	0.3053	0.5082	2.98	0.0665	0.3966	1.01	0.0201	0.3931	0.36
0.1523	0.4807	0.3171	0.5576	2.61	0.0769	0.4579	0.82	0.0238	0.4567	0.24
0.1497	0.3465	0.3971	0.341	2.75	0.1068	0.4458	1.21	0.0337	0.4489	0.39
0.1542	0.3512	0.428	0.3356	2.99	0.1083	0.4604	1.26	0.0342	0.4624	0.41
0.0021	1.871	0.8266	1.284	2.21	0.2561	0.4112	2.10	0.0819	0.1298	2.07
0.0628	1.873	0.8207	1.264	2.21	0.2639	0.4362	1.89	0.0910	0.2306	0.74
0.1149	1.872	0.8165	1.253	2.18	0.2655	0.509	1.39	0.0852	0.3543	0.33
0.1247	1.873	0.892	1.249	2.97	0.2656	0.5294	1.25	0.0857	0.3808	0.22
0.2017	1.939	0.9188	1.339	2.41	0.3779	0.6915	1.28	0.1264	0.6213	0.15
0.2292	1.936	0.9229	1.317	2.49	0.3844	0.745	0.95	0.1279	0.6915	0.14

Table G.24. Parameters of fitted truncated normal distribution for W_{ij}, $a_i = a_j$ with I/Q maximally flat lowpass filters BT=0.6, $E_b = 1$ and GMSK BT=0.3.

e_{ij}	d_{ij}	Eb/N0=0dB σ=0.7687			Eb/N0=4dB σ=0.4889			Eb/N0=6dB σ=0.39		
		σ_W	μ_W	error [%]	σ_W	μ_W	error [%]	σ_W	μ_W	error [%]
0.1265	0.482	2.208	1.216	3.39	1.016	0.7095	3.21	0.706	0.6043	3.16
0.1446	0.4659	2.124	1.325	3.28	1.016	0.7308	3.14	0.7482	0.6034	3.24
0.1414	0.3338	2.025	1.098	3.28	0.9565	0.4873	3.25	0.6916	0.3585	3.38
0.1439	0.3366	2.068	1.046	3.22	0.9505	0.5011	3.35	0.8107	0.2189	3.89
0.0055	1.942	3.656	4.654	3.00	2.023	3.019	2.41	1.58	2.411	2.22
0.0718	1.929	3.904	4.401	3.43	2.034	2.941	2.49	1.775	2.29	3.49
0.1051	1.914	3.551	4.43	2.94	1.996	2.875	2.55	1.536	2.286	2.48
0.1139	1.916	3.537	4.413	3.00	2.003	2.897	2.58	1.843	2.206	3.94
0.1469	1.973	3.64	4.587	2.89	2.067	2.979	2.63	1.615	2.369	2.47
0.1874	1.959	3.908	4.389	3.45	2.065	2.941	2.61	1.614	2.351	2.48

e_{ij}	d_{ij}	Eb/N0=10dB σ=0.2451			Eb/N0=20dB σ=0.0771			Eb/N0=30dB σ=0.0244		
		σ_W	μ_W	error [%]	σ_W	μ_W	error [%]	σ_W	μ_W	error [%]
0.1265	0.482	0.3543	0.5022	2.94	0.0767	0.3848	1.18	0.0230	0.3795	0.29
0.1446	0.4659	0.3678	0.5351	2.53	0.0858	0.4358	1.05	0.0266	0.4334	0.39
0.1414	0.3338	0.4168	0.3036	3.07	0.1147	0.4201	1.49	0.0361	0.4236	0.55
0.1439	0.3366	0.4229	0.3086	2.98	0.1156	0.4278	1.39	0.0365	0.4313	0.50
0.0055	1.942	0.9607	1.529	2.02	0.2999	0.485	1.96	0.0943	0.1535	1.93
0.0718	1.929	0.962	1.502	2.19	0.3103	0.5108	1.88	0.1165	0.2621	0.97
0.1051	1.914	0.9515	1.48	2.14	0.3105	0.5461	1.57	0.1058	0.3352	0.42
0.1139	1.916	1.113	1.434	3.62	0.3117	0.5612	1.48	0.1068	0.3584	0.40
0.1469	1.973	1.004	1.543	2.26	0.4218	0.5951	2.79	0.1456	0.4618	0.22
0.1874	1.959	1.015	1.531	2.26	0.4036	0.6794	1.65	0.1432	0.5788	0.15

Table G.25. Parameters of fitted truncated normal distribution for W_{ij}, $a_i = a_j$ with Gaussian I/Q lowpass filters BT=0.4, $E_b = 1$ and GMSK BT=0.5.

e_{ij}	d_{ij}	Eb/N0=0dB σ=0.6528 σ_W	μ_W	error [%]	Eb/N0=4dB σ=0.4123 σ_W	μ_W	error [%]	Eb/N0=6dB σ=0.327 σ_W	μ_W	error [%]
0.0995	0.4064	1.491	0.8063	3.21	0.7942	0.402	3.63	0.4943	0.4361	3.11
0.1026	0.4009	1.509	0.8008	3.19	0.7108	0.5026	3.15	0.4989	0.4415	3.05
0.1045	0.2849	1.404	0.6854	3.27	0.6809	0.2941	3.24	0.5001	0.2222	3.30
0.1052	0.2859	1.407	0.6842	3.23	0.673	0.3105	3.34	0.4981	0.2216	3.30
0.0053	1.749	2.589	3.344	2.91	1.716	2.071	3.82	1.149	1.713	2.44
0.0535	1.777	2.568	3.258	2.87	1.483	2.108	2.58	1.151	1.679	2.44
0.0626	1.803	2.893	3.03	3.75	1.47	2.066	2.66	1.146	1.655	2.49
0.0634	1.803	2.58	3.188	2.96	1.66	2.003	3.60	1.135	1.662	2.52
0.2556	1.848	2.651	3.324	2.95	1.576	2.2	2.72	1.245	1.784	2.61
0.2002	1.873	2.64	3.252	3.02	1.552	2.124	2.76	1.217	1.723	2.63

e_{ij}	d_{ij}	Eb/N0=10dB σ=0.2055 σ_W	μ_W	error [%]	Eb/N0=20dB σ=0.0628 σ_W	μ_W	error [%]	Eb/N0=30dB σ=0.0205 σ_W	μ_W	error [%]
0.0995	0.4064	0.2432	0.3807	2.85	0.0533	0.301	0.93	0.0162	0.2985	0.32
0.1026	0.4009	0.2526	0.3893	2.94	0.0555	0.31	0.98	0.0170	0.3078	0.30
0.1045	0.2849	0.3028	0.2218	2.91	0.0824	0.3107	1.36	0.0259	0.313	0.46
0.1052	0.2859	0.3089	0.215	2.82	0.0824	0.3134	1.40	0.0259	0.3155	0.45
0.0053	1.749	0.7068	1.092	2.29	0.2207	0.3462	2.14	0.0694	0.11	2.17
0.0535	1.777	0.8464	1.028	3.84	0.2336	0.3606	2.24	0.0938	0.1769	1.54
0.0626	1.803	0.8353	1.008	3.8	0.2236	0.3779	1.79	0.0722	0.2106	0.58
0.0634	1.803	0.7017	1.058	2.36	0.2253	0.3796	1.77	0.0721	0.2124	0.59
0.2556	1.848	0.834	1.236	2.5	0.3389	0.8162	0.48	0.1098	0.768	0.15
0.2002	1.873	0.8046	1.157	2.60	0.3353	0.6812	0.81	0.1083	0.6228	0.14

Table G.26. Parameters of fitted truncated normal distribution for W_{ij}, $a_i = a_j$ with Gaussian I/Q lowpass filters BT=0.5, $E_b = 1$ and GMSK BT=0.5.

e_{ij}	d_{ij}	Eb/N0=0dB σ=0.7181			Eb/N0=4dB σ=0.4663			Eb/N0=6dB σ=0.365		
		σ_W	μ_W	error [%]	σ_W	μ_W	error [%]	σ_W	μ_W	error [%]
0.0849	0.3669	1.84	1.053	3.22	0.8394	0.5293	3.27	0.58	0.4263	3.17
0.0868	0.3638	1.839	1.066	3.19	0.8448	0.5375	3.18	0.5929	0.4244	3.16
0.0872	0.2581	1.729	0.9976	3.26	0.7862	0.4071	3.26	0.5382	0.2969	3.39
0.0876	0.2586	1.76	0.952	3.32	0.7805	0.4277	3.32	0.5444	0.2917	3.33
0.0016	1.835	3.21	4.17	2.75	2.025	2.614	3.46	1.61	2.075	3.59
0.0307	1.849	3.236	4.147	2.81	1.817	2.663	2.54	1.401	2.124	2.27
0.0431	1.862	3.231	4.103	2.86	1.805	2.628	2.49	1.385	2.114	2.36
0.0435	1.862	3.217	4.095	2.84	1.808	2.639	2.50	1.481	2.102	2.79
0.1932	1.898	3.269	4.211	2.88	1.872	2.724	2.55	1.462	2.197	2.34
0.1623	1.911	3.254	4.171	2.93	1.88	2.711	2.52	1.464	2.168	2.39

e_{ij}	d_{ij}	Eb/N0=10dB σ=0.2278			Eb/N0=20dB σ=0.0733			Eb/N0=30dB σ=0.023		
		σ_W	μ_W	error [%]	σ_W	μ_W	error [%]	σ_W	μ_W	error [%]
0.0849	0.3669	0.2921	0.3369	2.91	0.0608	0.2597	1.47	0.0179	0.2546	0.41
0.0868	0.3638	0.2911	0.3418	2.85	0.0624	0.2658	1.36	0.0186	0.2604	0.40
0.0872	0.2581	0.357	0.1286	3.91	0.0858	0.2596	1.66	0.0271	0.2617	0.60
0.0876	0.2586	0.314	0.1818	3.31	0.0861	0.2606	1.75	0.0271	0.2626	0.56
0.0016	1.835	0.8614	1.364	2.14	0.267	0.4324	1.99	0.0846	0.1365	1.95
0.0307	1.849	0.8593	1.351	2.13	0.2674	0.433	2.01	0.0940	0.1557	1.89
0.0431	1.862	0.8622	1.338	2.17	0.2691	0.4373	2.00	0.0925	0.1801	1.12
0.0435	1.862	0.856	1.346	2.19	0.2675	0.4387	1.96	0.0940	0.1812	1.28
0.1932	1.898	0.9297	1.434	2.28	0.3692	0.6725	1.37	0.1312	0.5858	0.22
0.1623	1.911	1.056	1.354	3.63	0.3622	0.6079	1.72	0.1295	0.5036	0.20

Table G.27. Parameters of fitted truncated normal distribution for W_{ij}, $a_i = a_j$ with Gaussian I/Q lowpass filters BT=0.6, $E_b = 1$ and GMSK BT=0.5

e_{ij}	d_{ij}	Eb/N0=0dB σ=0.7982			Eb/N0=4dB σ=0.5082			Eb/N0=6dB σ=0.3977		
		σ_W	μ_W	error [%]	σ_W	μ_W	error [%]	σ_W	μ_W	error [%]
0.0751	0.3417	2.171	1.333	3.29	0.9649	0.6162	3.3	0.6524	0.4606	3.18
0.0764	0.3397	2.182	1.295	3.30	0.9544	0.6199	3.24	0.6644	0.4474	3.27
0.0765	0.2408	2.156	1.183	3.21	0.8957	0.5307	3.32	0.6175	0.3363	3.29
0.0766	0.241	2.095	1.218	3.27	0.8952	0.5308	3.25	0.6014	0.3646	3.35
0.0006	1.883	3.792	4.906	2.88	2.128	3.162	2.40	1.627	2.525	2.22
0.0177	1.89	3.801	4.868	2.90	2.116	3.147	2.41	1.647	2.509	2.32
0.0353	1.897	3.83	4.853	2.83	2.101	3.124	2.46	1.627	2.499	2.31
0.0356	1.897	3.827	4.855	2.83	2.121	3.133	2.52	1.632	2.515	2.24
0.1489	1.927	3.888	4.926	2.85	2.163	3.21	2.49	1.67	2.558	2.27
0.1334	1.934	3.895	4.925	2.87	2.175	3.194	2.55	1.658	2.554	2.26

e_{ij}	d_{ij}	Eb/N0=10dB σ=0.251			Eb/N0=20dB σ=0.0798			Eb/N0=30dB σ=0.0252		
		σ_W	μ_W	error [%]	σ_W	μ_W	error [%]	σ_W	μ_W	error [%]
0.0751	0.3417	0.3327	0.31	3.05	0.0667	0.2342	1.73	0.0192	0.2253	0.45
0.0764	0.3397	0.3322	0.3176	3.08	0.0669	0.237	1.56	0.0197	0.2291	0.54
0.0765	0.2408	0.3251	0.1806	3.38	0.0893	0.2249	2.02	0.0279	0.229	0.73
0.0766	0.241	0.3289	0.1783	3.35	0.0895	0.2263	2.03	0.0278	0.2294	0.67
0.0006	1.883	0.9956	1.603	1.98	0.311	0.5075	1.91	0.0977	0.1607	1.86
0.0177	1.89	0.996	1.595	2.05	0.3092	0.5051	1.86	0.1002	0.1671	1.88
0.0353	1.897	0.9976	1.593	2.10	0.3124	0.5104	1.87	0.1056	0.184	1.67
0.0356	1.897	0.9935	1.589	2.08	0.3107	0.5117	1.91	0.1057	0.1844	1.57
0.1489	1.927	1.038	1.655	2.10	0.3801	0.6333	1.80	0.148	0.4608	0.37
0.1334	1.934	1.02	1.639	2.11	0.3721	0.6114	1.85	0.1449	0.4253	0.35

Table G.28. Parameters of fitted truncated normal distribution for W_{ij}, $a_i = a_j$ with I/Q maximally flat lowpass filters BT=0.4, $E_b = 1$ and GMSK BT=0.5.

e_{ij}	d_{ij}	Eb/N0=0dB σ=0.6436			Eb/N0=4dB σ=0.4058			Eb/N0=6dB σ=0.3224		
		σ_W	μ_W	error [%]	σ_W	μ_W	error [%]	σ_W	μ_W	error [%]
0.1045	0.4127	1.443	0.7293	3.05	0.6922	0.4807	3.25	0.4721	0.4524	3.10
0.1079	0.4082	1.449	0.74	3.18	0.6825	0.5099	3.13	0.5044	0.4499	3.36
0.1089	0.2898	1.363	0.582	3.14	0.6833	0.2416	3.28	0.5011	0.2032	3.46
0.1096	0.2907	1.373	0.5633	3.12	0.6547	0.2842	3.34	0.5016	0.2033	3.40
0.0028	1.761	2.513	3.199	2.88	1.44	2.065	2.58	1.119	1.654	2.42
0.0653	1.785	2.484	3.091	3.00	1.437	2.003	2.57	1.107	1.606	2.52
0.0549	1.809	2.484	2.972	2.93	1.413	1.949	2.75	1.097	1.553	2.68
0.0556	1.809	2.649	2.908	3.52	1.408	1.945	2.71	1.097	1.556	2.65
0.2914	1.856	2.583	3.153	3.06	1.54	2.09	2.71	1.24	1.723	2.79
0.2285	1.878	2.588	3.008	3.04	1.506	1.995	2.92	1.197	1.622	2.78

e_{ij}	d_{ij}	Eb/N0=10dB σ=0.2021			Eb/N0=20dB σ=0.0644			Eb/N0=30dB σ=0.0201		
		σ_W	μ_W	error [%]	σ_W	μ_W	error [%]	σ_W	μ_W	error [%]
0.1045	0.4127	0.232	0.3963	2.93	0.0520	0.3151	0.91	0.0159	0.3133	0.29
0.1079	0.4082	0.2381	0.4075	2.72	0.0550	0.3252	0.77	0.0171	0.3234	0.24
0.1089	0.2898	0.3116	0.2259	2.89	0.0818	0.3248	1.20	0.0259	0.3263	0.42
0.1096	0.2907	0.3159	0.2265	2.90	0.0826	0.3258	1.18	0.0260	0.3283	0.45
0.0028	1.761	0.6844	1.042	2.35	0.2149	0.333	2.24	0.0679	0.1049	2.16
0.0653	1.785	0.6913	1.019	2.44	0.2781	0.3395	3.89	0.0991	0.203	1.21
0.0549	1.809	0.6795	0.9895	2.40	0.2142	0.3525	1.91	0.0666	0.19	0.82
0.0556	1.809	0.6778	0.9954	2.45	0.2137	0.3535	1.99	0.0664	0.1918	0.79
0.2914	1.856	0.8421	1.222	2.57	0.3338	0.9052	0.31	0.107	0.874	0.16
0.2285	1.878	0.8052	1.105	2.62	0.3601	0.7239	1.48	0.1073	0.689	0.19

Table G.29. Parameters of fitted truncated normal distribution for W_{ij}, $a_i = a_j$ with I/Q maximally flat lowpass filters BT=0.5, $E_b = 1$ and GMSK BT=0.5.

e_{ij}	d_{ij}	Eb/N0=0dB σ=0.7081			Eb/N0=4dB σ=0.444			Eb/N0=6dB σ=0.3561		
		σ_W	μ_W	error [%]	σ_W	μ_W	error [%]	σ_W	μ_W	error [%]
0.0886	0.37	1.693	0.9451	3.24	0.7851	0.5102	3.24	0.5399	0.4244	3.20
0.0907	0.3693	1.723	0.9199	3.18	0.7946	0.511	3.17	0.5454	0.4319	3.14
0.0903	0.2614	1.608	0.8548	3.24	0.7345	0.3622	3.24	0.5238	0.2539	3.39
0.0903	0.2614	1.65	0.8004	3.21	0.7608	0.3372	3.24	0.5222	0.2623	3.39
0.0109	1.87	3.016	3.936	2.86	1.74	2.555	2.42	1.341	2.026	2.30
0.0412	1.877	3.062	3.858	2.96	1.751	2.497	2.44	1.335	1.994	2.47
0.0174	1.884	3.026	3.798	2.94	1.714	2.431	2.57	1.384	1.942	2.79
0.0175	1.884	3.023	3.762	2.95	1.714	2.439	2.70	1.324	1.954	2.50
0.2393	1.92	3.112	3.901	2.89	1.799	2.552	2.74	1.415	2.056	2.53
0.2045	1.926	3.083	3.818	2.99	1.79	2.501	2.73	1.391	2.013	2.64

e_{ij}	d_{ij}	Eb/N0=10dB σ=0.222			Eb/N0=20dB σ=0.0714			Eb/N0=30dB σ=0.0223		
		σ_W	μ_W	error [%]	σ_W	μ_W	error [%]	σ_W	μ_W	error [%]
0.0886	0.37	0.2964	0.3374	3.46	0.0581	0.2705	1.21	0.0174	0.266	0.39
0.0907	0.3693	0.2755	0.3564	2.82	0.0618	0.2767	1.00	0.0187	0.2721	0.26
0.0903	0.2614	0.3076	0.1822	3.29	0.0849	0.2684	1.50	0.0267	0.271	0.50
0.0903	0.2614	0.3153	0.173	3.16	0.0846	0.2692	1.54	0.0267	0.2708	0.52
0.0109	1.87	0.8249	1.287	2.19	0.2558	0.412	2.11	0.0830	0.1329	1.95
0.0412	1.877	0.8239	1.269	2.25	0.2639	0.4106	2.27	0.1004	0.1607	1.98
0.0174	1.884	0.8166	1.24	2.31	0.2561	0.3929	2.24	0.0812	0.1337	1.95
0.0175	1.884	0.8126	1.243	2.34	0.299	0.3828	3.67	0.0818	0.1336	2.00
0.2393	1.92	0.9218	1.37	2.37	0.3753	0.7619	1.13	0.1282	0.7179	0.15
0.2045	1.926	0.8949	1.311	2.52	0.3649	0.6626	1.63	0.1305	0.6142	0.17

Table G.30. Parameters of fitted truncated normal distribution for W_{ij}, $a_i = a_j$ with I/Q maximally flat lowpass filters BT=0.5, $E_b = 1$ and GMSK BT=0.5.

e_{ij}	d_{ij}	Eb/N0=0dB σ=0.7687			Eb/N0=4dB σ=0.4889			Eb/N0=6dB σ=0.39		
		σ_W	μ_W	error [%]	σ_W	μ_W	error [%]	σ_W	μ_W	error [%]
0.0745	0.3355	2.022	1.139	3.21	0.9041	0.5496	3.27	0.6157	0.423	3.21
0.0756	0.3373	1.968	1.2	3.29	0.8938	0.5627	3.27	0.6159	0.4298	3.26
0.0754	0.2382	1.929	1.064	3.26	0.844	0.4504	3.29	0.5758	0.3029	3.36
0.0750	0.2376	1.95	1.025	3.21	0.8397	0.4499	3.28	0.5659	0.3131	3.38
0.0124	1.944	3.652	4.663	2.99	2.024	3.023	2.41	1.582	2.413	2.22
0.0169	1.94	3.622	4.598	2.85	2.041	2.972	2.51	1.566	2.379	2.29
0.0122	1.937	3.599	4.523	2.89	2.349	2.818	3.80	1.549	2.329	2.47
0.0125	1.937	3.582	4.497	2.99	2.035	2.938	2.54	1.858	2.237	3.98
0.1896	1.966	3.652	4.614	2.84	2.078	3.013	2.60	1.609	2.402	2.5
0.1798	1.962	3.654	4.576	2.93	2.075	2.973	2.60	1.606	2.386	2.42

e_{ij}	d_{ij}	Eb/N0=10dB σ=0.2451			Eb/N0=20dB σ=0.0771			Eb/N0=30dB σ=0.0244		
		σ_W	μ_W	error [%]	σ_W	μ_W	error [%]	σ_W	μ_W	error [%]
0.0745	0.3355	0.3033	0.3101	3.04	0.0627	0.2312	1.50	0.0184	0.2236	0.37
0.0756	0.3373	0.3334	0.2968	3.55	0.0658	0.2349	1.35	0.0198	0.2268	0.38
0.0754	0.2382	0.307	0.171	3.45	0.0862	0.2223	1.79	0.0269	0.2258	0.68
0.0750	0.2376	0.3105	0.168	3.38	0.0857	0.2214	1.8	0.0268	0.2247	0.63
0.0124	1.944	0.962	1.53	2.00	0.3407	0.4765	3.10	0.0957	0.1563	1.83
0.0169	1.94	0.9615	1.509	2.21	0.2959	0.4795	2.05	0.0987	0.1566	2.08
0.0122	1.937	0.9569	1.486	2.20	0.2979	0.4726	2.03	0.0946	0.1526	1.97
0.0125	1.937	0.948	1.488	2.22	0.3543	0.4548	3.79	0.0944	0.1531	2.03
0.1896	1.966	1.01	1.572	2.26	0.3833	0.6817	1.68	0.1482	0.5707	0.31
0.1798	1.962	0.9976	1.552	2.18	0.3739	0.6587	1.72	0.1454	0.5425	0.57

Table G.31. Parameters of fitted truncated normal distribution for W_{ij}, $a_i = a_j$ with I/Q Gaussian filter BT=0.4, $E_b = 1$ and MSK.

e_{ij}	d_{ij}	Eb/N0=0dB σ=0.6528			Eb/N0=4dB σ=0.4123			Eb/N0=6dB σ=0.327		
		σ_W	μ_W	error [%]	σ_W	μ_W	error [%]	σ_W	μ_W	error [%]
0.0635	0.3114	1.41	0.7307	3.22	0.6762	0.3481	3.35	0.4628	0.3014	3.41
0.0640	0.2202	1.428	0.7022	3.26	0.6436	0.3831	3.22	0.4527	0.3087	3.14
0.0005	1.747	1.344	0.666	3.23	0.5968	0.2921	3.20	0.4214	0.1936	3.34
0.0481	1.768	1.337	0.6642	3.17	0.598	0.2949	3.36	0.4183	0.1939	3.31
0.0010	1.788	2.599	3.33	2.89	1.474	2.151	2.56	1.156	1.717	2.45
0.2243	1.815	2.567	3.275	2.92	1.48	2.112	2.51	1.146	1.69	2.46

e_{ij}	d_{ij}	Eb/N0=10dB σ=0.2055			Eb/N0=20dB σ=0.0628			Eb/N0=30dB σ=0.0205		
		σ_W	μ_W	error [%]	σ_W	μ_W	error [%]	σ_W	μ_W	error [%]
0.0635	0.3114	0.2339	0.2495	3.38	0.0463	0.1952	1.18	0.0138	0.1905	0.36
0.0640	0.2202	0.2332	0.2501	3.25	0.0461	0.1949	1.22	0.0138	0.1904	0.24
0.0005	1.747	0.2399	0.1243	3.26	0.0656	0.1898	1.62	0.0206	0.192	0.52
0.0481	1.768	0.2425	0.1215	3.23	0.0655	0.1896	1.59	0.0207	0.192	0.61
0.0010	1.788	0.7051	1.092	2.30	0.2203	0.3456	2.17	0.0696	0.109	2.17
0.2243	1.815	0.7114	1.078	2.34	0.27	0.3493	3.54	0.0983	0.1743	1.44

Table G.32. Parameters of fitted truncated normal distribution for W_{ij}, $a_i = a_j$ with Gaussian I/Q lowpass filters BT=0.5, $E_b = 1$ and MSK.

e_{ij}	d_{ij}	Eb/N0=0dB σ=0.7181			Eb/N0=4dB σ=0.4663			Eb/N0=6dB σ=0.365		
		σ_W	μ_W	error [%]	σ_W	μ_W	error [%]	σ_W	μ_W	error [%]
0.0438	0.2568	2.051	0.5811	3.60	0.7472	0.4467	3.28	0.5048	0.3208	3.26
0.0439	0.1816	1.736	0.9806	3.24	0.7537	0.4408	3.18	0.5041	0.321	3.27
2.658e	1.834	1.662	0.9792	3.23	0.7092	0.391	3.26	0.4623	0.269	3.33
0.0384	1.845	1.677	0.9557	3.38	0.7045	0.404	3.32	0.4746	0.2593	3.28
0.0220	1.856	3.381	4.094	3.17	1.803	2.692	2.47	1.394	2.14	2.35
0.1647	1.874	3.297	4.147	2.85	1.813	2.677	2.50	1.399	2.128	2.36

e_{ij}	d_{ij}	Eb/N0=10dB σ=0.2278			Eb/N0=20dB σ=0.0733			Eb/N0=30dB σ=0.023		
		σ_W	μ_W	error [%]	σ_W	μ_W	error [%]	σ_W	μ_W	error [%]
0.0438	0.2568	0.2489	0.1981	3.13	0.0483	0.141	1.98	0.0135	0.1314	0.55
0.0439	0.1816	0.2473	0.2009	3.19	0.0481	0.1409	1.88	0.0135	0.1314	0.43
2.658e	1.834	0.236	0.1213	3.45	0.0634	0.1271	1.96	0.0194	0.1315	0.78
0.0384	1.845	0.2357	0.1215	3.39	0.0633	0.1274	2.08	0.0193	0.1315	0.77
0.0220	1.856	0.8588	1.356	2.12	0.2684	0.433	2.01	0.0851	0.1364	1.97
0.1647	1.874	0.8589	1.358	2.08	0.2715	0.4385	1.95	0.1002	0.1656	1.92

Table G.33. Parameters of fitted truncated normal distribution for W_{ij}, $a_i = a_j$ with Gaussian I/Q lowpass filters BT=0.6, $E_b = 1$ and MSK.

e_{ij}	d_{ij}	Eb/N0=0dB σ=0.7982			Eb/N0=4dB σ=0.5082			Eb/N0=6dB σ=0.3977		
		σ_W	μ_W	error [%]	σ_W	μ_W	error [%]	σ_W	μ_W	error [%]
0.0316	0.2179	2.053	1.279	3.32	0.8715	0.5244	3.29	0.5657	0.3634	3.25
0.0316	0.1541	2.08	1.225	3.33	0.867	0.5202	3.24	0.5973	0.3257	3.44
7.467e	1.883	2.027	1.227	3.30	0.8309	0.4972	3.34	0.5379	0.3231	3.29
0.0299	1.89	2.031	1.207	3.22	0.8204	0.509	3.34	0.544	0.3183	3.29
0.0248	1.897	3.836	4.899	2.85	2.132	3.161	2.44	1.98	2.4	3.99
0.1232	1.91	3.854	4.882	2.91	2.12	3.158	2.42	1.639	2.516	2.24

e_{ij}	d_{ij}	Eb/N0=10dB σ=0.251			Eb/N0=20dB σ=0.0798			Eb/N0=30dB σ=0.0252		
		σ_W	μ_W	error [%]	σ_W	μ_W	error [%]	σ_W	μ_W	error [%]
0.0316	0.2179	0.262	0.1876	3.32	0.0498	0.1071	2.32	0.0129	0.0948	0.62
0.0316	0.1541	0.2706	0.1811	3.13	0.0495	0.1072	2.25	0.0128	0.0948	0.70
7.467e	1.883	0.244	0.1401	3.33	0.0615	0.0847	2.61	0.0181	0.0944	1.05
0.0299	1.89	0.2509	0.1365	3.47	0.0622	0.0848	2.49	0.0180	0.0944	0.98
0.0248	1.897	0.9952	1.603	2.00	0.3105	0.5083	1.92	0.0972	0.1599	1.90
0.1232	1.91	1.005	1.598	2.09	0.3103	0.5107	1.89	0.1067	0.1756	1.80

Table G.34. Parameters of fitted truncated normal distribution for W_{ij}, $a_i = a_j$ with I/Q maximally flat lowpass filters BT=0.4, $E_b = 1$ and MSK.

e_{ij}	d_{ij}	Eb/N0=0dB σ=0.6436			Eb/N0=4dB σ=0.4058			Eb/N0=6dB σ=0.3224		
		σ_W	μ_W	error [%]	σ_W	μ_W	error [%]	σ_W	μ_W	error [%]
0.0700	0.3248	1.356	0.6711	3.10	0.6225	0.3916	3.14	0.4374	0.3325	3.24
0.0701	0.2296	1.361	0.6637	3.21	0.6228	0.3905	3.17	0.4319	0.3378	3.13
0.0060	1.76	1.297	0.5734	3.10	0.6082	0.2287	3.17	0.4233	0.1783	3.50
0.0617	1.777	1.307	0.5487	3.08	0.5824	0.2656	3.31	0.4233	0.1771	3.54
0.0244	1.794	2.512	3.198	2.88	1.439	2.066	2.57	1.26	1.607	3.46
0.2669	1.823	2.489	3.106	3.01	1.435	2.012	2.62	1.108	1.617	2.54

e_{ij}	d_{ij}	Eb/N0=10dB σ=0.2021			Eb/N0=20dB σ=0.0644			Eb/N0=30dB σ=0.0201		
		σ_W	μ_W	error [%]	σ_W	μ_W	error [%]	σ_W	μ_W	error [%]
0.0700	0.3248	0.2136	0.2817	2.86	0.0481	0.2138	0.86	0.0146	0.21	0.22
0.0701	0.2296	0.2138	0.2815	2.75	0.0478	0.2139	0.79	0.0146	0.2099	0.17
0.0060	1.76	0.2456	0.133	3.33	0.0675	0.2089	1.40	0.0214	0.21	0.46
0.0617	1.777	0.2459	0.1332	3.25	0.0679	0.2082	1.4	0.0214	0.2101	0.49
0.0244	1.794	0.6846	1.042	2.34	0.215	0.3333	2.23	0.0681	0.1059	2.16
0.2669	1.823	0.6932	1.023	2.44	0.2351	0.3546	2.54	0.0995	0.2014	0.97

Table G.35. Parameters of fitted truncated normal distribution for W_{ij}, $a_i = a_j$ with I/Q maximally flat lowpass filters BT=0.5, $E_b = 1$ and MSK.

e_{ij}	d_{ij}	Eb/N0=0dB σ=0.7081			Eb/N0=4dB σ=0.444			Eb/N0=6dB σ=0.3561		
		σ_W	μ_W	error [%]	σ_W	μ_W	error [%]	σ_W	μ_W	error [%]
0.0488	0.2722	1.602	0.8843	3.26	0.7083	0.426	3.27	0.4759	0.3205	3.34
0.0491	0.1925	1.624	0.8583	3.21	0.7905	0.3277	3.65	0.48	0.3182	3.27
0.0068	1.872	1.869	0.4207	3.91	0.6682	0.34	3.23	0.4497	0.2307	3.31
0.0609	1.876	1.582	0.7933	3.21	0.6904	0.3223	3.2	0.4548	0.2308	3.36
0.0822	1.88	3.017	3.943	2.86	1.742	2.559	2.42	1.343	2.029	2.30
0.2235	1.899	3.466	3.699	3.81	1.755	2.518	2.48	1.344	2.011	2.43

e_{ij}	d_{ij}	Eb/N0=10dB σ=0.222			Eb/N0=20dB σ=0.0714			Eb/N0=30dB σ=0.0223		
		σ_W	μ_W	error [%]	σ_W	μ_W	error [%]	σ_W	μ_W	error [%]
0.0488	0.2722	0.2339	0.2233	3.19	0.0510	0.1556	1.25	0.0151	0.1466	0.27
0.0491	0.1925	0.2337	0.2229	3.11	0.0512	0.1558	1.19	0.0151	0.1466	0.22
0.0068	1.872	0.235	0.1201	3.58	0.0658	0.1438	1.80	0.0204	0.1472	0.64
0.0609	1.876	0.2409	0.1143	3.30	0.0656	0.1443	1.77	0.0203	0.1472	0.65
0.0822	1.88	0.8262	1.288	2.19	0.2563	0.4119	2.11	0.0824	0.1312	2.01
0.2235	1.899	0.8285	1.281	2.21	0.3221	0.4144	3.73	0.104	0.2094	1.26

Table G.36. Parameters of fitted truncated normal distribution for W_{ij}, $a_i = a_j$ with I/Q maximally flat lowpass filters BT=0.6, $E_b = 1$ and MSK.

e_{ij}	d_{ij}	Eb/N0=0dB σ=0.7687			Eb/N0=4dB σ=0.4889			Eb/N0=6dB σ=0.39		
		σ_W	μ_W	error [%]	σ_W	μ_W	error [%]	σ_W	μ_W	error [%]
0.0327	0.2284	1.932	1.076	3.25	0.8255	0.467	3.3	0.5414	0.3312	3.21
0.0337	0.1615	1.881	1.124	3.31	0.8067	0.4779	3.24	0.5407	0.3284	3.29
0.0033	1.948	1.87	1.045	3.26	0.7734	0.4407	3.29	0.5069	0.2846	3.31
0.0589	1.945	1.89	1.011	3.19	0.7766	0.4298	3.31	0.5055	0.2839	3.29
0.1212	1.941	3.661	4.674	2.99	2.028	3.029	2.42	1.585	2.417	2.22
0.1844	1.955	3.964	4.484	3.49	2.047	2.998	2.49	1.578	2.402	2.3

e_{ij}	d_{ij}	Eb/N0=10dB σ=0.2451			Eb/N0=20dB σ=0.0771			Eb/N0=30dB σ=0.0244		
		σ_W	μ_W	error [%]	σ_W	μ_W	error [%]	σ_W	μ_W	error [%]
0.0327	0.2284	0.2559	0.1876	3.35	0.0521	0.1114	1.64	0.0148	0.0983	0.23
0.0337	0.1615	0.2491	0.1942	3.24	0.0517	0.1112	1.62	0.0147	0.0983	0.27
0.0033	1.948	0.2331	0.1335	3.33	0.0648	0.0929	2.92	0.0187	0.1009	0.90
0.0589	1.945	0.2362	0.1325	3.36	0.0611	0.0936	2.57	0.0187	0.1009	0.90
0.1212	1.941	0.9632	1.533	2.02	0.3007	0.4864	1.96	0.0942	0.1537	1.96
0.1844	1.955	0.9699	1.526	2.17	0.3075	0.5114	1.89	0.1122	0.2409	0.96

APPENDIX H

TABLES OF NORMALIZED ENVELOPE DISTANCES FOR GMSK BT=0.3 WITH 3-SAMPLE METRIC

Table H.1. Normalized envelope distances of GMSK BT=0.3 for 3-sample metric with Gaussian filter BT=0.4.

	w1/1	w2/1	w3/-1	w4/-1	w5/1	w6/1	w7/-1	w8/-1	w9/1	w10/1	w11/-1	w12/-1	w13/1	w14/1	w15/-1	w16/-1
w1/1	0	0.164	0.922	1.068	0.164	0.155	0.946	1.038	0.061	0.019	0.946	0.922	0.138	0.061	1.038	1.068
w2/1	0.164	0	0.605	0.915	0.131	0.157	0.569	0.946	0.233	0.061	0.915	0.716	0.267	0.126	1.068	0.798
w3/-1	0.922	0.605	0	0.157	0.716	0.344	0.157	0.155	0.716	0.922	0.267	0.014	0.344	0.605	0.138	0.267
w4/-1	1.068	0.915	0.157	0	0.798	0.716	0.131	0.164	0.915	0.946	0.233	0.267	0.605	0.569	0.061	0.126
w5/1	0.164	0.131	0.716	0.798	0	0.157	0.915	1.068	0.126	0.061	0.569	0.605	0.267	0.233	0.946	0.915
w6/1	0.155	0.157	0.344	0.716	0.157	0	0.605	0.922	0.267	0.138	0.605	0.344	0.014	0.267	0.922	0.716
w7/-1	0.946	0.569	0.157	0.131	0.915	0.605	0	0.164	0.798	1.068	0.126	0.267	0.716	0.915	0.061	0.233
w8/-1	1.038	0.946	0.155	0.164	1.068	0.922	0.164	0	1.068	1.038	0.061	0.138	0.922	0.946	0.019	0.061
w9/1	0.061	0.233	0.716	0.915	0.126	0.267	0.798	1.068	0	0.164	0.915	0.605	0.157	0.131	0.946	0.569
w10/1	0.019	0.061	0.922	0.946	0.061	0.138	1.068	1.038	0.164	0	1.068	0.922	0.155	0.164	1.038	0.946
w11/-1	0.946	0.915	0.267	0.233	0.569	0.605	0.126	0.061	0.915	1.068	0	0.157	0.716	0.798	0.164	0.131
w12/-1	0.922	0.716	0.014	0.267	0.605	0.344	0.267	0.138	0.605	0.922	0.157	0	0.344	0.716	0.155	0.157
w13/1	0.138	0.267	0.344	0.605	0.267	0.014	0.716	0.922	0.157	0.155	0.716	0.344	0	0.157	0.922	0.605
w14/1	0.061	0.126	0.605	0.569	0.233	0.267	0.915	0.946	0.131	0.164	0.798	0.716	0.157	0	1.068	0.915
w15/-1	1.038	1.068	0.138	0.061	0.946	0.922	0.061	0.019	0.946	1.038	0.164	0.155	0.922	1.068	0	0.164
w16/-1	1.068	0.798	0.267	0.126	0.915	0.716	0.233	0.061	0.569	0.946	0.131	0.157	0.605	0.915	0.164	0

Table H.2. Normalized envelope distances of GMSK BT=0.3 for 3-sample metric with Gaussian filter BT=0.5

	w1/1	w2/1	w3/-1	w4/-1	w5/1	w6/1	w7/-1	w8/-1	w9/1	w10/1	w11/-1	w12/-1	w13/1	w14/1	w15/-1	w16/-1
w1/1	0	0.153	0.995	1.129	0.153	0.149	1.04	1.133	0.064	0.011	1.04	0.995	0.132	0.064	1.133	1.129
w2/1	0.153	0	0.708	0.989	0.128	0.148	0.707	1.04	0.171	0.064	0.989	0.785	0.224	0.121	1.129	0.871
w3/-1	0.995	0.708	0	0.148	0.785	0.435	0.148	0.149	0.785	0.995	0.224	0.022	0.435	0.708	0.132	0.224
w4/-1	1.129	0.989	0.148	0	0.871	0.785	0.128	0.153	0.989	1.04	0.171	0.224	0.708	0.707	0.064	0.121
w5/1	0.153	0.128	0.785	0.871	0	0.148	0.989	1.129	0.121	0.064	0.707	0.708	0.224	0.171	1.04	0.989
w6/1	0.149	0.148	0.435	0.785	0.148	0	0.708	0.995	0.224	0.132	0.708	0.435	0.022	0.224	0.995	0.785
w7/-1	1.04	0.707	0.148	0.128	0.989	0.708	0	0.153	0.871	1.129	0.121	0.224	0.785	0.989	0.064	0.171
w8/-1	1.133	1.04	0.149	0.153	1.129	0.995	0.153	0	1.129	1.133	0.064	0.132	0.995	1.04	0.011	0.064
w9/1	0.064	0.171	0.785	0.989	0.121	0.224	0.871	1.129	0	0.153	0.989	0.708	0.148	0.128	1.04	0.707
w10/1	0.011	0.064	0.995	1.04	0.064	0.132	1.129	1.133	0.153	0	1.129	0.995	0.149	0.153	1.133	1.04
w11/-1	1.04	0.989	0.224	0.171	0.707	0.708	0.121	0.064	0.989	1.129	0	0.148	0.785	0.871	0.153	0.128
w12/-1	0.995	0.785	0.022	0.224	0.708	0.435	0.224	0.132	0.708	0.995	0.148	0	0.435	0.785	0.149	0.148
w13/1	0.132	0.224	0.435	0.708	0.224	0.022	0.785	0.995	0.148	0.149	0.785	0.435	0	0.148	0.995	0.708
w14/1	0.064	0.121	0.708	0.707	0.171	0.224	0.989	1.04	0.128	0.153	0.871	0.785	0.148	0	1.129	0.989
w15/-1	1.133	1.129	0.132	0.064	1.04	0.995	0.064	0.011	1.04	1.133	0.153	0.149	0.995	1.129	0	0.153
w16/-1	1.129	0.871	0.224	0.121	0.989	0.785	0.171	0.064	0.707	1.04	0.128	0.148	0.708	0.989	0.153	0

Table H.3. Normalized envelope distances of GMSK BT=0.3 for 3-sample metric with Gaussian filter BT=0.6.

	w1/1	w2/1	w3/-1	w4/-1	w5/1	w6/1	w7/-1	w8/-1	w9/1	w10/1	w11/-1	w12/-1	w13/1	w14/1	w15/-1	w16/-1
w1/1	0	0.145	1.037	1.163	0.145	0.143	1.097	1.189	0.079	0.007	1.097	1.037	0.128	0.079	1.189	1.163
w2/1	0.145	0	0.771	1.033	0.125	0.142	0.792	1.097	0.129	0.079	1.033	0.826	0.197	0.118	1.163	0.914
w3/-1	1.037	0.771	0	0.142	0.826	0.489	0.142	0.143	0.826	1.037	0.197	0.022	0.489	0.771	0.128	0.197
w4/-1	1.163	1.033	0.142	0	0.914	0.826	0.125	0.145	1.033	1.097	0.129	0.197	0.771	0.792	0.079	0.118
w5/1	0.145	0.125	0.826	0.914	0	0.142	1.033	1.163	0.118	0.079	0.792	0.771	0.197	0.129	1.097	1.033
w6/1	0.143	0.142	0.489	0.826	0.142	0	0.771	1.037	0.197	0.128	0.771	0.489	0.022	0.197	1.037	0.826
w7/-1	1.097	0.792	0.142	0.125	1.033	0.771	0	0.145	0.914	1.163	0.118	0.197	0.826	1.033	0.079	0.129
w8/-1	1.189	1.097	0.143	0.145	1.163	1.037	0.145	0	1.163	1.189	0.079	0.128	1.037	1.097	0.007	0.079
w9/1	0.079	0.129	0.826	1.033	0.118	0.197	0.914	1.163	0	0.145	1.033	0.771	0.142	0.125	1.097	0.792
w10/1	0.007	0.079	1.037	1.097	0.079	0.128	1.163	1.189	0.145	0	1.163	1.037	0.143	0.145	1.189	1.097
w11/-1	1.097	1.033	0.197	0.129	0.792	0.771	0.118	0.079	1.033	1.163	0	0.142	0.826	0.914	0.145	0.125
w12/-1	1.037	0.826	0.022	0.197	0.771	0.489	0.197	0.128	0.771	1.037	0.142	0	0.489	0.826	0.143	0.142
w13/1	0.128	0.197	0.489	0.771	0.197	0.022	0.826	1.037	0.142	0.143	0.826	0.489	0	0.142	1.037	0.771
w14/1	0.079	0.118	0.771	0.792	0.129	0.197	1.033	1.097	0.125	0.145	0.914	0.826	0.142	0	1.163	1.033
w15/-1	1.189	1.163	0.128	0.079	1.097	1.037	0.079	0.007	1.097	1.189	0.145	0.143	1.037	1.163	0	0.145
w16/-1	1.163	0.914	0.197	0.118	1.033	0.826	0.129	0.079	0.792	1.097	0.125	0.142	0.771	1.033	0.145	0

Table H.4. Normalized envelope distances of GMSK BT=0.3 for 3-sample metric with maximally flat filter BT=0.4.

	w1/1	w2/1	w3/-1	w4/-1	w5/1	w6/1	w7/-1	w8/-1	w9/1	w10/1	w11/-1	w12/-1	w13/1	w14/1	w15/-1	w16/-1
w1/1	0	0.166	0.929	1.083	0.166	0.159	0.949	1.048	0.063	0.015	0.949	0.929	0.137	0.063	1.048	1.083
w2/1	0.166	0	0.601	0.922	0.134	0.159	0.558	0.949	0.26	0.063	0.922	0.72	0.277	0.125	1.083	0.81
w3/-1	0.929	0.601	0	0.159	0.72	0.342	0.159	0.159	0.72	0.929	0.277	0.029	0.342	0.601	0.137	0.277
w4/-1	1.083	0.922	0.159	0	0.81	0.72	0.134	0.166	0.922	0.949	0.26	0.277	0.601	0.558	0.063	0.125
w5/1	0.166	0.134	0.72	0.81	0	0.159	0.922	1.083	0.125	0.063	0.558	0.601	0.277	0.26	0.949	0.922
w6/1	0.159	0.159	0.342	0.72	0.159	0	0.601	0.929	0.277	0.137	0.601	0.342	0.029	0.277	0.929	0.72
w7/-1	0.949	0.558	0.159	0.134	0.922	0.601	0	0.166	0.81	1.083	0.125	0.277	0.72	0.922	0.063	0.26
w8/-1	1.048	0.949	0.159	0.166	1.083	0.929	0.166	0	1.083	1.048	0.063	0.137	0.929	0.949	0.015	0.063
w9/1	0.063	0.26	0.72	0.922	0.125	0.277	0.81	1.083	0	0.166	0.922	0.601	0.159	0.134	0.949	0.558
w10/1	0.015	0.063	0.929	0.949	0.063	0.137	1.083	1.048	0.166	0	1.083	0.929	0.159	0.166	1.048	0.949
w11/-1	0.949	0.922	0.277	0.26	0.558	0.601	0.125	0.063	0.922	1.083	0	0.159	0.72	0.81	0.166	0.134
w12/-1	0.929	0.72	0.029	0.277	0.601	0.342	0.277	0.137	0.601	0.929	0.159	0	0.342	0.72	0.159	0.159
w13/1	0.137	0.277	0.342	0.601	0.277	0.029	0.72	0.929	0.159	0.159	0.72	0.342	0	0.159	0.929	0.601
w14/1	0.063	0.125	0.601	0.558	0.26	0.277	0.922	0.949	0.134	0.166	0.81	0.72	0.159	0	1.083	0.922
w15/-1	1.048	1.083	0.137	0.063	0.949	0.929	0.063	0.015	0.949	1.048	0.166	0.159	0.929	1.083	0	0.166
w16/-1	1.083	0.81	0.277	0.125	0.922	0.72	0.26	0.063	0.558	0.949	0.134	0.159	0.601	0.922	0.166	0

Table H.5. Normalized envelope distances of GMSK BT=0.3 for 3-sample metric with maximally flat filter BT=0.5

	w1/1	w2/1	w3/-1	w4/-1	w5/1	w6/1	w7/-1	w8/-1	w9/1	w10/1	w11/-1	w12/-1	w13/1	w14/1	w15/-1	w16/-1
w1/1	0	0.154	1.022	1.167	0.154	0.152	1.065	1.168	0.062	0.002	1.065	1.022	0.124	0.062	1.168	1.167
w2/1	0.154	0	0.726	1.017	0.131	0.149	0.72	1.065	0.201	0.062	1.017	0.806	0.229	0.114	1.167	0.906
w3/-1	1.022	0.726	0	0.149	0.806	0.453	0.149	0.152	0.806	1.022	0.229	0.053	0.453	0.726	0.124	0.229
w4/-1	1.167	1.017	0.149	0	0.906	0.806	0.131	0.154	1.017	1.065	0.201	0.229	0.726	0.72	0.062	0.114
w5/1	0.154	0.131	0.806	0.906	0	0.149	1.017	1.167	0.114	0.062	0.72	0.726	0.229	0.201	1.065	1.017
w6/1	0.152	0.149	0.453	0.806	0.149	0	0.726	1.022	0.229	0.124	0.726	0.453	0.053	0.229	1.022	0.806
w7/-1	1.065	0.72	0.149	0.131	1.017	0.726	0	0.154	0.906	1.167	0.114	0.229	0.806	1.017	0.062	0.201
w8/-1	1.168	1.065	0.152	0.154	1.167	1.022	0.154	0	1.167	1.168	0.062	0.124	1.022	1.065	0.002	0.062
w9/1	0.062	0.201	0.806	1.017	0.114	0.229	0.906	1.167	0	0.154	1.017	0.726	0.149	0.131	1.065	0.72
w10/1	0.002	0.062	1.022	1.065	0.062	0.124	1.167	1.168	0.154	0	1.167	1.022	0.152	0.154	1.168	1.065
w11/-1	1.065	1.017	0.229	0.201	0.72	0.726	0.114	0.062	1.017	1.167	0	0.149	0.806	0.906	0.154	0.131
w12/-1	1.022	0.806	0.053	0.229	0.726	0.453	0.229	0.124	0.726	1.022	0.149	0	0.453	0.806	0.152	0.149
w13/1	0.124	0.229	0.453	0.726	0.229	0.053	0.806	1.022	0.149	0.152	0.806	0.453	0	0.149	1.022	0.726
w14/1	0.062	0.114	0.726	0.72	0.201	0.229	1.017	1.065	0.131	0.154	0.906	0.806	0.149	0	1.167	1.017
w15/-1	1.168	1.167	0.124	0.062	1.065	1.022	0.062	0.002	1.065	1.168	0.154	0.152	1.022	1.167	0	0.154
w16/-1	1.167	0.906	0.229	0.114	1.017	0.806	0.201	0.062	0.72	1.065	0.131	0.149	0.726	1.017	0.154	0

Table H.6. Normalized envelope distances of GMSK BT=0.3 for 3-sample metric with maximally flat filter BT=0.6.

	w1/1	w2/1	w3/-1	w4/-1	w5/1	w6/1	w7/-1	w8/-1	w9/1	w10/1	w11/-1	w12/-1	w13/1	w14/1	w15/-1	w16/-1
w1/1	0	0.143	1.089	1.222	0.143	0.144	1.15	1.257	0.071	0.005	1.15	1.089	0.113	0.071	1.257	1.222
w2/1	0.143	0	0.822	1.086	0.126	0.141	0.847	1.15	0.146	0.071	1.086	0.868	0.187	0.105	1.222	0.972
w3/-1	1.089	0.822	0	0.141	0.868	0.537	0.141	0.144	0.868	1.089	0.187	0.066	0.537	0.822	0.113	0.187
w4/-1	1.222	1.086	0.141	0	0.972	0.868	0.126	0.143	1.086	1.15	0.146	0.187	0.822	0.847	0.071	0.105
w5/1	0.143	0.126	0.868	0.972	0	0.141	1.086	1.222	0.105	0.071	0.847	0.822	0.187	0.146	1.15	1.086
w6/1	0.144	0.141	0.537	0.868	0.141	0	0.822	1.089	0.187	0.113	0.822	0.537	0.066	0.187	1.089	0.868
w7/-1	1.15	0.847	0.141	0.126	1.086	0.822	0	0.143	0.972	1.222	0.105	0.187	0.868	1.086	0.071	0.146
w8/-1	1.257	1.15	0.144	0.143	1.222	1.089	0.143	0	1.222	1.257	0.071	0.113	1.089	1.15	0.005	0.071
w9/1	0.071	0.146	0.868	1.086	0.105	0.187	0.972	1.222	0	0.143	1.086	0.822	0.141	0.126	1.15	0.847
w10/1	0.005	0.071	1.089	1.15	0.071	0.113	1.222	1.257	0.143	0	1.222	1.089	0.144	0.143	1.257	1.15
w11/-1	1.15	1.086	0.187	0.146	0.847	0.822	0.105	0.071	1.086	1.222	0	0.141	0.868	0.972	0.143	0.126
w12/-1	1.089	0.868	0.066	0.187	0.822	0.537	0.187	0.113	0.822	1.089	0.141	0	0.537	0.868	0.144	0.141
w13/1	0.113	0.187	0.537	0.822	0.187	0.066	0.868	1.089	0.141	0.144	0.868	0.537	0	0.141	1.089	0.822
w14/1	0.071	0.105	0.822	0.847	0.146	0.187	1.086	1.15	0.126	0.143	0.972	0.868	0.141	0	1.222	1.086
w15/-1	1.257	1.222	0.113	0.071	1.15	1.089	0.071	0.005	1.15	1.257	0.143	0.144	1.089	1.222	0	0.143
w16/-1	1.222	0.972	0.187	0.105	1.086	0.868	0.146	0.071	0.847	1.15	0.126	0.141	0.822	1.086	0.143	0

Table H.7. Normalized envelope distances of GMSK BT=0.5 for 3-sample metric with Gaussian filter BT=0.4.

	w1/1	w2/1	w3/-1	w4/-1	w5/1	w6/1	w7/-1	w8/-1	w9/1	w10/1	w11/-1	w12/-1	w13/1	w14/1	w15/-1	w16/-1
w1/1	0	0.105	0.997	1.086	0.105	0.102	0.957	1.022	0.053	0.005	0.957	0.997	0.063	0.053	1.022	1.086
w2/1	0.105	0	0.799	0.996	0.099	0.104	0.735	0.957	0.255	0.053	0.996	0.89	0.2	0.062	1.086	0.954
w3/-1	0.997	0.799	0	0.104	0.89	0.656	0.104	0.102	0.89	0.997	0.2	0.073	0.656	0.799	0.063	0.2
w4/-1	1.086	0.996	0.104	0	0.954	0.89	0.099	0.105	0.996	0.957	0.255	0.2	0.799	0.735	0.053	0.062
w5/1	0.105	0.099	0.89	0.954	0	0.104	0.996	1.086	0.062	0.053	0.735	0.799	0.2	0.255	0.957	0.996
w6/1	0.102	0.104	0.656	0.89	0.104	0	0.799	0.997	0.2	0.063	0.799	0.656	0.073	0.2	0.997	0.89
w7/-1	0.957	0.735	0.104	0.099	0.996	0.799	0	0.105	0.954	1.086	0.062	0.2	0.89	0.996	0.053	0.255
w8/-1	1.022	0.957	0.102	0.105	1.086	0.997	0.105	0	1.086	1.022	0.053	0.063	0.997	0.957	0.005	0.053
w9/1	0.053	0.255	0.89	0.996	0.062	0.2	0.954	1.086	0	0.105	0.996	0.799	0.104	0.099	0.957	0.735
w10/1	0.005	0.053	0.997	0.957	0.053	0.063	1.086	1.022	0.105	0	1.086	0.997	0.102	0.105	1.022	0.957
w11/-1	0.957	0.996	0.2	0.255	0.735	0.799	0.062	0.053	0.996	1.086	0	0.104	0.89	0.954	0.105	0.099
w12/-1	0.997	0.89	0.073	0.2	0.799	0.656	0.2	0.063	0.799	0.997	0.104	0	0.656	0.89	0.102	0.104
w13/1	0.063	0.2	0.656	0.799	0.2	0.073	0.89	0.997	0.104	0.102	0.89	0.656	0	0.104	0.997	0.799
w14/1	0.053	0.062	0.799	0.735	0.255	0.2	0.996	0.957	0.099	0.105	0.954	0.89	0.104	0	1.086	0.996
w15/-1	1.022	1.086	0.063	0.053	0.957	0.997	0.053	0.005	0.957	1.022	0.105	0.102	0.997	1.086	0	0.105
w16/-1	1.086	0.954	0.2	0.062	0.996	0.89	0.255	0.053	0.735	0.957	0.099	0.104	0.799	0.996	0.105	0

Table H.8. Normalized envelope distances of GMSK BT=0.5 for 3-sample metric with Gaussian filter BT=0.5

	w1/1	w2/1	w3/-1	w4/-1	w5/1	w6/1	w7/-1	w8/-1	w9/1	w10/1	w11/-1	w12/-1	w13/1	w14/1	w15/-1	w16/-1
w1/1	0	0.087	1.089	1.158	0.087	0.086	1.061	1.122	0.03	0.001	1.061	1.089	0.043	0.03	1.122	1.158
w2/1	0.087	0	0.932	1.088	0.084	0.087	0.895	1.061	0.193	0.03	1.088	0.986	0.162	0.043	1.158	1.047
w3/-1	1.089	0.932	0	0.087	0.986	0.795	0.087	0.086	0.986	1.089	0.162	0.085	0.795	0.932	0.043	0.162
w4/-1	1.158	1.088	0.087	0	1.047	0.986	0.084	0.087	1.088	1.061	0.193	0.162	0.932	0.895	0.03	0.043
w5/1	0.087	0.084	0.986	1.047	0	0.087	1.088	1.158	0.043	0.03	0.895	0.932	0.162	0.193	1.061	1.088
w6/1	0.086	0.087	0.795	0.986	0.087	0	0.932	1.089	0.162	0.043	0.932	0.795	0.085	0.162	1.089	0.986
w7/-1	1.061	0.895	0.087	0.084	1.088	0.932	0	0.087	1.047	1.158	0.043	0.162	0.986	1.088	0.03	0.193
w8/-1	1.122	1.061	0.086	0.087	1.158	1.089	0.087	0	1.158	1.122	0.03	0.043	1.089	1.061	0.001	0.03
w9/1	0.03	0.193	0.986	1.088	0.043	0.162	1.047	1.158	0	0.087	1.088	0.932	0.087	0.084	1.061	0.895
w10/1	0.001	0.03	1.089	1.061	0.03	0.043	1.158	1.122	0.087	0	1.158	1.089	0.086	0.087	1.122	1.061
w11/-1	1.061	1.088	0.162	0.193	0.895	0.932	0.043	0.03	1.088	1.158	0	0.087	0.986	1.047	0.087	0.084
w12/-1	1.089	0.986	0.085	0.162	0.932	0.795	0.162	0.043	0.932	1.089	0.087	0	0.795	0.986	0.086	0.087
w13/1	0.043	0.162	0.795	0.932	0.162	0.085	0.986	1.089	0.087	0.086	0.986	0.795	0	0.087	1.089	0.932
w14/1	0.03	0.043	0.932	0.895	0.193	0.162	1.088	1.061	0.084	0.087	1.047	0.986	0.087	0	1.158	1.088
w15/-1	1.122	1.158	0.043	0.03	1.061	1.089	0.03	0.001	1.061	1.122	0.087	0.086	1.089	1.158	0	0.087
w16/-1	1.158	1.047	0.162	0.043	1.088	0.986	0.193	0.03	0.895	1.061	0.084	0.087	0.932	1.088	0.087	0

Table H.9. Normalized envelope distances of GMSK BT=0.5 for 3-sample metric with Gaussian filter BT=0.6.

	w1/1	w2/1	w3/-1	w4/-1	w5/1	w6/1	w7/-1	w8/-1	w9/1	w10/1	w11/-1	w12/-1	w13/1	w14/1	w15/-1	w16/-1
w1/1	0	0.076	1.142	1.199	0.076	0.076	1.125	1.182	0.017	0	1.125	1.142	0.035	0.017	1.182	1.199
w2/1	0.076	0	1.009	1.142	0.075	0.076	0.992	1.125	0.148	0.017	1.142	1.043	0.133	0.035	1.199	1.101
w3/-1	1.142	1.009	0	0.076	1.043	0.876	0.076	0.076	1.043	1.142	0.133	0.081	0.876	1.009	0.035	0.133
w4/-1	1.199	1.142	0.076	0	1.101	1.043	0.075	0.076	1.142	1.125	0.148	0.133	1.009	0.992	0.017	0.035
w5/1	0.076	0.075	1.043	1.101	0	0.076	1.142	1.199	0.035	0.017	0.992	1.009	0.133	0.148	1.125	1.142
w6/1	0.076	0.076	0.876	1.043	0.076	0	1.009	1.142	0.133	0.035	1.009	0.876	0.081	0.133	1.142	1.043
w7/-1	1.125	0.992	0.076	0.075	1.142	1.009	0	0.076	1.101	1.199	0.035	0.133	1.043	1.142	0.017	0.148
w8/-1	1.182	1.125	0.076	0.076	1.199	1.142	0.076	0	1.199	1.182	0.017	0.035	1.142	1.125	0	0.017
w9/1	0.017	0.148	1.043	1.142	0.035	0.133	1.101	1.199	0	0.076	1.142	1.009	0.076	0.075	1.125	0.992
w10/1	0	0.017	1.142	1.125	0.017	0.035	1.199	1.182	0.076	0	1.199	1.142	0.076	0.076	1.182	1.125
w11/-1	1.125	1.142	0.133	0.148	0.992	1.009	0.035	0.017	1.142	1.199	0	0.076	1.043	1.101	0.076	0.075
w12/-1	1.142	1.043	0.081	0.133	1.009	0.876	0.133	0.035	1.009	1.142	0.076	0	0.876	1.043	0.076	0.076
w13/1	0.035	0.133	0.876	1.009	0.133	0.081	1.043	1.142	0.076	0.076	1.043	0.876	0	0.076	1.142	1.009
w14/1	0.017	0.035	1.009	0.992	0.148	0.133	1.142	1.125	0.075	0.076	1.101	1.043	0.076	0	1.199	1.142
w15/-1	1.182	1.199	0.035	0.017	1.125	1.142	0.017	0	1.125	1.182	0.076	0.076	1.142	1.199	0	0.076
w16/-1	1.199	1.101	0.133	0.035	1.142	1.043	0.148	0.017	0.992	1.125	0.075	0.076	1.009	1.142	0.076	0

Table H.10. Normalized envelope distances of GMSK BT=0.5 for 3-sample metric with maximally flat filter BT=0.4.

	w1/1	w2/1	w3/-1	w4/-1	w5/1	w6/1	w7/-1	w8/-1	w9/1	w10/1	w11/-1	w12/-1	w13/1	w14/1	w15/-1	w16/-1
w1/1	0	0.109	1.006	1.102	0.109	0.107	0.957	1.033	0.065	0.002	0.957	1.006	0.055	0.065	1.033	1.102
w2/1	0.109	0	0.798	1.005	0.104	0.108	0.726	0.957	0.291	0.065	1.005	0.892	0.228	0.054	1.102	0.968
w3/-1	1.006	0.798	0	0.108	0.892	0.653	0.108	0.107	0.892	1.006	0.228	0.107	0.653	0.798	0.055	0.228
w4/-1	1.102	1.005	0.108	0	0.968	0.892	0.104	0.109	1.005	0.957	0.291	0.228	0.798	0.726	0.065	0.054
w5/1	0.109	0.104	0.892	0.968	0	0.108	1.005	1.102	0.054	0.065	0.726	0.798	0.228	0.291	0.957	1.005
w6/1	0.107	0.108	0.653	0.892	0.108	0	0.798	1.006	0.228	0.055	0.798	0.653	0.107	0.228	1.006	0.892
w7/-1	0.957	0.726	0.108	0.104	1.005	0.798	0	0.109	0.968	1.102	0.054	0.228	0.892	1.005	0.065	0.291
w8/-1	1.033	0.957	0.107	0.109	1.102	1.006	0.109	0	1.102	1.033	0.065	0.055	1.006	0.957	0.002	0.065
w9/1	0.065	0.291	0.892	1.005	0.054	0.228	0.968	1.102	0	0.109	1.005	0.798	0.108	0.104	0.957	0.726
w10/1	0.002	0.065	1.006	0.957	0.065	0.055	1.102	1.033	0.109	0	1.102	1.006	0.107	0.109	1.033	0.957
w11/-1	0.957	1.005	0.228	0.291	0.726	0.798	0.054	0.065	1.005	1.102	0	0.108	0.892	0.968	0.109	0.104
w12/-1	1.006	0.892	0.107	0.228	0.798	0.653	0.228	0.055	0.798	1.006	0.108	0	0.653	0.892	0.107	0.108
w13/1	0.055	0.228	0.653	0.798	0.228	0.107	0.892	1.006	0.108	0.107	0.892	0.653	0	0.108	1.006	0.798
w14/1	0.065	0.054	0.798	0.726	0.291	0.228	1.005	0.957	0.104	0.109	0.968	0.892	0.108	0	1.102	1.005
w15/-1	1.033	1.102	0.055	0.065	0.957	1.006	0.065	0.002	0.957	1.033	0.109	0.107	1.006	1.102	0	0.109
w16/-1	1.102	0.968	0.228	0.054	1.005	0.892	0.291	0.065	0.726	0.957	0.104	0.108	0.798	1.005	0.109	0

Table H.11. Normalized envelope distances of GMSK BT=0.5 for 3-sample metric with maximally flat filter BT=0.5

	w1/1	w2/1	w3/-1	w4/-1	w5/1	w6/1	w7/-1	w8/-1	w9/1	w10/1	w11/-1	w12/-1	w13/1	w14/1	w15/-1	w16/-1
w1/1	0	0.049	1.194	1.214	0.049	0.048	1.145	1.168	0.06	0.006	1.145	1.194	0.082	0.06	1.168	1.214
w2/1	0.049	0	1.125	1.194	0.048	0.049	1.076	1.145	0.223	0.06	1.194	1.145	0.203	0.082	1.214	1.168
w3/-1	1.194	1.125	0	0.049	1.145	1.076	0.049	0.048	1.145	1.194	0.203	0.269	1.076	1.125	0.082	0.203
w4/-1	1.214	1.194	0.049	0	1.168	1.145	0.048	0.049	1.194	1.145	0.223	0.203	1.125	1.076	0.06	0.082
w5/1	0.049	0.048	1.145	1.168	0	0.049	1.194	1.214	0.082	0.06	1.076	1.125	0.203	0.223	1.145	1.194
w6/1	0.048	0.049	1.076	1.145	0.049	0	1.125	1.194	0.203	0.082	1.125	1.076	0.269	0.203	1.194	1.145
w7/-1	1.145	1.076	0.049	0.048	1.194	1.125	0	0.049	1.168	1.214	0.082	0.203	1.145	1.194	0.06	0.223
w8/-1	1.168	1.145	0.048	0.049	1.214	1.194	0.049	0	1.214	1.168	0.06	0.082	1.194	1.145	0.006	0.06
w9/1	0.06	0.223	1.145	1.194	0.082	0.203	1.168	1.214	0	0.049	1.194	1.125	0.049	0.048	1.145	1.076
w10/1	0.006	0.06	1.194	1.145	0.06	0.082	1.214	1.168	0.049	0	1.214	1.194	0.048	0.049	1.168	1.145
w11/-1	1.145	1.194	0.203	0.223	1.076	1.125	0.082	0.06	1.194	1.214	0	0.049	1.145	1.168	0.049	0.048
w12/-1	1.194	1.145	0.269	0.203	1.125	1.076	0.203	0.082	1.125	1.194	0.049	0	1.076	1.145	0.048	0.049
w13/1	0.082	0.203	1.076	1.125	0.203	0.269	1.145	1.194	0.049	0.048	1.145	1.076	0	0.049	1.194	1.125
w14/1	0.06	0.082	1.125	1.076	0.223	0.203	1.194	1.145	0.048	0.049	1.168	1.145	0.049	0	1.214	1.194
w15/-1	1.168	1.214	0.082	0.06	1.145	1.194	0.06	0.006	1.145	1.168	0.049	0.048	1.194	1.214	0	0.049
w16/-1	1.214	1.168	0.203	0.082	1.194	1.145	0.223	0.06	1.076	1.145	0.048	0.049	1.125	1.194	0.049	0

Table H.12. Normalized envelope distances of GMSK BT=0.5 for 3-sample metric with maximally flat filter BT=0.6.

	w1/1	w2/1	w3/-1	w4/-1	w5/1	w6/1	w7/-1	w8/-1	w9/1	w10/1	w11/-1	w12/-1	w13/1	w14/1	w15/-1	w16/-1
w1/1	0	0.033	1.299	1.296	0.033	0.032	1.265	1.264	0.058	0.003	1.265	1.299	0.121	0.058	1.264	1.296
w2/1	0.033	0	1.267	1.299	0.032	0.033	1.234	1.265	0.184	0.058	1.299	1.265	0.216	0.121	1.296	1.264
w3/-1	1.299	1.267	0	0.033	1.265	1.234	0.033	0.032	1.265	1.299	0.216	0.311	1.234	1.267	0.121	0.216
w4/-1	1.296	1.299	0.033	0	1.264	1.265	0.032	0.033	1.299	1.265	0.184	0.216	1.267	1.234	0.058	0.121
w5/1	0.033	0.032	1.265	1.264	0	0.033	1.299	1.296	0.121	0.058	1.234	1.267	0.216	0.184	1.265	1.299
w6/1	0.032	0.033	1.234	1.265	0.033	0	1.267	1.299	0.216	0.121	1.267	1.234	0.311	0.216	1.299	1.265
w7/-1	1.265	1.234	0.033	0.032	1.299	1.267	0	0.033	1.264	1.296	0.121	0.216	1.265	1.299	0.058	0.184
w8/-1	1.264	1.265	0.032	0.033	1.296	1.299	0.033	0	1.296	1.264	0.058	0.121	1.299	1.265	0.003	0.058
w9/1	0.058	0.184	1.265	1.299	0.121	0.216	1.264	1.296	0	0.033	1.299	1.267	0.033	0.032	1.265	1.234
w10/1	0.003	0.058	1.299	1.265	0.058	0.121	1.296	1.264	0.033	0	1.296	1.299	0.032	0.033	1.264	1.265
w11/-1	1.265	1.299	0.216	0.184	1.234	1.267	0.121	0.058	1.299	1.296	0	0.033	1.265	1.264	0.033	0.032
w12/-1	1.299	1.265	0.311	0.216	1.267	1.234	0.216	0.121	1.267	1.299	0.033	0	1.234	1.265	0.032	0.033
w13/1	0.121	0.216	1.234	1.267	0.216	0.311	1.265	1.299	0.033	0.032	1.265	1.234	0	0.033	1.299	1.267
w14/1	0.058	0.121	1.267	1.234	0.184	0.216	1.299	1.265	0.032	0.033	1.264	1.265	0.033	0	1.296	1.299
w15/-1	1.264	1.296	0.121	0.058	1.265	1.299	0.058	0.003	1.265	1.264	0.033	0.032	1.299	1.296	0	0.033
w16/-1	1.296	1.264	0.216	0.121	1.299	1.265	0.184	0.058	1.234	1.265	0.032	0.033	1.267	1.299	0.033	0

Table H.13. Normalized envelope distances of MSK for 3-sample metric with Gaussian filter BT=0.4.

	w1/1	w2/1	w3/-1	w4/-1	w5/1	w6/1	w7/-1	w8/-1	w9/1	w10/1	w11/-1	w12/-1	w13/1	w14/1	w15/-1	w16/-1
w1/1	0	0.064	1.034	1.081	0.064	0.063	0.97	1.017	0.048	0	0.97	1.034	0.001	0.048	1.017	1.081
w2/1	0.064	0	0.921	1.034	0.063	0.064	0.857	0.97	0.224	0.048	1.034	0.97	0.176	0.001	1.081	1.017
w3/-1	1.034	0.921	0	0.064	0.97	0.857	0.064	0.063	0.97	1.034	0.176	0.128	0.857	0.921	0.001	0.176
w4/-1	1.081	1.034	0.064	0	1.017	0.97	0.063	0.064	1.034	0.97	0.224	0.176	0.921	0.857	0.048	0.001
w5/1	0.064	0.063	0.97	1.017	0	0.064	1.034	1.081	0.001	0.048	0.857	0.921	0.176	0.224	0.97	1.034
w6/1	0.063	0.064	0.857	0.97	0.064	0	0.921	1.034	0.176	0.001	0.921	0.857	0.128	0.176	1.034	0.97
w7/-1	0.97	0.857	0.064	0.063	1.034	0.921	0	0.064	1.017	1.081	0.001	0.176	0.97	1.034	0.048	0.224
w8/-1	1.017	0.97	0.063	0.064	1.081	1.034	0.064	0	1.081	1.017	0.048	0.001	1.034	0.97	0	0.048
w9/1	0.048	0.224	0.97	1.034	0.001	0.176	1.017	1.081	0	0.064	1.034	0.921	0.064	0.063	0.97	0.857
w10/1	0	0.048	1.034	0.97	0.048	0.001	1.081	1.017	0.064	0	1.081	1.034	0.063	0.064	1.017	0.97
w11/-1	0.97	1.034	0.176	0.224	0.857	0.921	0.001	0.048	1.034	1.081	0	0.064	0.97	1.017	0.064	0.063
w12/-1	1.034	0.97	0.128	0.176	0.921	0.857	0.176	0.001	0.921	1.034	0.064	0	0.857	0.97	0.063	0.064
w13/1	0.001	0.176	0.857	0.921	0.176	0.128	0.97	1.034	0.064	0.063	0.97	0.857	0	0.064	1.034	0.921
w14/1	0.048	0.001	0.921	0.857	0.224	0.176	1.034	0.97	0.063	0.064	1.017	0.97	0.064	0	1.081	1.034
w15/-1	1.017	1.081	0.001	0.048	0.97	1.034	0.048	0	0.97	1.017	0.064	0.063	1.034	1.081	0	0.064
w16/-1	1.081	1.017	0.176	0.001	1.034	0.97	0.224	0.048	0.857	0.97	0.063	0.064	0.921	1.034	0.064	0

Table H.14. Normalized envelope distances of MSK for 3-sample metric with Gaussian filter BT=0.5

	w1/1	w2/1	w3/-1	w4/-1	w5/1	w6/1	w7/-1	w8/-1	w9/1	w10/1	w11/-1	w12/-1	w13/1	w14/1	w15/-1	w16/-1
w1/1	0	0.043	1.137	1.165	0.043	0.043	1.093	1.121	0.038	0	1.093	1.137	0.022	0.038	1.121	1.165
w2/1	0.043	0	1.066	1.137	0.043	0.043	1.022	1.093	0.164	0.038	1.137	1.093	0.137	0.022	1.165	1.121
w3/-1	1.137	1.066	0	0.043	1.093	1.022	0.043	0.043	1.093	1.137	0.137	0.131	1.022	1.066	0.022	0.137
w4/-1	1.165	1.137	0.043	0	1.121	1.093	0.043	0.043	1.137	1.093	0.164	0.137	1.066	1.022	0.038	0.022
w5/1	0.043	0.043	1.093	1.121	0	0.043	1.137	1.165	0.022	0.038	1.022	1.066	0.137	0.164	1.093	1.137
w6/1	0.043	0.043	1.022	1.093	0.043	0	1.066	1.137	0.137	0.022	1.066	1.022	0.131	0.137	1.137	1.093
w7/-1	1.093	1.022	0.043	0.043	1.137	1.066	0	0.043	1.121	1.165	0.022	0.137	1.093	1.137	0.038	0.164
w8/-1	1.121	1.093	0.043	0.043	1.165	1.137	0.043	0	1.165	1.121	0.038	0.022	1.137	1.093	0	0.038
w9/1	0.038	0.164	1.093	1.137	0.022	0.137	1.121	1.165	0	0.043	1.137	1.066	0.043	0.043	1.093	1.022
w10/1	0	0.038	1.137	1.093	0.038	0.022	1.165	1.121	0.043	0	1.165	1.137	0.043	0.043	1.121	1.093
w11/-1	1.093	1.137	0.137	0.164	1.022	1.066	0.022	0.038	1.137	1.165	0	0.043	1.093	1.121	0.043	0.043
w12/-1	1.137	1.093	0.131	0.137	1.066	1.022	0.137	0.022	1.066	1.137	0.043	0	1.022	1.093	0.043	0.043
w13/1	0.022	0.137	1.022	1.066	0.137	0.131	1.093	1.137	0.043	0.043	1.093	1.022	0	0.043	1.137	1.066
w14/1	0.038	0.022	1.066	1.022	0.164	0.137	1.137	1.093	0.043	0.043	1.121	1.093	0.043	0	1.165	1.137
w15/-1	1.121	1.165	0.022	0.038	1.093	1.137	0.038	0	1.093	1.121	0.043	0.043	1.137	1.165	0	0.043
w16/-1	1.165	1.121	0.137	0.022	1.137	1.093	0.164	0.038	1.022	1.093	0.043	0.043	1.066	1.137	0.043	0

Table H.15. Normalized envelope distances of MSK for 3-sample metric with Gaussian filter BT=0.6.

	w1/1	w2/1	w3/-1	w4/-1	w5/1	w6/1	w7/-1	w8/-1	w9/1	w10/1	w11/-1	w12/-1	w13/1	w14/1	w15/-1	w16/-1
w1/1	0	0.031	1.196	1.213	0.031	0.031	1.164	1.182	0.029	0	1.164	1.196	0.024	0.029	1.182	1.213
w2/1	0.031	0	1.147	1.196	0.031	0.031	1.115	1.164	0.123	0.029	1.196	1.164	0.105	0.024	1.213	1.182
w3/-1	1.196	1.147	0	0.031	1.164	1.115	0.031	0.031	1.164	1.196	0.105	0.113	1.115	1.147	0.024	0.105
w4/-1	1.213	1.196	0.031	0	1.182	1.164	0.031	0.031	1.196	1.164	0.123	0.105	1.147	1.115	0.029	0.024
w5/1	0.031	0.031	1.164	1.182	0	0.031	1.196	1.213	0.024	0.029	1.115	1.147	0.105	0.123	1.164	1.196
w6/1	0.031	0.031	1.115	1.164	0.031	0	1.147	1.196	0.105	0.024	1.147	1.115	0.113	0.105	1.196	1.164
w7/-1	1.164	1.115	0.031	0.031	1.196	1.147	0	0.031	1.182	1.213	0.024	0.105	1.164	1.196	0.029	0.123
w8/-1	1.182	1.164	0.031	0.031	1.213	1.196	0.031	0	1.213	1.182	0.029	0.024	1.196	1.164	0	0.029
w9/1	0.029	0.123	1.164	1.196	0.024	0.105	1.182	1.213	0	0.031	1.196	1.147	0.031	0.031	1.164	1.115
w10/1	0	0.029	1.196	1.164	0.029	0.024	1.213	1.182	0.031	0	1.213	1.196	0.031	0.031	1.182	1.164
w11/-1	1.164	1.196	0.105	0.123	1.115	1.147	0.024	0.029	1.196	1.213	0	0.031	1.164	1.182	0.031	0.031
w12/-1	1.196	1.164	0.113	0.105	1.147	1.115	0.105	0.024	1.147	1.196	0.031	0	1.115	1.164	0.031	0.031
w13/1	0.024	0.105	1.115	1.147	0.105	0.113	1.164	1.196	0.031	0.031	1.164	1.115	0	0.031	1.196	1.147
w14/1	0.029	0.024	1.147	1.115	0.123	0.105	1.196	1.164	0.031	0.031	1.182	1.164	0.031	0	1.213	1.196
w15/-1	1.182	1.213	0.024	0.029	1.164	1.196	0.029	0	1.164	1.182	0.031	0.031	1.196	1.213	0	0.031
w16/-1	1.213	1.182	0.105	0.024	1.196	1.164	0.123	0.029	1.115	1.164	0.031	0.031	1.147	1.196	0.031	0

Table H.16. Normalized envelope distances of MSK for 3-sample metric with maximally flat filter BT=0.4.

	w1/1	w2/1	w3/-1	w4/-1	w5/1	w6/1	w7/-1	w8/-1	w9/1	w10/1	w11/-1	w12/-1	w13/1	w14/1	w15/-1	w16/-1
w1/1	0	0.07	1.05	1.099	0.07	0.07	0.98	1.032	0.061	0.006	0.98	1.05	0.024	0.061	1.032	1.099
w2/1	0.07	0	0.93	1.05	0.07	0.07	0.86	0.98	0.266	0.061	1.05	0.98	0.217	0.024	1.099	1.032
w3/-1	1.05	0.93	0	0.07	0.98	0.86	0.07	0.07	0.98	1.05	0.217	0.194	0.86	0.93	0.024	0.217
w4/-1	1.099	1.05	0.07	0	1.032	0.98	0.07	0.07	1.05	0.98	0.266	0.217	0.93	0.86	0.061	0.024
w5/1	0.07	0.07	0.98	1.032	0	0.07	1.05	1.099	0.024	0.061	0.86	0.93	0.217	0.266	0.98	1.05
w6/1	0.07	0.07	0.86	0.98	0.07	0	0.93	1.05	0.217	0.024	0.93	0.86	0.194	0.217	1.05	0.98
w7/-1	0.98	0.86	0.07	0.07	1.05	0.93	0	0.07	1.032	1.099	0.024	0.217	0.98	1.05	0.061	0.266
w8/-1	1.032	0.98	0.07	0.07	1.099	1.05	0.07	0	1.099	1.032	0.061	0.024	1.05	0.98	0.006	0.061
w9/1	0.061	0.266	0.98	1.05	0.024	0.217	1.032	1.099	0	0.07	1.05	0.93	0.07	0.07	0.98	0.86
w10/1	0.006	0.061	1.05	0.98	0.061	0.024	1.099	1.032	0.07	0	1.099	1.05	0.07	0.07	1.032	0.98
w11/-1	0.98	1.05	0.217	0.266	0.86	0.93	0.024	0.061	1.05	1.099	0	0.07	0.98	1.032	0.07	0.07
w12/-1	1.05	0.98	0.194	0.217	0.93	0.86	0.217	0.024	0.93	1.05	0.07	0	0.86	0.98	0.07	0.07
w13/1	0.024	0.217	0.86	0.93	0.217	0.194	0.98	1.05	0.07	0.07	0.98	0.86	0	0.07	1.05	0.93
w14/1	0.061	0.024	0.93	0.86	0.266	0.217	1.05	0.98	0.07	0.07	1.032	0.98	0.07	0	1.099	1.05
w15/-1	1.032	1.099	0.024	0.061	0.98	1.05	0.061	0.006	0.98	1.032	0.07	0.07	1.05	1.099	0	0.07
w16/-1	1.099	1.032	0.217	0.024	1.05	0.98	0.266	0.061	0.86	0.98	0.07	0.07	0.93	1.05	0.07	0

Table H.17. Normalized envelope distances of MSK for 3-sample metric with maximally flat filter BT=0.5

	w1/1	w2/1	w3/-1	w4/-1	w5/1	w6/1	w7/-1	w8/-1	w9/1	w10/1	w11/-1	w12/-1	w13/1	w14/1	w15/-1	w16/-1
w1/1	0	0.049	1.194	1.214	0.049	0.048	1.145	1.168	0.06	0.006	1.145	1.194	0.082	0.06	1.168	1.214
w2/1	0.049	0	1.125	1.194	0.048	0.049	1.076	1.145	0.223	0.06	1.194	1.145	0.203	0.082	1.214	1.168
w3/-1	1.194	1.125	0	0.049	1.145	1.076	0.049	0.048	1.145	1.194	0.203	0.269	1.076	1.125	0.082	0.203
w4/-1	1.214	1.194	0.049	0	1.168	1.145	0.048	0.049	1.194	1.145	0.223	0.203	1.125	1.076	0.06	0.082
w5/1	0.049	0.048	1.145	1.168	0	0.049	1.194	1.214	0.082	0.06	1.076	1.125	0.203	0.223	1.145	1.194
w6/1	0.048	0.049	1.076	1.145	0.049	0	1.125	1.194	0.203	0.082	1.125	1.076	0.269	0.203	1.194	1.145
w7/-1	1.145	1.076	0.049	0.048	1.194	1.125	0	0.049	1.168	1.214	0.082	0.203	1.145	1.194	0.06	0.223
w8/-1	1.168	1.145	0.048	0.049	1.214	1.194	0.049	0	1.214	1.168	0.06	0.082	1.194	1.145	0.006	0.06
w9/1	0.06	0.223	1.145	1.194	0.082	0.203	1.168	1.214	0	0.049	1.194	1.125	0.049	0.048	1.145	1.076
w10/1	0.006	0.06	1.194	1.145	0.06	0.082	1.214	1.168	0.049	0	1.214	1.194	0.048	0.049	1.168	1.145
w11/-1	1.145	1.194	0.203	0.223	1.076	1.125	0.082	0.06	1.194	1.214	0	0.049	1.145	1.168	0.049	0.048
w12/-1	1.194	1.145	0.269	0.203	1.125	1.076	0.203	0.082	1.125	1.194	0.049	0	1.076	1.145	0.048	0.049
w13/1	0.082	0.203	1.076	1.125	0.203	0.269	1.145	1.194	0.049	0.048	1.145	1.076	0	0.049	1.194	1.125
w14/1	0.06	0.082	1.125	1.076	0.223	0.203	1.194	1.145	0.048	0.049	1.168	1.145	0.049	0	1.214	1.194
w15/-1	1.168	1.214	0.082	0.06	1.145	1.194	0.06	0.006	1.145	1.168	0.049	0.048	1.194	1.214	0	0.049
w16/-1	1.214	1.168	0.203	0.082	1.194	1.145	0.223	0.06	1.076	1.145	0.048	0.049	1.125	1.194	0.049	0

Table H.18. Normalized envelope distances of MSK for 3-sample metric with maximally flat filter BT=0.6.

	w1/1	w2/1	w3/-1	w4/-1	w5/1	w6/1	w7/-1	w8/-1	w9/1	w10/1	w11/-1	w12/-1	w13/1	w14/1	w15/-1	w16/-1
w1/1	0	0.033	1.299	1.296	0.033	0.032	1.265	1.264	0.058	0.003	1.265	1.299	0.121	0.058	1.264	1.296
w2/1	0.033	0	1.267	1.299	0.032	0.033	1.234	1.265	0.184	0.058	1.299	1.265	0.216	0.121	1.296	1.264
w3/-1	1.299	1.267	0	0.033	1.265	1.234	0.033	0.032	1.265	1.299	0.216	0.311	1.234	1.267	0.121	0.216
w4/-1	1.296	1.299	0.033	0	1.264	1.265	0.032	0.033	1.299	1.265	0.184	0.216	1.267	1.234	0.058	0.121
w5/1	0.033	0.032	1.265	1.264	0	0.033	1.299	1.296	0.121	0.058	1.234	1.267	0.216	0.184	1.265	1.299
w6/1	0.032	0.033	1.234	1.265	0.033	0	1.267	1.299	0.216	0.121	1.267	1.234	0.311	0.216	1.299	1.265
w7/-1	1.265	1.234	0.033	0.032	1.299	1.267	0	0.033	1.264	1.296	0.121	0.216	1.265	1.299	0.058	0.184
w8/-1	1.264	1.265	0.032	0.033	1.296	1.299	0.033	0	1.296	1.264	0.058	0.121	1.299	1.265	0.003	0.058
w9/1	0.058	0.184	1.265	1.299	0.121	0.216	1.264	1.296	0	0.033	1.299	1.267	0.033	0.032	1.265	1.234
w10/1	0.003	0.058	1.299	1.265	0.058	0.121	1.296	1.264	0.033	0	1.296	1.299	0.032	0.033	1.264	1.265
w11/-1	1.265	1.299	0.216	0.184	1.234	1.267	0.121	0.058	1.299	1.296	0	0.033	1.265	1.264	0.033	0.032
w12/-1	1.299	1.265	0.311	0.216	1.267	1.234	0.216	0.121	1.267	1.299	0.033	0	1.234	1.265	0.032	0.033
w13/1	0.121	0.216	1.234	1.267	0.216	0.311	1.265	1.299	0.033	0.032	1.265	1.234	0	0.033	1.299	1.267
w14/1	0.058	0.121	1.267	1.234	0.184	0.216	1.299	1.265	0.032	0.033	1.264	1.265	0.033	0	1.296	1.299
w15/-1	1.264	1.296	0.121	0.058	1.265	1.299	0.058	0.003	1.265	1.264	0.033	0.032	1.299	1.296	0	0.033
w16/-1	1.296	1.264	0.216	0.121	1.299	1.265	0.184	0.058	1.234	1.265	0.032	0.033	1.267	1.299	0.033	0

APPENDIX I

Table I.1. Envelope distance of GMSK BT=0.3 for the selected waveforms by RW-ICIC.

Complex Envelope Waveform/Symbol	$w_{4i} + jw_{4q}$ (w2/+1)	$w_{2i} + jw_{2q}$ (w6/+1)	$w_{1i} + jw_{1q}$ (w4/-1)	$w_{3i} + jw_{3q}$ (w8/-1)
$w_{4i} + jw_{4q}$ (w2/+1)	0	0.157	0.915	0.946
$w_{2i} + jw_{2q}$ (w6/+1)	0.157	0	0.716	0.922
$w_{1i} + jw_{1q}$ (w4/-1)	0.915	0.716	0	0.164
$w_{3i} + jw_{3q}$ (w8/-1)	0.946	0.922	0.13	0

Table I.2. Envelope distance of GMSK BT=0.3 for the selected waveforms by RW-ICICI.

Complex Envelope (Waveform/Symbol)	$w_{3i} - jw_{3q}$ (w1/+1)	$w_{1i} - jw_{1q}$ (w5/+1)	$w_{2i} - jw_{2q}$ (w3/-1)	$w_{4i} - jw_{4q}$ (w7/-1)
$w_{3i} - jw_{3q}$ (w1/+1)	0	0.164	0.922	0.946
$w_{1i} - jw_{1q}$ (w5/+1)	0.164	0	0.716	0.915
$w_{2i} - jw_{2q}$ (w3/-1)	0.922	0.716	0	0.157
$w_{4i} - jw_{4q}$ (w7/-1)	0.946	0.915	0.157	0

Table I.3. Envelope distance of GMSK BT=0.3 for the selected waveforms by RW-ICIC.

Complex Envelope (Waveform/Symbol)	$-w_{3i}+jw_{3q}$ (w10/+1)	$-w_{1i}+jw_{1q}$ (w14/+1)	$-w_{2i}+jw_{2q}$ (w12/-1)	$-w_{4i}+jw_{4q}$ (w16/-1)
$-w_{3i}+jw_{3q}$ (w10/+1)	0	0.164	0.922	0.946
$-w_{1i}+jw_{1q}$ (w14/+1)	0.164	0	0.716	0.915
$-w_{2i}+jw_{2q}$ (w12/-1)	0.922	0.716	0	0.157
$-w_{4i}+jw_{4q}$ (w16/-1)	0.946	0.915	0.13	0

Table I.4. Envelope distance of GMSK BT=0.3 for the selected waveforms by RW-ICIC.

Complex Envelope (Waveform/Symbol)	$-w_{2i}-jw_{2q}$ (w9/+1)	$-w_{4i}-jw_{4q}$ (w13/+1)	$-w_{1i}-jw_{1q}$ (w11/-1)	$-w_{3i}-jw_{3q}$ (w15/-1)
$-w_{2i}-jw_{2q}$ (w9/+1)	0	0.157	0.915	0.946
$-w_{4i}-jw_{4q}$ (w13/+1)	0.157	0	0.716	0.922
$-w_{1i}-jw_{1q}$ (w11/-1)	0.915	0.716	0	0.164
$-w_{3i}-jw_{3q}$ (w15/-1)	0.946	0.922	0.164	0

APPENDIX J

Table J.1. Correlation coefficients between L_{ij} in E_b/N_0=10dB.

Lij	L1,1	L1,2	L1,3	L1,4	L1,5	L1,6	L1,7	L1,8	L1,9	L1,10	L1,11	L1,12	L1,13	L1,14	L1,15	L1,16
L1,1	1	0.063	0.018	0.02	0.071	0.179	0.016	0.02	0.133	0.138	0.006	0.009	0.123	0.135	0.01	0.01
L1,2	0.063	1	0.141	0	0.046	0.55	0.129	0.029	0.02	0.09	0.123	0.323	0.014	0.038	0.135	0.35
L1,3	0.018	0.141	1	0.959	0.327	0.229	0.936	0.89	0.152	0.191	0.044	0.048	0.056	0.08	0.081	0.026
L1,4	0.02	0	0.959	1	0.347	0.177	0.889	0.928	0.151	0.185	0.017	0.026	0.063	0.086	0.024	0.006
L1,5	0.071	0.046	0.327	0.347	1	0.555	0.127	0.131	0.02	0.07	0.142	0.156	0.015	0.017	0.022	0.01
L1,6	0.179	0.55	0.229	0.177	0.555	1	0.135	0.071	0.043	0.106	0.151	0.245	0.023	0.054	0.086	0.193
L1,7	0.016	0.129	0.936	0.889	0.127	0.135	1	0.951	0.192	0.187	0.126	0.051	0.122	0.11	0.07	0.01
L1,8	0.02	0.029	0.89	0.928	0.131	0.071	0.951	1	0.2	0.189	0.07	0.085	0.136	0.124	0.011	0.029
L1,9	0.133	0.02	0.152	0.151	0.02	0.043	0.192	0.2	1	0.918	0.047	0.022	0.92	0.894	0.068	0.036
L1,10	0.138	0.09	0.191	0.185	0.07	0.106	0.187	0.189	0.918	1	0.125	0.138	0.797	0.918	0.134	0.142
L1,11	0.006	0.123	0.044	0.017	0.142	0.151	0.126	0.07	0.047	0.125	1	0.935	0.066	0.138	0.949	0.887
L1,12	0.009	0.323	0.048	0.026	0.156	0.245	0.051	0.085	0.022	0.138	0.935	1	0.005	0.108	0.889	0.959
L1,13	0.123	0.014	0.056	0.063	0.015	0.023	0.122	0.136	0.92	0.797	0.066	0.005	1	0.92	0.082	0.015
L1,14	0.135	0.038	0.08	0.086	0.017	0.054	0.11	0.124	0.894	0.918	0.138	0.108	0.92	1	0.148	0.111
L1,15	0.01	0.135	0.081	0.024	0.022	0.086	0.07	0.011	0.068	0.134	0.949	0.889	0.082	0.148	1	0.928
L1,16	0.01	0.35	0.026	0.006	0.01	0.193	0.01	0.029	0.036	0.142	0.887	0.959	0.015	0.111	0.928	1

Lij	L2,1	L2,2	L2,3	L2,4	L2,5	L2,6	L2,7	L2,8	L2,9	L2,10	L2,11	L2,12	L2,13	L2,14	L2,15	L2,16
L2,1	1	0.057	0.326	0.224	0.49	0.113	0.336	0.214	0.203	0.069	0.128	0.072	0.217	0.106	0.143	0.083
L2,2	0.057	1	0.01	0.009	0.171	0.05	0.01	0.009	0.072	0.121	0.015	0.014	0.067	0.112	0.017	0.019
L2,3	0.326	0.01	1	0.945	0.027	0.294	0.943	0.863	0.383	0.075	0.129	0.008	0.389	0.021	0.183	0.037
L2,4	0.224	0.009	0.945	1	0.012	0.332	0.903	0.937	0.342	0.101	0.022	0.046	0.332	0.018	0.071	0.002
L2,5	0.49	0.171	0.027	0.012	1	0.475	0.119	0.083	0.165	0.096	0.158	0.094	0.162	0.062	0.103	0.009
L2,6	0.113	0.05	0.294	0.332	0.475	1	0.126	0.14	0.024	0.022	0.139	0.146	0.027	0.03	0.007	0.055
L2,7	0.336	0.01	0.943	0.903	0.119	0.126	1	0.934	0.403	0.106	0.214	0.07	0.425	0.035	0.191	0.022
L2,8	0.214	0.009	0.863	0.937	0.083	0.14	0.934	1	0.353	0.132	0.094	0.029	0.359	0.079	0.059	0.025
L2,9	0.203	0.072	0.383	0.342	0.165	0.024	0.403	0.353	1	0.639	0.553	0.468	0.951	0.62	0.559	0.466
L2,10	0.069	0.121	0.075	0.101	0.096	0.022	0.106	0.132	0.639	1	0.086	0.077	0.59	0.923	0.098	0.096
L2,11	0.128	0.015	0.129	0.022	0.158	0.139	0.214	0.094	0.553	0.086	1	0.929	0.592	0.107	0.957	0.872
L2,12	0.072	0.014	0.008	0.046	0.094	0.146	0.07	0.029	0.468	0.077	0.929	1	0.508	0.099	0.875	0.937
L2,13	0.217	0.067	0.389	0.332	0.162	0.027	0.425	0.359	0.951	0.59	0.592	0.508	1	0.654	0.567	0.465
L2,14	0.106	0.112	0.021	0.018	0.062	0.03	0.035	0.079	0.62	0.923	0.107	0.099	0.654	1	0.122	0.12
L2,15	0.143	0.017	0.183	0.071	0.103	0.007	0.191	0.059	0.559	0.098	0.957	0.875	0.567	0.122	1	0.915
L2,16	0.083	0.019	0.037	0.002	0.009	0.055	0.022	0.025	0.466	0.096	0.872	0.937	0.465	0.12	0.915	1

Lij	L3,1	L3,2	L3,3	L3,4	L3,5	L3,6	L3,7	L3,8	L3,9	L3,10	L3,11	L3,12	L3,13	L3,14	L3,15	L3,16
L3,1	1	0.945	0.014	0.22	0.923	0.857	0.131	0.057	0.001	0.105	0.53	0.119	0.121	0.222	0.083	0.389
L3,2	0.945	1	0.013	0.318	0.847	0.895	0.117	0.101	0.047	0.22	0.518	0.118	0.145	0.313	0.038	0.442
L3,3	0.014	0.013	1	0.056	0.016	0.036	0.053	0.146	0.015	0.016	0.068	0.106	0.041	0.018	0.111	0.069
L3,4	0.22	0.318	0.056	1	0.256	0.348	0.036	0.547	0.069	0.142	0.013	0.077	0.04	0.13	0.113	0.226
L3,5	0.923	0.847	0.016	0.256	1	0.897	0.075	0.199	0.092	0.007	0.438	0.09	0.03	0.056	0.075	0.361
L3,6	0.857	0.895	0.036	0.348	0.897	1	0.048	0.206	0.039	0.12	0.475	0.19	0.004	0.148	0.11	0.33
L3,7	0.131	0.117	0.053	0.036	0.075	0.048	1	0.58	0.261	0.221	0.21	0.064	0.357	0.322	0.097	0.021
L3,8	0.057	0.101	0.146	0.547	0.199	0.206	0.58	1	0.202	0.06	0.107	0.134	0.213	0.106	0.086	0.108
L3,9	0.001	0.047	0.015	0.069	0.092	0.039	0.261	0.202	1	0.92	0.335	0.113	0.892	0.842	0.112	0.45
L3,10	0.105	0.22	0.016	0.142	0.007	0.12	0.221	0.06	0.92	1	0.363	0.141	0.849	0.942	0.12	0.549
L3,11	0.53	0.518	0.068	0.013	0.438	0.475	0.21	0.107	0.335	0.363	1	0.644	0.307	0.416	0.651	0.026
L3,12	0.119	0.118	0.106	0.077	0.09	0.19	0.064	0.134	0.113	0.141	0.644	1	0.215	0.146	0.813	0.639
L3,13	0.121	0.145	0.041	0.04	0.03	0.004	0.357	0.213	0.892	0.849	0.307	0.215	1	0.893	0.142	0.491
L3,14	0.222	0.313	0.018	0.13	0.056	0.148	0.322	0.106	0.842	0.942	0.416	0.146	0.893	1	0.076	0.543
L3,15	0.083	0.038	0.111	0.113	0.075	0.11	0.097	0.086	0.112	0.12	0.651	0.813	0.142	0.076	1	0.665
L3,16	0.389	0.442	0.069	0.226	0.361	0.33	0.021	0.108	0.45	0.549	0.026	0.639	0.491	0.543	0.665	1

Lij	L4,1	L4,2	L4,3	L4,4	L4,5	L4,6	L4,7	L4,8	L4,9	L4,10	L4,11	L4,12	L4,13	L4,14	L4,15	L4,16
L4,1	1	0.958	0.006	0.003	0.914	0.876	0.108	0.147	0.081	0.065	0.545	0.546	0.202	0.208	0.092	0.113
L4,2	0.958	1	0.14	0.002	0.871	0.929	0.168	0.134	0.038	0.107	0.539	0.569	0.152	0.237	0.079	0.097
L4,3	0.006	0.14	1	0.07	0.058	0.144	0.505	0.102	0.318	0.118	0.018	0.031	0.285	0.106	0.013	0.031
L4,4	0.003	0.002	0.07	1	0.006	0.003	0.182	0.049	0.011	0.008	0.073	0.066	0.017	0.015	0.128	0.114
L4,5	0.914	0.871	0.058	0.006	1	0.937	0.012	0.079	0.015	0.015	0.451	0.441	0.058	0.042	0.086	0.103
L4,6	0.876	0.929	0.144	0.003	0.937	1	0.108	0.063	0.024	0.049	0.454	0.483	0.019	0.1	0.063	0.081
L4,7	0.108	0.168	0.505	0.182	0.012	0.108	1	0.488	0.008	0.097	0.169	0.167	0.023	0.128	0.092	0.059
L4,8	0.147	0.134	0.102	0.049	0.079	0.063	0.488	1	0.227	0.215	0.204	0.221	0.327	0.337	0.075	0.116
L4,9	0.081	0.038	0.318	0.011	0.015	0.024	0.008	0.227	1	0.935	0.337	0.332	0.943	0.899	0.098	0.011
L4,10	0.065	0.107	0.118	0.008	0.015	0.049	0.097	0.215	0.935	1	0.339	0.348	0.859	0.931	0.136	0.077
L4,11	0.545	0.539	0.018	0.073	0.451	0.454	0.169	0.204	0.337	0.339	1	0.952	0.378	0.389	0.658	0.643
L4,12	0.546	0.569	0.031	0.066	0.441	0.483	0.167	0.221	0.332	0.348	0.952	1	0.39	0.417	0.608	0.678
L4,13	0.202	0.152	0.285	0.017	0.058	0.019	0.023	0.327	0.943	0.859	0.378	0.39	1	0.94	0.073	0.028
L4,14	0.208	0.237	0.106	0.015	0.042	0.1	0.128	0.337	0.899	0.931	0.389	0.417	0.94	1	0.111	0.033
L4,15	0.092	0.079	0.013	0.128	0.086	0.063	0.092	0.075	0.098	0.136	0.658	0.608	0.073	0.111	1	0.924
L4,16	0.113	0.097	0.031	0.114	0.103	0.081	0.059	0.116	0.011	0.077	0.643	0.678	0.028	0.033	0.924	1

Table J.2. Correlation coefficients between L_{ij} in E_b/N_0=10dB.

Lij	L5,1	L5,2	L5,3	L5,4	L5,5	L5,6	L5,7	L5,8	L5,9	L5,10	L5,11	L5,12	L5,13	L5,14	L5,15	L5,16
L5,1	1	0.481	0.046	0.058	0.056	0.101	0.141	0.156	0.112	0.078	0.331	0.325	0.216	0.205	0.208	0.22
L5,2	0.481	1	0.124	0.038	0.183	0.504	0.179	0.126	0.066	0.095	0.126	0.026	0.169	0.173	0.091	0.014
L5,3	0.046	0.124	1	0.939	0.011	0.168	0.931	0.879	0.077	0.056	0.11	0.014	0.506	0.473	0.065	0.029
L5,4	0.058	0.038	0.939	1	0.018	0.024	0.876	0.917	0.113	0.087	0.049	0.049	0.475	0.476	0.006	0.005
L5,5	0.056	0.183	0.011	0.018	1	0.061	0.011	0.014	0.123	0.135	0.018	0.017	0.076	0.082	0.012	0.013
L5,6	0.101	0.504	0.168	0.024	0.061	1	0.159	0.022	0.029	0.014	0.107	0.286	0.047	0.004	0.114	0.321
L5,7	0.141	0.179	0.931	0.876	0.011	0.159	1	0.96	0.088	0.068	0.243	0.144	0.585	0.553	0.121	0.031
L5,8	0.156	0.126	0.879	0.917	0.014	0.022	0.96	1	0.111	0.085	0.212	0.19	0.568	0.562	0.074	0.07
L5,9	0.112	0.066	0.077	0.113	0.123	0.029	0.088	0.111	1	0.921	0.054	0.008	0.661	0.624	0.093	0.025
L5,10	0.078	0.095	0.056	0.087	0.135	0.014	0.068	0.085	0.921	1	0.121	0.084	0.591	0.639	0.142	0.105
L5,11	0.331	0.126	0.11	0.049	0.018	0.107	0.243	0.212	0.054	0.121	1	0.94	0.402	0.39	0.932	0.898
L5,12	0.325	0.026	0.014	0.049	0.017	0.286	0.144	0.19	0.008	0.084	0.94	1	0.368	0.37	0.855	0.941
L5,13	0.216	0.169	0.506	0.475	0.076	0.047	0.585	0.568	0.661	0.591	0.402	0.368	1	0.951	0.339	0.314
L5,14	0.205	0.173	0.473	0.476	0.082	0.004	0.553	0.562	0.624	0.639	0.39	0.37	0.951	1	0.344	0.332
L5,15	0.208	0.091	0.065	0.006	0.012	0.114	0.121	0.074	0.093	0.142	0.932	0.855	0.339	0.344	1	0.933
L5,16	0.22	0.014	0.029	0.005	0.013	0.321	0.031	0.07	0.025	0.105	0.898	0.941	0.314	0.332	0.933	1

Lij	L6,1	L6,2	L6,3	L6,4	L6,5	L6,6	L6,7	L6,8	L6,9	L6,10	L6,11	L6,12	L6,13	L6,14	L6,15	L6,16
L6,1	1	0.554	0.204	0.198	0.576	0.17	0.106	0.063	0.117	0.101	0.103	0.21	0.144	0.105	0.064	0.207
L6,2	0.554	1	0.047	0.082	0.019	0.048	0.113	0.122	0.001	0.117	0.323	0.365	0.081	0.213	0.227	0.267
L6,3	0.204	0.047	1	0.894	0.339	0.039	0.892	0.855	0.343	0.082	0.141	0.01	0.171	0.467	0.11	0.035
L6,4	0.198	0.082	0.894	1	0.237	0.013	0.841	0.922	0.358	0.059	0.027	0.042	0.088	0.436	0.024	0.104
L6,5	0.576	0.019	0.339	0.237	1	0.07	0.307	0.202	0.218	0.127	0.117	0.05	0.096	0.004	0.127	0.084
L6,6	0.17	0.048	0.039	0.013	0.07	1	0.012	0.009	0.07	0.118	0.015	0.039	0.113	0.07	0.009	0.007
L6,7	0.106	0.113	0.892	0.841	0.307	0.012	1	0.942	0.446	0.02	0.303	0.149	0.114	0.52	0.209	0.049
L6,8	0.063	0.122	0.855	0.922	0.202	0.009	0.942	1	0.38	0.074	0.198	0.116	0.126	0.536	0.08	0.005
L6,9	0.117	0.001	0.343	0.358	0.218	0.07	0.446	0.38	1	0.657	0.518	0.468	0.636	0.018	0.527	0.433
L6,10	0.101	0.117	0.082	0.059	0.127	0.118	0.02	0.074	0.657	1	0.043	0.111	0.81	0.647	0.086	0.072
L6,11	0.103	0.323	0.141	0.027	0.117	0.015	0.303	0.198	0.518	0.043	1	0.889	0.124	0.426	0.942	0.841
L6,12	0.21	0.365	0.01	0.042	0.05	0.039	0.149	0.116	0.468	0.111	0.889	1	0.19	0.315	0.842	0.886
L6,13	0.144	0.081	0.171	0.088	0.096	0.113	0.114	0.126	0.636	0.81	0.124	0.19	1	0.643	0.12	0.084
L6,14	0.105	0.213	0.467	0.436	0.004	0.07	0.52	0.536	0.018	0.647	0.426	0.315	0.643	1	0.373	0.353
L6,15	0.064	0.227	0.11	0.024	0.127	0.009	0.209	0.08	0.527	0.086	0.942	0.842	0.12	0.373	1	0.919
L6,16	0.207	0.267	0.035	0.104	0.084	0.007	0.049	0.005	0.433	0.072	0.841	0.886	0.084	0.353	0.919	1

Lij	L7,1	L7,2	L7,3	L7,4	L7,5	L7,6	L7,7	L7,8	L7,9	L7,10	L7,11	L7,12	L7,13	L7,14	L7,15	L7,16
L7,1	1	0.932	0.128	0.087	0.936	0.859	0.014	0.213	0.032	0.048	0.116	0.322	0.03	0.09	0.186	0.311
L7,2	0.932	1	0.117	0.121	0.9	0.942	0.017	0.339	0.026	0.192	0.081	0.384	0.079	0.22	0.169	0.355
L7,3	0.128	0.117	1	0.483	0.326	0.293	0.075	0.115	0.021	0.023	0.015	0.064	0.176	0.162	0.034	0.01
L7,4	0.087	0.121	0.483	1	0.008	0.026	0.201	0.485	0.008	0.098	0.062	0.155	0.088	0.147	0.094	0.162
L7,5	0.936	0.9	0.326	0.008	1	0.942	0.016	0.228	0.014	0.051	0.053	0.291	0.055	0.011	0.149	0.297
L7,6	0.859	0.942	0.293	0.026	0.942	1	0.018	0.331	0.031	0.174	0.023	0.342	0.01	0.125	0.133	0.33
L7,7	0.014	0.017	0.075	0.201	0.016	0.018	1	0.056	0.014	0.011	0.116	0.072	0.01	0.01	0.128	0.078
L7,8	0.213	0.339	0.115	0.485	0.228	0.331	0.056	1	0.081	0.143	0.082	0.198	0.075	0.124	0.043	0.184
L7,9	0.032	0.026	0.021	0.008	0.014	0.031	0.014	0.081	1	0.913	0.086	0.452	0.938	0.874	0.06	0.452
L7,10	0.048	0.192	0.023	0.098	0.051	0.174	0.011	0.143	0.913	1	0.077	0.543	0.874	0.96	0.049	0.533
L7,11	0.116	0.081	0.015	0.062	0.053	0.023	0.116	0.082	0.086	0.077	1	0.646	0.06	0.062	0.924	0.615
L7,12	0.322	0.384	0.064	0.155	0.291	0.342	0.072	0.198	0.452	0.543	0.646	1	0.494	0.57	0.575	0.949
L7,13	0.03	0.079	0.176	0.088	0.055	0.01	0.01	0.075	0.938	0.874	0.06	0.494	1	0.927	0.035	0.454
L7,14	0.09	0.22	0.162	0.147	0.011	0.125	0.01	0.124	0.874	0.96	0.062	0.57	0.927	1	0.036	0.529
L7,15	0.186	0.169	0.034	0.094	0.149	0.133	0.128	0.043	0.06	0.049	0.924	0.575	0.035	0.036	1	0.628
L7,16	0.311	0.355	0.01	0.162	0.297	0.33	0.078	0.184	0.452	0.533	0.615	0.949	0.454	0.529	0.628	1

Lij	L8,1	L8,2	L8,3	L8,4	L8,5	L8,6	L8,7	L8,8	L8,9	L8,10	L8,11	L8,12	L8,13	L8,14	L8,15	L8,16
L8,1	1	0.951	0.079	0.131	0.928	0.889	0.033	0.013	0.061	0.049	0.059	0.085	0.116	0.104	0.111	0.135
L8,2	0.951	1	0.148	0.126	0.89	0.936	0.126	0.009	0.02	0.105	0.042	0.067	0.079	0.156	0.103	0.119
L8,3	0.079	0.148	1	0.554	0.19	0.243	0.559	0.175	0.18	0.068	0.011	0.017	0.232	0.135	0.078	0.017
L8,4	0.131	0.126	0.554	1	0.349	0.325	0.049	0.058	0.007	0.039	0.013	0.042	0.135	0.121	0.059	0.013
L8,5	0.928	0.89	0.19	0.349	1	0.96	0	0.012	0.042	0.066	0.016	0.007	0.009	0.024	0.111	0.091
L8,6	0.889	0.936	0.243	0.325	0.96	1	0.141	0.01	0.009	0.122	0.004	0.005	0.012	0.084	0.109	0.083
L8,7	0.033	0.126	0.559	0.049	0	0.141	1	0.066	0.34	0.125	0.026	0.023	0.319	0.119	0.072	0.005
L8,8	0.013	0.009	0.175	0.058	0.012	0.01	0.066	1	0.008	0.008	0.136	0.125	0.007	0.004	0.144	0.139
L8,9	0.061	0.02	0.18	0.007	0.042	0.009	0.34	0.008	1	0.929	0.129	0.046	0.96	0.89	0.151	0.058
L8,10	0.049	0.105	0.068	0.039	0.066	0.122	0.125	0.008	0.929	1	0.168	0.117	0.89	0.951	0.147	0.094
L8,11	0.059	0.042	0.011	0.013	0.016	0.004	0.026	0.136	0.129	0.168	1	0.92	0.121	0.152	0.918	0.892
L8,12	0.085	0.067	0.017	0.042	0.007	0.005	0.023	0.125	0.046	0.117	0.92	1	0.031	0.097	0.798	0.92
L8,13	0.116	0.079	0.232	0.135	0.009	0.012	0.319	0.007	0.96	0.89	0.121	0.031	1	0.936	0.149	0.045
L8,14	0.104	0.156	0.135	0.121	0.024	0.084	0.119	0.004	0.89	0.951	0.152	0.097	0.936	1	0.139	0.077
L8,15	0.111	0.103	0.078	0.059	0.111	0.109	0.072	0.144	0.151	0.147	0.918	0.798	0.149	0.139	1	0.918
L8,16	0.135	0.119	0.017	0.013	0.091	0.083	0.005	0.139	0.058	0.094	0.892	0.92	0.045	0.077	0.918	1

Table J.3. Correlation coefficients between L_{ij} in E_b/N_0=10dB.

Lij	L9,1	L9,2	L9,3	L9,4	L9,5	L9,6	L9,7	L9,8	L9,9	L9,10	L9,11	L9,12	L9,13	L9,14	L9,15	L9,16
L9,1	1	0.648	0.065	0.082	0.923	0.6	0.09	0.101	0.134	0.086	0.073	0.048	0.007	0.085	0.113	0.087
L9,2	0.648	1	0.462	0.547	0.632	0.951	0.465	0.559	0.081	0.206	0.359	0.402	0.022	0.163	0.36	0.414
L9,3	0.065	0.462	1	0.931	0.085	0.501	0.939	0.876	0.018	0.067	0.041	0.002	0.159	0.101	0.044	0.09
L9,4	0.082	0.547	0.931	1	0.105	0.585	0.878	0.959	0.017	0.126	0.022	0.135	0.148	0.161	0.097	0.223
L9,5	0.923	0.632	0.085	0.105	1	0.668	0.11	0.125	0.121	0.126	0.002	0.044	0.035	0.052	0.066	0.019
L9,6	0.6	0.951	0.501	0.585	0.668	1	0.465	0.566	0.075	0.214	0.337	0.396	0.034	0.158	0.354	0.424
L9,7	0.09	0.465	0.939	0.878	0.11	0.465	1	0.916	0.026	0.075	0	0.044	0.033	0.017	0.019	0.034
L9,8	0.101	0.559	0.876	0.959	0.125	0.566	0.916	1	0.021	0.145	0.064	0.186	0.008	0.108	0.054	0.195
L9,9	0.134	0.081	0.018	0.017	0.121	0.075	0.026	0.021	1	0.058	0.01	0.013	0.062	0.189	0.01	0.014
L9,10	0.086	0.206	0.067	0.126	0.126	0.214	0.075	0.145	0.058	1	0.228	0.333	0.126	0.482	0.209	0.337
L9,11	0.073	0.359	0.041	0.022	0.002	0.337	0	0.064	0.01	0.228	1	0.942	0.329	0.001	0.934	0.9
L9,12	0.048	0.402	0.002	0.135	0.044	0.396	0.044	0.186	0.013	0.333	0.942	1	0.297	0.036	0.854	0.94
L9,13	0.007	0.022	0.159	0.148	0.035	0.034	0.033	0.008	0.062	0.126	0.329	0.297	1	0.489	0.129	0.119
L9,14	0.085	0.163	0.101	0.161	0.052	0.158	0.017	0.108	0.189	0.482	0.001	0.036	0.489	1	0.104	0.138
L9,15	0.113	0.36	0.044	0.097	0.066	0.354	0.019	0.054	0.01	0.209	0.934	0.854	0.129	0.104	1	0.931
L9,16	0.087	0.414	0.09	0.223	0.019	0.424	0.034	0.195	0.014	0.337	0.9	0.94	0.119	0.138	0.931	1

Lij	L10,1	L10,2	L10,3	L10,4	L10,5	L10,6	L10,7	L10,8	L10,9	L10,10	L10,11	L10,12	L10,13	L10,14	L10,15	L10,16
L10,1	1	0.916	0.147	0.137	0.915	0.796	0.147	0.142	0.082	0.147	0.143	0.144	0.102	0.079	0.139	0.133
L10,2	0.916	1	0.036	0.069	0.89	0.919	0.047	0.085	0.012	0.145	0.111	0.104	0.035	0.022	0.153	0.139
L10,3	0.147	0.036	1	0.936	0.111	0.017	0.959	0.886	0.305	0.007	0.04	0.06	0.234	0.163	0.075	0.042
L10,4	0.137	0.069	0.936	1	0.144	0.084	0.893	0.951	0.107	0.006	0.023	0.038	0.136	0.144	0.063	0.12
L10,5	0.915	0.89	0.111	0.144	1	0.921	0.12	0.158	0.034	0.141	0.034	0.026	0.036	0.002	0.074	0.061
L10,6	0.796	0.919	0.017	0.084	0.921	1	0.032	0.104	0.017	0.131	0.017	0.007	0.004	0.032	0.094	0.078
L10,7	0.147	0.047	0.959	0.893	0.12	0.032	1	0.928	0.325	0.008	0.012	0.04	0.177	0.019	0.014	0.02
L10,8	0.142	0.085	0.886	0.951	0.158	0.104	0.928	1	0.106	0.009	0.011	0.072	0.063	0.016	0	0.063
L10,9	0.082	0.012	0.305	0.107	0.034	0.017	0.325	0.106	1	0.059	0.006	0.148	0.551	0.026	0.03	0.129
L10,10	0.147	0.145	0.007	0.006	0.141	0.131	0.008	0.009	0.059	1	0.018	0.016	0.177	0.077	0.018	0.014
L10,11	0.143	0.111	0.04	0.023	0.034	0.017	0.012	0.011	0.006	0.018	1	0.96	0.188	0.341	0.926	0.889
L10,12	0.144	0.104	0.06	0.038	0.026	0.007	0.04	0.072	0.148	0.016	0.96	1	0.24	0.32	0.885	0.934
L10,13	0.102	0.035	0.234	0.136	0.036	0.004	0.177	0.063	0.551	0.177	0.188	0.24	1	0.587	0.067	0.136
L10,14	0.079	0.022	0.163	0.144	0.002	0.032	0.019	0.016	0.026	0.077	0.341	0.32	0.587	1	0.117	0.115
L10,15	0.139	0.153	0.075	0.063	0.074	0.094	0.014	0	0.03	0.018	0.926	0.885	0.067	0.117	1	0.951
L10,16	0.133	0.139	0.042	0.12	0.061	0.078	0.02	0.063	0.129	0.014	0.889	0.934	0.136	0.115	0.951	1

Lij	L11,1	L11,2	L11,3	L11,4	L11,5	L11,6	L11,7	L11,8	L11,9	L11,10	L11,11	L11,12	L11,13	L11,14	L11,15	L11,16
L11,1	1	0.938	0.341	0.342	0.932	0.862	0.1	0.155	0.076	0.037	0.009	0.119	0.017	0.047	0.212	0.107
L11,2	0.938	1	0.324	0.335	0.9	0.941	0.032	0.116	0	0.041	0.01	0.31	0.066	0.03	0.227	0.008
L11,3	0.341	0.324	1	0.949	0.4	0.371	0.65	0.574	0.556	0.538	0.078	0.045	0.47	0.434	0.227	0.179
L11,4	0.342	0.335	0.949	1	0.38	0.363	0.612	0.624	0.517	0.525	0.082	0.005	0.431	0.43	0.216	0.185
L11,5	0.932	0.9	0.4	0.38	1	0.942	0.07	0.145	0.204	0.177	0.017	0.108	0.065	0.007	0.329	0.128
L11,6	0.862	0.941	0.371	0.363	0.942	1	0.004	0.105	0.112	0.16	0.016	0.281	0.024	0.01	0.324	0.03
L11,7	0.1	0.032	0.65	0.612	0.07	0.004	1	0.922	0.059	0.079	0.124	0.026	0.051	0.079	0.103	0.066
L11,8	0.155	0.116	0.574	0.624	0.145	0.105	0.922	1	0.032	0.047	0.135	0.02	0.023	0.048	0.07	0.098
L11,9	0.076	0	0.556	0.517	0.204	0.112	0.059	0.032	1	0.959	0.005	0.163	0.926	0.87	0.132	0.162
L11,10	0.037	0.041	0.538	0.525	0.177	0.16	0.079	0.047	0.959	1	0.007	0.021	0.871	0.909	0.151	0.109
L11,11	0.009	0.01	0.078	0.082	0.017	0.016	0.124	0.135	0.005	0.007	1	0.061	0.003	0.009	0.065	0.192
L11,12	0.119	0.31	0.045	0.005	0.108	0.281	0.026	0.02	0.163	0.021	0.061	1	0.172	0.026	0.098	0.486
L11,13	0.017	0.066	0.47	0.431	0.065	0.024	0.051	0.023	0.926	0.871	0.003	0.172	1	0.937	0.073	0.103
L11,14	0.047	0.03	0.434	0.43	0.007	0.01	0.079	0.048	0.87	0.909	0.009	0.026	0.937	1	0.085	0.014
L11,15	0.212	0.227	0.227	0.216	0.329	0.324	0.103	0.07	0.132	0.151	0.065	0.098	0.073	0.085	1	0.491
L11,16	0.107	0.008	0.179	0.185	0.128	0.03	0.066	0.098	0.162	0.109	0.192	0.486	0.103	0.014	0.491	1

Lij	L12,1	L12,2	L12,3	L12,4	L12,5	L12,6	L12,7	L12,8	L12,9	L12,10	L12,11	L12,12	L12,13	L12,14	L12,15	L12,16
L12,1	1	0.922	0.118	0.378	0.941	0.844	0.53	0.078	0.205	0.083	0.119	0.009	0.114	0.01	0.059	0.212
L12,2	0.922	1	0.084	0.351	0.842	0.886	0.433	0.072	0.038	0.014	0.09	0.011	0.038	0.103	0.2	0.25
L12,3	0.118	0.084	1	0.647	0.125	0.199	0.64	0.814	0.14	0.149	0.069	0.114	0.203	0.121	0.118	0.073
L12,4	0.378	0.351	0.647	1	0.428	0.308	0.032	0.671	0.53	0.546	0.013	0.076	0.48	0.454	0.091	0.209
L12,5	0.941	0.842	0.125	0.428	1	0.891	0.517	0.034	0.301	0.202	0.11	0.013	0.142	0.037	0.102	0.313
L12,6	0.844	0.886	0.199	0.308	0.891	1	0.469	0.113	0.134	0.102	0.059	0.042	0	0.048	0.205	0.345
L12,7	0.53	0.433	0.64	0.032	0.517	0.469	1	0.648	0.412	0.348	0.211	0.075	0.313	0.328	0.112	0.003
L12,8	0.078	0.072	0.814	0.671	0.034	0.113	0.648	1	0.077	0.131	0.092	0.123	0.138	0.12	0.082	0.119
L12,9	0.205	0.038	0.14	0.53	0.301	0.134	0.412	0.077	1	0.944	0.315	0.017	0.893	0.845	0.116	0.109
L12,10	0.083	0.014	0.149	0.546	0.202	0.102	0.348	0.131	0.944	1	0.215	0.015	0.855	0.922	0.072	0.12
L12,11	0.119	0.09	0.069	0.013	0.11	0.059	0.211	0.092	0.315	0.215	1	0.055	0.35	0.255	0.572	0.017
L12,12	0.009	0.011	0.114	0.076	0.013	0.042	0.075	0.123	0.017	0.015	0.055	1	0.044	0.016	0.158	0.058
L12,13	0.114	0.038	0.203	0.48	0.142	0	0.313	0.138	0.893	0.855	0.35	0.044	1	0.897	0.222	0.062
L12,14	0.01	0.103	0.121	0.454	0.037	0.048	0.328	0.12	0.845	0.922	0.255	0.016	0.897	1	0.213	0.089
L12,15	0.059	0.2	0.118	0.091	0.102	0.205	0.112	0.082	0.116	0.072	0.572	0.158	0.222	0.213	1	0.564
L12,16	0.212	0.25	0.073	0.209	0.313	0.345	0.003	0.119	0.109	0.12	0.017	0.058	0.062	0.089	0.564	1

Table J.4. Correlation coefficients between L_{ij} in E_b/N_0=10dB.

Lij	L13,1	L13,2	L13,3	L13,4	L13,5	L13,6	L13,7	L13,8	L13,9	L13,10	L13,11	L13,12	L13,13	L13,14	L13,15	L13,16
L13,1	1	0.655	0.107	0.044	0.653	0.812	0.088	0.098	0.117	0.107	0.077	0.11	0.112	0.117	0.093	0.043
L13,2	0.655	1	0.473	0.532	0.018	0.639	0.445	0.545	0.004	0.125	0.347	0.326	0.069	0.23	0.366	0.43
L13,3	0.107	0.473	1	0.89	0.325	0.197	0.888	0.846	0.345	0.19	0.036	0.013	0.038	0.035	0.111	0.146
L13,4	0.044	0.532	0.89	1	0.431	0.133	0.838	0.941	0.305	0.085	0.044	0.153	0.014	0.131	0.205	0.309
L13,5	0.653	0.018	0.325	0.431	1	0.637	0.333	0.359	0.218	0.121	0.44	0.477	0.071	0.008	0.539	0.525
L13,6	0.812	0.639	0.197	0.133	0.637	1	0.115	0.147	0.078	0.156	0.098	0.192	0.112	0.082	0.133	0.126
L13,7	0.088	0.445	0.888	0.838	0.333	0.115	1	0.919	0.236	0.175	0.115	0.049	0.012	0.07	0.031	0.025
L13,8	0.098	0.545	0.846	0.941	0.359	0.147	0.919	1	0.196	0.034	0.018	0.11	0.012	0.139	0.067	0.194
L13,9	0.117	0.004	0.345	0.305	0.218	0.078	0.236	0.196	1	0.549	0.065	0.037	0.053	0.03	0.137	0.124
L13,10	0.107	0.125	0.19	0.085	0.121	0.156	0.175	0.034	0.549	1	0.18	0.192	0.167	0.572	0.044	0.091
L13,11	0.077	0.347	0.036	0.044	0.44	0.098	0.115	0.018	0.065	0.18	1	0.893	0.019	0.25	0.921	0.844
L13,12	0.11	0.326	0.013	0.153	0.477	0.192	0.049	0.11	0.037	0.192	0.893	1	0.042	0.35	0.852	0.893
L13,13	0.112	0.069	0.038	0.014	0.071	0.112	0.012	0.012	0.053	0.167	0.019	0.042	1	0.059	0.017	0.018
L13,14	0.117	0.23	0.035	0.131	0.008	0.082	0.07	0.139	0.03	0.572	0.25	0.35	0.059	1	0.211	0.31
L13,15	0.093	0.366	0.111	0.205	0.539	0.133	0.031	0.067	0.137	0.044	0.921	0.852	0.017	0.211	1	0.943
L13,16	0.043	0.43	0.146	0.309	0.525	0.126	0.025	0.194	0.124	0.091	0.844	0.893	0.018	0.31	0.943	1

Lij	L14,1	L14,2	L14,3	L14,4	L14,5	L14,6	L14,7	L14,8	L14,9	L14,10	L14,11	L14,12	L14,13	L14,14	L14,15	L14,16
L14,1	1	0.924	0.111	0.152	0.64	0.592	0.129	0.169	0.081	0.054	0.1	0.07	0.02	0.121	0.096	0.077
L14,2	0.924	1	0.028	0.09	0.624	0.663	0.061	0.125	0.052	0.085	0.128	0.101	0.014	0.112	0.125	0.107
L14,3	0.111	0.028	1	0.946	0.371	0.369	0.942	0.866	0.043	0.328	0.045	0.012	0.261	0.011	0.199	0.155
L14,4	0.152	0.09	0.946	1	0.38	0.392	0.903	0.934	0.13	0.335	0.033	0.093	0.1	0.014	0.208	0.238
L14,5	0.64	0.624	0.371	0.38	1	0.95	0.337	0.338	0.178	0.217	0.46	0.458	0.015	0.077	0.556	0.546
L14,6	0.592	0.663	0.369	0.392	0.95	1	0.318	0.333	0.171	0.228	0.46	0.497	0.038	0.071	0.564	0.584
L14,7	0.129	0.061	0.942	0.903	0.337	0.318	1	0.94	0.015	0.229	0.008	0.024	0.296	0.006	0.086	0.047
L14,8	0.169	0.125	0.866	0.934	0.338	0.333	0.94	1	0.106	0.22	0.015	0.051	0.113	0.008	0.075	0.118
L14,9	0.081	0.052	0.043	0.13	0.178	0.171	0.015	0.106	1	0.491	0.028	0.114	0.465	0.156	0.115	0.167
L14,10	0.054	0.085	0.328	0.335	0.217	0.228	0.229	0.22	0.491	1	0.053	0.037	0.091	0.043	0.175	0.162
L14,11	0.1	0.128	0.045	0.033	0.46	0.46	0.008	0.015	0.028	0.053	1	0.936	0.053	0.027	0.912	0.87
L14,12	0.07	0.101	0.012	0.093	0.458	0.497	0.024	0.051	0.114	0.037	0.936	1	0.144	0.018	0.872	0.927
L14,13	0.02	0.014	0.261	0.1	0.015	0.038	0.296	0.113	0.465	0.091	0.053	0.144	1	0.035	0.004	0.135
L14,14	0.121	0.112	0.011	0.014	0.077	0.071	0.006	0.008	0.156	0.043	0.027	0.018	0.035	1	0.02	0.015
L14,15	0.096	0.125	0.199	0.208	0.556	0.564	0.086	0.075	0.115	0.175	0.912	0.872	0.004	0.02	1	0.958
L14,16	0.077	0.107	0.155	0.238	0.546	0.584	0.047	0.118	0.167	0.162	0.87	0.927	0.135	0.015	0.958	1

Lij	L15,1	L15,2	L15,3	L15,4	L15,5	L15,6	L15,7	L15,8	L15,9	L15,10	L15,11	L15,12	L15,13	L15,14	L15,15	L15,16
L15,1	1	0.927	0.11	0.164	0.951	0.888	0.088	0.144	0.053	0.001	0.021	0.078	0.065	0.011	0.016	0.13
L15,2	0.927	1	0.028	0.113	0.89	0.96	0.039	0.138	0.024	0.02	0.008	0.188	0.039	0.003	0.012	0.348
L15,3	0.11	0.028	1	0.919	0.091	0.015	0.919	0.791	0.067	0.092	0.03	0.022	0.002	0.018	0.116	0.051
L15,4	0.164	0.113	0.919	1	0.149	0.107	0.892	0.916	0.053	0.077	0.004	0.013	0.02	0.038	0.128	0.004
L15,5	0.951	0.89	0.091	0.149	1	0.936	0.073	0.139	0.107	0.058	0.136	0.145	0.031	0.024	0.011	0.127
L15,6	0.888	0.96	0.015	0.107	0.936	1	0.031	0.139	0.033	0.075	0.148	0.241	0.061	0.035	0.01	0.325
L15,7	0.088	0.039	0.919	0.892	0.073	0.031	1	0.915	0.133	0.156	0.03	0.015	0.1	0.117	0.129	0.024
L15,8	0.144	0.138	0.791	0.916	0.139	0.139	0.915	1	0.129	0.143	0.081	0.087	0.139	0.148	0.134	0.054
L15,9	0.053	0.024	0.067	0.053	0.107	0.033	0.133	0.129	1	0.95	0.128	0.15	0.937	0.892	0.007	0.118
L15,10	0.001	0.02	0.092	0.077	0.058	0.075	0.156	0.143	0.95	1	0.13	0.08	0.889	0.93	0.014	0.045
L15,11	0.021	0.008	0.03	0.004	0.136	0.148	0.03	0.081	0.128	0.13	1	0.555	0.323	0.343	0.056	0.051
L15,12	0.078	0.188	0.022	0.013	0.145	0.241	0.015	0.087	0.15	0.08	0.555	1	0.244	0.189	0.167	0.557
L15,13	0.065	0.039	0.002	0.02	0.031	0.061	0.1	0.139	0.937	0.889	0.323	0.244	1	0.959	0.008	0.135
L15,14	0.011	0.003	0.018	0.038	0.024	0.035	0.117	0.148	0.892	0.93	0.343	0.189	0.959	1	0.012	0.009
L15,15	0.016	0.012	0.116	0.128	0.011	0.01	0.129	0.134	0.007	0.014	0.056	0.167	0.008	0.012	1	0.043
L15,16	0.13	0.348	0.051	0.004	0.127	0.325	0.024	0.054	0.118	0.045	0.051	0.557	0.135	0.009	0.043	1

Lij	L16,1	L16,2	L16,3	L16,4	L16,5	L16,6	L16,7	L16,8	L16,9	L16,10	L16,11	L16,12	L16,13	L16,14	L16,15	L16,16
L16,1	1	0.917	0.562	0.134	0.958	0.874	0.559	0.109	0.183	0.039	0.098	0.01	0.182	0.059	0.153	0.018
L16,2	0.917	1	0.466	0.128	0.876	0.937	0.472	0.107	0.02	0.039	0.012	0.052	0.037	0.009	0.065	0.021
L16,3	0.562	0.466	1	0.666	0.587	0.507	0.951	0.595	0.407	0.342	0.164	0.028	0.38	0.324	0.225	0.073
L16,4	0.134	0.128	0.666	1	0.117	0.105	0.63	0.919	0.04	0.083	0.078	0.025	0.022	0.02	0.124	0.123
L16,5	0.958	0.876	0.587	0.117	1	0.93	0.557	0.099	0.213	0.085	0.154	0.131	0.132	0.019	0.138	0.014
L16,6	0.874	0.937	0.507	0.105	0.93	1	0.48	0.09	0.077	0.027	0.1	0.144	0.002	0.046	0.057	0.013
L16,7	0.559	0.472	0.951	0.63	0.557	0.48	1	0.646	0.374	0.325	0.173	0.014	0.36	0.318	0.207	0.079
L16,8	0.109	0.107	0.595	0.919	0.099	0.09	0.646	1	0.127	0.151	0.119	0.032	0.09	0.12	0.081	0.13
L16,9	0.183	0.02	0.407	0.04	0.213	0.077	0.374	0.127	1	0.932	0.105	0.125	0.941	0.903	0.33	0.017
L16,10	0.039	0.039	0.342	0.083	0.085	0.027	0.325	0.151	0.932	1	0.075	0.129	0.856	0.935	0.207	0.013
L16,11	0.098	0.012	0.164	0.078	0.154	0.1	0.173	0.119	0.105	0.075	1	0.488	0.01	0.023	0.466	0.194
L16,12	0.01	0.052	0.028	0.025	0.131	0.144	0.014	0.032	0.125	0.129	0.488	1	0.295	0.325	0.133	0.05
L16,13	0.182	0.037	0.38	0.022	0.132	0.002	0.36	0.09	0.941	0.856	0.01	0.295	1	0.943	0.326	0.013
L16,14	0.059	0.009	0.324	0.02	0.019	0.046	0.318	0.12	0.903	0.935	0.023	0.325	0.943	1	0.226	0.011
L16,15	0.153	0.065	0.225	0.124	0.138	0.057	0.207	0.081	0.33	0.207	0.466	0.133	0.326	0.226	1	0.066
L16,16	0.018	0.021	0.073	0.123	0.014	0.013	0.079	0.13	0.017	0.013	0.194	0.05	0.013	0.011	0.066	1